

University at Albany, State University of New York

Scholars Archive

Geology Theses and Dissertations

Atmospheric and Environmental Sciences

2003

Late Holocene hydrologic and climatic variability in the Walker Lake basin, Nevada and California

Fasong Yuan

University at Albany, State University of New York

Follow this and additional works at: https://scholarsarchive.library.albany.edu/cas_daes_geology_etd

Recommended Citation

Yuan, Fasong, "Late Holocene hydrologic and climatic variability in the Walker Lake basin, Nevada and California" (2003). *Geology Theses and Dissertations*. 117.

https://scholarsarchive.library.albany.edu/cas_daes_geology_etd/117

This Dissertation is brought to you for free and open access by the Atmospheric and Environmental Sciences at Scholars Archive. It has been accepted for inclusion in Geology Theses and Dissertations by an authorized administrator of Scholars Archive. For more information, please contact scholarsarchive@albany.edu.

LATE HOLOCENE HYDROLOGIC AND
CLIMATIC VARIABILITY IN THE WALKER
LAKE BASIN, NEVADA AND CALIFORNIA

By

Fasong Yuan

A Dissertation

Submitted to the University at Albany, State University of New York

in Partial Fulfillment of

the Requirements for the Degree of

Doctor of Philosophy

College of Arts & Sciences

Department of Earth & Atmospheric Sciences

2003

ABSTRACT

Oxygen and carbon isotopic measurements of the total inorganic carbon (TIC) fraction of sediments from Walker Lake (Nevada, USA) were completed at a decadal-scale resolution spanning the last ~3000 years. On the basis of radiocarbon dating of the total organic fraction of cored sediments, the late Holocene isotope record recorded a relatively dry climate in Period LH-1 (1000 BC to AD 800), a relatively wet climate punctuated by a few severe droughts in Period LH-2 (AD 800 to 1900), and an anthropogenic perturbation era (LH-h: 1900-2000). Relatively high accumulation rates in Period LH-2 (AD 800 to 1900) provided detailed information on climatic and hydrologic variability in this region. Coupled with the tree-ring-based Sacramento River flow record, the radiocarbon-based age model was refined for the interval of AD 800 through 1900. A high-resolution (3.5 year per sample) TIC $\delta^{18}\text{O}$ record spanning the last 1200 years was generated to reflect fluctuations in winter snowfall of the Sierra Nevada. This TIC $\delta^{18}\text{O}$ record shows at least two prolonged droughts that occurred during the Medieval Warm Epoch, which are chronologically well consistent with previous findings (STINE, 1994). Time series analyses on the TIC $\delta^{18}\text{O}$ and the Sacramento River flow records reveal that interdecadal and centennial modes of climate variability persisted over the last millennium. PDO-like interdecadal oscillations that centered in the periods of 50-90 yr were almost in phase with thermal fluctuations in ocean climate of the California Current, suggesting that interdecadal climate oscillations in the Sierra Nevada were intimately linked with the Pacific dynamics. The underlying centennial to multicentennial variability corresponding to the Medieval Warm Epoch and the Little Ice Age comprise the major share of total variance. In addition, the TIC $\delta^{18}\text{O}$ record of Walker Lake is visually well correlated with the polar ice-core-based cosmogenic nuclide production and the Rice Lake Mg/Ca records. This suggests that some centennial oscillations in winter precipitation of the Sierra Nevada were associated with solar activity over the last millennium.

ACKNOWLEDGMENTS

I have benefited from many people who offered their thoughtful ideas, suggestions, and encouragement through my dissertation research. No list is exhaustive nor words expressive enough of my deep appreciation to these people. First thanks go to my advisor, Dr. Braddock K. Linsley, who gave me a great opportunity to come to the United States to pursue my Ph. D program at the University at Albany. As one of his students, I have learned a lot from him. His guidance and supervision are vital in pursuit of my dissertation research. I was impressed by his patience and wisdom in explanation and/discussion when I had questions. By no means, without his physical and mental support, it would be very difficult for me to accomplish this dissertation. Next, I would like to thank Dr. Larry V. Benson in the U. S. Geological Survey, who first acquainted me with Walker Lake and helped me to collect high-quality sediment cores. His expertise has guided me to the right direction. Moreover, he provided me a great deal of background information about Walker Lake. I am indebted to Mr. Stephen S. Howe for his help in running mass spectrometer and Dr. Donald T. Rodbell in the Union College for his assistance in running coulometer. Thanks are also due to Dr. Karen I. Mohr, one of my committee members. I thank Dr. John W. Delano for his generous support during the early stage of this dissertation research. Special thanks go to Dr. Andrei Lapenis, who taught the course of Advanced Climatology, in which I have learned a lot about global climate history over the past few thousand years. I am equally appreciative to all the professors from whom I have taken courses. I also thank the people in the main office of the Department of Earth and Atmospheric Sciences.

I have received distant instructions from Dr. Richard Forester of U. S. Geological Survey for microfossil (Ostracode) identification. I appreciate Dr. Steve Lund of the University of Southern California, Dr. Joe Smoot of the U. S. Geological Survey, Dr. Robert Richards and Dr. Alan Heyvaert of the University of California at Davis for their assistance in core acquisition. I also thank Dr. Jack McGeehin of the U. S. Geological Survey for radiocarbon dating analysis on cored sediments. In

addition, John Heggeness of Nevada Division of Environmental Protection kindly provided me brand new results of water chemistry and temperature measurements of the Walker River and Walker Lake.

This dissertation work was supported by the Department of Earth and Atmospheric Sciences at the University at Albany and the arid climate program of the U.S. Geological Survey.

I thank my colleagues at the University at Albany: Bin Zhu, Youshe Li, Chul Lim, and Elizabeth Scott. Special thanks go to Haiyan Liu, who helped me cut box cores manually.

Last but not the least acknowledgment goes to my parents and parents-in-law for their continuous support over the years and to my wife Meihua Yu and my son Rick Yuan. This dissertation is dedicated to Meihua Yu and Rick Yuan.

TABLE OF CONTENTS

ABSTRACT	ii
ACKNOWLEDGMENTS	iii
LIST OF TABLES	vii
LIST OF FIGURES.....	viii
PREFACE.....	1
CHAPTER 1 GENERAL INTRODUCTION.....	3
1.1 Lakes in the western Great Basin.....	4
1.2 Climate of the western Great Basin.....	5
1.3 Late Holocene paleoclimate of the western Great Basin	10
1.4 Walker Lake and its drainage basin.....	13
1.5 Objective of this dissertation research.....	16
CHAPTER 2 OXYGEN ISOTOPES IN THE WALKER RIVER AND WALKER LAKE SURFACE WATER SYSTEM.....	19
2.1 Abstract	19
2.2 Introduction.....	19
2.3 Walker Lake Hydrology.....	20
2.4 Surface Water $\delta^{18}\text{O}$	26
2.5 Oxygen Isotopic Modeling.....	29
2.6 Results and Discussion	32
CHAPTER 3 COMPARISON OF HISTORICAL LAKE LEVELS AND DOWN-CORE ISOTOPIC SIGNATURES FROM WALKER LAKE	39
3.1 Abstract	39
3.2 Introduction.....	40
3.3 Method and Materials.....	41
3.4 Results.....	43
3.5 Discussion.....	48
CHAPTER 4 LATE HOLOCENE LACUSTRINE GEOCHEMICAL AND ISOTOPIC RECORD OF WALKER LAKE	60
4.1 Abstract	60
4.2 Introduction.....	60
4.3 Methods and Results.....	64
4.3.1 Core WLC84-8.....	66
4.3.2 Core WLC002.....	68
4.3.3 Core WLC001	70
4.4 Core Chronology.....	73
4.4.1 Reservoir Effect.....	73
4.4.2 Age Model.....	77
4.5 Discussion.....	78
4.5.1 Period LH-1, 1000BC to 800AD.....	78
4.5.2 Period LH-2, 800AD to 1900AD.....	81
4.5.3 Period LH-h, 1900 to 2000AD.....	87
4.6 Conclusion	87

CHAPTER 5 CENTENNIAL AND INTERDECADAL CLIMATE VARIABILITY IN THE WALKER LAKE BASIN SINCE AD 800.....	89
5.1 Abstract	89
5.2 Introduction.....	90
5.3 Isotopic responses to climatic changes.....	92
5.4 Age model revision	99
5.5 Spectral analysis.....	102
5.6 Results and discussion	102
5.6.1 Interdecadal climatic oscillations	102
5.6.2 Centennial timescale variability	109
APPENDIX 1 A WINDOWS PROGRAM FOR PALEOLAKE LEVEL RECONSTRUCTION FROM THE OXYGEN ISOTOPIC RECORD OF CLOSED-BASIN LAKE CARBONATES.....	113
A1.1 Abstract	113
A1.2 Introduction.....	113
A1.3 Program description.....	115
A1.3.1 Data acquisition and validation.....	116
A1.3.2 Model parameters and physical settings.....	117
A1.3.3 Modeling modules	118
A1.4 Discussion.....	119
APPENDIX 2 RECONSTRUCTION OF LATE HOLOCENE EFFECTIVE MOISTURE AVAILABILITY IN THE WALKER LAKE BASIN	120
A2.1 Abstract	120
A2.2 Introduction.....	121
A2.3 Reconstruction Model	123
A2.4 Model Data Acquisition	125
A2.4.1 Lake Water $\delta^{18}\text{O}_L$	125
A2.4.2 River Flow $\delta^{18}\text{O}_R$	126
A2.4.3 Model Parameters.....	128
A2.5 Model Results	129
A2.6 Validation	132
A2.6.1 Walker River Discharge.....	132
A2.6.2 Oxygen Isotopes.....	134
A2.7 Discussion.....	137
APPENDIX 3 RESULTS OF MEASUREMENTS OF TOTAL INORGANIC CARBON, TOTAL CARBON, OXYGEN AND CARBON ISOTOPIC COMPOSITIONS	141
A3.1 Box-core WLB-003C.....	141
A3.2 Piston Core WLC002.....	144
A3.3 Piston Core WLC-001	155
REFERENCE	156
VITA	166

LIST OF TABLES

<i>Number</i>	<i>Page</i>
Table 1-1 Water chemistry of the Walker River and Walker Lake	14
Table 2-1 Surface waters and their oxygen isotopic signatures.....	27
Table 2-2 Lunar monthly limnologic and climatic data and normalized lunar monthly values of river flow, on-lake precipitation, and evaporation that are taken from Pyramid Lake	30
Table 4-1 Standard deviations and mean relative errors of carbon and oxygen isotopic analyses	66
Table 4-2 Estimates of the reservoir effect of Walker Lake.....	76
Table 4-3 Calibrated radiocarbon dates of the TOC fraction of WLC001 and WLC002	77
Table 5-1 Revised calendar ages	100
Table A2-1 Input data and parameter values for reconstruction of the Walker Lake levels during the past 3,000 years	131
Table A3-1 Geochemical and isotopic results of bulk sediments from box-core WLB-003C	142
Table A3-2 Stable isotopic results of ostracode shells (<i>L. ceriotuberosa</i>) from box core WLB-003C	144
Table A3-3 Geochemical and isotopic results of bulk sediments from piston core WLC002	145
Table A3-4 Geochemical and isotopic results of bulk sediments from piston core WLC001	156

LIST OF FIGURES

<i>Number</i>	<i>Page</i>
Figure 1-1 Drainage of streams emanating from the Sierra Nevada, California and Nevada	4
Figure 1-2 Correlation analyses of historical (1940-2000) river flow data in drainages on both sides of the Sierra Nevada	7
Figure 1-3 Comparison of historic instrumental river flow of the West Walker River (WWR) near Coleville, California and the Yuba River (YR) near Marysville, California	8
Figure 1-4 Comparison of the PDO index and the West Walker River discharge near Coleville, California	9
Figure 1-5 Comparison of 40-year moving averages of tree-ring based paleoclimatic records of the western U.S.	11
Figure 1-6 Comparison of reconstructed Mono Lake levels and a $\delta^{18}\text{O}$ record from Pyramid Lake	12
Figure 1-7 Walker Lake temperature and dissolved oxygen profiles	16
Figure 2-1 Walker Lake drainage basin, Nevada and California showing location of the Walker River and Walker Lake	21
Figure 2-2 Historic instrumental precipitation records of Walker Lake and its adjacent areas gleaned from National Climate Data Center (NCDC)	21
Figure 2-3 Long-term monthly precipitations near Walker Lake and its adjacent areas	22
Figure 2-4 Long-term mean monthly river discharge of the Walker River at gauging stations near Wabuska, Coleville, and Wellington	22
Figure 2-5 A histogram shows variations in the percentage of river discharge at the Wabuska gauging station passing through the Schurz gauging station	23
Figure 2-6 Linear correlation of river discharge of the Walker River near the Wabuska and Schurz	24
Figure 2-7 Positive linear stream correlation of river discharge between the Walker River and lake volume change of Walker Lake	24
Figure 2-8 Plots of Walker Lake hypsometric data	25

Figure 2-9 Walker Lake long-term mean annual evaporation rate estimation through least square root error	26
Figure 2-10 Variations in $\delta^{18}\text{O}$ of stream water near the Wabuska gauging station	27
Figure 2-11 Comparison of measured lake level elevation and lake water $\delta^{18}\text{O}$ for the period of 1975-1995	28
Figure 2-12 Hydrologic balance simulation using fixed rates of on-lake precipitation and evaporation	31
Figure 2-13 Lake water $\delta^{18}\text{O}$ simulations through using a variety of f_{ad}	33
Figure 2-14 Comparison of model simulation results through HIBAL and Paleolake	34
Figure 2-15 Results of HIBAL model experiments (I)	35
Figure 2-16 Results of HIBAL model experiments (II)	37
Figure 3-1 Instrumental records of the total dissolved solid (TDS) and total alkalinity (TA) of Walker Lake	41
Figure 3-2 Bathymetry and sediment core sites in Walker Lake	42
Figure 3-3 Results of measurements of the total inorganic carbon (TIC) and total organic carbon (TOC) of cored sediments from WLB-003C	44
Figure 3-4 Results of measurements of TIC $\delta^{13}\text{C}$ and TIC $\delta^{18}\text{O}$ of cored sediments from WLB-003C	46
Figure 3-5 Positive correlation between TIC $\delta^{13}\text{C}$ and TIC $\delta^{18}\text{O}$ of cored sediments (WLB-003C)	46
Figure 3-6 Plot of Walker Lake isotopic data: $\delta^{13}\text{C}$ vs. $\delta^{18}\text{O}$	47
Figure 3-7 Results of measurements of $\delta^{13}\text{C}$ and $\delta^{18}\text{O}$ preserved in down-core ostracode shells (<i>L. ceriotuberosa</i>) of cored sediments from WLB-003C	47
Figure 3-8 Computed $\delta^{18}\text{O}_L$ record from down-core ostracode $\delta^{18}\text{O}$	49
Figure 3-9 Comparison between the 3-point running average computed $\delta^{18}\text{O}_L$ and instrumental $\delta^{18}\text{O}_L$ records	49
Figure 3-10 Plot of age model for WLB-003C: age vs. depth	50

Figure 3-11 72-year records of TIC, TOC, TIC $\delta^{13}\text{C}$, TIC $\delta^{18}\text{O}$ from WLB-003C and their comparison with historical lake level record	52
Figure 3-12 A direct comparison between TOC of down-core sediments and river discharge of the Walker River	53
Figure 3-13 Comparison of lake water $\delta^{13}\text{C}$ and lake level elevation	54
Figure 3-14 Comparison of TIC $\delta^{18}\text{O}$ and ostracode $\delta^{18}\text{O}$ from cored sediments (WLB-003C)	58
Figure 4-1 Results of measurements of oxygen and carbon isotopes from WLC84-8	67
Figure 4-2 TIC, $\delta^{13}\text{C}$, and $\delta^{18}\text{O}$ results were performed on the total inorganic carbon fraction of sediments from core WLC002	68
Figure 4-3 Comparison of TIC $\delta^{18}\text{O}$ records derived from WLC84-8 and WLC002.....	69
Figure 4-4 Stratigraphic correlations between WLC001 and WLC002	71
Figure 4-5 TIC $\delta^{13}\text{C}$ and $\delta^{18}\text{O}$ records derived from piston core WLC001	72
Figure 4-6 $\delta^{13}\text{C}$ records from WLC001 and WLC002	72
Figure 4-7 $\delta^{18}\text{O}$ records from WLC001 and WLC002	73
Figure 4-8 Direct comparison of historic lake level record (USGS) and the raw $\delta^{18}\text{O}$ record from the uppermost section of WLC002	74
Figure 4-9 $\delta^{18}\text{O}$ records of WLB-003C and the uppermost section of WLC002	76
Figure 4-10 Plot of calibrated ^{14}C ages vs. depth for WLC002	78
Figure 4-11 3000-year records of TIC, magnetic susceptibility, TIC $\delta^{13}\text{C}$, and TIC $\delta^{18}\text{O}$ of Walker Lake	79
Figure 4-12 Late Holocene variations in lake level of Pyramid and Walker Lakes	80
Figure 4-13 High-resolution 1200-year records of TIC, magnetic susceptibility, $\delta^{13}\text{C}$, and $\delta^{18}\text{O}$ of Walker Lake	81
Figure 4-14 Comparison of $\delta^{18}\text{O}$ records from Walker Lake and Pyramid Lake	83
Figure 4-15 Comparison of sediment-based record of Walker Lake and tree-ring based records in adjacent areas	85

Figure 4-16 Comparison of magnetic susceptibility, TIC, and $\delta^{13}\text{C}$ records with the tree-ring based river flow record of the Sacramento River	86
Figure 5-1 Steady state lake elevation of Walker Lake corresponding to long-term average value of the Walker River discharge	93
Figure 5-2 Oxygen isotopic responses to oscillatory changes in the Walker River discharge with a wavelength of 5-yr	95
Figure 5-3 Oxygen isotopic responses to oscillatory changes in the Walker River discharge with a wavelength of 25-yr	96
Figure 5-4 Oxygen isotopic responses to oscillatory changes in the Walker River discharge with a wavelength of 100-yr	96
Figure 5-5 Relationship between the amplitude of oscillations in the $\delta^{18}\text{O}_L$ and the amplitude of fluctuations in the Walker River discharge	97
Figure 5-6 Relationship between the amplitude of oscillations in the $\delta^{18}\text{O}$ of lake water and the mean value of the Walker River discharge	98
Figure 5-7 Relationship between the amplitude of oscillations in the $\delta^{18}\text{O}$ of lake water and the frequency component of oscillations in the Walker River discharge	98
Figure 5-8 Relationship between the amplitude of oscillations in the $\delta^{18}\text{O}$ of lake water and the $\delta^{18}\text{O}$ value of the Walker River discharge	99
Figure 5-9 Plots of revised age model and original $\delta^{18}\text{O}$ results from Walker Lake	101
Figure 5-10 Plots of revised age model, original and simulated $\delta^{18}\text{O}$ results from Walker Lake	101
Figure 5-11. Singular spectrum analysis on time series from Walker Lake for the intervals from 800 to 1900AD.....	105
Figure 5-12. Singular spectrum analysis on time series of the tree-ring based Sacramento River flow record for the intervals from AD 869 to 1900.....	106
Figure 5-13 Comparison of the tree-ring reconstructed Sacramento River flow, Walker Lake $\delta^{18}\text{O}$, and Santa Barbara $\delta^{18}\text{O}$ records.....	107
Figure 5-14 Regression analysis of the winter mean $5^\circ \times 5^\circ$ surface temperature against the West Walker River discharge.....	108
Figure 5-15. Correlation of paleoclimate and paleo-solar proxies	110

Figure A1-1 A block diagram lists the major modules or components of the program	116
Figure A1-2 A model parameter settings panel consists of four categories, geometric, hydrologic, isotopic, and dynamic settings	118
Figure A2-1 Comparison of measured and computed $\delta^{18}\text{O}_L$ records for Walker Lake	127
Figure A2-2 Responses of lake level elevation and $\delta^{18}\text{O}_L$ to change in river discharge of the Walker River	128
Figure A2-3 Lake steady-state $\delta^{18}\text{O}_L$ affected by river $\delta^{18}\text{O}_L$ and f_{ad}	129
Figure A2-4 The TIC $\delta^{18}\text{O}$ record from Walker Lake divided into three stages with distinctive average $\delta^{18}\text{O}$ values	131
Figure A2-5 Reconstruction of the Walker Lake levels (elevations) during the last 3,000 years ..	133
Figure A2-6 Reconstructed lake level elevation of Walker Lake and stream discharge of the Walker River during the late Holocene	134
Figure A2-7 Comparing reconstructed river flow record of the Walker River with tree-ring based river flow record of the Sacramento River	135
Figure A2-8 Comparing HIBAL model-derived $\delta^{18}\text{O}$ results with measured down-core TIC $\delta^{18}\text{O}$ data from topmost section of WLC002	136
Figure A2-9 Comparing measured down-core TIC $\delta^{18}\text{O}$ record with HIBAL model-derived $\delta^{18}\text{O}$ results using reconstructed river flow of the Walker River	137
Figure A2-10 Down-core TIC $\delta^{18}\text{O}$ data and HIBAL model-derived $\delta^{18}\text{O}$ results using reconstructed river flow of the Walker River spanning 1000BC to 2000 AD	138
Figure A2-11 Modeled fluctuations in the Walker River discharge, Walker Lake elevations and $\delta^{18}\text{O}$	140

PREFACE

People of the Anasazi culture appeared in Nevada as early as 300BC and began raising crops and developed irrigation between ~AD 700 and 1100 (ENCYCLOPEDIA, 1999). The Anasazi culture expanded widely after AD 900, reached maximum extent about AD 1100, and shrank drastically around AD 1300 (SMITH, 2002). The history of the Anasazi is a mystery as we do not know why the Anasazi population shrank suddenly in ~AD 1300. One of the possible causes is attributed to the severe drought that occurred from AD 1276 to 1299 (SMITH, 2002). Paleoclimatic records (like tree-rings and dated tree stumps) suggest that the climate was relatively dry in the period from AD 900 to 1400, compared to the subsequent five centuries in this area. These results seem to implicate that the Anasazi people developed and boomed during the relatively dry intervals of the last millennium. This is contradictory to the conventional wisdom. However, the oxygen isotopic signal extracted from Walker Lake carbonate sediments forces me to tell a different story about the climate during the last millennium.

This research has been focused on reconstructing hydrologic and climatic variability using Walker Lake sedimentary deposits. On June 19, 2000, I participated in the core acquisition team that was supervised by Dr. L. Benson of the U.S. Geological Survey. Two piston cores and one box core were collected as part of a USGS project and were kindly provided to me by Dr. L. Benson. I splitted and sliced the cores and prepared samples to extract geochemical and isotopic signals preserved in down-core carbonate sediments. The carbon and oxygen isotopic analyses were performed in the Stable Isotope Laboratory at the University at Albany with the assistance of S. Howe and the coulometric analyses were conducted in Dr. D. Rodbell's laboratory at the Union College. Dr. J. McGeehin (USGS) kindly performed the radiocarbon dating analyses.

This dissertation research takes advantage of previous work by Dr. L. Benson (USGS) and his co-workers. They have generated and compiled important background data pertinent to the oxygen and carbon isotopic composition in the Walker River and Walker Lake surface water systems. These data serve as an important information source to decipher the isotopic signals extracted from down-core sediments. In chapter 2 and 3, I use this important background data to examine the distribution of oxygen and carbon isotopes and their responses to changes in hydrologic conditions and to establish a linkage between lake level and down-core carbonate $\delta^{18}\text{O}$ composition. The isotopic results from the piston cores are reported in Chapter 4. In the last chapter, i.e., Chapter 5, I attempt to detect the climatic variability or modes through spectral analyses on the oxygen isotopic signal of the Walker River during the last ~1000 years.

It is hoped that the results and methods presented in this dissertation will refine our understanding in the history of the climate and its variability over the last ~3000 years in this climatically critical region.

CHAPTER 1 GENERAL INTRODUCTION

Climate-driven hydrologic variability has direct social and economic impacts. Of primary concern to society are hydrologic extremes, such as droughts and floods. In the western U. S., droughts have severe societal impacts partially due to the dependence of the agriculture industry on limited water resources. Even short-lived droughts have exacted large economic costs. For example, the Dust Bowl drought of the 1930s impacted an expansive region of the western and mid-continental U. S. (WOODHOUSE and OVERPECK, 1998), which displaced millions of people and cost \$1 billion in federal support (DEMENOCA, 2001). More recently, the drought of the late 1980s that affected the west coast of the U.S. led to an economic loss of \$39 billion (RIEBSAME et al., 1991). As observed, a decadal to interdecadal re-occurring pattern of droughts that occurred over the last century has created considerable interest in the frequency and duration of such events. In addition, water resource planning for such vulnerable and populous regions as California usually requires detailed information on the hydrological variability imposed by the climate system. There is a clear need to develop a more thorough understanding of the climate conditions that result in western U.S. droughts and also of past drought recurrence intervals.

The El Niño Southern Oscillation (ENSO) is the most important mode of interannual climate variability (GLANTZ, 1996), affecting most of the tropics and subtropics and many regions along western and eastern margins of the Pacific Ocean. The interannual mode of ENSO is well documented in modern instrumental records. More recently it has become appreciated that the low-frequency (decadal to interdecadal time scales) behavior of ENSO may be as significant as that associated with the coupled atmosphere-ocean mode of interannual ENSO (NRC, 1998). However, the spatial and temporal variability of low-frequency ENSO behavior remains uncertain in part because the instrumental record is too short to allow assessment of the full range of interdecadal to centennial time

scale variability of ENSO and currently the paleoclimatic records that have been generated are insufficient in achieving detailed histories for different climate variables at a regional scale (JONES et al., 2001).

In an attempt to refine our understanding of climatic and hydrologic variability in the western United States, this research has focused on extracting paleoclimatic information for sediments in Walker Lake (Nevada, USA). In spite of the fact that Walker Lake is geographically situated on a correlation hinge point with respect to the interannual mode of ENSO climate today, it is not clear how the low-frequency modes (>10 years) of ENSO behave in this critical region. The paleo-record of past changes in Walker Lake basin hydrologic conditions developed as part of this research is high-resolution (near triennial) for the last millennium.

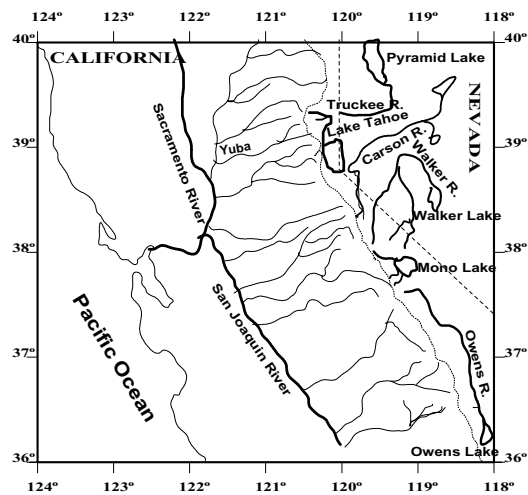


Figure 1-1. Drainage of streams emanating from the Sierra Nevada, California and Nevada (After *Benson et al.*, 2002).

1.1 Lakes in the western Great Basin

There are primarily five major lakes in the western Great Basin (Pyramid Lake, Lake Tahoe, Walker Lake, Mono Lake, and Owens Lake) (Figure 1-1). These lakes, located on the leeside of the Sierra Nevada, are fed by rivers and streams that have headwaters in the Sierra Nevada. Lake Tahoe is the

deepest while Owens Lake has become a playa due to river diversion to the Los Angeles Aqueduct (LEVY et al., 1999). All lakes except Lake Tahoe at present remain in hydrologic closure.

Human activities such as agricultural irrigations, dam constructions and artificial river diversions have altered the natural hydrologic conditions, and resulted in desiccation and /or lowered lake levels in most closed-basin lakes in the western Great Basin (BENSON et al., 2002). Reconstructions of the pristine lake levels for the Great Basin lakes suggested that most of the lakes experienced nearly synchronous variations in size during historical intervals (MILNE and BENSON, 1987).

The lake level of a closed basin lake is an effective indicator of changes in drainage basin hydrologic conditions, which are usually controlled by precipitation, runoff, and evaporation. The closed basin lakes of the western Great Basin, are primarily fed by stream flow and /or runoff that originate from the Sierra snowpack and water loss of these lakes is mainly through evaporation. Changes in the Sierra snowpack and /or evaporation rates influence the water budget of these lakes. Such changes ultimately result in lake levels rising or dropping. These changes in hydrologic balance can be registered in water and down-core biogeochemistry. Under certain circumstances, some of the proxy records extracted from sediments from these lakes are expected to contain a regional-scale paleoclimate signal (BENSON et al., 2002; BENSON et al., 1991; BRADBURY, 1987; BRADBURY et al., 1989; LI, 1995a; LI et al., 2000).

1.2 Climate of the western Great Basin

There are primarily four storm trajectories that influence the western U.S. Great Basin: polar Pacific, subtropical Pacific, continental, and Gulf storm tracks (HOUGHTON, 1969). The modern climatic regime of the western Great Basin is dominated by low-pressure storm systems driven by westerly winds moving off the Pacific Ocean. During the warmer months of the year, these westerlies lie far to the north. During the winter, the westerlies shift southward and bring Pacific storm systems onto the coast of California, where they encounter the Sierra Nevada. Forced upward, their air masses are cooled and condensed, and as a result drop massive amounts of precipitation (mostly snowfall) on the ranges of the Sierra Nevada (GRAYSON, 1993).

Since the western Great Basin lies in the rain shadow east of the Sierra Nevada, the climate of the area is arid to semiarid. Based on instrumental data documented by National Climate Data Center (NCDC), the precipitation in Walker Lake and its adjacent areas is low with annual mean precipitation ranging from 12.5 to 19.1 cm. The long-term (1930-1995) monthly mean values of precipitation exhibit a strong seasonal pattern, where this area receives more precipitation in winter and spring than in the summer. In contrast, the evaporation rate is high. From north to south, the long-term annual mean evaporation ranges from 125 cm in Pyramid Lake to 150 cm in Owens Lake (BENSON and PAILLET, 2002).

River flow and /or runoff are the primary water source of the lakes in this region. Most stream flow is fed by melting water of the snowpack on the Sierra Nevada. Fluctuations in stream discharge lag a few months to variations in precipitation in this area. As a result, stream discharge is usually higher in spring-summer than other seasons. Because snow-melt from the Sierra Nevada serves as the primary source of headwaters for rivers flowing into the Great Basin lakes, there exists a high correlation of annual stream discharge between the rivers in the region. For example, the discharge of the West Walker River (WWR) near Coleville is strongly correlated with that of the Truckee River near Reno (Figure 1-2A). Moreover, there exists a strong positive correlation of stream discharge between the WWR near Coleville and the Yuba River near Marysville even though these drainages are located on opposite sides of the Sierra's (Figure 1-2B) (BENSON et al., 2002).

The climate of the western U.S. is influenced in a complex way by ENSO. Precipitation is low in the Pacific Northwest and high in the desert Southwest during El Niño events (REDMOND and KOCH, 1991). Since the western Great Basin is geographically situated on a hinge point between the U.S. Northwest and Southwest, the correlation between precipitation and ENSO indices over the last century is very weak. However, instrumental stream discharge records of the WWR near Coleville and the Yuba River near Marysville back to 1940 (Figure 1-3) reveal two pronounced wet intervals that are coincident with the recent two very strong ENSO events of 1982-83 and 1997-98. This is probably

associated with the noted Pacific-wide climatic regime shift in 1976 (GRAHAM, 1994; MANTUA et al., 1997; TRENBERTH and HURRELL, 1994).

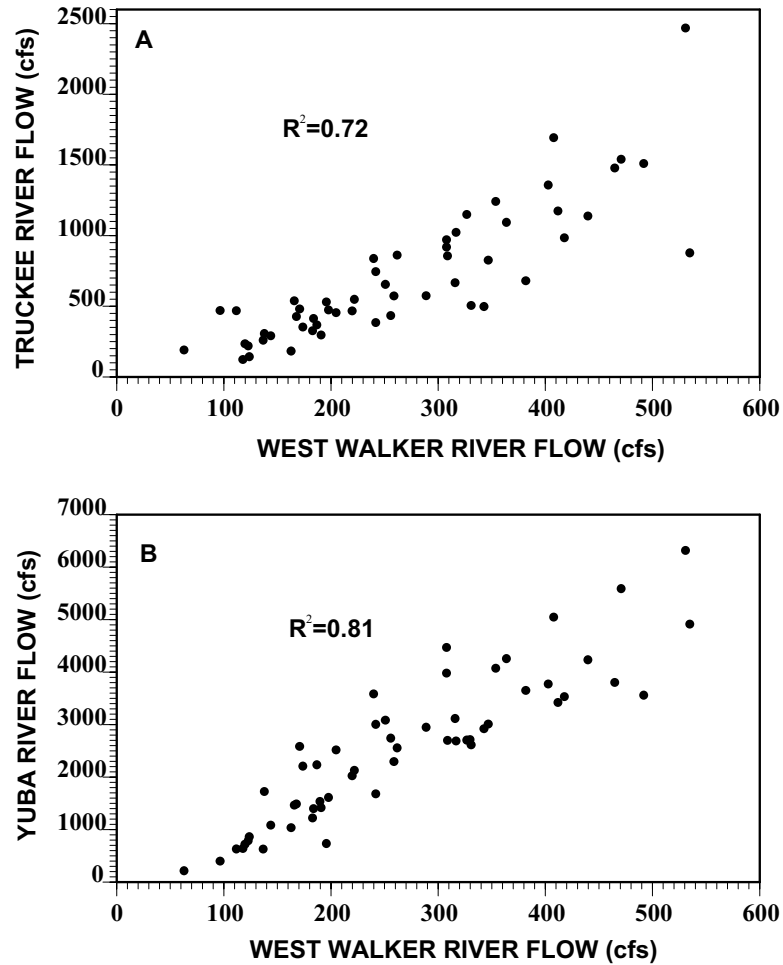


Figure 1-2. Correlation analyses of historical (1940-2000) river flow data in drainages on both sides of the Sierra Nevada. A: Stream flow correlation between the West Walker River (WWR) near Coleville, California and the Truckee River (TR) at Reno, Nevada. B: Stream flow correlation between WWR and the Yuba River (YR) near Marysville, California. Note that river flow data were taken from USGS water resources website, <http://water.usgs.gov> and calendar yearly average values were calculated. The English unit of cfs denotes cubic feet per second. Gage sites selected are considered to be only minimally effected by water diversions.

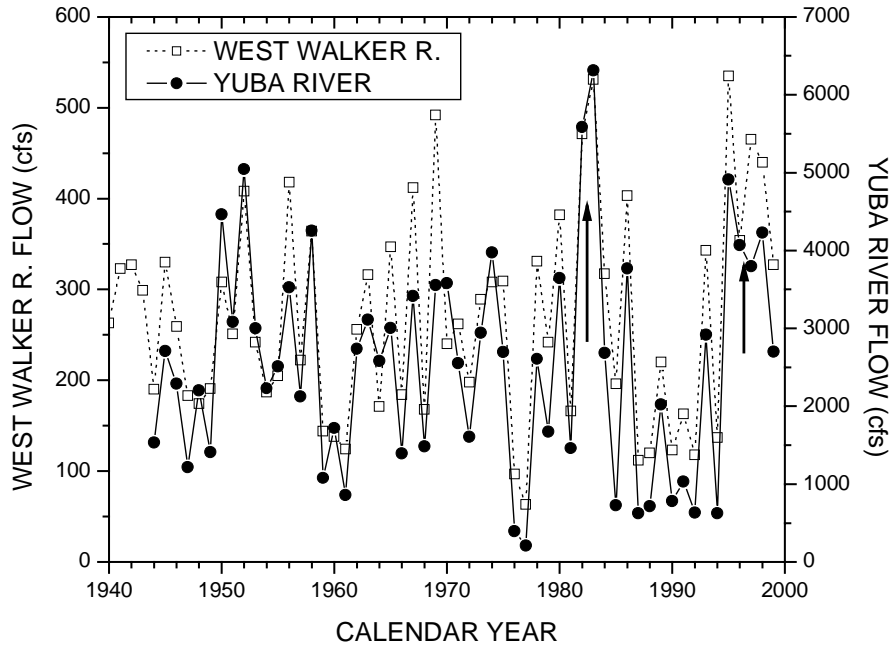


Figure 1-3. Comparison of instrumental river flow of the West Walker River (WWR) near Coleville, California and the Yuba River (YR) near Marysville, California. Solid arrows indicate the two exceptionally strong ENSO events of 1982/83 and 1997/98 (original data from USGS website, <http://water.usgs.gov>).

Decadal and interdecadal climate modes of coupled atmosphere-ocean variability have recently been recognized in instrumental records (GHIL and VAUTARD, 1991; MANTUA et al., 1997; ZHANG et al., 1997). Moreover, the 15- and 25-year periodicities detected in a 135-year-long historic instrumental temperature record (JONES et al., 1986) have been confirmed in much longer annual resolution proxy records of coral cores and varve sediments (BIONDI et al., 1997; QUINN et al., 1996). Mantua et al. (1997) defined a Pacific Decadal Oscillation (PDO) index based on North Pacific Sea Surface Temperature (SST) back to 1900. During the positive phase of PDO index, the SST of the Central North Pacific is cooler than average while SST in the Gulf of Alaska and along the Pacific coast of North America is warmer than average. In general, there is not a robust correlation on year-to-year scale between variations in WWR flow and the PDO (Figure 1-4A). However, comparison of low-frequency variations of the WWR flow and PDO index records back to 1940 reveals an intricate pattern

of associations. During intervals when the PDO index is positive, the WWR flow tends to be positively correlated with the PDO while during times when the PDO index is negative the WWR flow tends to be negatively correlated with the PDO (Figure 1-4B). This indicates that the low-frequency mode of SST variability on interdecadal time-scales over the Pacific Ocean is associated with fluctuations in winter precipitation of the Sierra Nevada and consequently affected the stream flow like the WWR in the Walker River Drainage Basin.

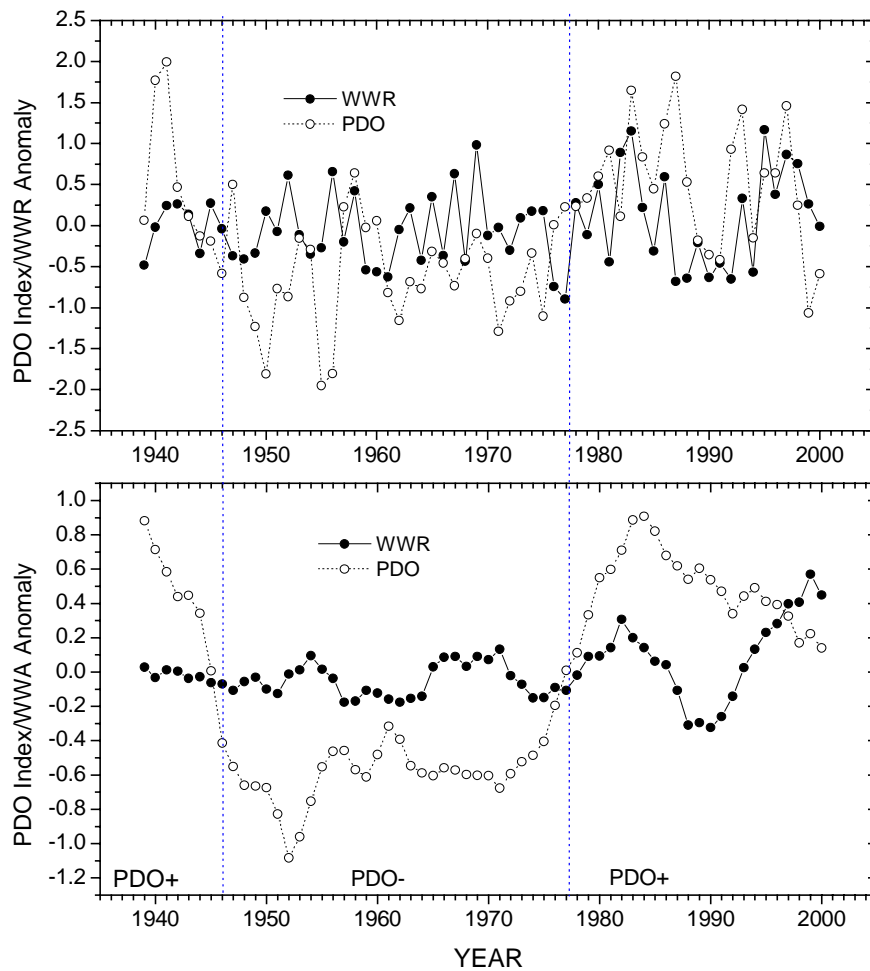


Figure 1-4. Comparison of the PDO index (open circles; Mantua et al., 1997) and the West Walker River (WWR) flow anomaly near Coleville, California (solid dots; USGS). PDO index used is the annual mean value and WWR anomaly is calculated through expression: $(Q_i - Q_e)/(2\delta)$. Upper Panel: Year to year comparison. Lower Panel: 9-point running average comparison. Two vertical dashed lines denote two climate regime shifts that occurred in 1946 and 1977, respectively.

1.3 Late Holocene paleoclimate of the western Great Basin

Our understanding of the climate system is greatly hampered by the shortness of instrumental records. The vast majority of terrestrial instrumental records span less than 50 years, which are most likely already influenced by human activities (BARNETT et al., 1999). In the western Great Basin, the longest stream gauging records extend back to 1900 while most of the continuous remote gauging readings only extend back to 1940. In addition, many stream discharge records are affected by upstream irrigation and impoundments. To understand the full range of climate variability on decadal to interdecadal time-scales, it is crucial to extend the record of climate variability beyond the era of instrumental measurements. In comparing a coral-based ENSO reconstruction from the central Pacific (URBAN et al., 2000) with a tree-ring based drought index record from the coterminous U.S. (COOK et al., 1999), Cole et al. (2002) have suggested that the dry conditions to the southwestern U. S. appear to be initiated by La Niña events and reinforced by surface feedbacks during the past few centuries. Based on tree-ring records from western North America, a reconstructed PDO record back to 1700 (D'ARRIGO et al., 2001) suggests that decadal climatic shifts appear to occur prior to the era of instrumental record. In the western Great Basin, Benson et al. (2003b) identified five major oscillations in the hydrologic balance of Mono Lake from 1700 to 1941 and associated these oscillations with a tree-ring-based reconstruction of changes in the Sierra Nevada snowpack. They proposed that major oscillations in the moisture conditions of the Sierra Nevada are linked with the sign of the PDO with extreme droughts occurring during PDO maxima.

It is now recognized that interdecadal to centennial climate variability exists in coral, tree-ring, and lake sediment records spanning the last 500 to 1000 years (BENSON et al., 2002; LINSLEY et al., 2000; YU and ITO, 1999). In the western U.S., numerous tree-ring records (COOK et al., 1999; HUGHES and FUNKHOUSER, 1996; HUGHES and GRAUMLICH, 1996; MEKO et al., 2001) have revealed that there were consistent re-occurring decadal through interdecadal periods of drought that occurred in this region over the last 1-2 millennia (Figure 1-5). In contrast, there are some intervals that are out of phase

in this region, such as the intervals centered on 1400 and 900 years B.P. The Sacramento River flow record suggested a transition from high to low flow near 1350AD (MEKO et al., 2001) while other paleoclimatic evidence indicated an abrupt switch from extreme drought to very wet conditions at more southerly latitudes in the Sierra Nevada and the neighboring White Mountains (GRAUMLICH, 1993; HUGHES and FUNKHOUSER, 1996; HUGHES and GRAUMLICH, 1996; MEKO et al., 2001). Hughes and Funkhouser (1996) suggested that the hydrologic variability of recent centuries would differ from that of earlier centuries as decadal and multi-decadal droughts occurred more frequently before 1500AD than since. However, questions still remain about the spatial and temporal late-Holocene hydrologic variability in this region.

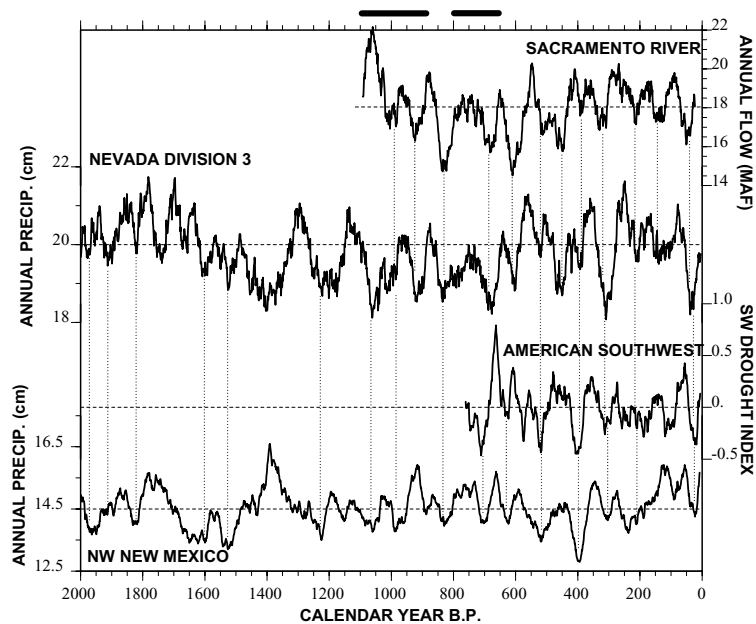


Figure 1-5. Comparison of 40-year moving averages of tree-ring based paleoclimatic records of the western U.S. (1) Sacramento River flow record (MEKO et al., 2001), MAF stands for million acre feet; (2) Nevada Division 3 precipitation record (HUGHES and GRAUMLICH, 1996); (3) American Southwest drought index (COOK et al., 1999); (4) Northwestern New Mexico precipitation record. Horizontal dashed lines denote mean values of each record while vertical dashed lines represent pervasive droughts in the regions (GRISSINO-MAYER, 1996). Two black bars denote two Medieval severe droughts that were previously proposed through dated tree stumps (STINE, 1994).

It has long been recognized that fluctuations in lake level are an indicator of climate (HALLEY, 1715) and closed basin lakes are thought to potentially preserve detailed paleoclimatic records due to

their sensitivity to changes in hydrologic balance. In Walker Lake, Benson et al. (1991) produced a series of proxy records derived from cored sediments. They suggested that wet intervals (high lake levels) occurred between 4.8 and 2.7ka, approximately at 1.25ka, and over last 300 years up until the anthropogenic lowering that began in 1922. They also concluded that droughts occurred around 2ka and 1ka BP. Based on a high-resolution $\delta^{18}\text{O}$ record derived from cored sediments in Pyramid Lake, Nevada, Benson et al. (2002) identified 18 multi-decadal to centennial droughts that occurred from 2740 to 110 years BP in this region. Most of these droughts, such as those that terminated at ~1120, ~860, ~760, ~640, ~540, and ~280 years BP (BENSON et al., 2002), were associated with droughts recorded in tree-ring based river flow data in the northern Sierra Nevada (MEKO et al., 2001) and other paleoclimatic records from dated tree stumps (STINE, 1994).

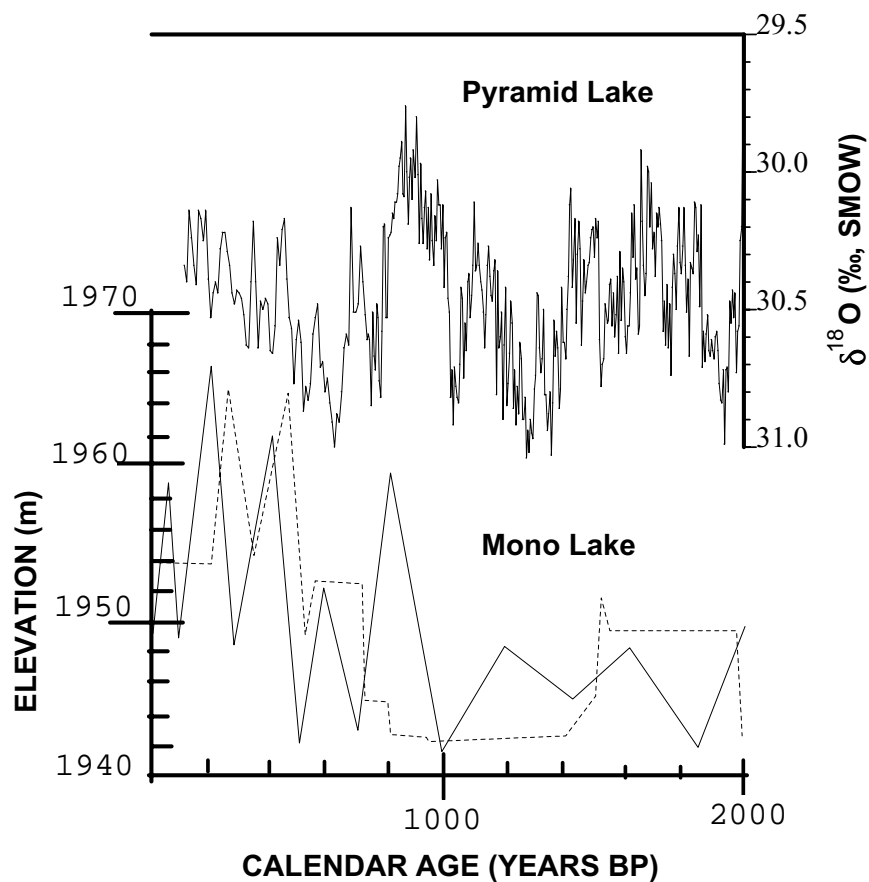


Figure 1-6. Comparison of reconstructed Mono Lake levels (solid line: Stine, 1990; dashed line: Li, 1995) and a $\delta^{18}\text{O}$ record (solid line: Benson et al., 2002) from Pyramid Lake.

However, there still exist many discrepancies among proxy records produced in the western Great Basin over the past few millennia. Using the $\delta^{18}\text{O}$ record recovered from analysis of bulk carbonate sediments in Mono Lake, Li (1995a) reconstructed the lake level history of Mono Lake over past 2000 years and suggested that generally wet and cold climates prevailed during the Little Ice Age (LIA) and dry and warm climates during the Medieval Warm Period (MWP). This interpretation is consistent with Stine's (1990) shoreline data from the same lake. However, a flood event or high lake-level interval that was centered at ~ 900 years BP in the shoreline data is absent in Li's (1995a) reconstruction for Mono lake level (Figure 1-6). Moreover, these two records are not completely consistent with published $\delta^{18}\text{O}$ records from Walker Lake (BENSON et al., 1991) and Pyramid Lake (BENSON et al., 2002). Thus, questions still remain regarding the regional extent and timing of the droughts recognized in this region.

1.4 Walker Lake and its drainage basin

Walker Lake, a terminal and saline lake, is located in western Nevada within the western U.S. Great Basin ($38^{\circ}42'\text{N}$, $118^{\circ}43'\text{W}$). It's long axis trends north and is about 27 km long and 8 km wide with maximum water depths exceeding 30 m. The lake has a large flat bottom with steep alluvial fans flanking the western shoreline and gentle but more extensive alluvial fans flanking the eastern shoreline (NEWTON and GROSSMAN, 1988). The lake is mostly fed by the Walker River and the drainage basin occupies $\sim 10,000$ km². The Walker River system consists of the East Walker River (EWR) and the West Walker River (WWR), with the WWR being the longer of the two forks. The WWR originates just below the divide that separates the Walker River Basin from Yosemite National Park to the west (Figure 1-1). The level of Walker Lake has dropped ~ 40 m since 1882 due to a substantial reduction ($\sim 60\%$) of river inflow resulting from increasing irrigation demands of upstream reaches (BENSON and LEACH, 1979). Today the only major water loss from this hydrologic system is evaporation (MILNE and BENSON, 1987). The water budget of the lake is negative because the amount of annual influent to the

lake is less than that of annual water loss through evaporation (THOMAS, 1995). This has resulted in a progressive lake level lowering over the past century. During the last two pronounced ENSO events of 1982-83 and 1997-98, however, the lake level was concurrently elevated when the Walker River drainage basin received abnormally high moisture (mostly snowfall on the Sierra Nevada).

Table 1-1. Water chemistry of the Walker River and Walker Lake. Chemical unit is in mM/L unless indicated

Chemical Species	Walker Lake				Walker River	
	1884	1966	1975-76	1999-03	1940-87	1992-98 ¹
PH	-	9.3	9.4	9.5	8.2	8.5
Calcium	0.56	0.11	0.27	0.20	0.26	0.94
Magnesium	1.60	5.10	5.59	6.24	0.10	0.38
Sodium	-	132	136	185	0.55	3.1
Potassium	-	4.10	4.19	-	0.038	-
Alk -HCO ₃	-	27.3	46.7	15.4	0.86	3.38
Chlorite	16.8	56.9	63.7	84.7	0.113	0.60
Sulfate	5.54	20.1	21.5	30.4	0.147	0.70
Silicate	0.13	0.01	0.01	-	0.12	-
Salinity ‰	2.5	8.6	10.0	12.4	-	0.33
Data Sources	Clarke (1924)	Rush (1970)	Benson et al. (1991)	NDEP (2003)	Benson et al. (1991)	NDEP (2003)

With the progressive drawdown of Walker Lake level during the last 100 years, the water chemistry and aquatic ecosystem have consequently changed. For example, water salinity has risen from 2.5 g L⁻¹ in 1884 (CLARKE, 1924) to ~10 g L⁻¹ in 1975-1976 (BENSON and SPENCER, 1983) to recent 12-13 g L⁻¹ (BEUTEL et al., 2001). *Candona caudata*, an ostracode lived in the lake prior to the drawdown, has become locally extinct in the lake (BRADBURY et al., 1989). Walker Lake has become an alkaline lake, containing considerable amounts of alkaline ions (Na⁺ + K⁺) balanced by hydrocarbonates (BENSON and SPENCER, 1983; KEMPE and KAZMIERCZAK, 1990). Water chemistry is characterized by

$\text{Na}^+ > \text{Mg}^{2+} > \text{K}^+ > \text{Ca}^{2+}$ and $\text{Cl}^- > \text{HCO}_3^- > \text{SO}_4^{2-}$ (see Table 1-1). Calcium in the lake water has become depleted due to a progressive enhancement of water alkalinity. The Mg/Ca molar ratio has become elevated from ~3 in 1884 to ~20 in 1975/76 to ~30 in 1999-2003 (NDEP, 2003). Calculation of saturation indices yields high supersaturations for calcite and extremely high values for dolomite (KEMPE and KAZMIERCZAK, 1990).

Today, the water temperature profile of Walker Lake has been extensively investigated (BEUTEL et al., 2001; NDEP, 2003) since Cooper and Koch's (1984) early efforts. Surface water temperature (water depth = 1 m) of Walker Lake ranges from 6.0 °C in winter to 22.5 °C in summer with an annual mean temperature of 14.5 °C (BENSON and SPENCER, 1983; COOPER and KOCH, 1984). Bottom water temperature ranges from 6.0 °C in winter to 9.5 °C in summer with annual average of 8.3 °C (BENSON and SPENCER, 1983; COOPER and KOCH, 1984). Typically circulation or overturn takes place after December and lasts until April or early May (KOCH et al., 1979). During this time period, the bottom waters become oxygenated and nutrients become homogeneously distributed throughout the lake. By the early summer, surface water temperatures begin to rise and the lake stratifies. The hypolimnion stagnates and becomes anoxic during summertime (BEUTEL et al., 2001), but prevailing winds sometimes produce large clockwise current gyres in the epilimnion (KOCH et al., 1979). Although Walker Lake surface level has lowered ~5 m since 1976/77, the thermal structure (i.e., temperature profile) of the lake remains unchanged (see figure 1-7) and the lake at present is still considered to be monomictic (BEUTEL et al., 2001).

The western shoreline of the lake is bounded by steep alluvial fans extending from the Wassuk Range, whereas the eastern shoreline is bounded by more gently sloping but extensive alluvial fans flanking the Gillis Range. The Walker River enters the lake on the northern margin and has formed a delta with extensive sand, silt, and clay flats (NEWTON and GROSSMAN, 1988). Spencer (1977) determined the predominant carbonate minerals present in Walker Lake cored sediments by XRD and

¹ Sampling site is at Schurz Bridge of the Lower Walker River.

suggested that monohydrocalcite appears to be the dominant carbonate mineral present in sediments deposited during the past 2000 years. High Mg/Ca molar ratios (> 2) inhibit the formation of other carbonate minerals and allow monohydrocalcite to precipitate (SPENCER, 1977).

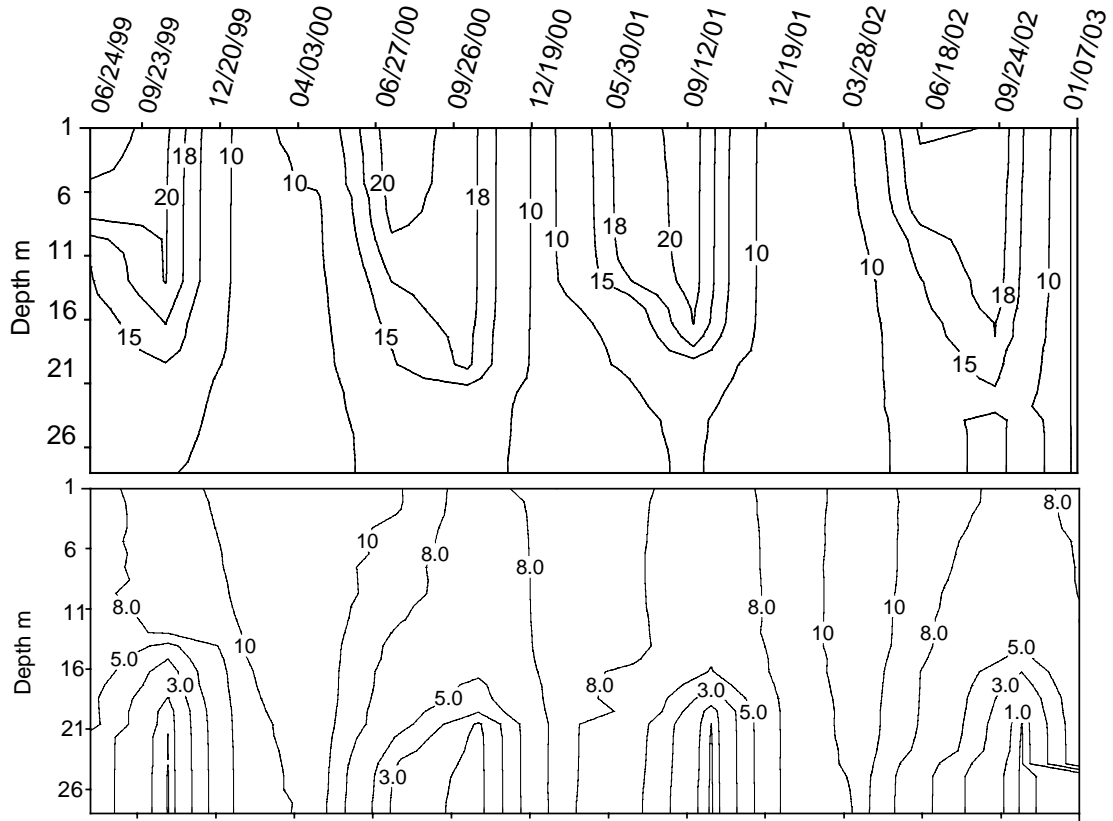


Figure 1-7. Temperature in °C (upper panel) and dissolved oxygen (DO) in mg L⁻¹ (lower panel). Original data from NDEP (2003).

1.5 Objective of this dissertation research

The central objective of this dissertation research is focused on the reconstruction of the last ~1000 years of climatic and hydrologic variability in the Walker Lake drainage basin through elemental and isotopic analyses of cored lake sediments. Because the Walker Lake basin is situated in a climatically critical region, the hydrographic history in this region during the past thousand years has the potential

to provide a wide range of climate and hydrologic variability on interdecadal to century-time scales.

While undertaking this research, I have attempted to address the following questions:

- 1). What is the climatic and hydrologic history over the past century in this region?
- 2). How does the $\delta^{18}\text{O}$ of lake water respond to the lake level changes and what is the exact connection between the lake level and the $\delta^{18}\text{O}$ of lake carbonates?
- 3). What is the history of lake level changes in the late Holocene? How many droughts can be identified in this lake? Can they be associated with the droughts that have been identified in Pyramid Lake and adjacent regions? How has the climate affected the late Holocene hydrologic pattern in this region?
- 4). What are the primary processes influencing the $\delta^{13}\text{C}$ value of down-core carbonates? What are the possible causes of the covariance of $\delta^{13}\text{C}$ and $\delta^{18}\text{O}$ observed in many aquatic systems?
- 5). What are the primary modes of climatic and hydrologic variability in this region over the last 1000 years?

To address these questions, two piston cores (WLC001 and WLC002) and one box core (WLB-003C) were collected as part of a USGS project and were kindly provided to me by Dr. L. Benson. I carefully cut the cores and prepared samples to extract geochemical and isotopic signals preserved in these cores. Isotopic analyses were performed in the Stable Isotope Laboratory at the University at Albany and coulometric analyses were conducted in Dr. D. Rodbell's laboratory in the Union College. I examine the distribution and temporal variability of oxygen and carbon isotopes in the aquatic system of Walker Lake and their responses to changes in hydrologic conditions in the interval of 1977 through 1995, in which detailed hydrologic and isotopic data are available through previous efforts made by Dr. L. Benson and his co-workers. In Chapter 2, I use a published hydrologic-isotopic model, HIBAL (BENSON and PAILLET, 2002) and a modified hydrologic-isotopic model of PaleoLake to simulate variations in the $\delta^{18}\text{O}$ of the surface water system of Walker Lake spanning 1977 to 1995. Changes in hydrologic conditions of Walker Lake over the last ~100 years are well documented and its hydrological

system is relatively simple. In Chapter 3, I present the isotopic results of the box core from this lake and compare the instrumental $\delta^{18}\text{O}$ data with down-core $\delta^{18}\text{O}$ results to test the reliability of down-core bulk inorganic carbonates as a faithful recorder of changes in lake water isotopic compositions. The results of isotopic and coulometric analyses of the piston cores are reported in Chapter 4. In the last chapter, i.e., Chapter 5, the climatic and hydrologic variability of Walker Lake spanning the last ~1200 years is investigated using spectral analyses on the $\delta^{18}\text{O}$ record of Walker Lake and the tree-ring-based Sacramento River flow record. Interdecadal and centennial modes of climate variability in winter precipitation of the Sierra Nevada have been detected.

CHAPTER 2 OXYGEN ISOTOPES IN THE WALKER RIVER AND WALKER LAKE SURFACE WATER SYSTEM

2.1 Abstract

Over the past several decades, the stable oxygen isotopic composition ($\delta^{18}\text{O}$) of ice cores and biogenic carbonates preserved in marine sediments has been used to examine climate variability in the late Quaternary. Similar records have been generated from lake sediments. In the terrestrial environment the $\delta^{18}\text{O}$ of carbonate sediments ($\delta^{18}\text{O}_c$) from closed-basin lakes has the potential to document basin-wide hydrologic and climatic variability. However, since the $\delta^{18}\text{O}$ value of lake water ($\delta^{18}\text{O}_L$) is affected by a number of hydrologic and climatic conditions, uncertainties remain in evaluating and interpreting the $\delta^{18}\text{O}_c$ signal acquired from down-core lacustrine carbonate sediments. To better understand the behavior of oxygen isotopes in the Walker River and Walker Lake surface water system, in this chapter I describe the results of applying a published hydrologic-isotopic model, HIBAL (BENSON and PAILLET, 2002) and a modified hydrologic-isotopic model (see Appendix 1 for details) to simulate variations in $\delta^{18}\text{O}_L$ of the Walker Lake surface water system spanning 1977 to 1995. Modeled results suggest that the overall trend of variations in $\delta^{18}\text{O}_L$ is affected by hydrologic conditions, i.e., hydrologic budget, while the seasonal variations in $\delta^{18}\text{O}_L$ are mainly controlled by seasonal oscillations in the hydrologic balance, evaporation, and limnological thermal structure.

2.2 Introduction

The $\delta^{18}\text{O}_c$ of lake inorganic carbonate sediments has been used in a number of lakes to reconstruct past terrestrial climatic variations (BENSON et al., 2002; BENSON et al., 1991; COVICH and STUIVER, 1974; LI et al., 2000; MCKENZIE and EBERLI, 1987; STUIVER, 1970). Fluctuations in the $\delta^{18}\text{O}_c$ record preserved in lake carbonates depend on the temperature and the $\delta^{18}\text{O}_L$ where the carbonates formed.

The later is usually determined by the hydrologic settings such as stream discharge, evaporation, on-lake precipitation, etc. In temperate lakes the $\delta^{18}\text{O}_c$ preserved in inorganic carbonate sediments usually reflects surface air temperature and lake surface temperature changes (VON GRAFENSTEIN et al., 1996; YU and EICHER, 1998), while in arid-semiarid closed-basin lakes it usually reflects changes of hydrologic conditions (BENSON et al., 1997; BENSON et al., 1996; HODELL et al., 1995; LI et al., 2000).

To narrow the uncertainty in interpreting the $\delta^{18}\text{O}_c$ signal preserved in down-core carbonate sediments, here I examine the hydrologic and isotopic system of the Walker Lake drainage basin and simulate variations in $\delta^{18}\text{O}_L$ of the Walker Lake surface water system spanning 1977 to 1995 through a published hydrologic-isotopic mode (HIBAL) and its simplified version called Paleolake.

2.3 Walker Lake Hydrology

Walker Lake is situated at the western margin of the U.S. Great Basin in western Nevada (Figure 2-1). Because it lies in the leeward side of the Sierra Nevada, the annual mean precipitation is low. Based on meteorological records between 1930 and 1997 from weather stations in this region (Figure 2-2), the annual mean precipitation rate ranges from 12.5 cm at Hawthorne to 13.9 cm at Yerington. Monthly mean precipitation exhibits a strong seasonal pattern where this area receives more precipitation in winter and spring than in summer (Figure 2-3). In contrast, stream flow of the Walker River is higher in late spring and early summer than other seasons because most streams in this drainage basin are fed by the snowmelt from the Sierra Nevada (Figure 2-4). The amount of water in the Walker River decreases from upstream to downstream reaches due to agricultural water consumption along the Walker River (BENSON and LEACH, 1979). For example, the amount of water flow in the West Walker River (WWR) near Coleville is 50% larger than that of the Walker River near Wabuska (THOMAS, 1995).

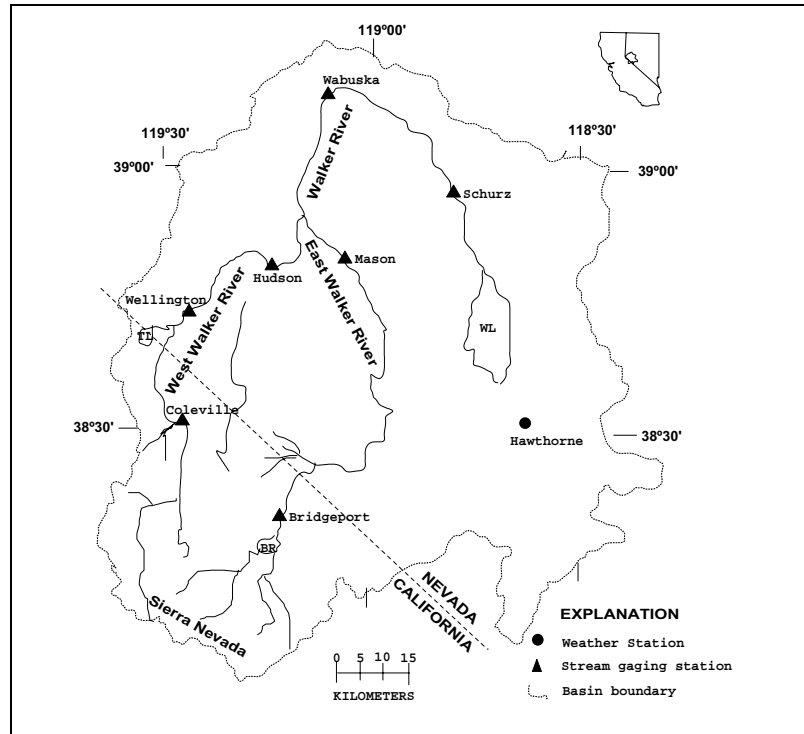


Figure 2-1. Walker Lake drainage basin, Nevada and California showing location of the Walker River and Walker Lake (BENSON and LEACH, 1979).

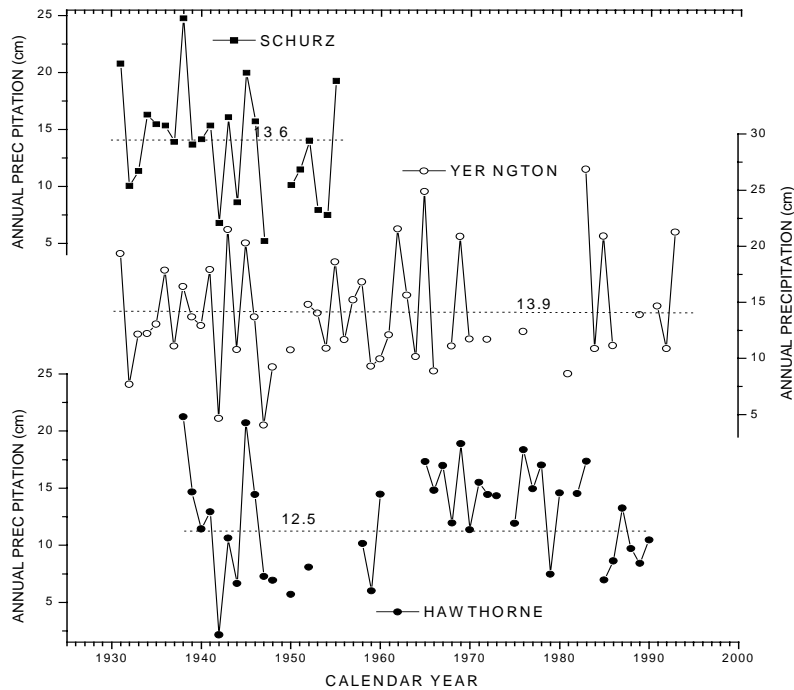


Figure 2-2. Historic instrumental precipitation records of Walker Lake and its adjacent areas (original data from National Climate Data Center). Horizontal dashed lines represent long-term averages of annual precipitation at each weather station indicated.

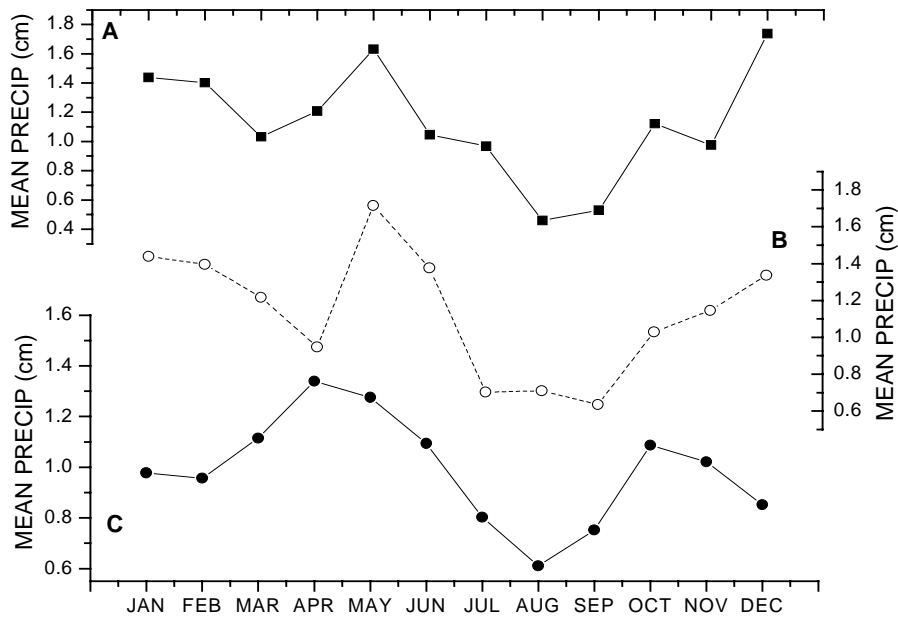


Figure 2-3. Precipitations climatologies near Walker Lake and its adjacent areas. A) Schurz Weather Station (1931-1945). B) Yellington Weather Station (1931-1993). C) Hawthorne Weather Station (1938-1990) (original data from NCDC).

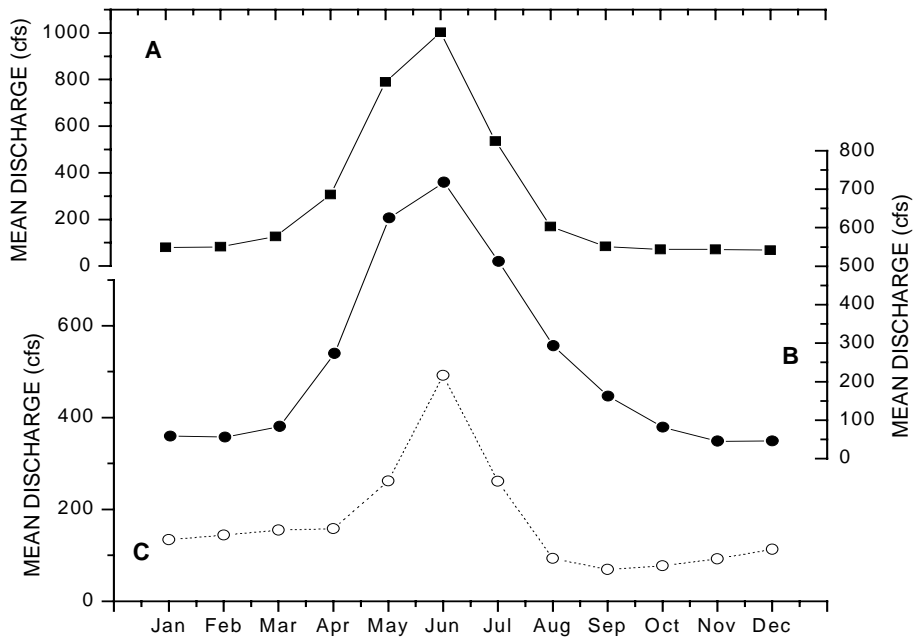


Figure 2-4 Average monthly river discharge of the Walker River at gauging stations near Coleville (A), Wellington (B), and Wabuska (C) (original data from US Geological Survey website <http://water.usgs.gov>).

The confluence of the WWR and the East Walker River (EWR) is located approximately 20 miles upstream from the Wabuska gauging station (Figure 2-1). The gauging station at Wabuska (operated by the USGS) has a continuous stream flow record back to 1944 and records an annual mean stream discharge of 0.16 km³. However, only about 88% of water passing Wabuska eventually enters Walker Lake according to annual discharge records from Schurz and Wabuska gauging stations spanning 1978 to 1995 (Figure 2-5). The amount of the stream flow near Schurz is highly correlated with the Wabuska gage record (Figure 2-6). This linear correlation will be used to correct the amount of the Walker River flow (near Wabuska) that eventually enters Walker Lake.

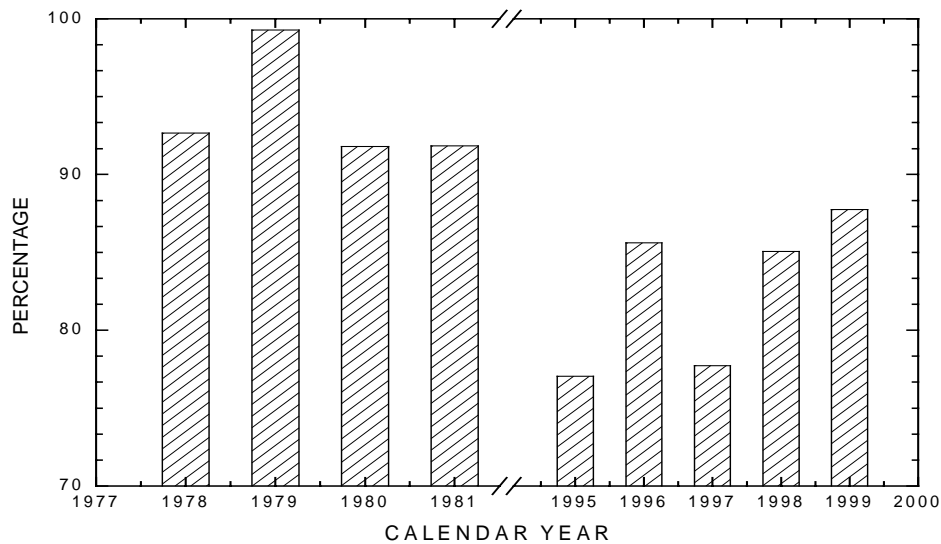


Figure 2-5 Histogram showing variations in the percentage of river discharge at the Wabuska gauging station passing through the Schurz gauging station (original data from USGS).

Since groundwater inflow and /or outflow are negligible (MILNE, 1987) and on-lake precipitation (P) is a minor component (<10 %) of the total water input to the lake, variations in lake level are primarily affected by stream flow (Q) and evaporation (E) according to the hydrologic mass balance. In fact, changes in lake volume (ΔV) vary linearly with the amount of Walker River flow (Figure 2-7). This also suggests that variations in the Walker River discharge are the primary contributor to lake volume changes over the past five decades or more.

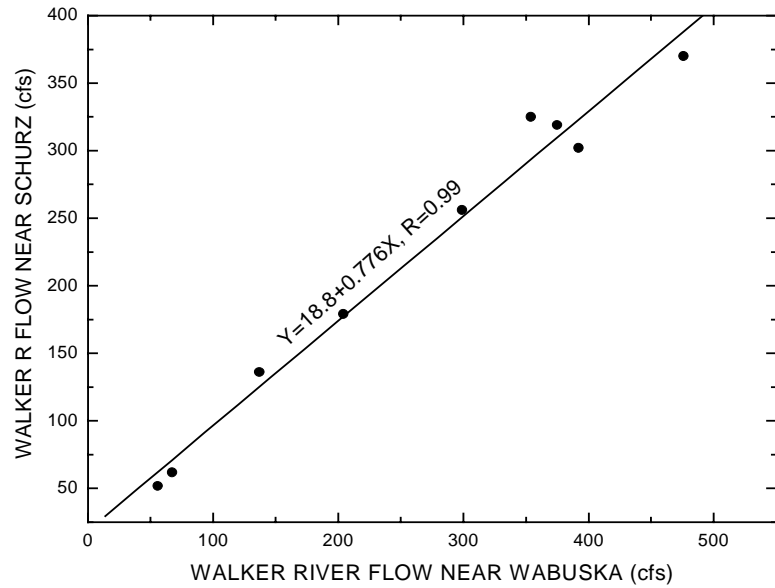


Figure 2-6 Linear correlation of river discharge of the Walker River near the Wabuska and Schurz based on the annual mean river discharge data spanning 1978 to 1999 (original data from USGS).

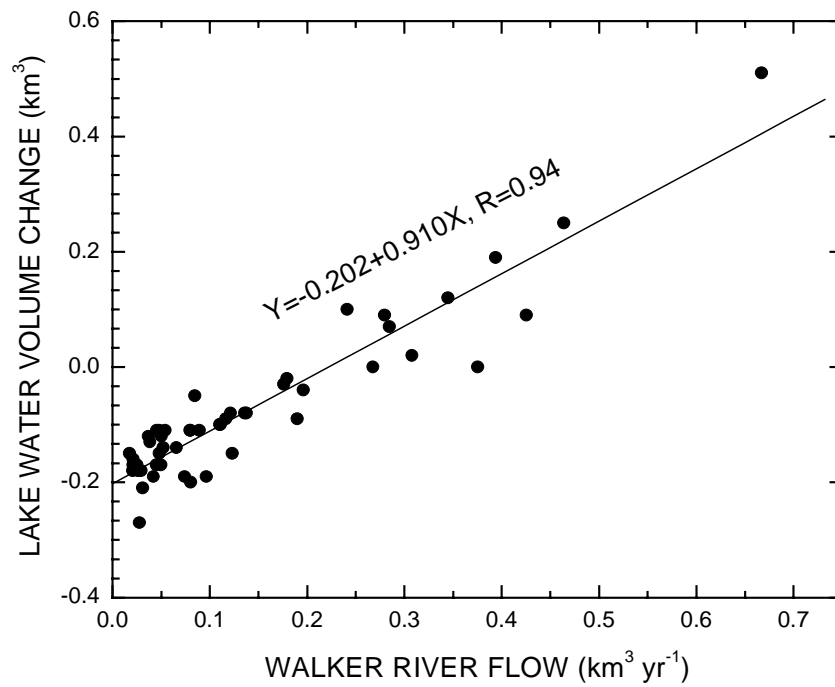


Figure 2-7 Positive linear stream correlation of river discharge between the Walker River and lake volume change of Walker Lake from 1945 to 1995 (original data from USGS).

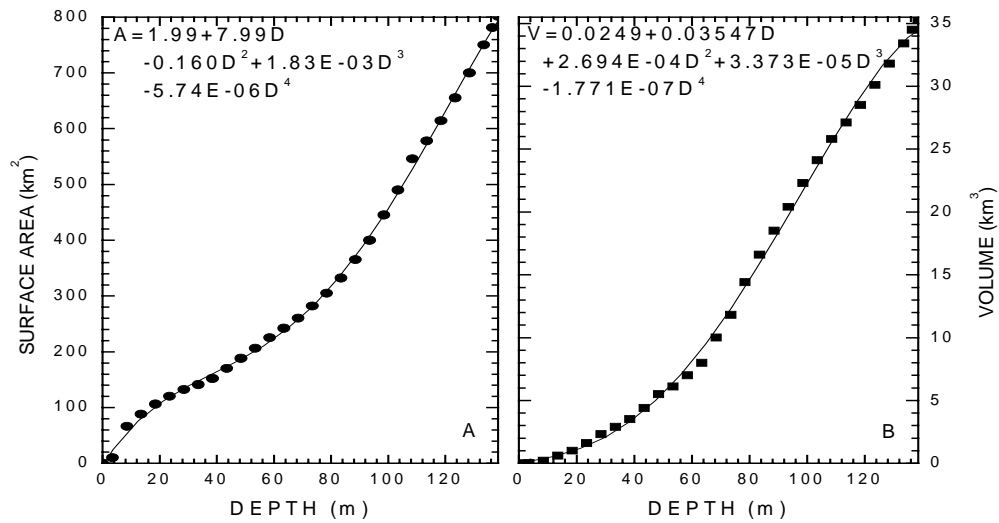


Figure 2-8 Plots of Walker Lake hypsometric data. A) Surface area vs. depth. B) Volume vs. depth (original data from *Dr. L. Benson, personal communication, 2001*).

Based on a straightforward water balance equation, $\frac{\Delta V}{\Delta t} = Q + P - E$, change in lake volume

is determined by the Walker Lake hypsometric settings (Figure 2-8A,B), and the amounts of the Walker River flow, on-lake precipitation, and evaporation. The long-term annual on-lake precipitation rate is 0.125 m. On the basis of the historical lake level record and the annual Walker River flow record (documented USGS), the long-term annual mean evaporation rate of Walker Lake can be estimated

through the least root mean square error (BENSON et al., 2002), $\xi = \sqrt{\frac{\sum_{i=1}^n (L_i^c - L_i^m)^2}{n}}$, where L_i^m is

the measured lake level and L_i^c is the lake level computed through the water mass balance equation.

The calendar-year stream flow record (1944 to 1999) of the Walker River near Wabuska is used and corrected through the stream flow correlation between the Wabuska and Schurz gauging stations (Figure 2-6). Computations indicate that long-term mean annual evaporation rate (1944-1995) is about 1.39 m (see Figure 2-9), which is close to *Milne's* (1987) estimate (1.35 m).

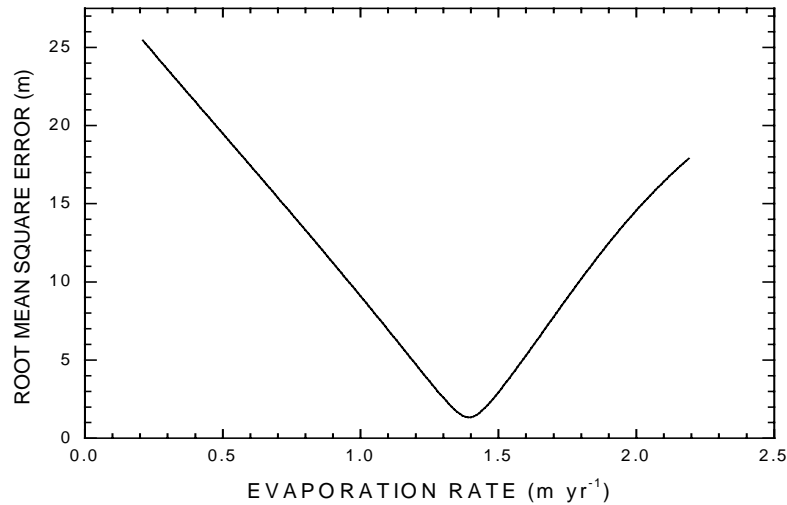


Figure 2-9 Walker Lake long-term mean annual evaporation rate estimated using corrected calendar-year inflow, fixed-rate (0.127 m yr⁻¹) of on-lake precipitation, and measured lake levels for the period 1944-1995. A long-term (1944-1995) average value of 1.39 m yr⁻¹ was obtained through the least root-mean-square error (difference) between measured and computed lake levels over the period 1944-1995 (original data from USGS).

2.4 Surface Water $\delta^{18}\text{O}$

In Walker Lake basin, there are three types of surface-water with distinct $\delta^{18}\text{O}$ ratios, $\delta^{18}\text{O}_L$ of lake water > $\delta^{18}\text{O}$ of on-lake precipitation ($\delta^{18}\text{O}_{PP}$) > $\delta^{18}\text{O}$ of stream water ($\delta^{18}\text{O}_R$) (Table 2-1). Because of the vast majority (>90%) of water in the Walker River is derived from Sierra Nevada snowmelt, the $\delta^{18}\text{O}_R$ is usually lower than any other components. The $\delta^{18}\text{O}_{PP}$ is related with the source of water vapor and ambient temperature when the water vapor condensation occurs. The $\delta^{18}\text{O}_{PP}$ at Sutcliffe, a weather station near Pyramid Lake, is -9.8 ± 4.4 (‰, VSMOW) (BENSON, 1994). In Walker Lake, direct measurement of the $\delta^{18}\text{O}_{PP}$ is not available. Since the evaporation/precipitation ratio is greater than 10, the contribution of on-lake precipitation to the $\delta^{18}\text{O}_L$ is relatively small. Thus, the $\delta^{18}\text{O}_{PP}$ value of precipitation at the Sutcliffe weather station was adopted for the isotopic simulation of Walker Lake.

Table 2-1 Surface waters and their oxygen isotopic signatures

Surface Water	Stream Water	Rainfall	Lake Water	Subtotal
Quantity ² (km ³)	0.155	0.019	2.50	2.67
%	5.8	0.71	93	100
$\delta^{18}\text{O}$ (‰, SMOW)	-13.6 \pm 0.6	-9.8 \pm 4.4	0 \pm 2	

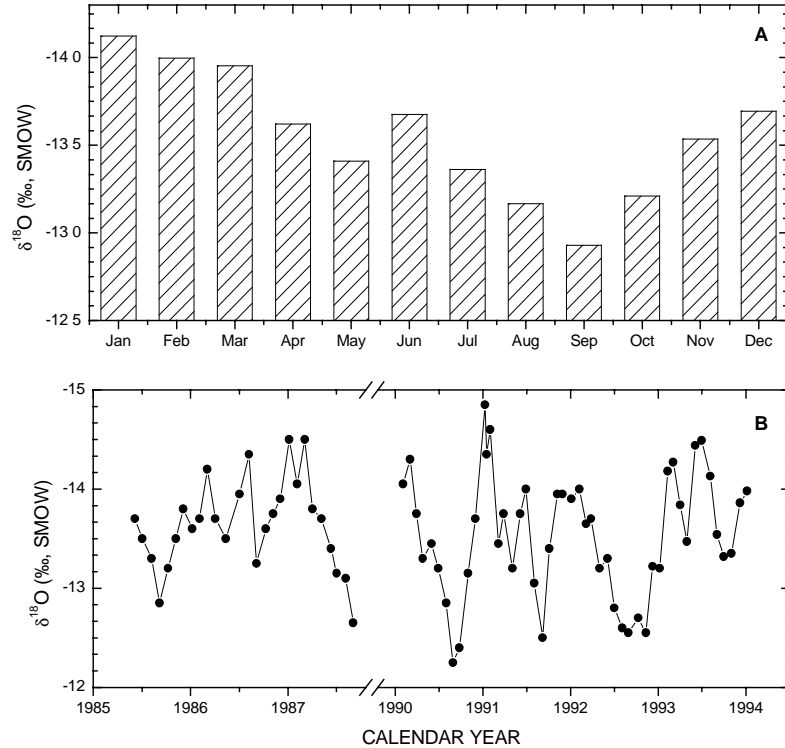


Figure 2-10 Variations in $\delta^{18}\text{O}$ of stream water near the Wabuska gauging station. A) Monthly mean $\delta^{18}\text{O}$. B) A time series of $\delta^{18}\text{O}$ record of stream water near the Wabuska gauging station (original data from Dr. L. Benson, personal communication, 2001).

The $\delta^{18}\text{O}_R$ of the Walker River flow at the Wabuska gauging station in the interval from 1985 to 1994 was measured by Dr. L. Benson of the USGS. The $\delta^{18}\text{O}_R$ tends to be higher in late summer than other seasons (Figure 2-10A), indicating that irrigation return-flow may alter the isotopic signature of the Walker River. The average $\delta^{18}\text{O}_R$ is -13.6 (‰, SMOW) with standard deviation of ± 0.6 (‰,

SMOW). Variations in the $\delta^{18}\text{O}_R$ observed are relatively small as the coefficient of variance (CV) is 4.4% (Figure 2-10B). Direct measurements of the $\delta^{18}\text{O}_L$ of Walker Lake back to 1977 have been previously published. Newton and Grossman (1988) reported an average $\delta^{18}\text{O}_L$ of Walker Lake of 2.8 ‰ (SMOW) based on the analysis of 13 samples collected from the lake in September 1977. Benson et al. (1996; 1991) reported 78 measurements of $\delta^{18}\text{O}_L$ that spanned 1981 to 1994. The results from 1977 to 1994 are shown in Figure 2-11. There was a negative correlation between the $\delta^{18}\text{O}_L$ and the lake surface elevation ($r^2= 0.94$, $n=56$) in the dry intervals from 1985 to 1994 when only a small amount of the Walker River flow entered the lake and the $\delta^{18}\text{O}_L$ was primarily affected by evaporation.

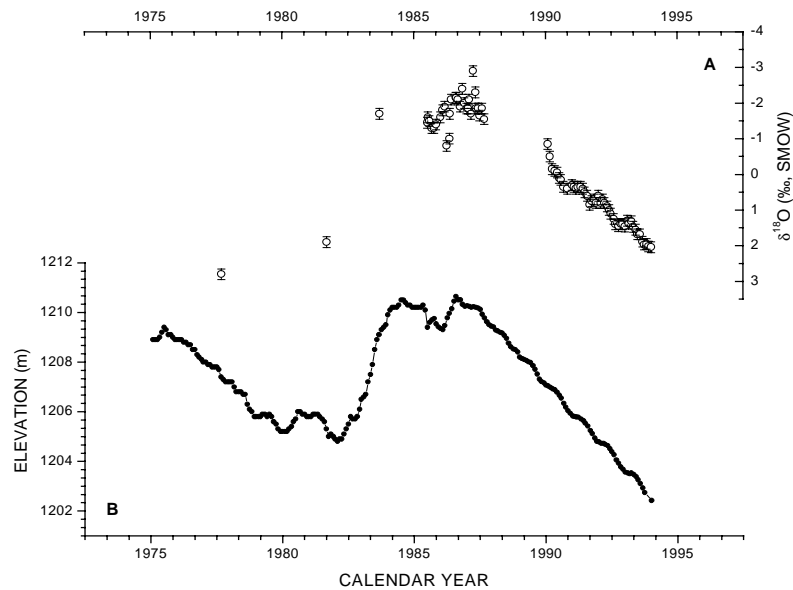


Figure 2-11 Comparison of measured lake level elevation and lake water $\delta^{18}\text{O}$ for the period of 1975-1995. The lake level elevation record was observed by USGS and the $\delta^{18}\text{O}$ data were taken from (BENSON et al., 1996; NEWTON and GROSSMAN, 1988; PENG and BROECKER, 1980).

However, change in $\delta^{18}\text{O}_L$ is not a simple linear function of hydrologic conditions (BENSON and WHITE, 1994). Other factors, such as limnological thermal structural and hypsometric properties of the lake may also play an important role in variations in the $\delta^{18}\text{O}_L$ (BENSON et al., 2002; BENSON and

² Stream flow is estimated based on long-term annual flow (174 cfs), while rainfall and lake water are estimated based on a lake surface area of 159 km².

PAILLET, 2002). Modern observations of the lake indicate that the lake exhibits strong seasonal stratification in summer and overturn in winter (BRADBURY et al., 1989; COOPER and KOCH, 1984). When Walker Lake becomes stratified, the surface waters become isolated from the deep water. Consequently, the $\delta^{18}\text{O}_L$ of surface water is much more variable than that of deep water. In addition, when the lake is shallow, the $\delta^{18}\text{O}_L$ becomes much more sensitive to changes in climatic and hydrologic conditions.

2.5 Oxygen Isotopic Modeling

As stated above, Walker Lake volume is affected by three major components, on-lake precipitation (P), stream flow (Q), and evaporation (E). The $\delta^{18}\text{O}_L$ (δ_L) is also affected by three major components with distinctive $\delta^{18}\text{O}$ values: on-lake precipitation (δ_P), stream flow (δ_Q), and evaporation (δ_E). Change in

the $\delta^{18}\text{O}_L$ (δ_L) is regulated by $\frac{\partial(V\delta_L)}{\partial t} = Q\delta_Q + P\delta_P + E\delta_E$ (GONFIANTINI, 1965; GONFIANTINI,

1986). The $\delta^{18}\text{O}$ value of water vapor leaving the lake is dependent on the $\delta^{18}\text{O}_L$ of lake surface water, the $\delta^{18}\text{O}$ and fraction of free water vapor overlying lake surface, and the relative humidity, and the water temperature, etc. The $\delta^{18}\text{O}$ of water vapor leaving lake surface may be estimated through following expression (BENSON and WHITE, 1994),

$$\delta_E = \frac{\alpha_{kin}(1 + \delta_L) - RHf_{ad}\alpha_{eq}\alpha_{kin}(1 + \delta_{ad})}{\alpha_{eq}(1 - RH) + RH\alpha_{eq}\alpha_{kin}(1 - f_{ad})} - 1 \dots\dots\dots(2.1)$$

where RH is the relative humidity of the boundary layer over the lake surface, δ_{ad} is the $\delta^{18}\text{O}$ of advected water vapor, α_{eq} and α_{kin} are the equilibrium and kinetic isotopic fractionation factors, and f_{ad} is the fraction of advected water vapor in the boundary layer over the lake surface. α_{eq} depends on lake surface water temperature and can be defined through Majoube's (1971) expression,

$$\alpha_{eq} = \exp(1137T^{-2} - 0.4156T^{-1} - 2.0667 \times 10^{-3}) \dots\dots\dots(2.2)$$

The surface water temperature (water depth = 1 m) ranges from 6.0 °C in winter to 22.5 °C in summer with an annual mean temperature of 14.5 °C (BENSON and SPENCER, 1983; COOPER and KOCH, 1984). Lunar monthly temperatures of Pyramid Lake (Table 2-2) are scaled to compute the concurrent lunar monthly α_{eq} for Walker Lake. The α_{kin} value of 0.994 is determined in previous studies (BENSON and PAILLET, 2002; MERLIVAT and JOUZEL, 1979). δ_{ad} is the $\delta^{18}\text{O}$ of advected water vapor from outside of the lake and the value of -21 ‰ (BENSON and WHITE, 1994) is applied. Lunar monthly relative humidity values, stream flow fraction, precipitation fraction, and evaporation fraction measured in Pyramid Lake are adapted (Table 2-2).

Table 2-2 Lunar monthly limnologic and climatic data and normalized lunar monthly values of river flow, on-lake precipitation, and evaporation that are taken from Pyramid Lake (BENSON and PAILLET, 2002).

Lunar Month	Mix Depth ³ (m)	Temp ⁴ (°C)	Humidity (%)	River Flow Fraction	Evap. Fraction	Precipitation Fraction
1	1000	6.66	0.73	0.0543	0.033	0.146
2	1000	7.08	0.68	0.0625	0.028	0.115
3	1000	7.83	0.55	0.0731	0.035	0.089
4	1000	10.05	0.47	0.1127	0.059	0.053
5	2	13.07	0.47	0.1696	0.079	0.070
6	5	16.41	0.46	0.1543	0.098	0.084
7	8	20.77	0.35	0.0882	0.129	0.030
8	12	23.15	0.37	0.0559	0.133	0.029
9	15	22.34	0.32	0.0491	0.124	0.030
10	17	20.00	0.41	0.0443	0.094	0.055
11	19	16.61	0.50	0.0381	0.069	0.051
12	21	12.62	0.64	0.0436	0.062	0.109
13	1000	9.02	0.67	0.0542	0.055	0.129

To determine the f_{ad} , I used corrected annual stream flow data at the Wabuska gauging station (refer to UGGS website, <http://water.usgs.gov>) as the primary input variable and the instrumental

³ Mix depth stands for the depth of surface mixing layer when lake becomes stratified, otherwise a number of 1000 is applied.

⁴ TEMP denotes surface water temperature.

$\delta^{18}\text{O}_L$ record spanning 1985 to 1994 (BENSON et al., 1996) as reference for the HIBAL model and determined the value of f_{ad} by fitting the modeled curve of $\delta^{18}\text{O}_L$ changes to that observed.

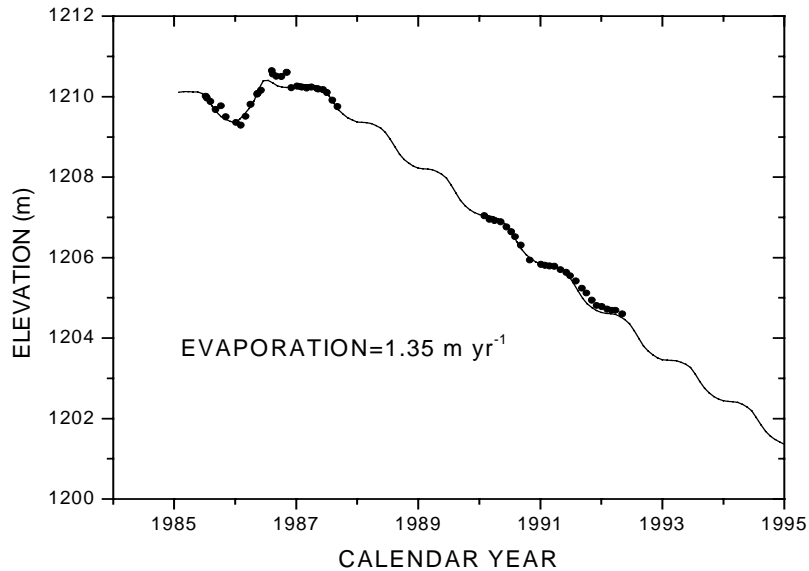


Figure 2-12 Hydrologic balance simulation using fixed rates of on-lake precipitation (0.127 m yr^{-1}) and evaporation (1.35 m yr^{-1}) (original lake elevation data from USGS).

The algorithm for the HIBAL model was kindly provided by Dr. Larry Benson of the U.S. Geological Survey. I modified the original Fortran source codes of HIBAL and converted them into Visual Basic macros for Microsoft Excel 2000. This Visual Basic program was then simplified and integrated into a comprehensive hydrologic basin model called Paleolake. Paleolake consists of three major components; hydrologic simulation, isotopic simulation, and lake level reconstruction (see Appendix 1 for details). The isotopic simulation component is a simplified version of HIBAL in which relative humidity, on-lake precipitation, and evaporation are treated as constant and the thermal structure of the lake is not taken into account. Paleolake uses corrected daily stream flow readings at the Wabuska gauging station⁵ and runs on an arbitrary user-defined time step⁶ while HIBAL uses corrected

⁵ River flow is corrected by multiplication of 90%.

⁶ The model can run hourly time step, but it will not increase the accuracy of model results, as the original data is usually in daily spacing.

monthly stream flow data in the Wabuska gauging station⁷ and the lunar monthly hydrologic and climatic data in Table 2-2 and runs on a constant monthly time step. Both programs require hypsometric data of the lake to establish relationships among volume, area and surface elevation. Before isotopic simulations, an average evaporation rate first needs to be estimated. In the interval from 1985 to 1994, an evaporation rate of 1.35 m yr⁻¹ is estimated by best-fit (see Figure 2-12), which is slightly lower than that calculated for the interval from 1944 to 1999 through least root mean square error technique (Figure 2-9).

2.6 Results and Discussion

As stated above, f_{ad} is tuned by the model itself. Paleolake can run in both modes, forward and backward. Assuming an annual mean RH value of 60%, I use the daily river flow data as the primary input variable and the $\delta^{18}O_L$ record as reference for the model to determine the value of f_{ad} by fitting the modeled curve of lake water $\delta^{18}O$ changes to that observed. A f_{ad} value of 30% is determined by this method running the model in both backward and forward modes (Figure 2-13A and 2-13B). Using fixed values of RH (60%) and f_{ad} determined, a Paleolake-modeled $\delta^{18}O_L$ record is produced and compared with the instrumental $\delta^{18}O_L$ record spanning 1977 to 1994 (Figure 2-14A). This modeled $\delta^{18}O$ curve captures the main features of the instrumental $\delta^{18}O_L$ record. In contrast, HIBAL only is run in forward mode. When a f_{ad} value of 33% is applied, HIBAL-modeled results fit the observed curve of lake water $\delta^{18}O$ well (Figure 2-14B), particularly in the interval from 1990 to 1994 in which modeled results remarkably capture most of variations in $\delta^{18}O_L$.

It is not surprising that the values of f_{ad} obtained through these two approaches are slightly different as an annual average RH of 51% (see Table 2-2) is applied in HIBAL simulation. Both f_{ad} and RH are important factors in regulating the isotopic distribution of the surface water system. With

⁷ River flow is corrected through the linear equation indicated in Figure 2-6.

an increase in either f_{ad} or RH , the model results tend to shift the $\delta^{18}\text{O}_L$ curve to lower average values (Figure 2-13B, forward method). An increase in f_{ad} can be offset by a decrease in RH during isotopic simulations. In fact, either f_{ad} or RH may change year to year. The f_{ad} value of $\sim 33\%$ was estimated according to hydrologic and climatic data in Table 2-2, in which most of the dataset is scaled from those measured in Pyramid Lake.

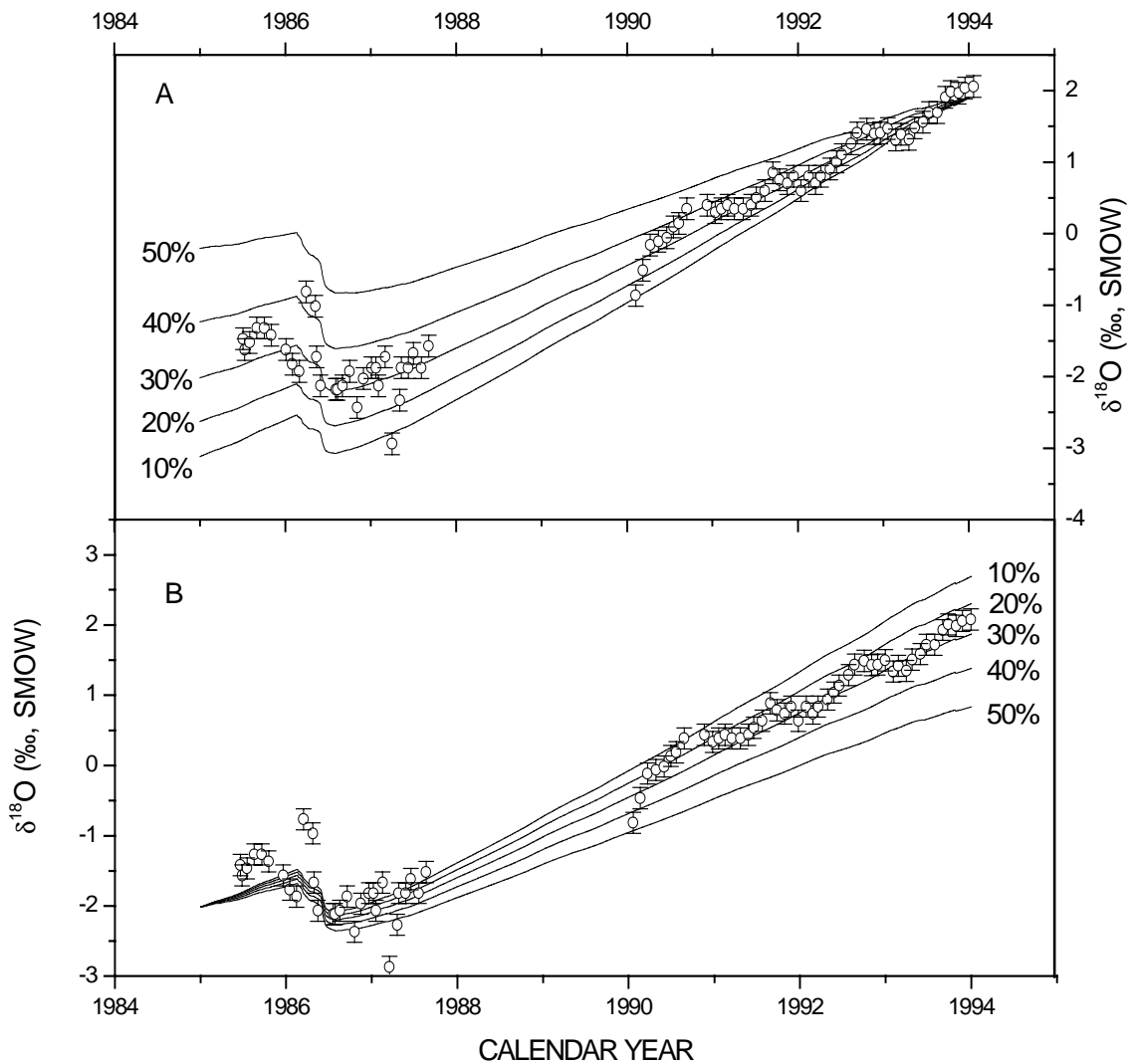


Figure 2-13 Lake water $\delta^{18}\text{O}$ simulations through Paleolake using various f_{ad} . A) Backward simulation method. B) Forward simulation method.

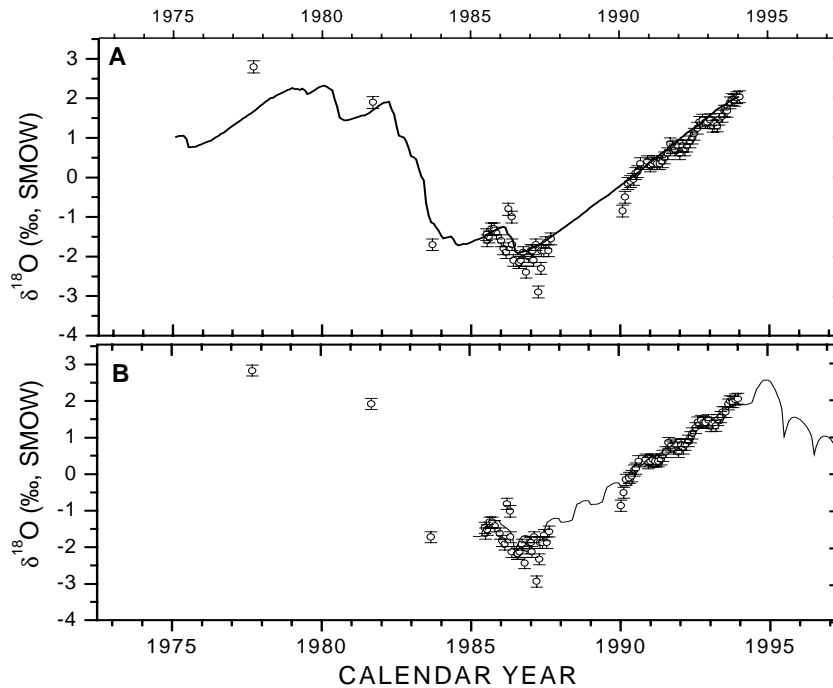


Figure 2-14 Comparison of model simulation results through Paleolake (A) and HIBAL (B). Note that the modeled results from HIBAL captured seasonal variations in lake water $\delta^{18}\text{O}$ while Paleolake are capable of reproducing the overall features of variations in lake water $\delta^{18}\text{O}$ (assuming $RH=60\%$ and $f_{ad}=0.3$). Open circles with error bar are measured data points (original data extracted from *Benson et al., 1996*).

In Table 2-2, there are six categories of parameters that may affect the isotopic distribution of the system. These parameters are used to reflect limnological, hydrologic, and the climatic annual cycle of the lake. For example, the mixing depth represents one of the limnological properties. Walker Lake has a thinner mixed layer in summer and early fall and overturns in winter and early spring (COOPER and KOCH, 1984). This limnological cycle is certainly related with hydrologic and climatic conditions of the lake. Hydrological closure, surface water temperature, and relatively high salinity are the primary factors that produce the distinct seasonal limnological pattern. Besides stream flow and on-lake precipitation, evaporation also exhibits a strong seasonal cycle that is higher in summer and early fall seasons and much lower in other seasons (BENSON and WHITE, 1994).

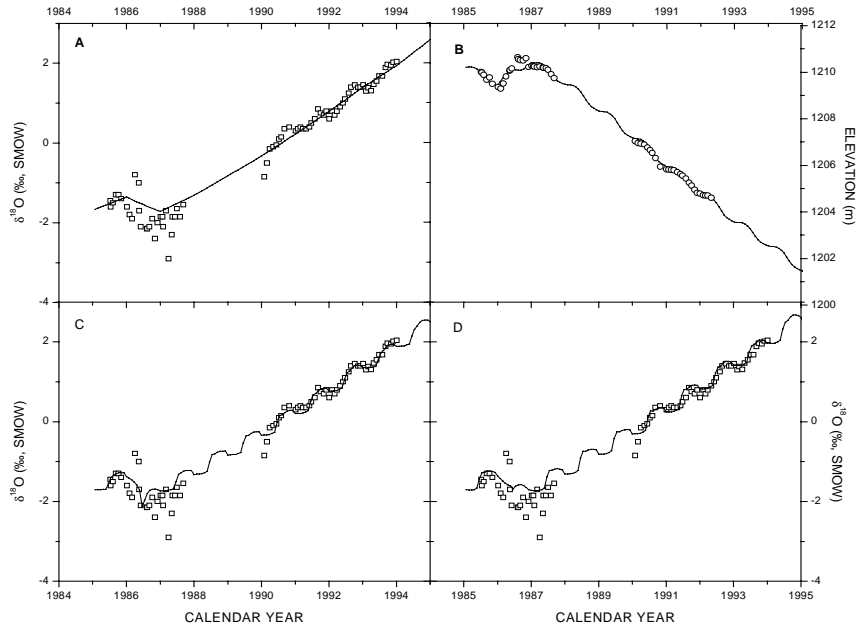


Figure 2-15 Results of HIBAL model experiments (I). Open squares are $\delta^{18}\text{O}$ or elevation values observed and solid curves are results of simulations using HIBAL. A) Assuming $f_{ad} = 0.25$, perennial fixed values of precipitation, evaporation, and water temperature, and full mixing conditions. B) Assuming perennial constant inflow. C) Assuming perennial constant rates of precipitation and $f_{ad} = 0.33$. D) Assuming perennial constant inflow and $f_{ad} = 0.30$.

HIBAL-modeled results capture most variations in $\delta^{18}\text{O}_L$ using the dataset in Table 2-2. To test the sensitivity of the response of $\delta^{18}\text{O}_L$ to these parameters, I removed the seasonal variations of the parameters in Table 2-2 and replaced them with annual averages. For example, the lunar monthly fractions of stream flow, on-lake precipitation, and evaporation are kept constant as 1/13. For water temperature and RH , their annual average values are applied, 14°C and 51%, respectively. The mixing depth is assigned to 1000 m⁸, which represents a perennial full mixing condition. Under these circumstances, HIBAL-modeled results are generated and presented in Figure 2-15A. These results are close to the Paleolake-modeled results except for the fact that HIBAL captures the fine or seasonal variations in $\delta^{18}\text{O}_L$.

In search for the primary contributors to seasonal variations in $\delta^{18}\text{O}_L$, I modified the dataset in Table 2-2 (using annual averages) and re-ran the HIBAL program. From 1985 to 1994, the climate was

relatively dry in this area. The Walker River discharge was very low with an average of 81 cubic feet per second (cfs), compared to an average of 184 cfs for the past six decades. Under such dry conditions, seasonal variations in river flow and on-lake precipitation have little impact on seasonal variations in lake volume or elevation since the results of hydrologic simulations with no seasonal variations in stream flow still capture most of seasonal variations in lake volume or elevation (Figure 2-15B). Also, seasonal variations in on-lake precipitation and inflow have little influence on seasonal variations in $\delta^{18}\text{O}_L$ (Figure 2-15C and 2-15D).

In contrast, seasonal variations in evaporation play an important role in affecting seasonal variations in lake volume and $\delta^{18}\text{O}_L$ since the results of the HIBAL simulations show no pronounced seasonal variations in either lake elevation or $\delta^{18}\text{O}_L$ (Figure 2-16A) when seasonal variations in evaporation are removed. Change in surface water temperature ultimately alters the limnological thermal structure of the lake and affects seasonal variations in $\delta^{18}\text{O}_L$ because the seasonal variations in $\delta^{18}\text{O}_L$ are substantially reduced when a perennial full mixing condition is applied (Figure 2-16B). However, seasonal changes in surface water temperature alone have little influence on seasonal variations in $\delta^{18}\text{O}_L$ since seasonal variations in $\delta^{18}\text{O}_L$ are still preserved when a perennial constant temperature of 14 °C is used (Figure 2-16C). Lastly, I use an average *RH* of 51% and re-ran the HIBAL model. The HIBAL-modeled results indicate that seasonal variations in $\delta^{18}\text{O}_L$ are also evident when *RH* is kept constant (Figure 2-16D). In Summary, among the parameters listed in Table 2-2, the results of HIBAL model experiments suggest that the overall trend of $\delta^{18}\text{O}_L$ is controlled by the Walker River discharge while the seasonal variations are primarily influenced by monthly evaporation rate and thermal structure of the lake.

⁸ This value is assigned for model calculation purpose.

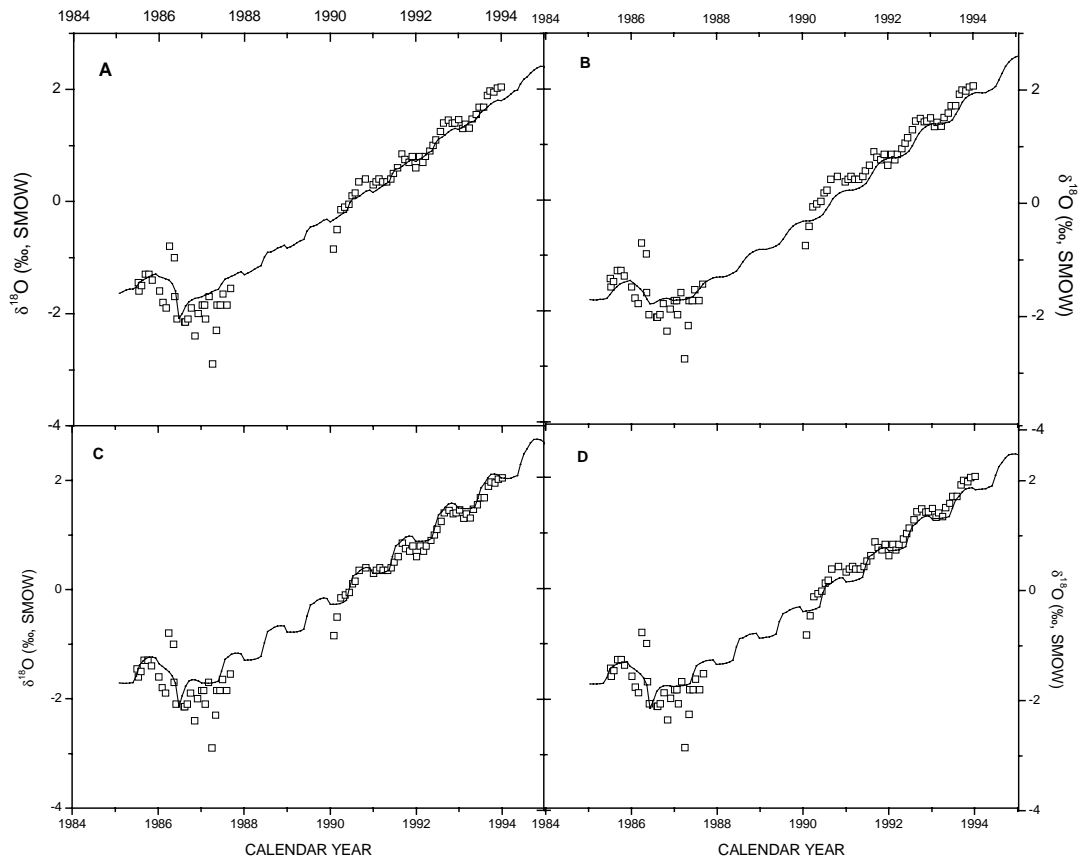


Figure 2-16 Results of HIBAL simulations (II). A) Assuming perennial constant rates of evaporation and $f_{ad} = 0.30$. B) Assuming $f_{ad} = 0.25$ and a perennial full mixing condition. C) Assuming perennial constant water temperature (14°C) and $f_{ad} = 0.35$. D) Assuming $f_{ad} = 0.25$ and $RH=51\%$.

As stated by Benson and Paillet (2002), hydrologic modeling usually has a much higher chance of success when isotopic simulation is confined to “interesting” parts of the record, in which some climatic parameters tend to be relatively well-constrained. This is also true in the Walker Lake isotopic simulations. For example, the HIBAL simulation does a better job for the interval from 1990 to 1995 than from 1985 to 1988. This is because there is little discharge to the lake during the period from 1990 to 1995. Model experiments demonstrate the ability of HIBAL to simulate changes in $\delta^{18}\text{O}_L$ of Walker Lake through adapting measured data from Pyramid Lake (except for stream flow and hypsometric data). However, such isotopic simulations are based on a well-defined hydrologic and isotopic system of the lake. The ultimate goal of hydrologic and isotopic model is to extract hydrological and climatic

information in the past on the basis of $\delta^{18}\text{O}_c$ signal preserved in down-core sediments. In fact, some of the parameters listed in Table 2-2, such as precipitation, evaporation, relative humidity etc, are directly related with climatic conditions, which are usually unknown for the past. To run the model, the modeler must assign appropriate values for these parameters. The simplest way is to adapt the value observed today. However, such modeled results are usually risky and speculative since the parameters in the past climate might differ from those of today. This is particularly true for the $\delta^{18}\text{O}_R$. The Walker River water is at present ^{18}O -enriched because some water has been used for irrigation (pre-evaporated) and returned the river with isotopically heavier signatures due to evaporation in field.

There are many uncertainties involved in the estimate of the parameters used in the models compared here. However, these parameters are known to have a range of values in this area. For example, in Walker Lake, long-term annual mean evaporation may range from 1.20 to 1.50 (m) and the $\delta^{18}\text{O}_R$ may range from -14 to -20 (‰, SMOW) over the past few thousand years. These two parameters are believed to be the primary factors that affect the $\delta^{18}\text{O}_L$ long-term evolution of the lake. Surface air temperature is also a key component of the climate in the past and it indirectly affects variations in $\delta^{18}\text{O}_L$ through several pathways. Changes in surface air temperature will alter evaporation rate, relative humidity, and thermal structure of the lake.

CHAPTER 3 COMPARISON OF HISTORICAL LAKE LEVELS AND DOWN-CORE ISOTOPIC SIGNATURES FROM WALKER LAKE

3.1 Abstract

The carbon ($\delta^{13}\text{C}$) and oxygen ($\delta^{18}\text{O}$) isotopic composition of authigenic or biogenic lacustrine carbonates have been used in numerous studies to extract information on terrestrial environmental changes in the past (COVICH and STUIVER, 1974; MCKENZIE, 1985; STUIVER, 1970; TALBOT and KELTS, 1990; TALBOT, 1990). Fluctuations in the $\delta^{18}\text{O}$ and $\delta^{13}\text{C}$ record preserved in down-core carbonate sediments usually depend on the ambient water temperature and the $\delta^{18}\text{O}$ and the dissolved inorganic carbon (DIC) $\delta^{13}\text{C}$ of host water where the carbonates form. In arid-semiarid closed-basin lakes, the source of variability in down-core $\delta^{18}\text{O}$ has usually been ascribed to changes in hydrological conditions, typically to the ratio of evaporation to precipitation. It has been assumed that when the amount of the ^{18}O -depleted surface water input exceeds that of water loss through evaporation, lake level rises and the $\delta^{18}\text{O}$ of lake water ($\delta^{18}\text{O}_L$) decreases and vice versa (BENSON, 1999). In contrast, the source of variability in down-core $\delta^{13}\text{C}$ is thought to relate primarily to the primary productivity instead of the surface water input (BENSON et al., 1991; BENSON and WHITE, 1994). Here I present a 72-year high-resolution (near-yearly temporal resolution) proxy record preserved in down-core sediments from Walker Lake, Nevada. Isotopic results indicate that there exists a strong covariance of the total inorganic fraction (TIC) $\delta^{18}\text{O}$ and TIC $\delta^{13}\text{C}$ of down-core inorganic carbonate in the lake sediments, while there is little correlation between ostracode $\delta^{18}\text{O}$ and ostracode $\delta^{13}\text{C}$. Direct comparison between the historical record of lake level and down-core $\delta^{18}\text{O}$ results indicates that the $\delta^{18}\text{O}$ of down-core carbonates in this setting has recorded the primary climatic and hydrologic events that occurred over the past seven decades.

3.2 Introduction

One source of information on changes in regional climatic and hydrologic conditions is down-core variations in lacustrine sedimentary carbonate (BENSON et al., 2002; BENSON et al., 1991; COVICH and STUIVER, 1974; DEAN, 2002; HODELL et al., 1995; STUIVER, 1970). Since most of organic and inorganic carbon in the sediments of Walker Lake are predominantly from in-lake source (MEYERS, 1990; TENZER et al., 1997), they are believed to be excellent recorders of hydrologic and geochemical conditions within the lake. The dominant carbon-bearing components are precipitated CaCO_3 and organic remains from a mixture of C3 phytoplankton, C4 bluegreen algae (MEYERS, 1990) and bivalved aquatic crustacean microfossil shells. Lake sediments also record other types of environmental information, such as nutrient status and aquatic fauna. Variations in these characteristics may be climatically and /or anthropogenically induced.

Walker Lake is presently a simple hydrological closed-basin lake situated at the western margin of the Great Basin in west-central Nevada. Walker Lake level varies in response to changes in discharge from the Walker River, the primary water source of the lake. Over the past century, the lake has experienced a massive drawdown beginning in 1922/23 due to increasing water consumptive demands and construction of water storage facilities in upstream reaches. As a result, the water chemistry and aquatic fauna of the lake have changed substantially. For example, both the concentrations of total dissolved solids (TDS) and alkalinity have at least doubled (Figure 3-1) since 1922. The ostracod *Candona caudata* lived in Walker Lake prior to its drawdown in 1920's (BRADBURY et al., 1989), and is presently absent from the lake. *Limnocythere ceriotuberosa* is the only abundant ostracode living near the lake water-sediment interface today (BRADBURY et al., 1989).

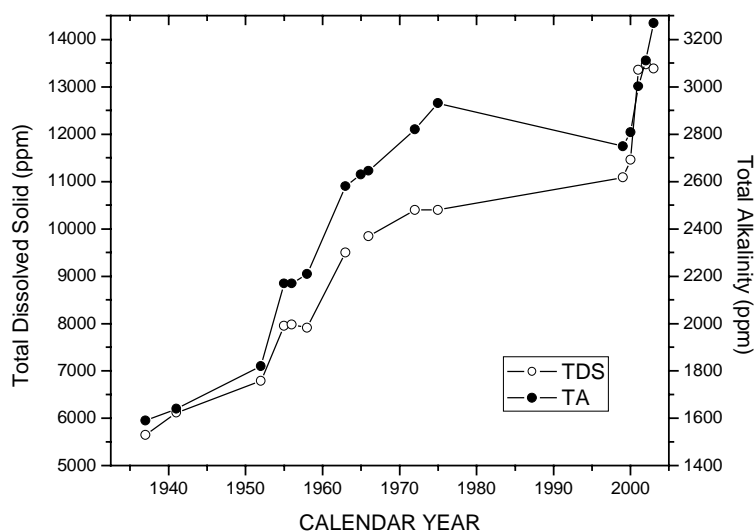


Figure 3-1. Instrumental records of the total dissolved solid (TDS) and total alkalinity (TA) of Walker Lake. Original data were taken from Benson and Spencer (1983) and NDEP (2003).

The purposes of this study are to report carbonate coulometric and isotopic results extracted from a box core collected from Walker Lake in June 2000, compare these results with the historical record of lake level, and examine how the history of variations in hydrological conditions of the lake is transferred to the sedimentary record.

3.3 Method and Materials

A 39.6 cm long boxcore (WLB-003C) was collected from one of the deepest portions of Walker Lake (Figure 3-2) in June 2000. The water depth was approximately 30 m. A distinct water-sediment interface was evident during boxcore recovery. The boxcore was carefully sealed and transferred to the University at Albany. Once it arrived at the University at Albany it was kept refrigerated storage at ~4 °C. WLB-003C was extruded vertically and sectioned at 0.5-cm intervals. Samples collected were separated into two portions, one was for microfossil analyses and the other was for coulometric analyses. Each sample from the microfossil portion was wet sieved (250 µm) and the coarse fraction transferred into an aluminum weighing dish and oven-dried at 60°C. The dried ostracode *L. ceriotuberosa* was hand-picked under a microscope with a pen brush, washed with deionized water to remove tiny

particulates stuck on valves, and oven-dried again at 60 °C. Because at the time when the samples were prepared the University at Albany stable isotope mass spectrometer needed more than 100 µg (ca. 10 to 15 shells) carbonate to get optimal results, every pair of two consecutive samples were merged prior to isotopic analyses. Samples from the other portion were washed several times in deionized water to remove soluble salts until their electrical conductivities were less than 3X those of Albany (New York) tap water. Washed samples were dried, homogenized, and soaked with 2.6% sodium hypochlorite for 6-8 hours to remove organic matter. The soaked sediments were vacuum-filtered with Whatman® glass microfibre filters (1.6 µm), rinsed with deionized water at least five times, and oven-dried at 60 °C prior to isotopic analysis (BENSON et al., 2002).

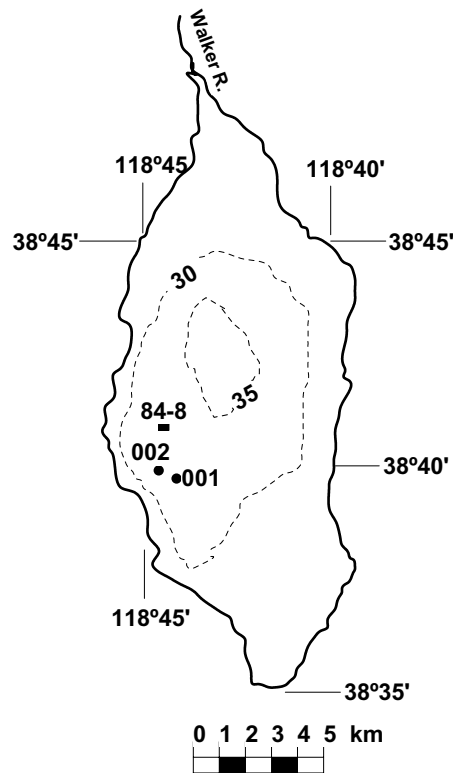


Figure 3-2 Bathymetry and sediment core sites in Walker Lake (After *Benson*, 1988). WLB-003C (not shown here) is very close to WLC002.

TIC analysis was conducted at Union College by accurately weighting 15 mg samples into a small Teflon boat. The boat was placed in the bottom of a sample flask and attached to the sample column assembly of an acidification unit. Total carbon (TC) analysis was conducted by accurately weighing 10 mg samples into an aluminum foil boat, which was then sealed. The boat was placed into a quartz ladle and introduced into the quartz combustion tube. Generated CO₂ through acidification (TIC) or combustion (TC, 950°C) was carried by CO₂ free inert gas into the analyzer of UIC coulometer. The detect limit was 0.08% C and the standard deviation for standards is 0.1%. The relative error of replicates is <2.0%. Total organic carbon (TOC) was determined by the difference of TC and TIC.

Carbon and oxygen isotopic analyses were performed on a Micromass Optima mass spectrometer with a MultiPrep automated sample preparation device. CO₂ was generated through orthophosphatic acidification. The isotopic results are reported relative to PDB, based on working standards calibrated against NBS-19. The overall precision (1- σ) of $\delta^{18}\text{O}$ and $\delta^{13}\text{C}$ are 0.04 ‰ and 0.02 ‰, respectively.

3.4 Results

Down-core carbonate chemistry is the primary recorder of changing geochemical and hydrological conditions of the lake. Over the past century, the molar Mg/Ca ratio has become progressively higher (from ~3 in 1884 to ~20 in 1975/76). As a result, calcite formation is severely inhibited and monohydrocalcite becomes the dominant carbonate precipitate (BENSON et al., 1991; SPENCER, 1977). The results of TIC and TOC are plotted vs. depth in figure 3-3. The weight % TIC fluctuates in a range of 1-4 (%C) with an average of 2.63 (%C). From a depth of 35 cm to 2 cm below sediment-water interface, the weight % TIC exhibits a progressive decreasing trend while the weight % TOC shows an opposite trend that is interrupted by three distinct TOC minima centered at depths of 15 cm, 8 cm, and 1.5 cm. The TIC and TOC are negatively correlated ($r = -0.63$, $n = 78$). Variations in weight % TIC in sediments are a function of inorganic carbonate precipitation, primary productivity, and accumulation of terrigenous clastic materials. Increases in primary productivity and clastic accumulation

will result in the dilution of sedimentary %TIC. It is plausible that the observed decreasing trend in %TIC is caused by increases in primary productivity (BENSON et al., 1991).

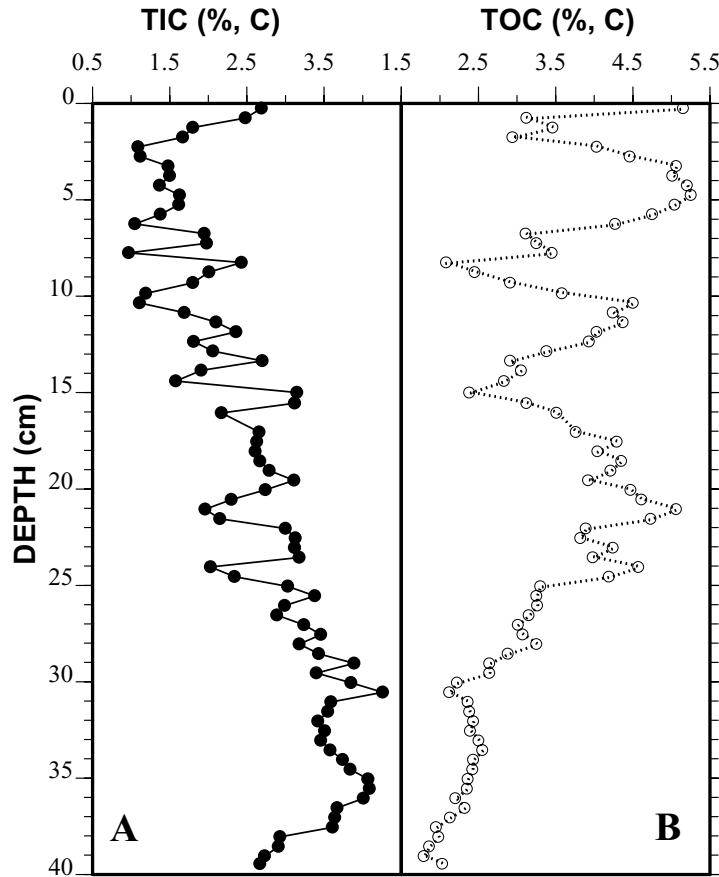


Figure 3-3. Results of measurements of the total inorganic carbon (TIC) and total organic carbon (TOC) of cored sediments from WLB-003C. A) TIC was measured by coulometric analysis. B). TOC was calculated by the difference of total carbon (TC) and TIC.

Carbon and oxygen isotopic analyses were performed on both ostracode shells and the bulk TIC fraction. The results of measurements of the TIC $\delta^{18}\text{O}$ and TIC $\delta^{13}\text{C}$ are shown in figure 3-4. The TIC $\delta^{18}\text{O}$ ranges from -4 to 4 ‰ (PDB) with an average of 0.7 ‰ (PDB) and the TIC $\delta^{13}\text{C}$ ranges from 1 to 4 ‰ (PDB) with an average of 3.2 ‰ (PDB). Both TIC $\delta^{18}\text{O}$ and TIC $\delta^{13}\text{C}$ progressively increase from a depth of 39.6 cm to 15 cm. TIC $\delta^{18}\text{O}$ and $\delta^{13}\text{C}$ variability becomes larger from a depth of 15 cm to the water-sediment interface. This is probably related to increases in isotopic sensitivity due to a

small lake volume and/or likely enhanced primary productivity (BENSON et al., 1991). The TIC $\delta^{18}\text{O}$ is positively correlated with the TIC $\delta^{13}\text{C}$ with a correlation coefficient of $r = 0.79$ (see Figure 3-5). However, the results of measurements of water samples from the lake indicate that there is no robust correlation between the water $\delta^{18}\text{O}$ and the DIC $\delta^{13}\text{C}$ (Figure 3-6). The results of measurements of the ostracode $\delta^{18}\text{O}$ and ostracode $\delta^{13}\text{C}$ are shown in figure 3-7. The values of ostracode $\delta^{18}\text{O}$ range from -0.5 to 10.5‰ (PDB) with an average of 4.8‰ (PDB) and the values of ostracode $\delta^{13}\text{C}$ range from -1.8 to 1.0‰ (PDB) with an average of -0.4‰ (PDB). The ostracode mean $\delta^{18}\text{O}$ is 4‰ heavier than the TIC mean $\delta^{18}\text{O}$ while the ostracode $\delta^{13}\text{C}$ is 3.6‰ lighter than the TIC $\delta^{13}\text{C}$. Since ostracode *L. ceriotuberosa* inhabits near water-sediment interface at a temperature of $\sim 8\text{ }^\circ\text{C}$ (BENSON and SPENCER, 1983) and most of inorganic CaCO_3 precipitates as whittings at a temperature of $\sim 22\text{ }^\circ\text{C}$ (BENSON et al., 1991), the difference of the $\delta^{18}\text{O}$ values between ostracode shells and TIC fraction can be ascribed to the temperature difference of epilimnion and bottom water, and the vital effect of ostracodes. As to $\delta^{13}\text{C}$, measurements of the DIC $\delta^{13}\text{C}$ in the lake spanning 1991 to 1994 reveal that DIC $\delta^{13}\text{C}$ fluctuates within 1.6 to 2.4‰ (PDB), with an average of 2.1‰ (PDB), suggesting that the DIC of the lake is in near isotopic equilibrium with atmospheric CO_2 (BENSON et al., 1996). The average value of ostracode $\delta^{13}\text{C}$ is lower than that of the DIC $\delta^{13}\text{C}$ while the average value of TIC $\delta^{13}\text{C}$ is higher than that of the DIC $\delta^{13}\text{C}$. The difference of the ostracode $\delta^{13}\text{C}$ and the TIC $\delta^{13}\text{C}$ can be ascribed to possible DIC $\delta^{13}\text{C}$ difference of host waters between epilimnion and hypolimnion. Also, it can be ascribed to the habitat of ostracodes, in which the DIC $\delta^{13}\text{C}$ is strongly influenced by releases of DIC with negative $\delta^{13}\text{C}$ through respiration and biodegradation of organic materials accumulated. In addition, the correlation between the ostracode $\delta^{18}\text{O}$ and the ostracode $\delta^{13}\text{C}$ is very weak ($r^2 = 0.09$, $n = 39$).

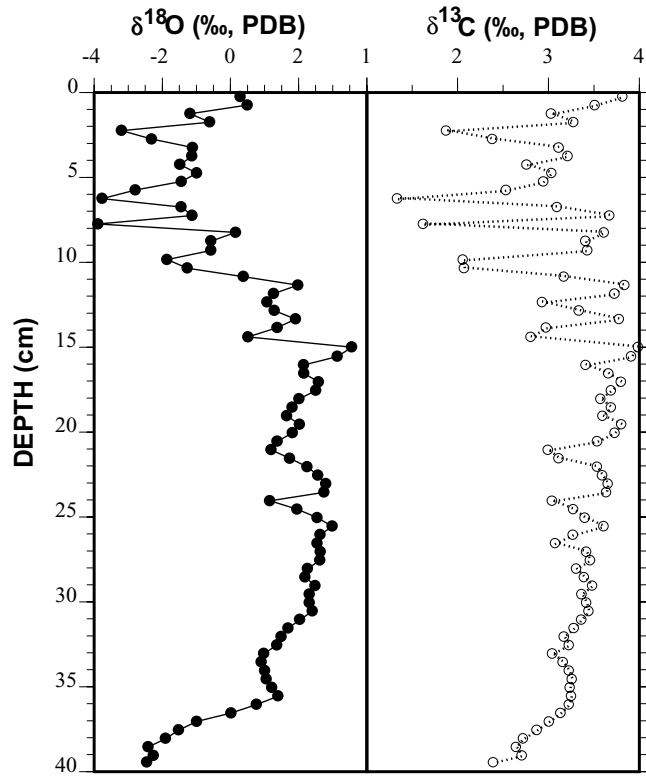


Figure 3-4. Results of measurements of TIC δ¹³C and TIC δ¹⁸O of cored sediments from WLB-003C.

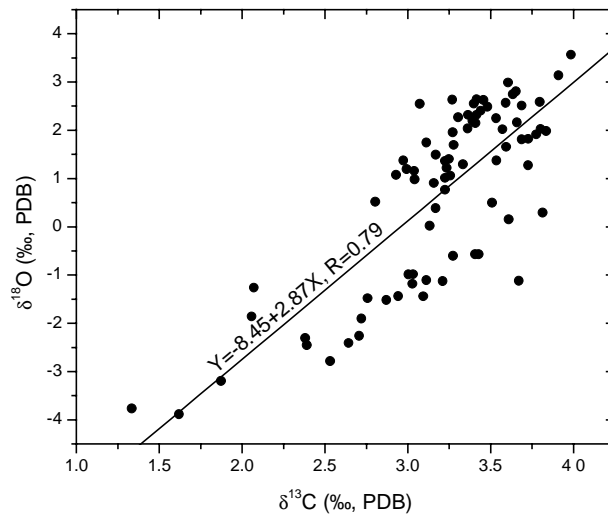


Figure 3-5. Positive correlation between TIC δ¹³C and TIC δ¹⁸O of cored sediments (WLB-003C)

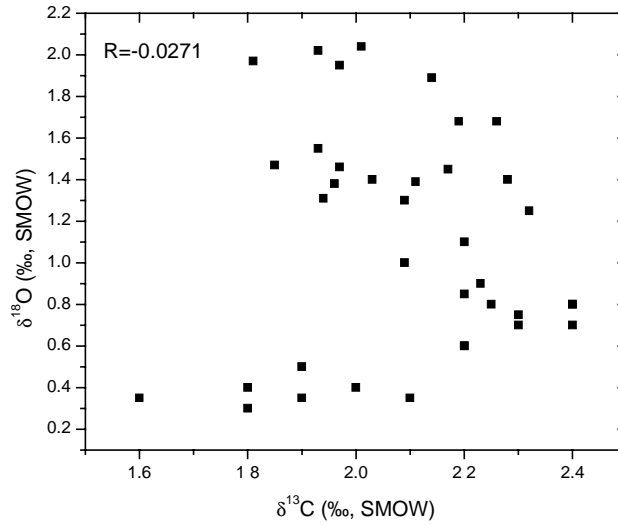


Figure 3-6. Plot of Walker Lake isotopic data: $\delta^{13}\text{C}$ vs. $\delta^{18}\text{O}$, based on the results of 37 measurements of lake water samples for the period of 1991-1994 (original data from *Benson et al.*, 1996).

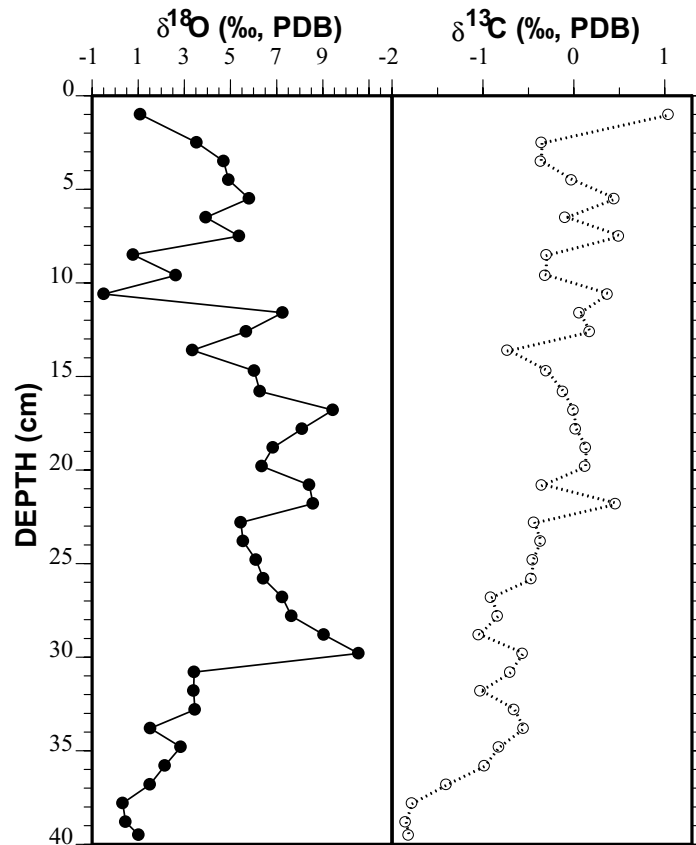


Figure 3-7. Results of measurements of $\delta^{13}\text{C}$ and $\delta^{18}\text{O}$ preserved in down-core ostracode shells (*L. ceriotuberosa*) of cored sediments from WLB-003C.

3.5 Discussion

Since Walker Lake has experienced a rapid and massive drawdown over the last century, the results of direct measurements of the $\delta^{18}\text{O}_L$ are crucial to understanding how the $\delta^{18}\text{O}_L$ varies in response to rapid changes in hydrologic conditions that are known. As stated above, the $\delta^{18}\text{O}$ signature preserved in TIC and ostracode shells usually reflects the $\delta^{18}\text{O}_L$ and ambient temperatures. On the basis of laboratory experiments, Xia et al. (1997b) developed an empirical equation for the oxygen isotopic fractionation of ostracode *C. rawsoni* valves in aquatic systems: $\delta^{18}O_L = \delta^{18}O_c + 0.179T - 3.943$, where T is the equilibrium temperature near the sediment-water interface in °C, $\delta^{18}O_L$ is the $\delta^{18}\text{O}$ value of host lake water in ‰ (SMOW), and $\delta^{18}O_o$ is the $\delta^{18}\text{O}$ value of ostracode shells in ‰ (PDB). The hypolimnion temperature varies gradually throughout the year in Walker Lake from ~6 °C in winter to ~10 °C in summer (BENSON and SPENCER, 1983). The $\delta^{18}\text{O}$ of hypolimnion water of the lake can be computed from the ostracode $\delta^{18}\text{O}$ record through this empirical equation (Figure 3-8). The error bar (± 0.35 ‰) is induced by the uncertainty in the bottom water temperature (6-10 °C). The computed values of $\delta^{18}\text{O}_L$ are subject to calibration through direct $\delta^{18}\text{O}_L$ measurements conducted during the past few decades, as the empirical equation used is derived from *C. rawsoni* instead of *L. ceriotuberosa*.

A direct comparison of the computed 3-point average $\delta^{18}\text{O}_L$ and the instrumental $\delta^{18}\text{O}_L$ results indicates that down-core ostracodes are an ideal recorder of the primary variations in the $\delta^{18}\text{O}_L$ spanning 1977 to 1995 (Figure 3-9). This comparison also suggests that the computed $\delta^{18}\text{O}_L$ values are overall ~0.5 ‰ higher than those of instrumental $\delta^{18}\text{O}_L$.

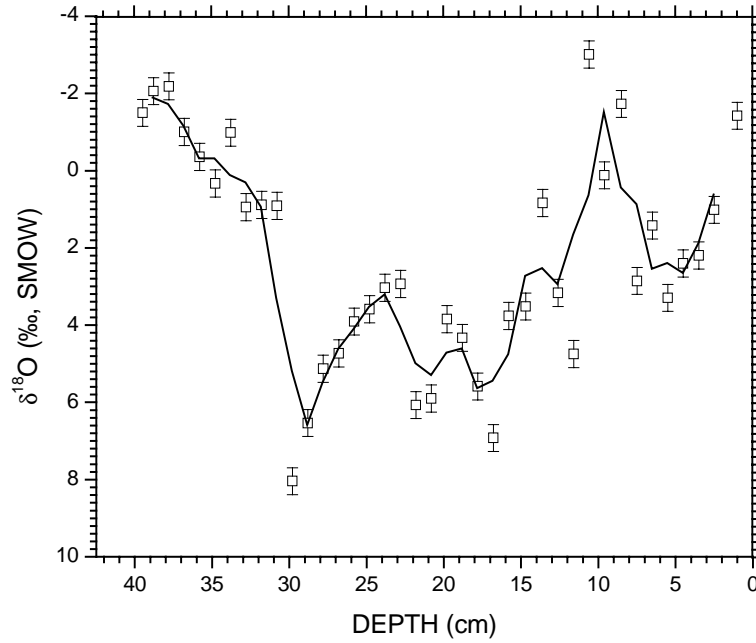


Figure 3-8. Computed $\delta^{18}\text{O}_L$ record from down-core ostracode $\delta^{18}\text{O}$ (see text for details). Errors of the computed $\delta^{18}\text{O}_L$ record (open squares with error bar) are induced by the uncertainty of water temperature ($6 \pm 2^\circ\text{C}$). The solid line represents 3-point running average of the computed $\delta^{18}\text{O}_L$ record.

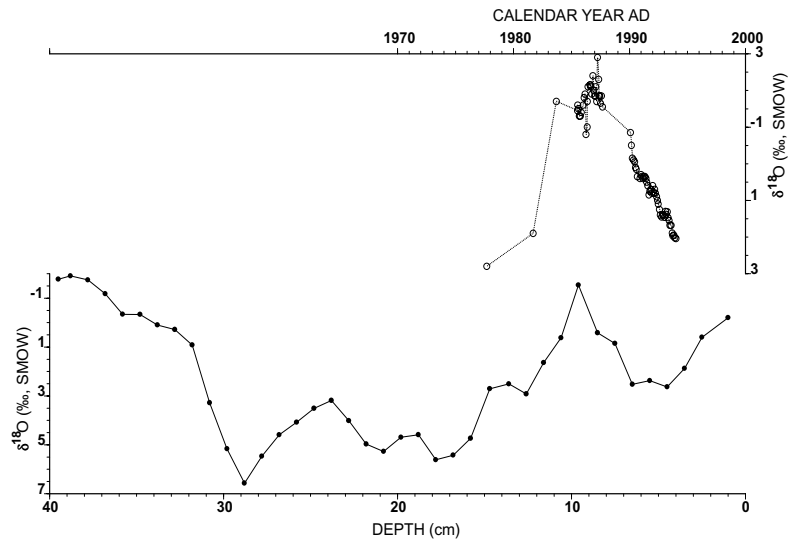


Figure 3-9. Comparison between the 3-point running average computed $\delta^{18}\text{O}_L$ and instrumental $\delta^{18}\text{O}_L$ records spanning 1985 to 1994. Original instrumental data were taken from Benson et al. (1996).

The bottom-most sediments in box core WLC-003C are equivalent to a depth of 29 cm in piston core WLC002 with a calendar age of ~1928 AD (refer to Chapter 4 in this dissertation). As the water-sediment interface was evident during box core recovery, the calendar age of the topmost sediments is assumed to be AD 2000. The comparison of proxy and instrumental $\delta^{18}\text{O}$ records supplies extra age constraints for WLC-003C. A second-order polynomial fit is made to establish an age model for box core WLC-003C (Figure 3-10). The sediment accumulation rate was apparently higher in uppermost sections than in the lower part of the core.

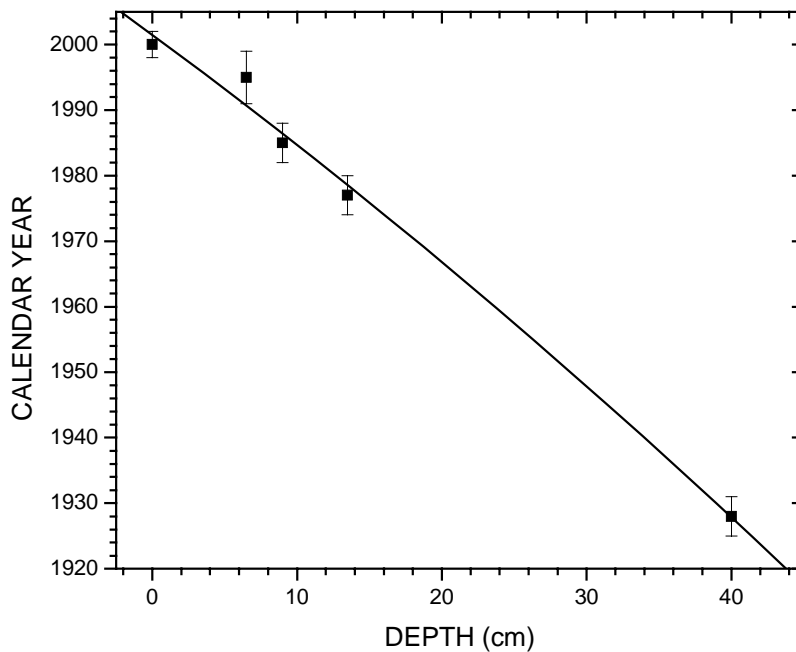


Figure 3-10. Plot of age model for WLC-003C: age vs. depth. The age of topmost sediments was assumed to be 2000AD as a sediment-water interface was preserved during core recovery. The age of bottommost sediments was assumed to be 1928AD (see Chapter 4 for details). Other age constraints were picked from figure 3-9 according to curve match. A 2nd order polynomial fit was performed to calculate the ages at various depths in the core.

The calendar age of sediments at various depths is calculated, through the second-order polynomial equation indicated in figure 3-10, to produce a 72-year proxy record of WLC-003C. This

box core spanning 1928-2000 recorded major changes in hydrological and isotopic conditions of the lake resulting from a combination of natural climatic variations and human-induced perturbations (Figure 3-11). At the beginning of the record, the %TIC, $\delta^{13}\text{C}$, and $\delta^{18}\text{O}$ records show abrupt increases in their values accompanying with the rapid lake level lowering beginning in 1922/23. This event is associated with human-induced perturbation due to increasing water demands in upstream reaches of the Walker River. The lake level is still dropping as a result of a negative hydrologic balance today (THOMAS, 1995). The record indicates relatively larger variations in TIC, TOC, $\delta^{13}\text{C}$, and $\delta^{18}\text{O}$ after 1976. This can be explained by increasing sensitivities as the lake has become smaller. During the two most recent large El Niño events of 1982/83 and 1997/98, Walker Lake level was raised by 3.6 and 1.2 m, respectively (USGS news release dated 09/03/1998). The values of TOC, $\delta^{13}\text{C}$, and $\delta^{18}\text{O}$ in general decrease with lake level rise and *vice versa*. Peak to peak correlations among records of TIC, $\delta^{13}\text{C}$, and $\delta^{18}\text{O}$ are apparently good in the interval from 1976 to 2000. The TOC record exhibits three relatively large cycles from 1965 to 2000. Sedimentary TOC is affected by a number of factors, such as biological primary productivity, organic decomposition, inorganic carbonate production, and input of terrigenous clastic materials. The TOC record is apparently associated with lake level changes. When the lake becomes smaller, nutrients like N and P tend to enrich and consequently lead to an increase in primary productivity (BENSON et al., 1996). Comparison of the Walker River flow and TOC record (see figure 3-12), however, suggests that higher % down-core TOC tend to be closely associated with increased stream discharge over the last several decades, indicating possible nutrient supply from the Walker River due to irrigation return-flow with high contents of nitrogen-bearing and phosphate fertilizer.

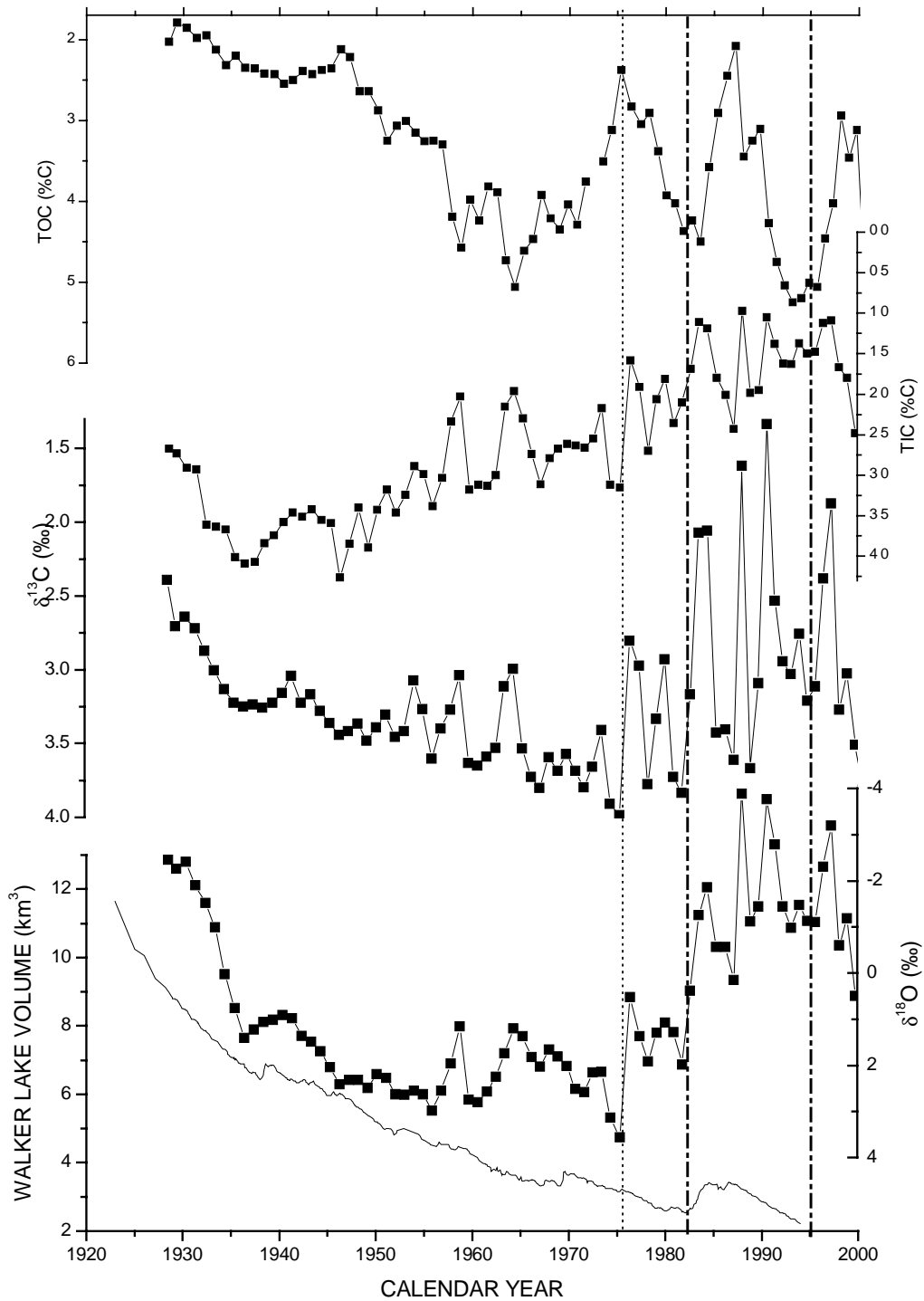


Figure 3-11. 72-year records of TIC, TOC, TIC $\delta^{13}\text{C}$, TIC $\delta^{18}\text{O}$ from WLB-003C and their comparison with historical lake level record (USGS). Vertical dotted line indicates a regime shift in 1976AD and two vertical dashed lines refer to the El Niño events of 1982/83 and 1997/98.

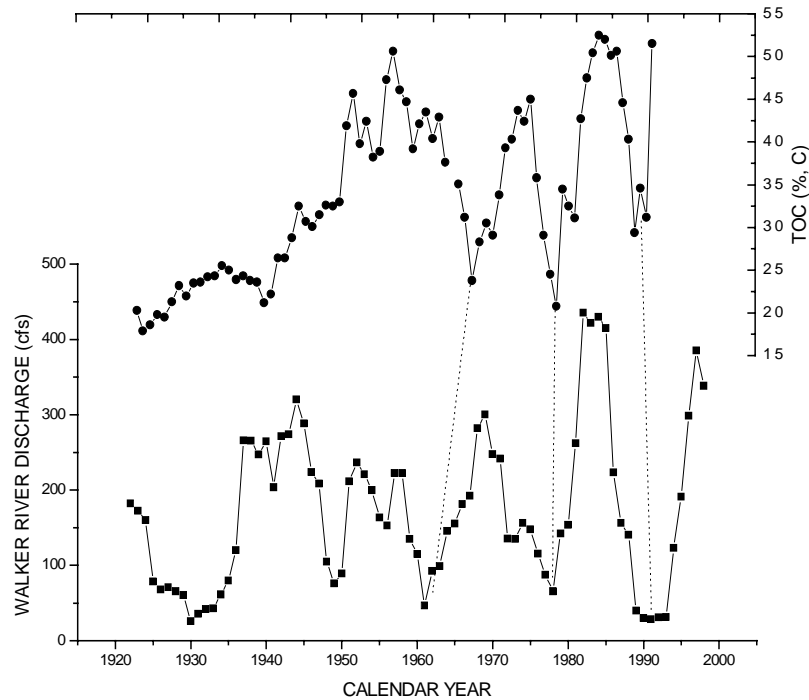


Figure 3-12. Comparison of down-core % TOC and the Walker River discharge. Dotted lines denote possible correlation between these two records. Note that the Walker River discharge data were taken from USGS and a five-point moving average was employed.

Changes in lake level or hydrological conditions usually lead to variations in TIC, TOC, $\delta^{13}\text{C}$ and $\delta^{18}\text{O}$ of the lake. TIC, TOC, and $\delta^{13}\text{C}$ are also associated with biological primary productivity and post-depositional diagenesis, which are indirectly linked with hydrological conditions, i.e., changes in hydrological conditions in general have indirect influence on these proxy indicators. In contrast, biological activities may have little effect on the $\delta^{18}\text{O}$ signal of the lake. Most variations in down-core $\delta^{18}\text{O}$ from a closed-basin lake are induced by changes in hydrologic and /or climatic conditions, such as river flow, evaporation, surface temperature, relative humidity, and wind speed etc. Although change in the $\delta^{18}\text{O}$ value of a closed-basin lake is not a simple function of the amount of change in lake volume (BENSON et al., 1991), model experiments indicate that the oxygen isotopic system is relatively simple because hydrologic models like Paleolake and HIBAL (BENSON and PAILLET, 2002) are capable of

simulating variations in $\delta^{18}\text{O}_L$ of Walker Lake over the last several decades, using just the historical stream flow record (refer to Chapter 2 and 5 in this dissertation).

Because Walker Lake is today an alkaline lake, 90% of the dissolved inorganic carbon (DIC) in the lake is in the form of HCO_3^- (BENSON et al., 1996). Results of measurements of the DIC $\delta^{13}\text{C}$ in Walker Lake back to 1966 have also been previously published. Peng and Broecker (1980) reported that the DIC $\delta^{13}\text{C}$ values of Walker Lake were 4.0‰, 3.0‰, and 3.0‰ in July 1966, September 1976, and May 1978, respectively. Based on measurements of 13 water samples collected from the lake in September 1977, Newton and Grossman (1988) reported an average $\delta^{13}\text{C}$ value of 2.8‰. In addition, Benson et al. (1996) presented 37 measurements for the $\delta^{13}\text{C}$ in Walker Lake during the interval from January 1991 to January 1995. These results are collected and shown in figure 3-13. In comparison with variations in the $\delta^{18}\text{O}_L$ observed (Figure 2-11), variations in the DIC $\delta^{13}\text{C}$ of Walker Lake are relatively small. As stated above, instrumental records in figure 3-13 show that lake DIC $\delta^{13}\text{C}$ appears to be associated with lake level change. For example, the DIC $\delta^{13}\text{C}$ was higher during relatively high stands in 1966 than during relatively low stands in 1990s.

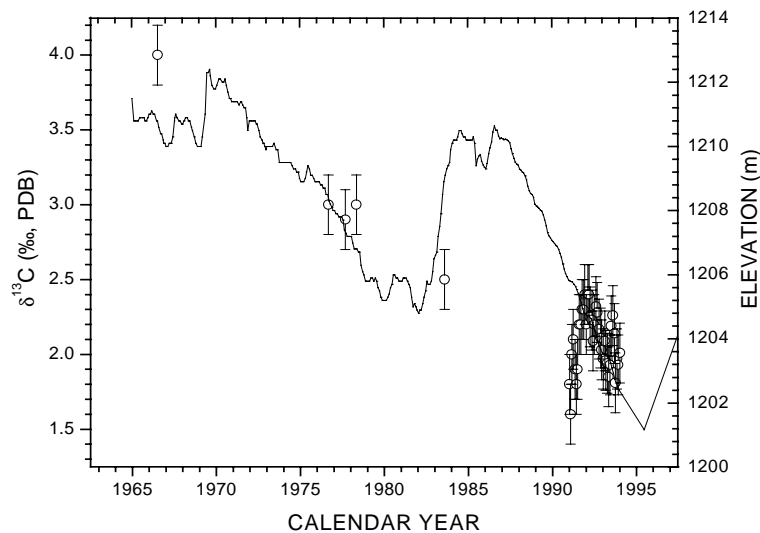


Figure 3-13. Comparison of lake water $\delta^{13}\text{C}$ and lake level elevation (carbon isotopic data originally from Benson et al., 1996 and lake elevation data taken from USGS).

However, the connection between $\delta^{13}\text{C}$ and lake level change is much more complicated. The processes that govern the variability of the DIC $\delta^{13}\text{C}$ of the lake are photosynthesis, respiration, CO_2 gas exchange, and preferential input of isotopically light ^{12}C DIC in stream flow (BENSON et al., 1996). The DIC $\delta^{13}\text{C}$ of the lake is -16‰ at the mouth of the Walker River in January 1979 (PENG and BROECKER, 1980), while it is $-10.1 \pm 0.8 \text{‰}$ at Wabuska gauge station based on 49 measurements of water samples collected during the period from February 1990 to January 1994 (BENSON et al., 1996). The DIC $\delta^{13}\text{C}$ value of the Walker River is presently controlled by the decay of C3 plant material (BENSON et al., 1991) that covers the $\delta^{13}\text{C}$ range between -23 and -34‰ , with an average close to -27‰ (BENEDICT, 1978; SMITH and EPSTEIN, 1971). However, the lower $\delta^{13}\text{C}$ of DIC in stream flow of the Walker River has little influence on the DIC $\delta^{13}\text{C}$ value of Walker Lake over seasonal, annual, and decadal time scales because the amount of DIC input ($0.33 \times 10^9 \text{ M yr}^{-1}$) is relatively small with respect to the DIC pool ($170 \times 10^9 \text{ M yr}^{-1}$) of Walker Lake (BENSON et al., 1996; BENSON et al., 1991).

CO_2 gas invasion across the air-water interface may play important role in influencing the DIC $\delta^{13}\text{C}$ value of Walker Lake. Mean CO_2 invasion rate for the lake is $17 \text{ M m}^{-2} \text{ yr}^{-1}$ (PENG and BROECKER, 1980), which is equivalent to $2.55 \times 10^9 \text{ M yr}^{-1}$, using a surface area of 150 km^2 . Isotopic and chemical reactions involve the transfer of CO_2 across the air-water interface and the hydration of dissolved CO_2 to HCO_3^- (HERCZEG and FAIRBANKS, 1987). Most of the isotopic fractionation takes place during hydration instead of during the transfer of CO_2 across the air-water interface (MOOK et al., 1974). The carbon isotopic fractionation between $\text{CO}_2(\text{g})$ and HCO_3^- is $\sim 8\text{‰}$ at 25°C to 11‰ at 0°C (MOOK et al., 1974). Based on measured $\delta^{13}\text{C}$ values near 2‰ from 1990 to 1995, Benson et al. (1996) claimed that the DIC of Walker Lake is in approximate isotopic equilibrium with atmospheric CO_2 .

Photosynthesis and respiration are also important factors affecting the DIC $\delta^{13}\text{C}$ value of Walker Lake. (MCKENZIE, 1985; MCKENZIE and EBERLI, 1987) suggested that the DIC of the epilimnion would become progressively enriched in ^{13}C as a result of an increase in the removal rate of

^{13}C -depleted organic matter. In fact, the carbon isotopic fractionation induced by plant photosynthesis depends on P_{CO_2} . Photosynthetic plants preferentially incorporate ^{12}C into their cells by 13‰ relative to $\text{CO}_2(\text{aq})$ when surface water $P_{\text{CO}_2} \geq$ atmospheric P_{CO_2} (CRAIG, 1953; HERCZEG and FAIRBANKS, 1987). When surface water P_{CO_2} is at low level, i.e., surface water $P_{\text{CO}_2} \ll$ atmospheric P_{CO_2} , however, the carbon isotopic fractionation that is induced by photosynthesis may be as low as 0‰ (CALDER and PARKER, 1973; DEUSER et al., 1968). In Walker Lake, P_{CO_2} has been reported to be relatively low (570 ppmV) in the early afternoon and high (1400 ppmV) in the morning (KEMPE and KAZMIERCZAK, 1990). Although no direct measurement on primary production in the lake has been made, Benson et al. (1996) argued that the lake may become more productive as it gets smaller. This notion is inconsistent with the data in figure 3-13 showing that the $\delta^{13}\text{C}$ value becomes progressively lower instead of higher with a decrease in lake level. Also, total respiration rate in the lake remains unknown. In addition, there may be other processes affecting $\delta^{13}\text{C}$ signal, such as wintertime CO_2 gas evasion (QUAY et al., 1986), carbonate burial rate, and water chemistry.

Covariance of $\delta^{13}\text{C}$ and $\delta^{18}\text{O}$ preserved in down-core carbonates has been used as an indicator of hydrologic closure of a lake (LI and KU, 1997a; TALBOT and KELTS, 1990). However, records generated from semi-closed to open hydrological lakes also show covariance of $\delta^{13}\text{C}$ and $\delta^{18}\text{O}$ (DEAN, 2002). In Walker Lake, the correlation between $\delta^{13}\text{C}$, and $\delta^{18}\text{O}$ records derived from the down-core TIC fraction of bulk carbonate sediments is relatively high while a correlation between $\delta^{13}\text{C}$ and $\delta^{18}\text{O}$ from ostracode shells is not evident. Direct measurements of lake surface water DIC $\delta^{13}\text{C}$ and $\delta^{18}\text{O}$ also show little correlation in the interval from January 1991 to January 1994 (Figure 3-6) (BENSON et al., 1996). Whether this instrumental record is too short or simply the covariance is just an artifact is an open question. McKenzie (1985) and McKenzie and Eberli (1987) suggested that the removal of ^{13}C -depleted organic matter would contribute to the enrichment of DIC ^{13}C pool of the epilimnion. This hypothesis, however, remains an open question as the covariance of $\delta^{13}\text{C}$ and $\delta^{18}\text{O}$ documented cannot

be explained satisfactorily by McKenzie's (1985) model. Results from laboratory experiments (SPERO et al., 1997) demonstrate that water chemistry (typically the alkalinity) play an important role in $\delta^{13}\text{C}$ and $\delta^{18}\text{O}$ values of planktonic foraminifera shells and suggest that there could be a common mechanism affecting the isotope ratio of both elements. I offer the hypothesis that the covariance of $\delta^{13}\text{C}$ and $\delta^{18}\text{O}$ in alkaline lake systems is simply because both elements come from the some source of HCO_3^- and /or CO_3^{2-} . The potential isotopic disequilibrium between water and DIC may be the key to this puzzle. The carbonate precipitation in highly alkaline aquatic systems is controlled by $p\text{CO}_2$ and $p\text{CO}_2$ can be changed by photosynthesis. Photosynthesis occurring in the limited layer of the epilimnion in a short period of time draws down $p\text{CO}_2$ and consequently triggers carbonate formation in the surrounding microenvironment where carbonate and /or hydro-carbonate have no time to reach isotopic equilibrium with the rest of DIC and water before carbonate precipitation. This potential isotopic disequilibrium mechanism may at least partially explain the covariance of $\delta^{13}\text{C}$ and $\delta^{18}\text{O}$ observed in down-core carbonates where overlying surface water may show no covariance. The lack of correlation between $\delta^{13}\text{C}$ and $\delta^{18}\text{O}$ from ostracode shells is most likely due to the relatively stable environmental conditions where carbonate and /or hydro-carbonate have enough time to reach isotopic equilibrium.

The $\delta^{18}\text{O}$ of ostracode shells is believed to be superior to that of authigenic carbonates to indicate variations in $\delta^{18}\text{O}_L$ due to a variety of reasons (HOLMES, 1996). In Walker Lake, the instrumental $\delta^{18}\text{O}$ record matches well with that of down-core *L. ceriotuberosa*. The $\delta^{18}\text{O}$ value of ostracodes from Walker Lake is heavier than that of authigenic carbonates, which can be ascribed to vital effect and relatively low temperature of bottom water relative to surface water. This is consistent with previous studies (BENSON et al., 1991), however, a comparison between the 5-point running average TIC $\delta^{18}\text{O}$ and 3-point running average ostracode $\delta^{18}\text{O}$ illustrates a complex picture (see figure 3-14), indicating the ostracode $\delta^{18}\text{O}$ is not always isotopically heavier than the TIC $\delta^{18}\text{O}$. For example, the values of the ostracode $\delta^{18}\text{O}$ and TIC $\delta^{18}\text{O}$ are very close in the intervals from 1928 to 1945 and

1975 to 1985. In addition, variability in the ostracode $\delta^{18}\text{O}$ is apparently larger than that in TIC $\delta^{18}\text{O}$. This apparently contradicts the stable environments near water-sediment interface where *L. ceriotuberosa* inhabits. This probably relates with the mobility and immaturity of *L. ceriotuberosa*, which have the potential to lead relatively large fluctuations in the $\delta^{18}\text{O}$ of ostracode shells.

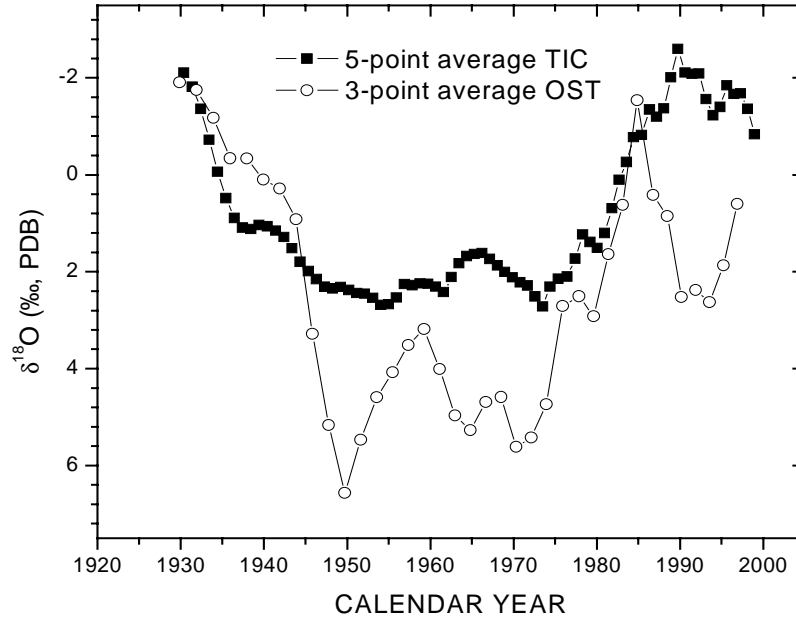


Figure 3-14. Comparison of TIC $\delta^{18}\text{O}$ (TIC) and ostracode $\delta^{18}\text{O}$ (OST) from cored sediments (WLB-003C).

Today, monohydrocalcite is the dominant carbonate precipitate in Walker Lake (SPENCER, 1977). Although the oxygen isotope fractionation factor for monohydrocalcite- H_2O is very close to that for calcite- H_2O ⁹ (JIMENEZ-LOPEZ et al., 2001), monohydrocalcite is metastable and subject to recrystallization. Isotopic fractionation between monohydrocalcite and calcite remains unknown, but systematic calculations for isotopic fractionation between calcite and aragonite (ZHENG, 1999; ZHOU

⁹ The oxygen isotope fractionation factors for monohydrocalcite- H_2O and calcite- H_2O (25°C, 1atm) are $27.8 \pm 0.1\text{‰}$ and $28.0 \pm 0.2\text{‰}$, respectively. Jimenez-Lopez C., Caballero E., Huertas F. J., and Romanek C. S. (2001) Chemical, mineralogical and isotope behavior, and phase transformation during the precipitation of calcium carbonate minerals from intermediate ionic solution at 25°C. *Geochimica et Cosmochimica Acta* **65**(19), 3219-3231.

and ZHENG, 2003) suggested that calcite was enriched in ^{18}O by 4.5‰ relative to aragonite at 25°C, whereas others suggested aragonite in some biogenic carbonates was enriched in ^{18}O relative to calcite (GROSSMAN and KU, 1986). Thus, the possible post-depositional alteration of carbonate precipitates complicates the interpretation of the carbonate $\delta^{18}\text{O}$ signal extracted from downcore sediments.

CHAPTER 4 LATE HOLOCENE LACUSTRINE GEOCHEMICAL AND ISOTOPIC RECORD OF WALKER LAKE

4.1 Abstract

To examine past hydrologic variability in one region of the US Western Great Basin, down-core measurements of total inorganic carbon (TIC), and inorganic carbon $\delta^{13}\text{C}$ and $\delta^{18}\text{O}$ have been completed on the last 3000 years of sediment accumulation in Walker Lake, Nevada. The age model is based on radiocarbon dating of the total organic fraction (TOC). This late Holocene proxy record is divided into three periods according to variations in TIC, $\delta^{13}\text{C}$, and $\delta^{18}\text{O}$ values. Period LH-1 (from 1000 BC to 800 AD) is characterized by low accumulation rate, relatively high values of $\delta^{18}\text{O}$, and low values of $\delta^{13}\text{C}$. The climate of Walker Lake in Period LH-1 appears to be relatively dry. Period LH-2 (from 800 AD to 1900 AD) is featured by high accumulation rates, relatively low values of $\delta^{18}\text{O}$, and high-frequency variations in TIC. The high accumulation rates in Period LH-2 make it possible to record detailed information on climatic and hydrologic variability during the past millennium in this region. In general, the climate in Period LH-2 was relatively wet and punctuated by a few severe droughts ending in 1150 AD, 1275 AD, 1340 AD, and 1500 AD. The climate of the first half millennium (1000-1500AD) was more variable than that of the second half since most of these severe droughts identified occurred within the interval from 1100 to 1500 AD. Lastly, Period LH-h (1900 to 2000 AD) is strongly marked by anthropogenic perturbations and featured with unprecedented increases in $\delta^{18}\text{O}$ values preserved in down-core carbonate sediments.

4.2 Introduction

The climate of the last millennium is conventionally termed by a simple sequence, a Medieval Warm Epoch (MWE), a Little Ice Age (LIA) and then globally extensive warming (BRADLEY, 2000). The MWE, also called as Medieval Warm Period (MWP) (CAMPBELL et al., 1998; CHU et al., 2002;

CIOCCALE, 1999; COOK et al., 2002; CROWLEY and LOWERY, 2000; DEMENOCAL, 2001; ESPER et al., 2002; GONG et al., 2000; HOFFMANN et al., 2001; JONES et al., 2001; KEIGWIN, 1996; PFISTER et al., 1998; VERSCHUREN et al., 2000; YU and ITO, 1999) or Medieval Climatic Anomaly (MCA) (BENSON et al., 2002; STINE, 1994), was termed by Lamb (1965) to designate the interval of 1080 through 1200 AD characterized by dry summers throughout Europe. However, it is debatable whether the global or hemispheric mean temperatures were higher during the MWE than in the 20th century (BRADLEY, 2000; CROWLEY and LOWERY, 2000; HUGHES and DIAZ, 1994). A number of proxy records show evidence for warmer conditions prevailing during the MWE. For example, results from a radiocarbon dated box core from the Bermuda Rise (KEIGWIN, 1996) suggested that sea surface temperature (SST) was ~ 1 °C warmer during the MWE (~1000 year BP) than today. A stacked water isotope record for Summit, central Greenland (HOFFMANN et al., 2001) indicated a warming of 0.6 °C during the MWE. On the basis of a tree-ring record of annual temperature in the Sierra Nevada Mountains, Scuderi (1993) suggested that warmer climatic conditions prevailed in the MWE (800 to 1200 AD). Tree-ring-based temperature reconstruction (ESPER et al., 2002) revealed a large-scale occurrence of the MWP (~1000 to 1300 AD) over the Northern Hemisphere extratropics. More recently, a tree-ring record from the South Island of New Zealand showed evidence for persistent above-average temperatures in the MWE and indicated a global occurrence of the MWE (COOK et al., 2002).

In fact, many areas in the world exhibited persistent drought episodes in the MWE. For example, a paleolimnological record of Lake Naivasha, Kenya (VERSCHUREN et al., 2000) suggested that equatorial east Africa was significantly drier in the MWE (~1000 to 1270 AD) than today. In tropical south China, a geochemical record from Lake Huguangyan also indicated dry climatic conditions in the MWE (880-1260 AD) (CHU et al., 2002). A reconstructed salinity record from Moon Lake, North Dakota (LAIRD et al., 1996) suggested an abrupt change in drought variability around 1200AD. However, in the central region of Argentina, geomorphologic and archeological data (CIOCCALE, 1999) suggested wet climatic conditions in plains accompanying with a recession of the Andean glaciers in MWE (1000 to 1400 AD).

In the western Great Basin, the climate of the MWE is not completely clear. Stine (1994) suggested two prolonged (century-scale) droughts from 910 to 1110 AD and from 1210 to 1350 AD according to dated tree stumps. Although Stine's (1994) results appear to be consistent with the tree-ring-based precipitation record of Nevada Division 3 (HUGHES and GRAUMLICH, 1996), the proposed century-scale drought from 910 to 1110 AD is at least partially opposite to a tree-ring based streamflow record of the Sacramento River (MEKO et al., 2001). For example, the streamflow of the Sacramento River prior to 1000 AD was in its highest point over the last 1130 years (see figure 1-5). Moreover, a lake-based oxygen isotopic record of Pyramid Lake (see figure 1-6; fig. 27 in BENSON et al., 2002) implicated that the climate of the MWE might not be necessarily dry in this region.

The Little Ice Age (LIA) appears in most paleoclimate records from the Northern Hemisphere, which occurred between 1500 and 1900 AD (BRADLEY and JONES, 1993; GROVE, 1988; JONES et al., 2001) and featured with glacier advances in both hemispheres (GROVE, 1988) and enhanced polar atmospheric circulation (HENDY et al., 2002; THOMPSON et al., 1986). In addition, paleoclimate records from tropical ice cores (THOMPSON et al., 1986), tropic Pacific corals (HENDY et al., 2002), and Antarctica ice cores (MOSLEY-THOMPSON et al., 1990) suggest that the LIA was a global-scale event. In most areas of the Northern hemisphere, the climate exhibited multicentury-scale periods of anomalously cold, dry conditions during the LIA (BRADLEY and JONES, 1993; GROVE, 1988; HENDY et al., 2002; LAMB, 1995). However, paleoclimate records from the Northern Great Plains suggest that the climate was relatively wetter during the LIA (1300-1850 AD) than during the MWE (1000-1200 AD) (LAIRD et al., 1998; LAIRD et al., 1996). In the western Great Basin, tree-ring based river flow (MEKO et al., 2001) and precipitation (HUGHES and GRAUMLICH, 1996) records also suggest the climate in the LIA was relatively wet relative to the MWE.

Lake sediments from closed basin lakes can be valuable recorders of climatic and hydrological changes in the past because of their sensitivity to concurrent hydrologic and geochemical conditions. Since the seminal work of Stuiver (1970) and Covich and Stuiver (1974), oxygen isotope ($\delta^{18}\text{O}$) geochemistry of authigenic carbonates has become a well-established technique in paleolimnology

(TALBOT and KELTS, 1990). Assuming that authigenic and biogenic carbonates precipitate in isotopic equilibrium with the environment, the $\delta^{18}\text{O}$ of lake sedimentary carbonates is a function of temperature and isotopic composition of the host water from which they were precipitated (BENSON and WHITE, 1994; CURTIS et al., 1996; HOLMES, 1996; MCKENZIE and HOLLANDER, 1993; XIA et al., 1997b). In contrast, the carbon isotopic composition ($\delta^{13}\text{C}$) of lake sedimentary carbonates, termed as an indirect indicator of climatic conditions (STUIVER, 1970), is primarily affected by the $\delta^{13}\text{C}$ of dissolved inorganic carbon (DIC) of host water, but with little influence of water temperature variations (HOLMES, 1996). Fluctuations in DIC $\delta^{13}\text{C}$ is controlled by a number of processes, such as aquatic CO_2 exchange with the atmosphere CO_2 , photosynthesis and respiration, and post-depositional diagenesis. In Walker Lake, historical instrumental records (lake level, stream gauging, and $\delta^{18}\text{O}$) demonstrate that fluctuations in water $\delta^{18}\text{O}$ are closely linked with changes in hydrological conditions. Fluctuations in water $\delta^{18}\text{O}$ are believed to be recorded in down-core carbonate sediments (see chapters 2 and 3).

Walker Lake and its adjacent lakes, Pyramid Lake, Mono Lake, Owens Lake in the southwestern U.S. Great Basin, have been extensively studied since Russell's (1885) pioneering work. The late Quaternary history of Walker Lake is confounded by possible diversions of the lower Walker River through Adrain Pass. Hutchinson (1937) suggested that Walker Lake apparently desiccated during post-Lahontan time because Walker Lake lacks any unique fish species. Based on physical and geochemical analyses of cored sediments from Walker Lake, Benson et al. (1991) suggested that Walker Lake was dry from 5,300 to 4,800 and 2,700 to 2,100 years BP. Paleolimnological analysis of ostracode and diatom fauna from the Walker Lake cores reveals that the lake desiccated prior to 4,700 and from 2,400 to 2,000 years BP (BRADBURY, 1987; BRADBURY et al., 1989). However, whether these times of desiccation were induced by climatic change is debatable. For example, Bradbury (1987) and Bradbury et al. (1989) believed that the latest desiccation (2,700 to 2,100 years BP) was induced by climatic change while Benson et al. (1991) argued they were related to the diversion of Walker River flowing north into the Carson Sink.

Relative to the entire Holocene, the late Holocene (2740 to 110 years BP) climate of Pyramid Lake was generally relatively wet, with droughts occurring on average, once every 150 years with persistent wet intervals between droughts ranging from 80 to 230 years (BENSON et al., 2002). Mono Lake, a closed-basin lake, is located ~150 km south of Walker Lake. Radiocarbon dating of fossil vegetation debris and identification of deltaic sequences shows that Mono Lake fluctuated over a vertical range of 40 m in response to oscillations in stream inflow and evaporation during the past 3,800 years (STINE, 1990). This indicates that long-term (sub-century to centuries time scale) effective inflow to Mono Basin over the past 3,800 years varied from >134% to < 68% of the modern mean value (STINE, 1990). On the basis of tree-ring data from the Sacramento River drainages (MEKO et al., 2001) variations in long-term (40 year running average) river flow of the Sacramento River over the past 1100 years were calculated to be only ~80% to 125% of the modern mean value (17.8 million acre feet yr⁻¹). If the past variations in the Sacramento River were applied into the Walker River basin, the calculated vertical range of the Walker Lake fluctuations from 1000 to 1900 AD would be less than 10 m (refer to Chapter 5 in this dissertation).

As part of my Ph.D. research on paleoclimate and paleohydrography of Walker Lake, I have analyzed the weight % total inorganic carbon (TIC) as well as $\delta^{18}\text{O}$ and $\delta^{13}\text{C}$ of the TIC fraction of cored sediments deposited over the last three thousand years. Based on radiocarbon dating of the total organic fraction of the cored sediments, a core chronology has been developed. This proxy record serves as the primary resource to reconstruct late Holocene climatic and hydrologic variability in Walker Lake.

4.3 Methods and Results

Dr. Larry Benson of the U. S. Geological Survey previously collected core WLC84-8 from the western basin of Walker Lake in 1984 (see Figure 3-2). The coring method and the results of extensive physical and geochemical analyses of core WLC84-8 were previously published in Benson et al. (1991). Core WLC84-8 is 12 m in length and was sectioned and sampled approximately every 10-cm by Dr. Larry Benson. Ostracode (*L. ceriotuberosa*) valves were hand picked from core WLC84-8 by Richard Forester

of the U.S. Geological Survey (BENSON et al., 1991). Two new piston cores (WLC001 and WLC002) were collected from the western basin of Walker Lake in ~30 m of water on June 19, 2000 by Dr. Larry Benson (USGS in Boulder), Dr. Steve Lund (University of Southern California), Dr. Joe Smoot (USGS in Reston), Dr. Bob Richards and Dr. Alan Heyvaert (University of California at Davis), and myself (see Figure 3-2). Core WLC001 is 5.62 m in length and core WLC002 is ~4.80 m. However, there was a loss of about 8-10 cm at the bottom of the uppermost section of WLC002 during core recovery. Both WLC001 and WLC002 were sectioned at every 1-cm and prepared in the Stable Isotope Laboratory at the University at Albany. Each bulk sediment sample taken from WLC001 and WLC002 was mixed with deionized water, shaken and then centrifuged for 15 min at 20,000 rpm using an International[®] Centrifuge (Model CS). After centrifugation, the electrical conductivity of the supernatant was measured and the supernatant was decanted. This procedure was repeated until the electronic conductivity was less than 3X that of tap water of Albany, New York. Washed samples from WLC001 and WLC002 were oven-dried at 60°C and homogenized with a mortar and pestle (BENSON et al., 2002). Both the bulk sediment sample from WLC84-8 and the dried and homogenized sample from WLC001 and WLC002 were soaked with 2.6% sodium hypochlorite for 6-8 hours to remove organic matter. The soaked sediments were vacuum-filtered with Whatman glass microfibre filters (1.6 µm), then rinsed with deionized water at least five times, and oven-dried at 60 °C prior to isotopic analyses (BENSON et al., 1996). With the assistance of Steve Howe (University at Albany), carbon and oxygen isotopic analyses were performed on a Micromass Optima gas-source mass spectrometer with a MultiPrep automated sample preparation device. The isotopic results are reported relative to Vienna Pee Dee Belemnite (VPDB) standard, based on working standards calibrated against NBS-19. The overall precisions (1-σ) of δ¹³C and δ¹⁸O (except for core WLC84-8 analyses) were less than 0.02% and 0.04%, respectively and mean relative errors of δ¹³C and δ¹⁸O are less than 1.7% except for core WLC84-8¹⁰ (Table 4-1).

¹⁰ WLC84-8 was not washed and homogenized due to the small amount of sediment material available prior to the organic

Table 4-1 Standard deviations and mean relative errors of carbon and oxygen analyses

CORE		Standard Deviation			Mean Relative Error		
		$\delta^{18}\text{O}$ (‰)	$\delta^{13}\text{C}$ (‰)	No of STDs	$\delta^{18}\text{O}$ (%)	$\delta^{13}\text{C}$ (%)	No of Replicates
WLC848	Inorganic Carbonates	0.03	0.02	5	5.6	16.3	8
	Ostracodes	0.03	0.01	17	-	-	-
WLC001	Inorganic Carbonates	0.03	0.01	11	0.9	1.1	7
WLC002	Inorganic Carbonates	0.04	0.02	89	1.7	1.5	59

TIC analysis was carried out in Union College with the assistance of Dr. Donald Rodbell (see Chapter 3 in this dissertation for details). The detection limit for TIC analysis was 0.08 %C and the standard deviation for standards is 0.1%. The relative error of replicates is <2.0%.

4.3.1 Core WLC84-8

The results of carbon and oxygen isotopic analyses for WLC84-8 are plotted against depth cm in Figure 4-1. The resolution is low as the samples were previously sectioned approximately every 10 cm and the relatively low precision of the carbon and oxygen isotopic analyses is apparently in part due to the heterogeneity of TIC-bearing material and the uncertainty of weight % TIC estimation of the sediments¹¹. Plots A and B are oxygen and carbon isotopic analysis results derived from the TIC fraction of bulk sediments while plots C and D are from ostracode (*L. ceriotuberosa*) shells.

matter removal procedure.

¹¹ Weight % TIC of WLC84-8 was previously estimated by Larry Benson through X-ray diffraction scans and the results were published in fig 11 in *Benson et al., 1991*.

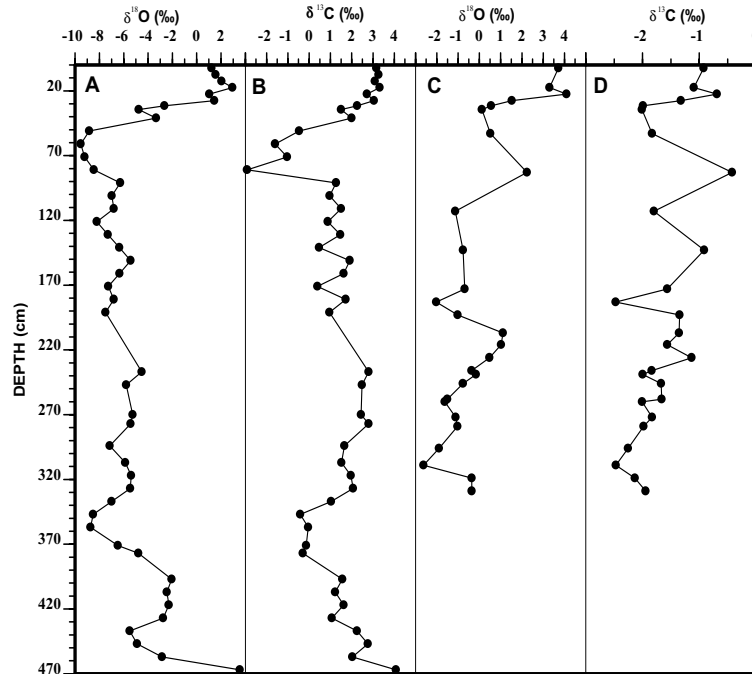


Figure 4-1. Results of measurements of oxygen and carbon isotopes from WLC84-8. A) TIC $\delta^{18}\text{O}$ record, B) TIC $\delta^{13}\text{C}$ record, C) $\delta^{18}\text{O}$ record of ostracod *L. ceriotuberosa* shells, D) $\delta^{13}\text{C}$ record of ostracod (*L. ceriotuberosa*) shells.

These isotopic results from bulk carbonate sediments and ostracode shells show maximum $\delta^{13}\text{C}$ and $\delta^{18}\text{O}$ values at a depth of ~ 20 cm. The transition in this interval is associated with the anthropogenically-induced lake level lowering that occurred starting in 1922/23. The ostracode $\delta^{13}\text{C}$ value is on average 3 ‰ lower than that of bulk carbonate sediments while the ostracode $\delta^{18}\text{O}$ values is on average 4 ‰ higher than that of bulk carbonate sediments. This is consistent with previous results from piston core WLC84-8 (BENSON et al., 1991) and box core WLC-003C (Chapter 3 in this dissertation). The difference of $\delta^{18}\text{O}$ values between ostracode and bulk carbonate sediments can be ascribed to vital effect (i.e., different organisms fractionate to varying degrees) (XIA et al., 1997a; XIA et al., 1997b) and the temperature difference between surface and bottom water (BENSON et al., 1991) since this ostracod (*L. ceriotuberosa*) tends to inhabit the water-sediment interface (BRADBURY et al., 1989; CHIVAS et al., 1985; HOLMES, 1996). The relatively ^{13}C -depleted ostracode shells may be in part related to the presence of organic material inside and /or outside of their valves since no sample

pre-treatment to remove organic matter was taken prior to isotopic analysis. $\delta^{18}\text{O}$ and $\delta^{13}\text{C}$ are positively correlated (for bulk carbonate, $r^2=0.55$, $n=45$; for ostracod shells, $r^2=0.57$, $n=27$). However, no correlation between ostracode $\delta^{18}\text{O}$ and ostracode $\delta^{13}\text{C}$ was found for the core WLC84-8 samples.

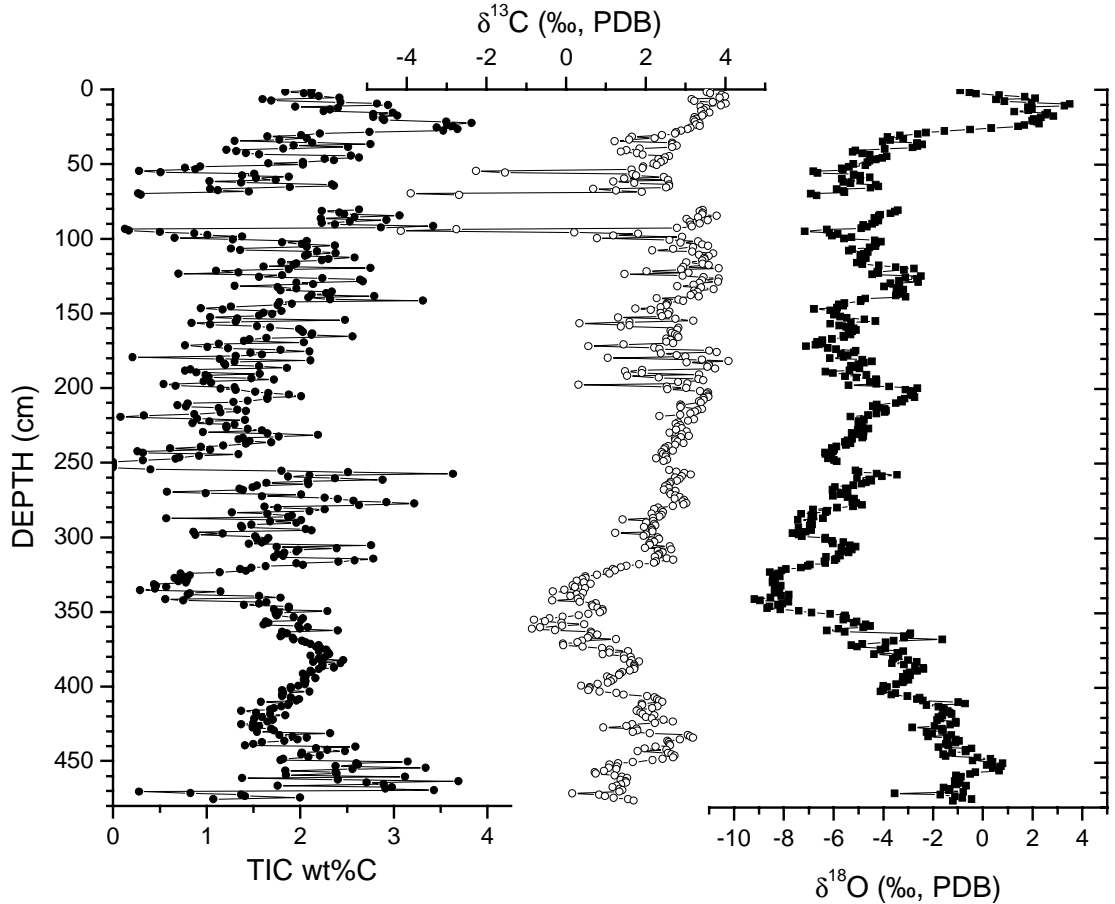


Figure 4-2. TIC, $\delta^{13}\text{C}$, and $\delta^{18}\text{O}$ results were performed on the total inorganic carbon fraction of sediments from core WLC002. Carbon and oxygen isotopic analyses were conducted after organic carbonate matter was removed by 2.6% NaClO solution.

4.3.2 Core WLC002

The TIC and isotopic results from the bulk carbonate content of WLC002 are plotted vs. depth cm in Figure 4-2. The gap indicated in the dataset is due to a loss of ~10-15 cm of core (previously estimated by Dr. S. Lund and Dr. J. Smoot) at the bottom of the uppermost core section during core recovery. Although $\delta^{18}\text{O}$ and $\delta^{13}\text{C}$ are not significantly correlated ($r^2 = 0.11$,

$n = 461$), the $\delta^{13}\text{C}$ minima are usually concurrent with the $\delta^{18}\text{O}$ minima as well as the TIC minima. In general, weight % TIC (Figure 4-2) shows larger variability than $\delta^{18}\text{O}$ and $\delta^{13}\text{C}$.

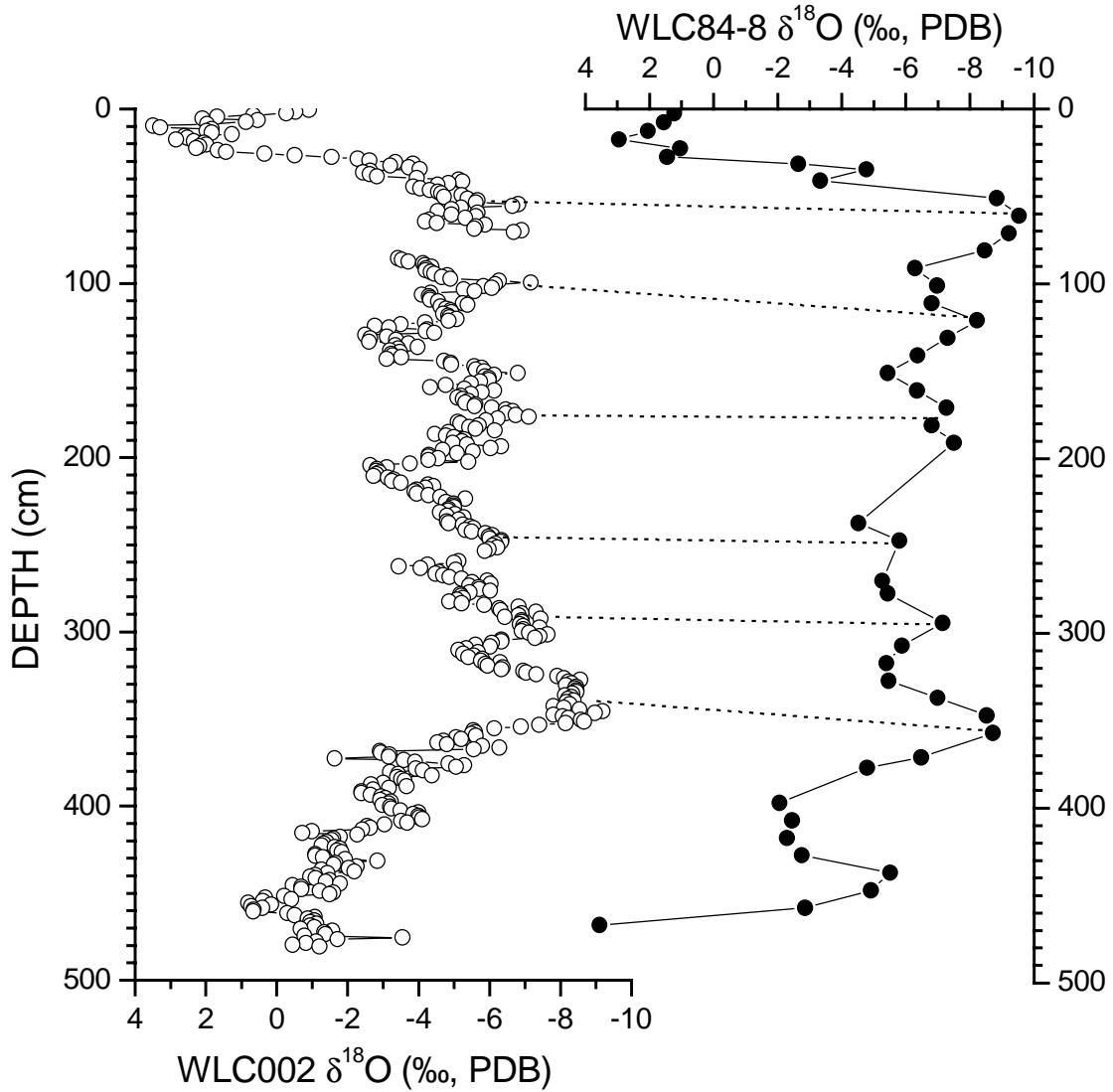


Figure 4-3. Comparison of TIC $\delta^{18}\text{O}$ records derived from WLC84-8 and WLC002. Note that the two records are generally consistent.

In the oldest part of the record $\delta^{18}\text{O}$ is higher except for the historical interval (0-45 cm) and then becomes progressively lower until it reaches a minimum of < -8 ‰ at depths of 330

to 360 cm. Due to anthropogenic lake lowering, $\delta^{18}\text{O}$ reaches a maximum of 3.5 ‰ at a depth 10 cm. The general features of this TIC $\delta^{18}\text{O}$ record are not only consistent in shape with the TIC $\delta^{18}\text{O}$ record of WLC84-8 also their absolute $\delta^{18}\text{O}$ values are very close (Figure 4-3).

4.3.3 Core WLC001

The stratigraphy of Core WLC001 is highly correlated with core WLC002 according to sedimentary structures, lithology, magnetic susceptibility (measured by Dr. Steve Lund), and radiocarbon dates (performed in the laboratory of Dr. J. McGeehin of the USGS). Ages depicted in Figure 4-4 are uncorrected radiocarbon dates of the TOC fraction from both cores WLC001 and WLC002. As the gap in core WLC002 is right above the most recent pronounced peak of magnetic susceptibility (Figure 4-4), 50 samples in the intervals 35 to 85 cm of core WLC001 were taken to splice across the gap in core WLC002. The carbon and oxygen isotopic results in this interval from WLC001 are plotted against depth cm in Figure 4-5. It is evident that $\delta^{18}\text{O}$ and $\delta^{13}\text{C}$ are positively correlated ($r^2 = 0.82$, $n = 50$). In addition, the $\delta^{18}\text{O}$ and $\delta^{13}\text{C}$ minima are concurrent with the maxima of silicic-clastic material. In conjunction with the $\delta^{18}\text{O}$ and $\delta^{13}\text{C}$ records of WLC002, both $\delta^{18}\text{O}$ and $\delta^{13}\text{C}$ from WLC001 clearly overlap with those from WLC002 (Figure 4-6 and 4-7). Core WLC001 apparently has lower average accumulation rates and /or is to a small degree more compacted than core WLC002. This is consistent with core correlations based on sedimentary features outlined in Figure 4-4. Based on analysis of these samples from WLC001, there is about 8-9 cm of sediment missing in the gap of WLC002.

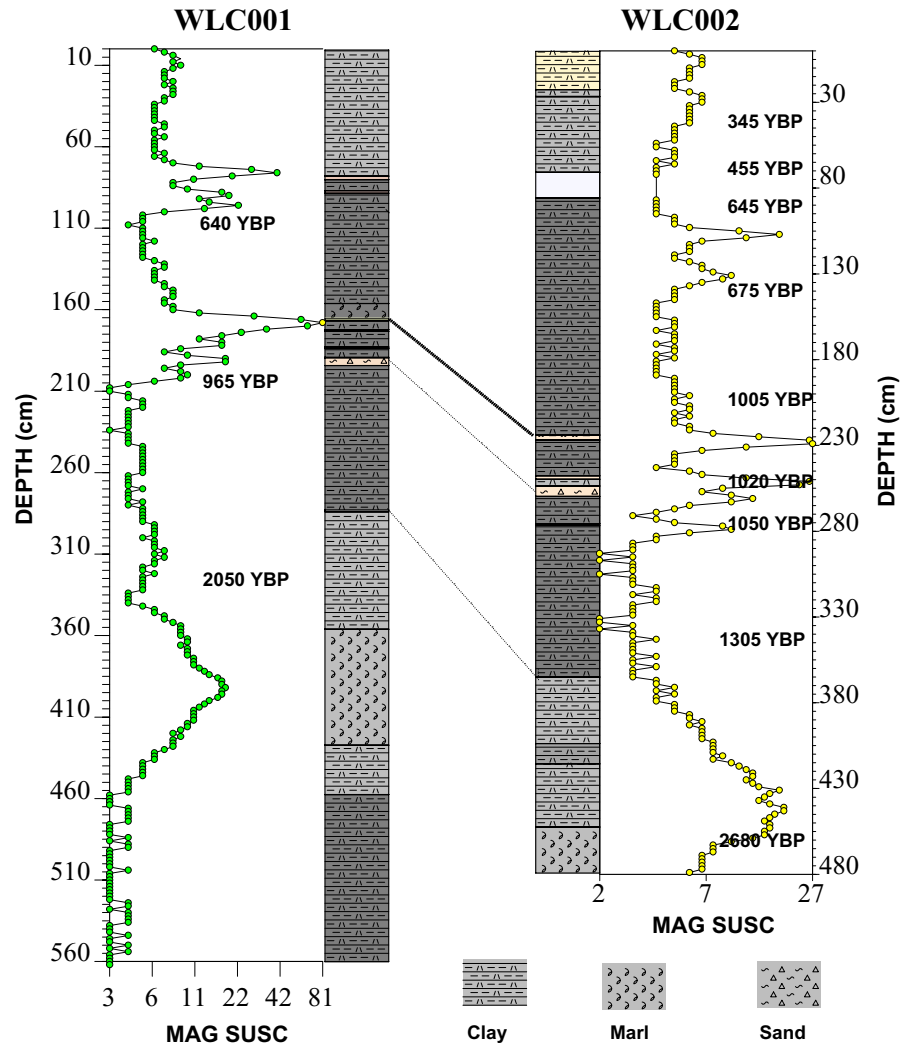


Figure 4-4. Stratigraphic correlations between WLC001 and WLC002. Magnetic susceptibility data were obtained by Dr. Steve Lund of the University of Southern California. Dates are uncorrected radiocarbon ages measured on the TOC fraction of carbonate materials of WLC001 and WLC002 by USGS.

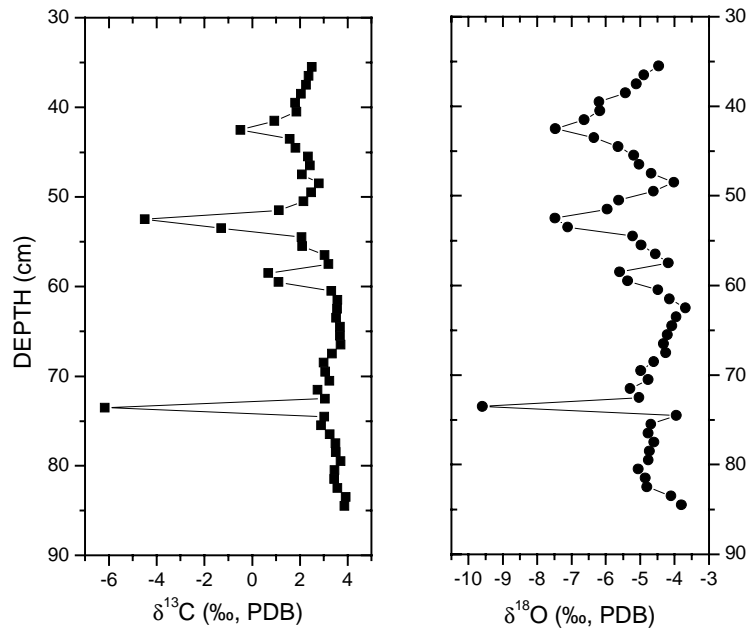


Figure 4-5. TIC $\delta^{13}\text{C}$ and TIC $\delta^{18}\text{O}$ records derived from piston core WLC001 to in the interval that spans the gap in WLC002.

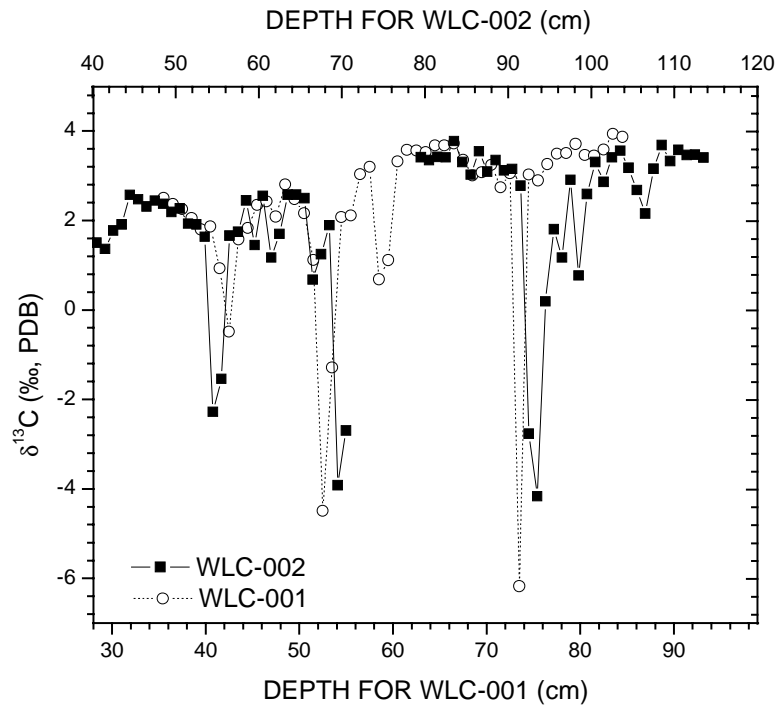


Figure 4-6. $\delta^{13}\text{C}$ records from WLC001 (open circles) and WLC002 (solid squares).

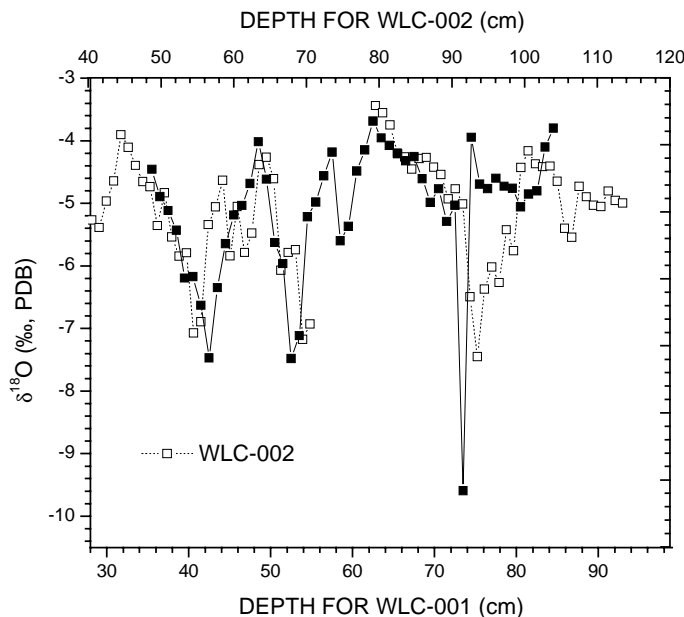


Figure 4-7. $\delta^{18}\text{O}$ records from WLC001 (solid square) and WLC002 (open square). In conjunction the $\delta^{13}\text{C}$ record presented in Figure 4-6, there is 8 cm loss at the bottom of the top segment of WLC002.

4.4 Core Chronology

4.4.1 Reservoir Effect

Because the radiocarbon-dated material is from the TOC fraction, that is mostly lake-derived organic matter (MEYERS, 1990), the reservoir effect of Walker Lake needs to be taken into account prior to ^{14}C date calibration. The reservoir effect on radiocarbon in Great Basin lakes is somewhat basin-specific. For example, Pyramid Lake has a 600-year reservoir effect (BENSON et al., 2003a; BENSON et al., 2002) while Mono Lake has a reservoir effect ranging from 1100 to 5300 years (BENSON et al., 2003a; BENSON et al., 1990). The reservoir effect is related with the residence time of the dissolved inorganic carbon (DIC) in the lake. Also, non-atmosphere borne carbon inputs, such as dissolution (weathering or reworking) of old carbonate sediments and DIC-bearing groundwater baseflow, will lead to lower $^{14}\text{C}/^{12}\text{C}$ ratio and apparently older ^{14}C dates.

One way to determine the reservoir effect of a lake is to compare radiocarbon dates and calendar ages of topmost sediments. If the calendar ages of topmost sediments can be determined through identification of regional and /or global historical events such as mining activities, river

diversions, and nuclear bomb tests, then these ages can be compared to radiocarbon ages of TOC in the same sediment horizons. In Walker Lake, two historical events are documented in down-core sediments; mining activities in 1860 (SMITH, 1998) and construction of Lake Topaz and Bridgeport reservoir completed in 1922/23.

A hydrological and isotopic balance modeling study on Pyramid Lake and Walker Lake (BENSON and PAILLET, 2002) suggested that the overall shapes of the lake volume and $\delta^{18}\text{O}$ records are similar and that minima and maxima in simulated TIC $\delta^{18}\text{O}$ records correspond to minima and maxima in the reconstructed lake volume records. The $\delta^{18}\text{O}$ signals preserved in carbonate sediments from the uppermost section of piston core WLC002 agree with this conclusion and have recorded the abrupt lake level lowering that began in 1922/23 due to an anthropogenically induced reduction of stream flow (Figure 4-8).

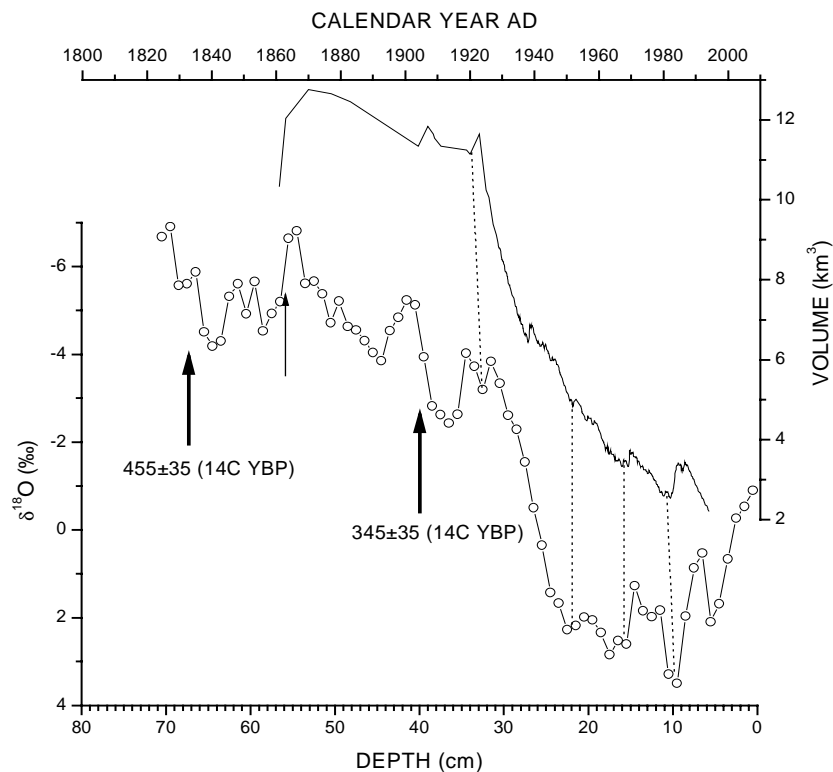


Figure 4-8. Direct comparison of historic lake level record (USGS) and the raw $\delta^{18}\text{O}$ record from the uppermost section of WLC002. Solid arrows refer to uncorrected radiocarbon dates and the thin arrow stands indicates a rise in Hg concentration due to Hg amalgamation processes around 1860 AD (*Michael Lico, personal communication, 2002*). Dotted lines denote possible correlation of these two records.

The sediments sampled at 40 cm with an uncorrected ^{14}C age of 345 ± 35 (CAMS87139) are right below the depth (~30 cm) with a marked $\delta^{18}\text{O}$ transition. In addition, an historical Hg record (*Michael Lico, personal communication, 2002*), derived from a piston core taken from the deep area of the same lake with the same coring platform that was used for WLC001 and WLC002, indicated that Hg started to move above background levels at 54 cm in the 1860s AD (SMITH, 1998) and back to background at 38 cm around ~1900 AD ¹². Hg analyses of digested sediment samples from one sibling box core of WLB-003C reveal that Hg concentration shifts back to normal levels at ~50 cm (*Alan Heyvaert, personal communication, 2002*). The Hg results from the box core and piston core are chronologically in excellent agreement as the age at 50 cm in the box core is equivalent to the age at 38 cm in piston core (Figure 4-9). The calendar age of sample CAMS87139 (with a depth of 40 cm) is in agreement with the upper limit of Hg excursion from the 1860s to the early 1900s. The calendar age for sample CAMS87140 (with a depth of 67 cm) is below the lower limit of the Hg excursion, i.e., older than 1860s AD. The slight core-top loss of WLC002 is trivial because there is a perfect match between the $\delta^{18}\text{O}$ records of WLC002 and WLB-003C (Figure 4-9). In conjunction with the historical lake volume changes ¹³, the upper bound calendar ages of CAMS87139 and CAMS87140 are 1900AD and 1830AD, respectively, since sedimentation rate may be higher in the upper section than in lower one. The lower bound calendar age of CAMS87139 is 1860AD while that of CAMS87140 remains unknown.

To define the reservoir effect (τ_r) of the lake, I assigned four τ_r 's and applied Calib 4.3 (STUIVER and REIMER, 1993; STUIVER et al., 1998) to calculate the calendar ages of CAMS87139 and CAMS87140. The calendar age is determined by the 50% median probability within 2- σ range (SMITH et al., 2002). Calculation results (Table 4-2) reveal that the reservoir effect of Walker Lake is approximately = 310 years in which the calibrated ages of both CAMS87139 and CAMS87140 are close to the age constraints derived above.

¹² Assuming constant sedimentation rate and no significant loss at the top of the core.

¹³ Lake volume is calculated using the polynomial function in Figure 2-8B in chapter 2 of this dissertation.

Table 4-2 Estimates of the reservoir effect of Walker Lake. Calendar year dates were calculated through applying the computer program Calib 4.3 (STUIVER and REIMER, 1993; STUIVER et al., 1998). Calibrated age is the 50% median probability (SMITH et al., 2002).

τ_r (years)	CAMS87139			CAMS87140		
	Calibrated (AD)	Year	2- σ range Year (AD)	Calibrated (AD)	Year	2- σ range Year (AD)
290	1865		1692-1955	1775		1660-1950
300	1875		1693-1955	1780		1665-1950
310	1895		1813-1955	1805		1668-1950
320	1895		1813-1955	1815		1671-1951

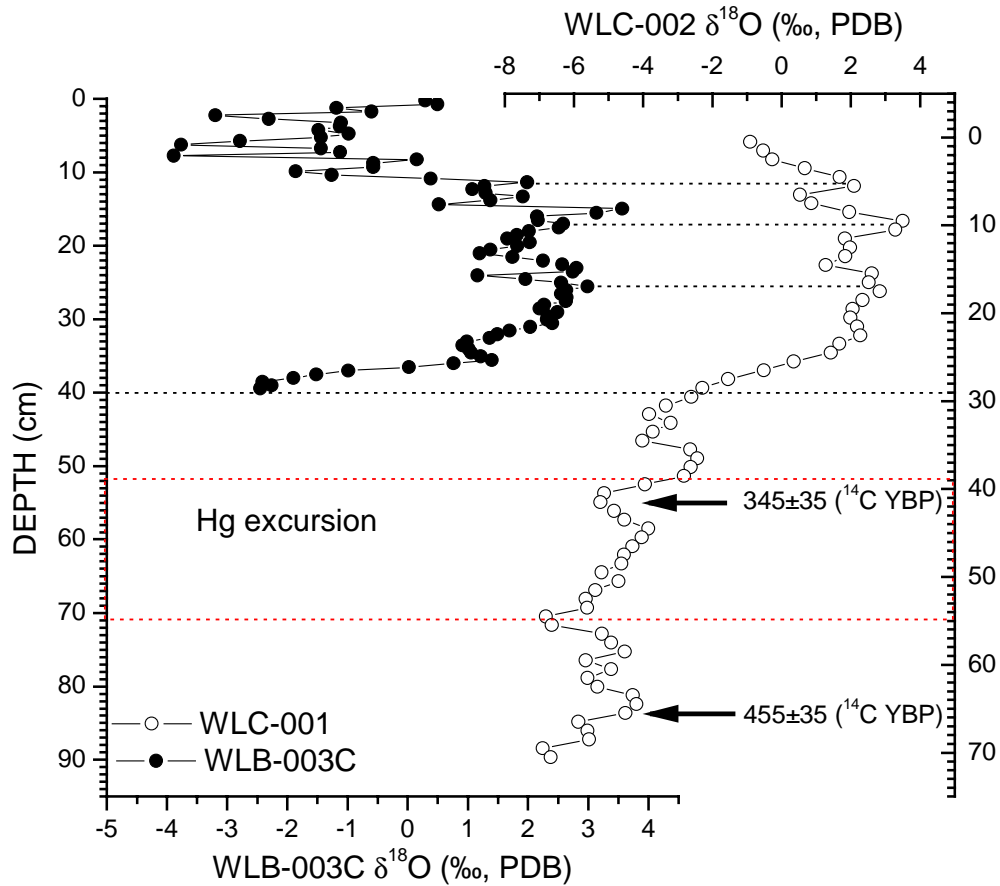


Figure 4-9. $\delta^{18}\text{O}$ records of WLB-003C (solid dots) and the uppermost section of WLC002 (open circles). Compared results indicate that topmost loss of WLC-002 is minor. Solid arrows refer to uncorrected radiocarbon dates.

4.4.2 Age Model

The radiocarbon ages from cores WLC001 and WLC002 were corrected into calendar year using the computer program Calib 4.3 (STUIVER and REIMER, 1993; STUIVER et al., 1998) and are presented in Table 4-3. All nine calendar ages of WLC002 are plotted vs. depth cm in Figure 4-10. A fourth-order polynomial fit was also performed to calculate the calendar age for carbonate materials at various depths.

Table 4-3 Calibrated radiocarbon dates of the TOC fraction of WLC001 and WLC002. Calendar year dates were calculated through using the computer program CALIB 4.3 (STUIVER and REIMER, 1993; STUIVER et al., 1998). Calibrated age is the 50 % median probability (SMITH et al., 2002). Note that dates of WLC001 (italic faced) were not used in age model construction because of apparent discrepancy in sedimentary accumulation (see figure 4-4 for details).

CAMS No.	Section No.	Depth (cm)	¹⁴ C Age ¹⁴ (yr BP)	Error (± yr)	Cal Year (AD/BC)	2-σ range (AD/BC)
87139	WLC002-5	40	35	35	1895	1813-1955
87140	WLC002-5	67	145	35	1805	1668-1950
87141	WLC002-4	84	335	35	1560	1476-1642
<i>87136</i>	<i>WLC001-5</i>	<i>105</i>	<i>330</i>	<i>35</i>	<i>1560</i>	<i>1479-1643</i>
87142	WLC002-4	135	365	35	1535	1447-1635
87143	WLC002-3	196	695	35	1295	1263-1390
<i>87137</i>	<i>WLC001-4</i>	<i>201</i>	<i>655</i>	<i>35</i>	<i>1350</i>	<i>1283-1396</i>
87144	WLC002-3	242	710	40	1290	1224-1390
87145	WLC002-3	267	740	45	1270	1209-1305
<i>87138</i>	<i>WLC001-2</i>	<i>326</i>	<i>1740</i>	<i>45</i>	<i>300</i>	<i>212-415</i>
87146	WLC002-2	333	995	35	1030	982-1158
87147	WLC002-1	452	2370	35	445BC	520-387BC

¹⁴ A 310-year reservoir effect was applied.

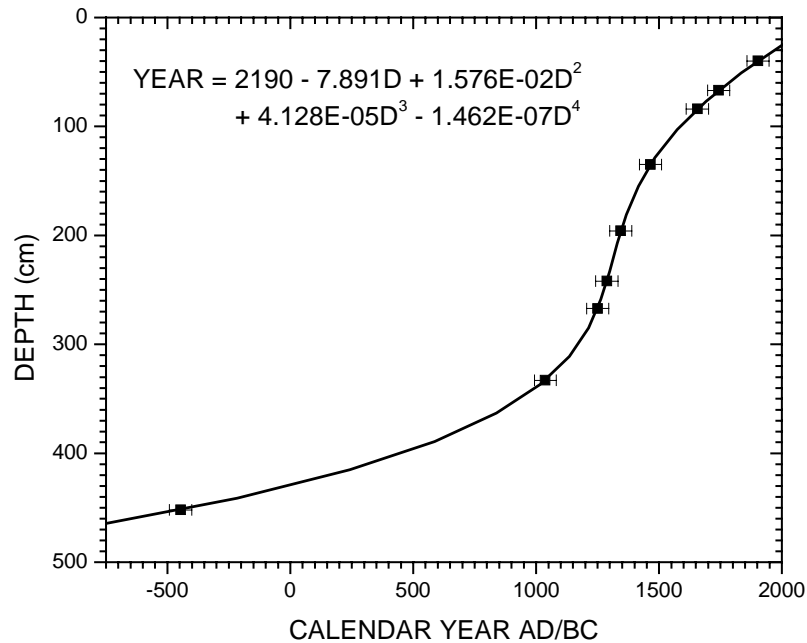


Figure 4-10. Plot of calibrated ^{14}C ages vs. depth for WLC002. Individual error bar is marked according to 2- σ range in Table 4-3. Solid line is a fourth-order polynomial fit of nine calibrated dates. Depth means the distance between the dated sample position and the water-sediment interface.

4.5 Discussion

The $\delta^{18}\text{O}$ results from WLC001 and WLC002 were merged to produce a high-resolution multi-proxy record spanning the last 3000 years (see Figure 4-11). The proxy record is characterized by lower accumulation rates and lower variability in % TIC, $\delta^{13}\text{C}$, and $\delta^{18}\text{O}$ prior to 800 AD. The values of magnetic susceptibility after 800 AD are relatively lower except for two pronounced excursions centered on ~1250 and ~1550 AD. On the basis of variations in magnetic susceptibility, TIC, $\delta^{13}\text{C}$, and $\delta^{18}\text{O}$, this late Holocene proxy record are divided into three periods; Period LH-1 (from 1000 BC to 800 AD), Period LH-2 (from 800 AD to 1900AD), Period LH-h (from 1900 AD to 2000AD). These intervals are discussed in more detail below.

4.5.1 Period LH-1, 1000BC to 800AD

The $\delta^{18}\text{O}$ values of down-core bulk carbonate sediments in Walker Lake are relatively high during Period LH-1 (Figure 4-11). The interval with highest $\delta^{18}\text{O}$ values (~0.8 ‰, PDB) is centered on

~400BC. This interval has the highest $\delta^{18}\text{O}$ of the entire late Holocene section from Walker Lake. In addition, the values of magnetic susceptibility are generally high during this period. This is interpreted to indicate that Walker Lake had a low stand at this time allowing terrestrial magnetic-bearing materials to reach in core sites. The average values of $\delta^{13}\text{C}$ are relatively low in this period, which probably indicates low primary productivity. This is consistent with low accumulation rates during Period LH-1.

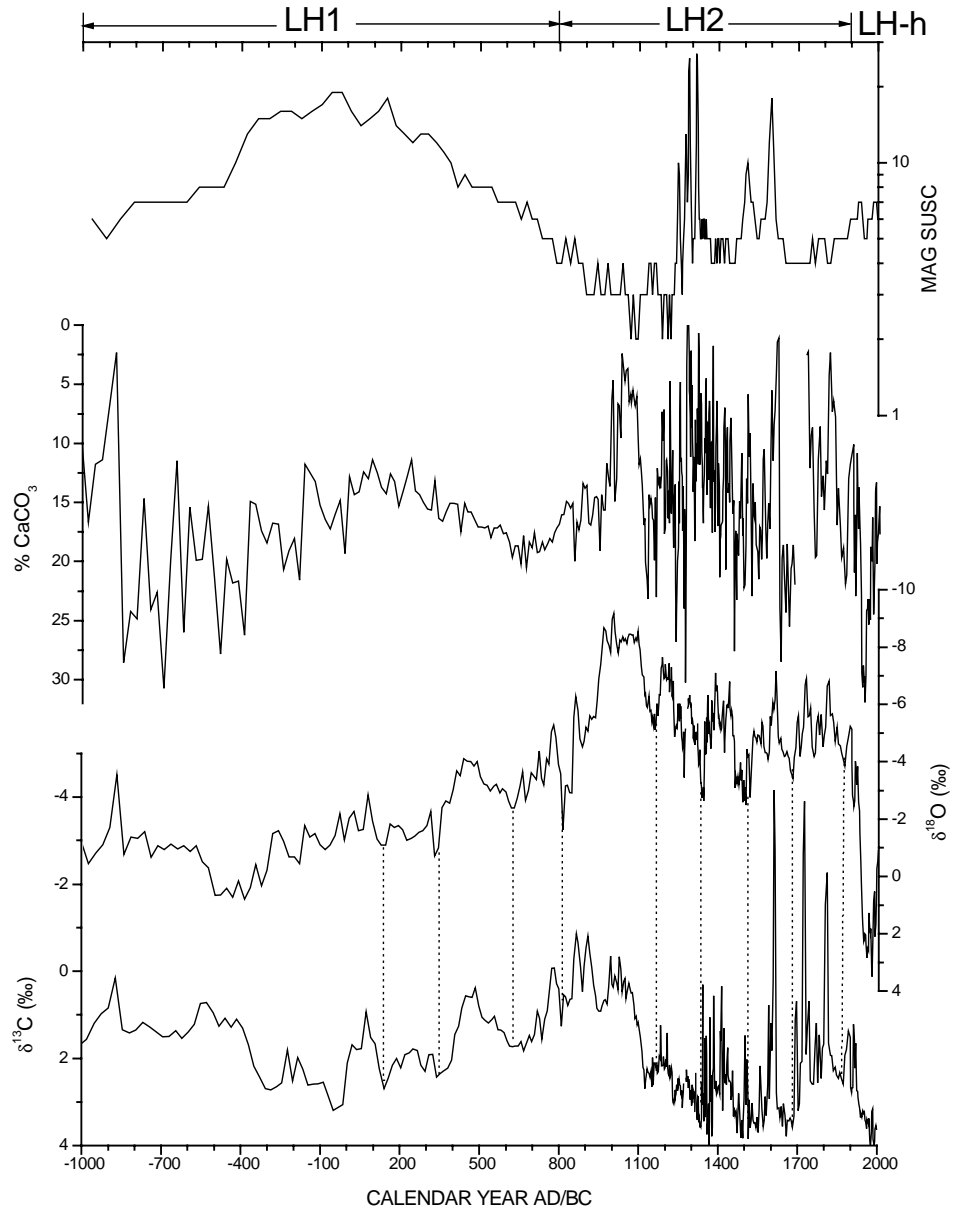


Figure 4-11. 3000-year records of TIC, magnetic susceptibility (Steve Lund), TIC $\delta^{13}\text{C}$, and TIC $\delta^{18}\text{O}$ of Walker Lake. Eight points were taken from WLC001 to fill the gap of WLC002. Vertical dotted lines denote correlation between $\delta^{13}\text{C}$ and $\delta^{18}\text{O}$.

On the basis of the core chronology (Figure 4-11), Walker Lake level elevation is interpreted to have been relatively low during Period LH-1. This result is comparable with previous findings except for the beginning of the period, in which previously results (BENSON and THOMPSON, 1987; BRADBURY, 1987; DAVIS, 1982) suggest that Walker Lake elevation was high (see Figure 4-12). A shallow brine Walker Lake (2400 to 2000 years BP) was documented in down-core limnological records of diatoms, ostracodes, and pollen (BRADBURY, 1987; BRADBURY et al., 1989). Benson et al. (1991) previously suggested relatively low lake levels during 2700-1250 years BP. However, whether the low lake stands during Period LH-1 were induced by climate changes or river diversions still remains uncertain. The fact that Mono Lake was also low during 1800-1000 years BP (STINE, 1990) favors climate-driving fluctuations in hydrologic conditions instead of river diversions.

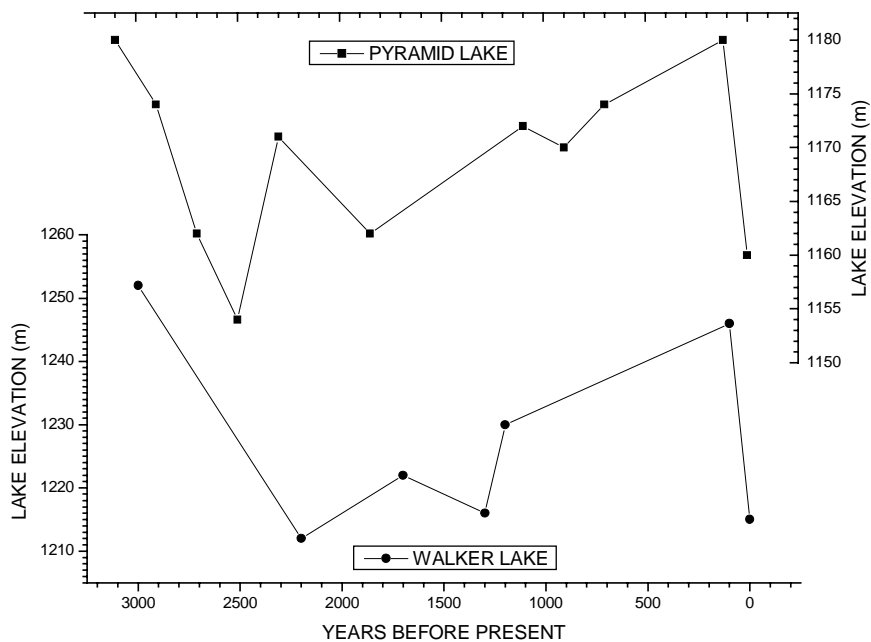


Figure 4-12 Late Holocene variations in lake level of Pyramid and Walker Lakes according to radiocarbon dated tufas and archaeological materials (after BRADBURY, 1987). Original data from Benson (1978) and Davis (1982)

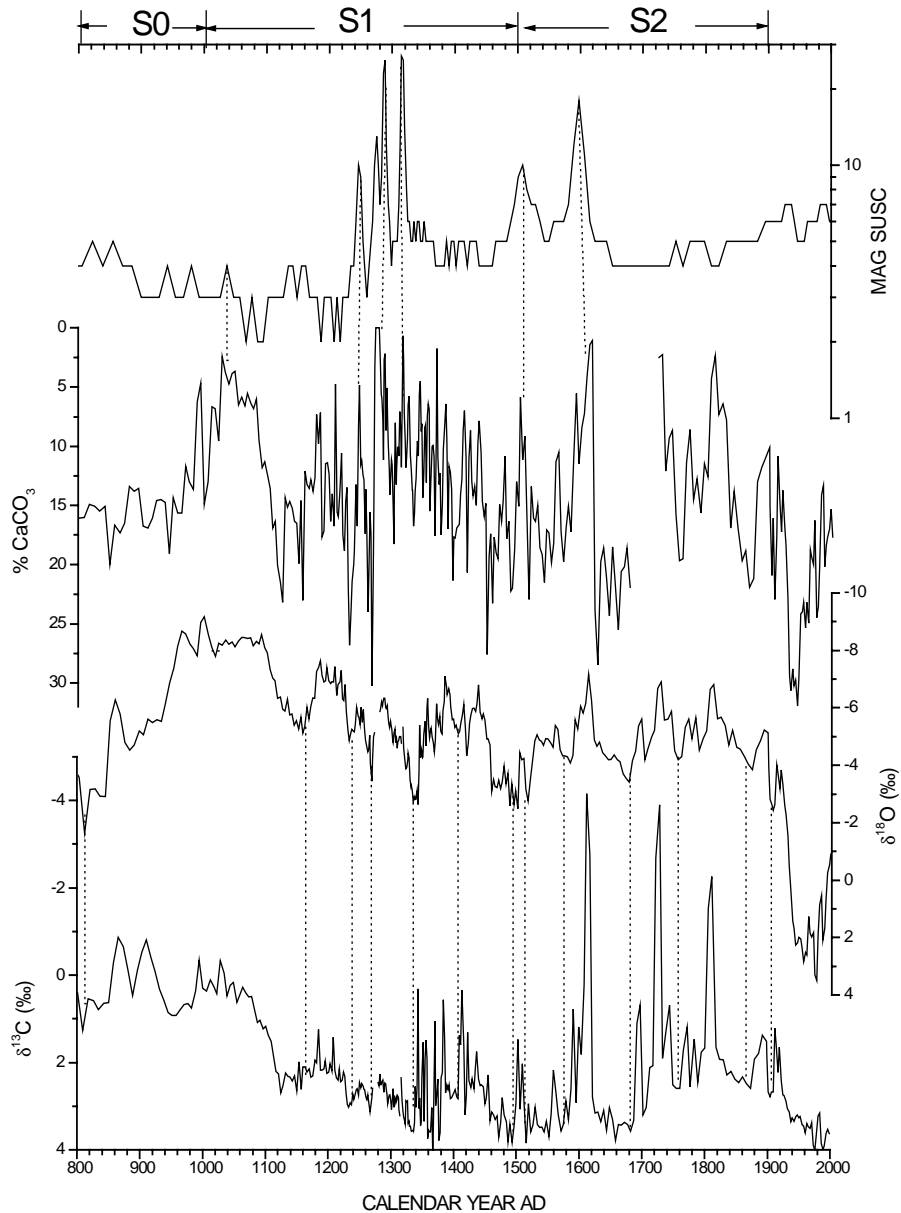


Figure 4-13. High-resolution (3.3 years per sample on average) 1200- year records of TIC, magnetic susceptibility (Steve Lund), $\delta^{13}\text{C}$, and $\delta^{18}\text{O}$ of Walker Lake. Dotted lines denote correlation between these records.

4.5.2 Period LH-2, 800AD to 1900AD

Down-core sediments in Period LH-2 are characterized by high accumulation rates with an average of $\sim 0.3 \text{ cm yr}^{-1}$. High-resolution records of magnetic susceptibility, TIC, $\delta^{13}\text{C}$, and $\delta^{18}\text{O}$ are shown in Figure 4-13. The TIC, $\delta^{13}\text{C}$, and $\delta^{18}\text{O}$ records exhibit several multi-decadal to centennial time

scale cycles. Minima $\delta^{13}\text{C}$ values are concurrent with the minima of TIC and magnetic susceptibility maxima are overall associated with the minima of TIC. On the basis of variations in $\delta^{18}\text{O}$ preserved in down-core bulk carbonate sediments, this period can be further subdivided into three stages; a rapid water-filling stage (S0) from 800 to 1000AD, an unstable high lake stand stage (S1) from 1000 to 1500AD, and a relatively stable lake level stage (S2) from 1500 to 1900 AD.

Although the $\delta^{18}\text{O}$ signal may not be used as a direct index of lake level or volume, the sign of its gradient may be an effective indicator of hydrologic balance. For example, from 810 to 1000 AD, the lake might have gained excessive stream inputs (i.e., positive hydrologic balance) as it experienced a large negative shift (-7.6‰) in lake carbonate $\delta^{18}\text{O}$ in stage S0 (Figure 4-13). The rapid negative shift in $\delta^{18}\text{O}$ values during S0 is unique in the late Holocene history of Walker Lake. This probably indicates a rapid water-filling event (such as abnormal floods and river diversions) beginning approximately 810AD with Walker Lake reaching its highest elevations of the late Holocene at the end of S0. In the following 130 years (960-1090 AD), the $\delta^{18}\text{O}$ signal shows small variations and suggests that the lake maintained a relatively high level. The lake appears to have experienced at least five major droughts ending in 1160, 1230, 1270, 1340, and 1500AD. The $\delta^{18}\text{O}$ values became progressively higher during S1, which is interpreted as the result of a long term lowering of the lake. The lake ultimately reached to a relatively stable stage (S2) of 1500-1900AD in that the $\delta^{18}\text{O}$ values show no significant temporal trends. The climate of Walker Lake appears to be more variable in stage S1 than in stage S2.

The $\delta^{18}\text{O}$ records from Pyramid Lake (BENSON et al., 2002) and Walker Lake are compared in Figure 4-14. Over most of the overlapping sections they show a high degree of similarity. I interpret this to indicate that much of the variance in each isotope record represents a regional climate signal. In general, the multi-decadal and centennial-scale $\delta^{18}\text{O}$ variations are much larger in Walker Lake than in Pyramid Lake. This is due to the smaller volume and hydrological closure of Walker Lake. It is evident that both records demonstrate a pronounced ^{18}O -depleted stage between 950 and 1100 AD. This observation suggests that lake levels in both Pyramid Lake and Walker Lake were relatively high from

950 to 1100 AD. If this interpretation is correct it contradicts Stine's (1994) tree-stump results that show drier conditions and lower lake levels during this time of the MWE, but agrees with the tree-ring-based streamflow record of the Sacramento River (see figure 4-15). In addition, both TIC $\delta^{18}\text{O}$ records of Pyramid Lake and Walker Lake show low lake stands in ~ 1265 , ~ 1335 , and ~ 1470 AD. Except for the proposed low stand of Walker Lake in 1265AD, the other two are also evident in tree-ring based river flow record (40-yr moving average) of the Sacramento River (MEKO et al., 2001).

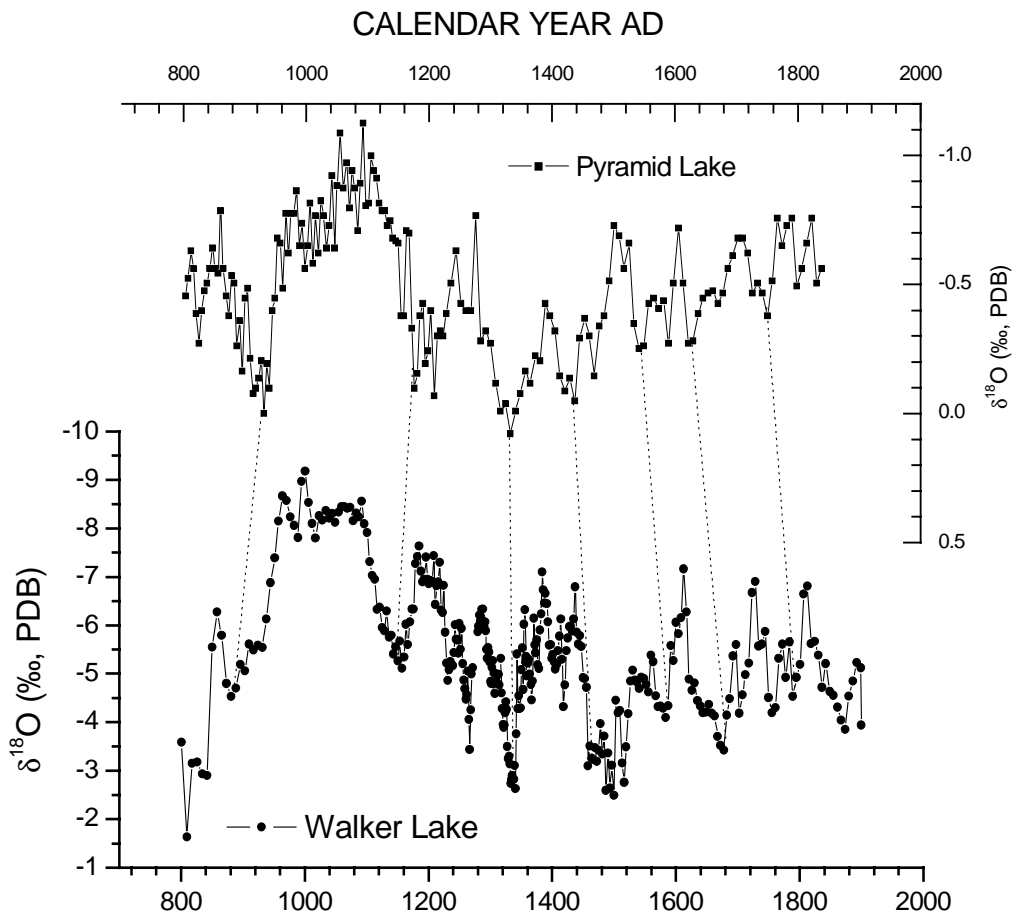


Figure 4-14. Comparison of $\delta^{18}\text{O}$ records from Walker Lake and Pyramid Lake (PLC97-1) (BENSON et al., 2002). Dashed lines denote possible correlation between these two $\delta^{18}\text{O}$ records.

The tree-ring based annual (July-June) precipitation record of Nevada Division 3 (HUGHES and GRAUMLICH, 1996) and tree-ring based stream flow record of the Sacramento River (MEKO et al., 2001) are compared with the $\delta^{18}\text{O}$ record of Walker Lake (Figure 4-15). Since historical river flow records on both sides of the Sierra Nevada are highly correlated (BENSON et al., 2002), the intervals that show apparent correlation between the Walker Lake $\delta^{18}\text{O}$ and both tree-ring based records are not unexpected. However, there are also significant discrepancies between these records. As pointed out above, the wet interval from 950 to 1100 AD is consistent with the interpreted high discharge in the river flow record of the Sacramento River. However, the Nevada Division 3 precipitation record shows a relatively dry interval. This dry interval ending in ~1340 AD is almost concurrent in all three records. The dry interval that ending in 1500 AD is consistent with low discharge of the Sacramento River but inconsistent with the Nevada Division 3 precipitation record. The Walker Lake $\delta^{18}\text{O}$ record is in general more consistent with the Sacramento River flow record than the Nevada Division 3 precipitation record. This is most likely due to the fact that both the Walker River and the Sacramento River share the same headwaters, the Sierra Nevada snowpack.

On the basis of the Sacramento River discharge record (MEKO et al., 2001), there were 11 droughts denoted as D1 to D11 (Figure 4-15) in this region over the last 1000 years. Eight of these droughts can be recognized in the $\delta^{18}\text{O}$ records of Walker Lake while three (D2, D5, and D7) are not evident in the $\delta^{18}\text{O}$ records (Figure 4-15). On the contrary, the $\delta^{18}\text{O}$ records of Pyramid Lake and Walker Lake show three brief wet intervals from 1065 to 1110 AD (D2), from 1370 to 1420 AD (D5), and from 1520 to 1570 AD (D7). Moreover, the tree-ring based streamflow record of the Sacramento River suggests that D3 (1140-1200 AD) and D5 are the most severe droughts while the $\delta^{18}\text{O}$ record of Walker River indicates that D4 (1290-1340 AD) and D6 (1480-1510 AD) are probably the most severe droughts over the last 1000 years.

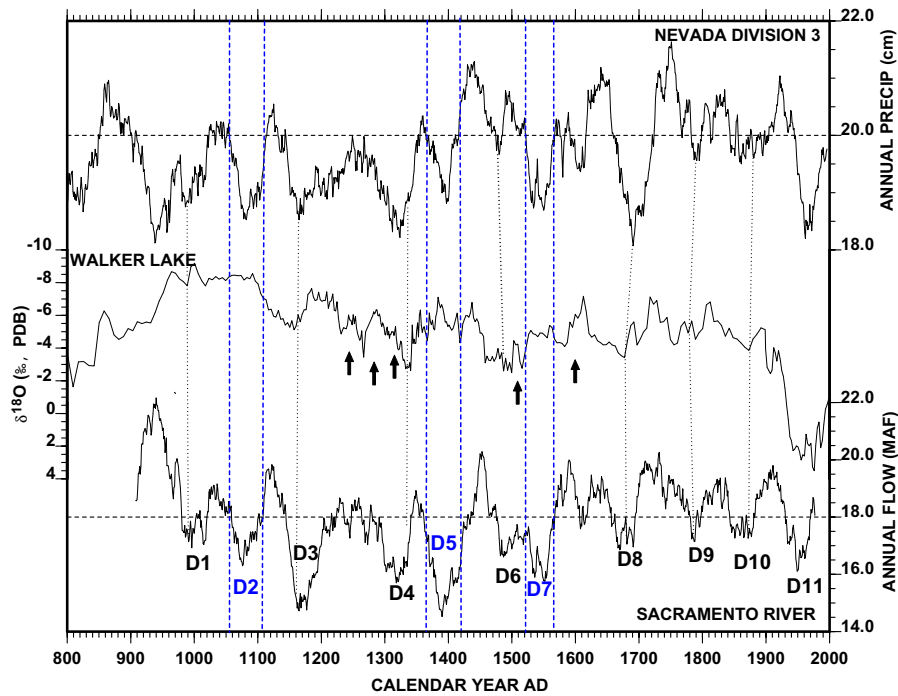


Figure 4-15. Comparison of sediment-based record of Walker Lake and tree-ring based records in adjacent areas. Proxy precipitation record of Nevada Division 3 and river flow record of the Sacramento River are 40-year moving averages of the data obtained by Hughes and Graumlich (1996) and Meko et al. (2001), respectively. D1 to D11 are 11 dry intervals evident in the Sacramento River flow record. The coarser solid line is also a 40-year moving average of $\delta^{18}\text{O}$ record from Walker Lake. Solid arrows represent the peaks of magnetic susceptibility.

The Walker Lake TIC $\delta^{13}\text{C}$ record is not as easily interpreted. The $\delta^{13}\text{C}$ record of Walker Lake and the streamflow record of the Sacramento River are only weakly correlatable (Figure 4-16). Wet intervals (high discharge) of the Sacramento River tend to correlate with minima of $\delta^{13}\text{C}$ and TIC values after 1550 AD, while the dry intervals are correlated with minima of $\delta^{13}\text{C}$ and TIC values before 1550 AD. The fact that the minima of $\delta^{13}\text{C}$ are concurrent with the minima of TIC values suggests the $\delta^{13}\text{C}$ is affected by biological productivity and /or TOC. In Chapter 3, I illustrated that downcore TOC content is associated with the stream discharge. When the stream discharge is larger, the Walker River tends to carry more nutrients to the lake and results in higher productivity or % TOC, which has the potential to produce a more negative signal of $\delta^{13}\text{C}$.

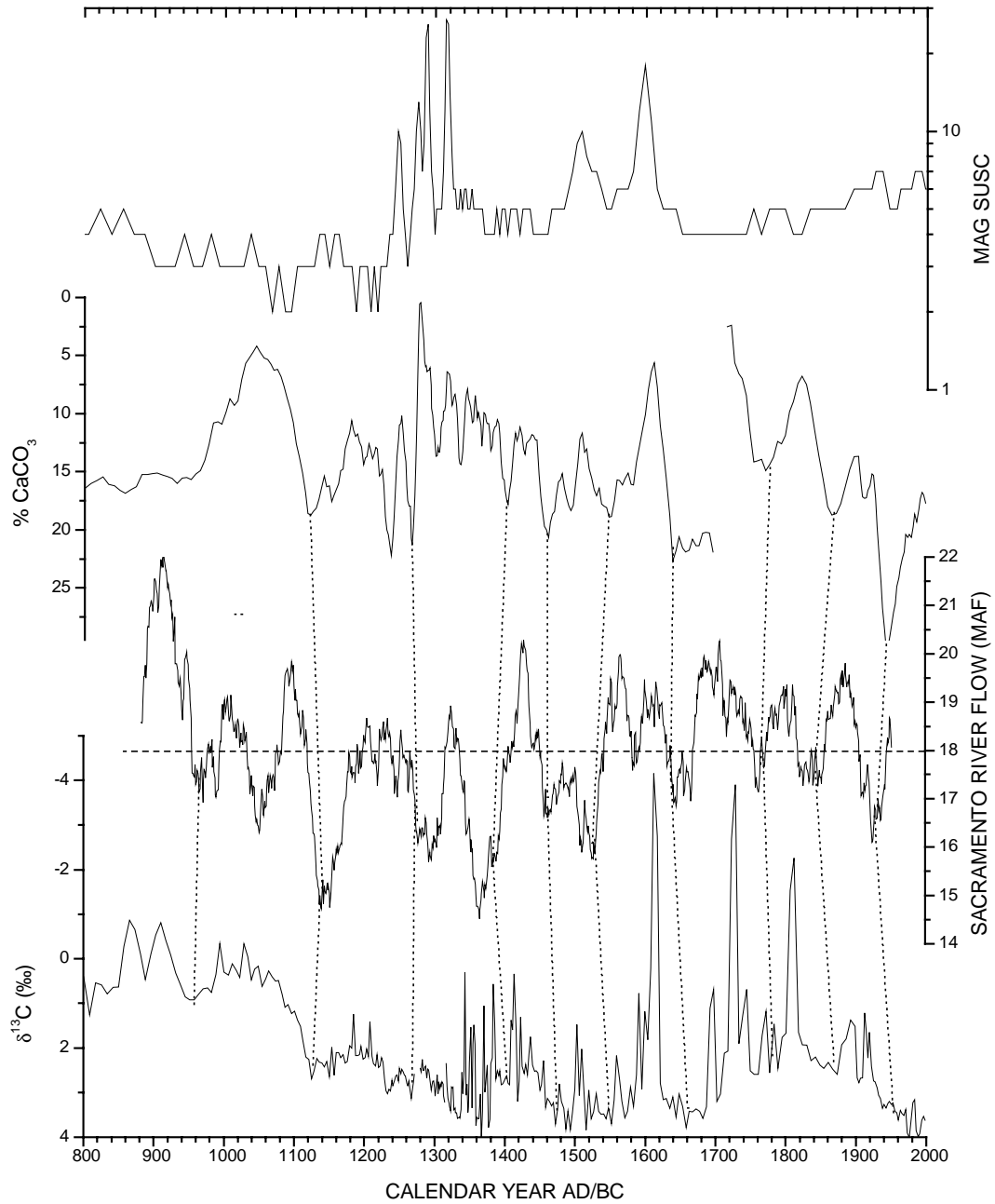


Figure 4-16. Comparison of magnetic susceptibility (Steve Lund), TIC, and $\delta^{13}\text{C}$ records from Walker Lake with the tree-ring based river flow record of the Sacramento River (MEKO et al., 2001). Vertical dashed lines are possible connections between these proxy records and horizontal dotted line denotes the average river discharge of the Sacramento River over the last 1130 years.

4.5.3 Period LH-h, 1900 to 2000AD

The boundary between Periods LH-2 and LH-h shows a ~ 7 ‰ increase in TIC $\delta^{18}\text{O}$. This period is characterized by positive $\delta^{18}\text{O}$ values of bulk carbonates induced by both anthropogenic perturbations and natural climate variations (see Chapter 3 for details).

4.6 Conclusion

On the basis of detailed radiocarbon chronology and down-core TIC $\delta^{18}\text{O}$, %TIC and magnetic susceptibility, the late Holocene climate in the Walker Lake basin has been divided into three periods (Period LH-1 from 1000BC to 800AD, Period LH-2 from 800 to 1900AD, and Period LH-h from 1900 to 2000AD). Period LH-1 is marked by relatively dry climate, with low lake level and relatively low sediment accumulation rates. Period LH-2 is relatively wet in the perspective of the entire late Holocene and further subdivided into 3 stages; S0 from 800 to 1000 AD, S1 from 1000 to 1500 AD, and S2 from 1500 to 1900. The lake was rapidly filled during S0 and reached to its highest elevations at the end of S0. Walker Lake experienced at least five major droughts during period S1 and became progressively lower until ~ 1500 AD when the lake began to maintain a relatively stable surface elevation (during S2). Without doubt, the historical record of Walker Lake (Period LH-h) documented the changing history of hydrologic conditions induced by anthropogenic perturbations and natural climatic variability.

The Period LH-1 $\delta^{18}\text{O}$ record from Walker Lake is not comparable with that from Pyramid Lake. The relative dry climate recorded in Walker Lake during this period has also been identified in a record of Mono Lake shoreline changes (STINE, 1990). This tends to support a climate-controlled story of lake level during Period LH-1. However, the rapid water-filling beginning in 810AD appears to be associated with potential river diversions. Antevs (1952) pointed out that Walker Lake desiccation before 800 AD was not induced by a sufficient dry climate. The rapid water-filling beginning in 810 AD is remarkably consistent with Antevs' (1952) story that the Walker River, used to be a tributary of Carson River, flowed south back to Walker Lake in ~ 810 AD. The Indians even have legends about the stream change (ANTEVS, 1952) and people of the Anazasi started raising crops and irrigation at almost the same time (ENCYCLOPEDIA, 1999). The relatively high resolution of the $\delta^{18}\text{O}$ record during Period

LH-2 from Walker Lake provides detailed information on fluctuations in lake level and volume. The Period LH-2 $\delta^{18}\text{O}$ record is in general correlated with that from Pyramid Lake. Besides, most of dry-wet episodes documented in the $\delta^{18}\text{O}$ records of both lakes are identifiable in the tree-ring based river flow record of the Sacramento River. This implies that the climatic signals documented in these proxy records are related to winter precipitation in the Sierra Nevada.

As discussed above, the Walker River diversion possibly occurred in ~800 AD. If this is the case, the $\delta^{18}\text{O}$ signal during Stage S0 (800-1000AD) may not reflect the climatic conditions then, because hydrologic and isotopic modeling experiments (see Chapter 5) suggest that the hydrologic system of Walker Lake may not reach to a near steady state until the beginning of Stage S1 (1000-1500AD). Stage S1 is equivalent to the MWE that are characterized by warm and dry conditions in most parts of the world. The progressive increases in the $\delta^{18}\text{O}$ record of Stage S1 tend to agree with dry climatic conditions revealed in other paleoclimatic records (HUGHES and GRAUMLICH, 1996; STINE, 1994). However, reconstruction of the lake level suggests that the overall climate during Stage S1 (1000-1500AD) or the MWE was relatively wet relative to Stage S2 (1500-1900AD) or the LIA (see Chapter 5).

CHAPTER 5 CENTENNIAL AND INTERDECADAL CLIMATE VARIABILITY IN THE WALKER LAKE BASIN SINCE AD 800

5.1 Abstract

Sediment cores from Walker Lake contain a high-resolution proxy climate record over the past millennium with at least basin-wide significance. Although the ENSO-like mode of interannual climate variability is strongly muted in this region over the last century, a decadal oscillation is evident in instrumental river flow records from the Sierra Nevada (LI and KU, 1997b), indicating that variations in hydrologic conditions of the Sierra Nevada are associated with the Pacific Decadal Oscillation (PDO) (BENSON et al., 2003b). In order to extract climatic and hydrologic variability of the past, I examined the responses of lake water $\delta^{18}\text{O}$ ($\delta^{18}\text{O}_L$) to changes in the discharge and the river flow $\delta^{18}\text{O}$ ($\delta^{18}\text{O}_R$). The results of model experiments suggest that fluctuations in $\delta^{18}\text{O}_R$ and the total discharge of river flow would result in nearly synchronous oscillations in $\delta^{18}\text{O}_L$. Because of chronological advantage in tree-ring based paleo-record, the age model for the $\delta^{18}\text{O}$ record of Walker Lake was revised according to the chronology of the tree-ring-based Sacramento River flow record. On the basis of this revised age model, a high-resolution record of downcore variations in TIC $\delta^{18}\text{O}$ ($\delta^{18}\text{O}_C$), spanning the last 1200 years with an average sample interval of 3.5 years, was generated. This revised $\delta^{18}\text{O}$ record of Walker Lake show two prolonged droughts that occurred during the Medieval Warm Epoch, which were previously identified through dated tree stumps (STINE, 1994). Time series analysis of this record using multitaper method (MTM) and singular spectral analysis (SSA) have been performed to detect the dominant modes of hydrologic and climatic oscillations over the last millennium. The results suggest that the $\delta^{18}\text{O}$ record of Walker Lake contains interdecadal and centennial climate variability. PDO-like interdecadal oscillations that centered in the periods of 50-90 yr were almost in phase with thermal fluctuations in ocean climate of the California Current, supporting that interdecadal climate variability in

the Sierra Nevada had a Pacific origin at least in the period of AD 800 to 1900. Compared to PDO-like interdecadal climate variations, the underlying centennial to multicentennial variability corresponding to the Medieval Warm Epoch and the Little Ice Age comprise the major share of total variance. In addition, the $\delta^{18}\text{O}$ record of Walker Lake is visually correlated with molar Mg/Ca ratio record of Rice Lake, North Dakota (FRITZ et al., 2000; YU and ITO, 1999; YU et al., 2002) and the ice-core-based cosmogenic nuclide production record (BARD et al., 2000; BARD et al., 2003). This suggests that at least some of centennial variability in the winter snowfall of the Sierra Nevada were associated with solar activity over the last millennium.

5.2 Introduction

The periodic nature of the climate change has been recognized at various timescales such as the Milankovitch orbital cycles, millennial-to-centennial-to-decadal periodicities, and interannual El Niño-Southern Oscillation (ENSO). Short timescale mode of climate like interannual ENSO variability are documented in historical instrumental records around the world (DEMENOCAL, 2001). Longer timescale ($>10^2$ yr) modes of climate variability are registered in paleoclimatic proxy records stored in tree rings, corals, ice cores, marine and lacustrine sediments. The unusual recent behavior of ENSO, such as the exceptionally strong warm (El Niño) events of 1982/83 and 1997/98, has highlighted the incomplete understanding of the ENSO phenomenon (RODBELL et al., 1999) and created considerable interest in the long-term evolution of ENSO and its relation to low-frequency climate forcing (MUÑOZ et al., 2002; RITTENOUR et al., 2000).

The background climate of the last 1200 years in the northern Hemisphere is contrasted with the Medieval Warm Epoch (MWE; 800-1450AD) and the Little Ice Age (LIA; 1450-1850AD). The behavior of ENSO phenomenon is likely modulated by long-term solar activity and /or greenhouse radiative forcing (KNUTSON et al., 1997; MANN et al., 2000). Increases in solar and /or greenhouse radiative forcing tend to decrease the amplitude of interannual ENSO variability (KNUTSON et al., 1997) or lengthen the period between El Niño events (ANDERSON, 1992). During the second half of LIA, a decadal mode of ENSO variability persisted and interannual ENSO variability was relatively

muted (DUNBAR et al., 1994; STAHLER et al., 1998). On the basis of a reconstruction of historical records and Nile flood history, Anderson (1992) suggested that lower frequency ENSO-like variability had a periodicity of ~90 yr during the MWE, indicating interannual ENSO modes were less dominant at that time.

Although the Walker River Drainage sits at a nodal point where there is in general a weaker statistical correlation between precipitation and ENSO over the last century, the drainage basin receives abnormal moisture during the recent two strong ENSO events of 1982/83 and 1997/98. Historical instrumental river flow records of the drainages on both sides of the Sierra Nevada exhibit a uniform decadal signal in this region, which is likely associated with the Pacific Decadal Oscillation (PDO) (MANTUA et al., 1997). Benson et al. (2003b) proposed that variations in the wetness of the Sierra Nevada are associated with changes in the sign of the PDO. Proxy records of prehistoric PDO variability have been obtained from tree rings, corals, and historical documentary records. However, most high-resolution records of PDO reconstruction have usually been limited to the past 2-3 centuries. For example, an irregular 14-year cycle has been detected in a proxy sea surface temperature (SST) record (AD 1726-1997) based on Sr/Ca analyses of a coral from Rarotonga in the South Pacific (LINSLEY et al., 2000). Northeast Pacific tree-ring records and reconstructions of the PDO back to AD 1700 suggest that a decadal mode is more dominant prior to the middle 1800s than afterwards, indicating a possible climate regime shift that occurred around that time (D'ARRIGO et al., 2001).

The oxygen isotopic composition ($\delta^{18}\text{O}$) of lacustrine authigenic or biogenic carbonate has been commonly used to examine paleoclimate variability (BENSON et al., 2002; COVICH and STUIVER, 1974; CURTIS et al., 1996; HODELL et al., 1995). For example, on the basis of high-resolution $\delta^{18}\text{O}_\text{C}$ records from cored sediments of Pyramid Lake, Nevada, Benson et al. (2002) suggested that the hydrologic balance of Pyramid Lake oscillated about every 150 years over the past 7630 years. Spectral analysis of the $\delta^{18}\text{O}_\text{C}$ signal measured on ostracode shells in a sediment core from Lake Punta Laguna (CURTIS et

al., 1996; HOPELL et al., 2001) also suggest the existence of century-scale climate modes (near 208 and 125 years) in the Yucatan Peninsula, Mexico.

The objectives of this part of dissertation are to examine possible responses of $\delta^{18}\text{O}_L$ to changes in hydrologic and isotopic conditions (typically the $\delta^{18}\text{O}_R$ and the amount of river flow) and retrieve climatic and hydrologic variability documented in the $\delta^{18}\text{O}_C$ record of Walker Lake over last ~1200 years.

5.3 Isotopic responses to climatic changes

The Walker River-Walker Lake surface water system has been the object of intensive hydrologic, chemical, isotopic, and biological studies over the last several decades (BENSON et al., 1991; BEUTEL et al., 2001; BRADBURY, 1987; BRADBURY et al., 1989; COOPER and KOCH, 1984; MILNE, 1987; NEWTON and GROSSMAN, 1988; SPENCER, 1977). The Walker River is the only major water source for Walker Lake. Hydrologic model experiments demonstrate that the hydrologic balance of Walker Lake can be simulated using fixed mean-annual rates of evaporation and on-lake precipitation, indicating that groundwater inflow or outflow is negligible (MILNE and BENSON, 1987). The long-term average values of the Walker River discharge during the intervals from 1871 to 1920 and from 1920 to 2000 are 445 ± 161 and 174 ± 169 cubic feet per second (cfs), respectively. 60% of stream flow of the Walker River has been taken in upstream reaches for agriculture purposes beginning in 1920 (BENSON and LEACH, 1979). Under natural environments, Walker Lake is able to achieve a hydrologic steady-state within a few decades. Walker Lake elevations are closely associated with the discharge of the Walker River (Figure 5-1). On the basis of the hypsometric settings of Walker Lake, the long-term (decadal scale) average value of the Walker River would vary within 1000 cfs, provided that Walker Lake remains under hydrologic closure. The historical average lake elevation (1242 m during 1860-1920) is slightly below the hydrologic steady-state elevation of 1253 m corresponding to the average river flow of 445 cfs (Figure 5-1).

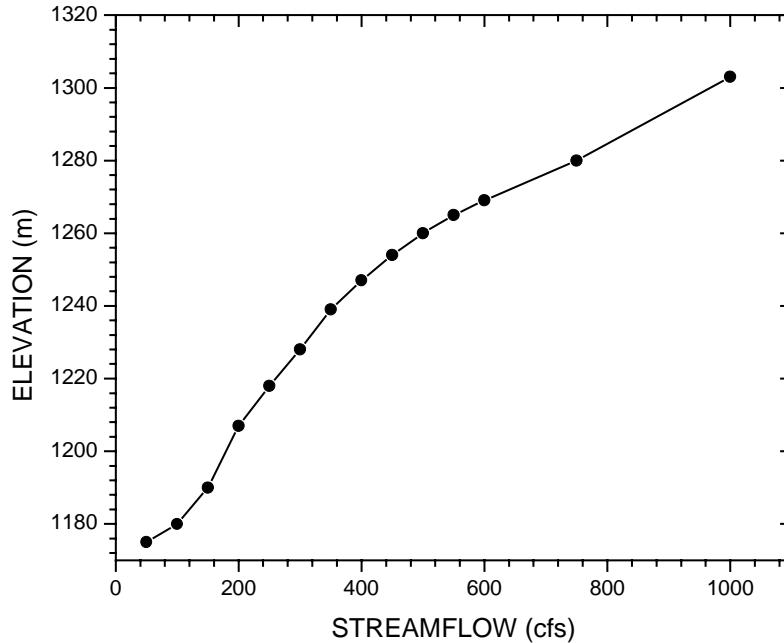


Figure 5-1. Steady-state lake elevation of Walker Lake corresponding to long-term average value of the Walker River discharge. The elevation of spilling sill is 1308.0 m and the lake bottom elevation is 1171.5 m (MILNE, 1987).

Walker Lake presently has not reached a hydrologic steady-state following the lowering that began in the early 1920s, as the actual lake elevation is slightly above to the steady-state level of 1198 m for the average river flow of 174 cfs. The average values of the reconstructed river flow of the Walker River are 330 cfs in the late Holocene, 550 cfs in the last millennium, and 640 cfs in MWE (1000 to 1430 AD) (see Chapter 5). The 20-year running average values of the reconstructed river flow of the late Holocene Walker River also varies within 1000 cfs, indicating that Walker Lake remained in hydrologic closure in the late Holocene.

Variations in the $\delta^{18}\text{O}_L$ have been successfully simulated using HIBAL (see chapter 2 in this dissertation). The natural river flow (Q) of the Walker River, as well as other climatic signals tends to fluctuate periodically, $Q = \sum_{i=1}^n A_i \sin\left(\frac{2\pi t}{\lambda_i}\right) + M$, where A is the amplitude of river discharge in cfs, λ the wavelength in year, t the time in year, M the mean value of river flow in cfs, $i=1, 2, \dots, n$ denoting n

principal components of river flow signal. To examine the response of $\delta^{18}\text{O}_L$ to variations in the amount of river flow of the Walker River, I assume $n=1$, $A=322$ cfs (2- σ of historical river flow record from 1871-1920 AD), $M=445$ cfs (the mean annual value of historical river flow record). Wavelength λ is assigned to be 5, 25, and 100 years to study the corresponding responses of $\delta^{18}\text{O}_L$ to interannual, interdecadal, and century-scale variations in river discharge. The HIBAL program is coded and integrated into Microsoft Excel 2000 via Macros functionality. HIBAL model parameters are determined by those observed in Pyramid Lake (Table 2-1). This program has been successfully used in $\delta^{18}\text{O}_L$ simulations of the Walker Lake surface water in a period of 1985-1994. Here I replace the actual discharge data with hypothetical discharge values that are generated through $Q = 322 \sin\left(\frac{2\pi t}{\lambda}\right) + 445$. HIBAL runs in a lunar monthly step fashion and records the 10th lunar month $\delta^{18}\text{O}_L$ values of the epilimnion and hypolimnion to represent carbonate precipitate $\delta^{18}\text{O}_C$ for the year¹⁵. Model experiments indicate that the initial response of $\delta^{18}\text{O}_L$ to change in river discharge is dependent on the initial hydrologic and isotopic conditions of the lake, such as the $\delta^{18}\text{O}_L$, the $\delta^{18}\text{O}_R$, and the lake elevation. However, the steady-state response of $\delta^{18}\text{O}_L$ to change in river discharge is independent of these initial hydrologic and isotopic conditions. In reality, the hydrologic balance may change before the steady-state $\delta^{18}\text{O}_L$ value is achieved because the climate tends to vary on all time scales (BENSON and PAILLET, 2002). In isotopic simulations, when hydrologic balance varies in a fixed time scale, an approximately steady-state $\delta^{18}\text{O}_L$ value is observed.

For the closed-basin Walker Lake $\delta^{18}\text{O}_L$ simulations, river flow (Q) is set to vary between 123 to 767 cfs. For interannual timescale mode of climate (discharge) variability, for example, wavelength $\lambda=5$ yr, the initial response of epilimnion $\delta^{18}\text{O}_L$ appears to be synchronous with change in river discharge while the initial response of hypolimnion $\delta^{18}\text{O}_L$ tends to lag by ~ 0.5 years changes in river

¹⁵ Model assumes that most inorganic carbonate precipitation occurs in this time interval.

discharge (Figure 5-2A and 5-2B). Under approximate steady-state conditions, the $\delta^{18}\text{O}_L$ values of epilimnion and hypolimnion vary in phase with changes in river discharge (Figure 5-2C and 5-2D). For interdecadal variations in river discharge (e.g., $\lambda=25$ yr), both the initial and steady-state responses of epilimnion and hypolimnion $\delta^{18}\text{O}_L$ tend to be synchronous with change in river discharge (Figure 5-3A, B, C, and D). However, for century-timescale like $\lambda=100$ yr, both the initial and steady-state responses of the epilimnion and hypolimnion $\delta^{18}\text{O}_L$ appear to lead by ~ 10 years changes in river discharge (Figure 5-4A, B, C, and D). If this result can be confirmed, the low-frequency $\delta^{18}\text{O}_L$ signal stored in down-core sediments can be used to predict the long-term future climate (discharge) changes. As this result is opposite to previous studies (BENSON and PAILLET, 2002), more modeling work is needed.

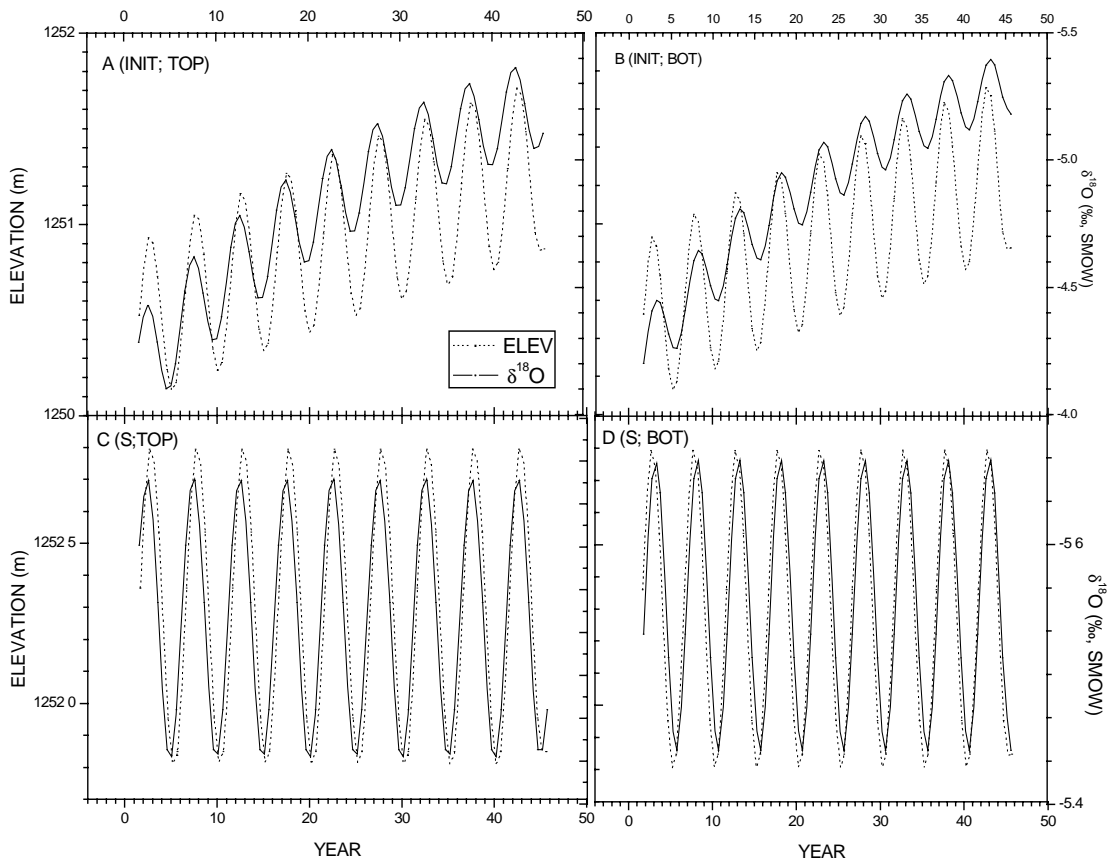


Figure 5-2. Oxygen isotopic responses to oscillatory changes in the Walker River discharge with a wavelength of 5-yr. A) Initial response of the top water. B) Initial response of the bottom water. C) Steady-state response of the top water. B) Steady-state response of the bottom water.

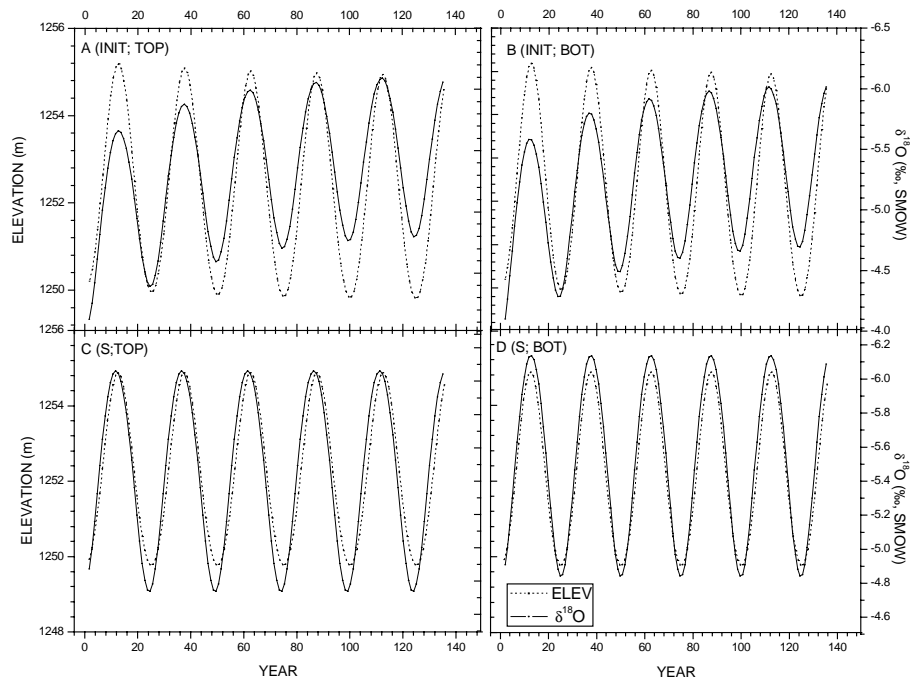


Figure 5-3. Oxygen isotopic responses to oscillatory changes in the Walker River discharge with a wavelength of 25-yr. A) Initial response of the top water. B) Initial response of the bottom water. C) Steady-state response of the top water. D) Steady-state response of the bottom water.

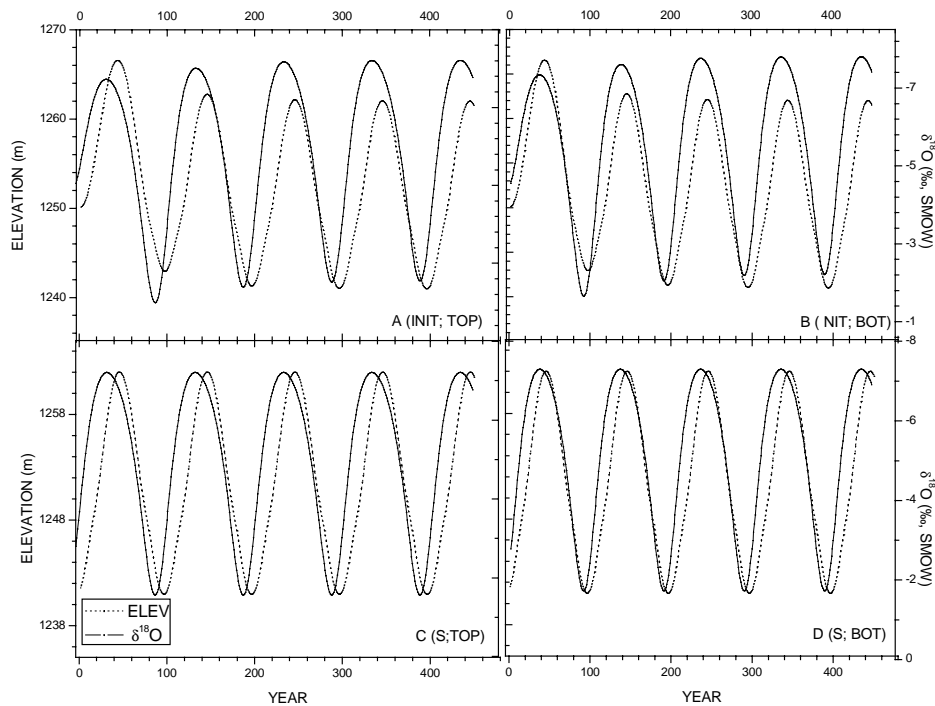


Figure 5-4. Oxygen isotopic responses to oscillatory changes in the Walker River discharge with a wavelength of 100-yr. A) Initial response of the top water. B) Initial response of the bottom water. C) Steady-state response of the top water. D) Steady-state response of the bottom water.

In Appendix 2 of this dissertation, I will discuss the isotopic relationship between lake water and river water, and suggested that the long-term average $\delta^{18}\text{O}_R$ can be inferred from the steady-state $\delta^{18}\text{O}_L$. In this section, the amplitude of variations in $\delta^{18}\text{O}_L$ that are induced by change in river discharge is addressed.

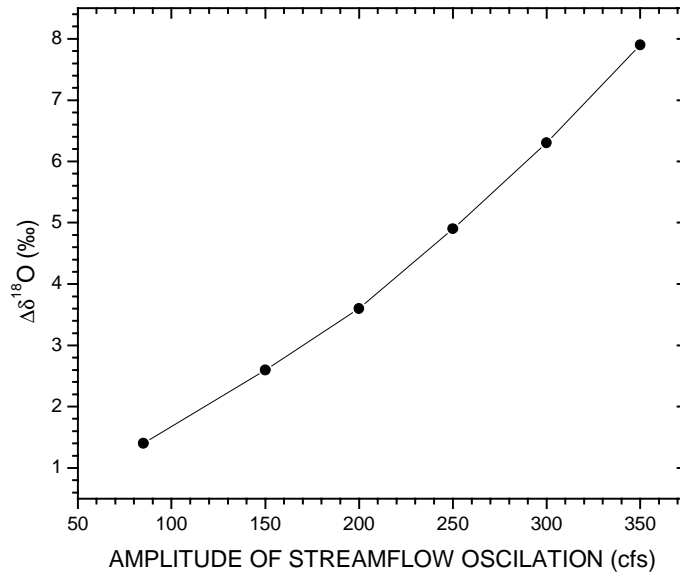


Figure 5-5. Relationship between the amplitude of oscillations in the $\delta^{18}\text{O}_w$ and the amplitude of fluctuations in the Walker River discharge.

The river discharge signal (function) can be decomposed into three components, the amplitude (A), the wavelength (λ) or frequency ($1/\lambda$), and the mean discharge value (M). The amplitude ($\Delta\delta^{18}\text{O} = \delta^{18}\text{O}_{\max} - \delta^{18}\text{O}_{\min}$) of variations in $\delta^{18}\text{O}_L$ increases in proportion to the amplitude of river discharge (Figure 5-5). However, it increases with the decrease in the mean value of river discharge (Figure 5-6), indicating that $\delta^{18}\text{O}_L$ is more sensitive when the lake is volumetrically smaller. The amplitude of variations in $\delta^{18}\text{O}_L$ is also in inverse proportion to the frequency of river flow signal (Figure 5-7). This means that the lower frequency component has larger spectral power. In addition, the amplitude of changes in river flow is positively correlated with the $\delta^{18}\text{O}_R$ (Figure 5-8).

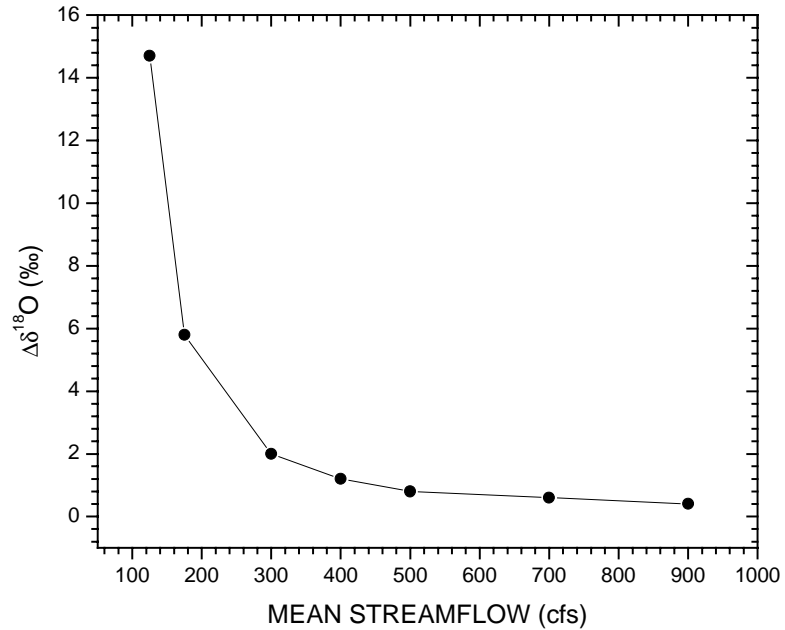


Figure 5-6. Relationship between the amplitude of oscillations in the $\delta^{18}\text{O}_L$ and the mean value of the Walker River discharge showing that the sensitivity of the $\delta^{18}\text{O}_L$ is exponentially proportional to the amount of stream flow when a lake becomes volumetrically small.

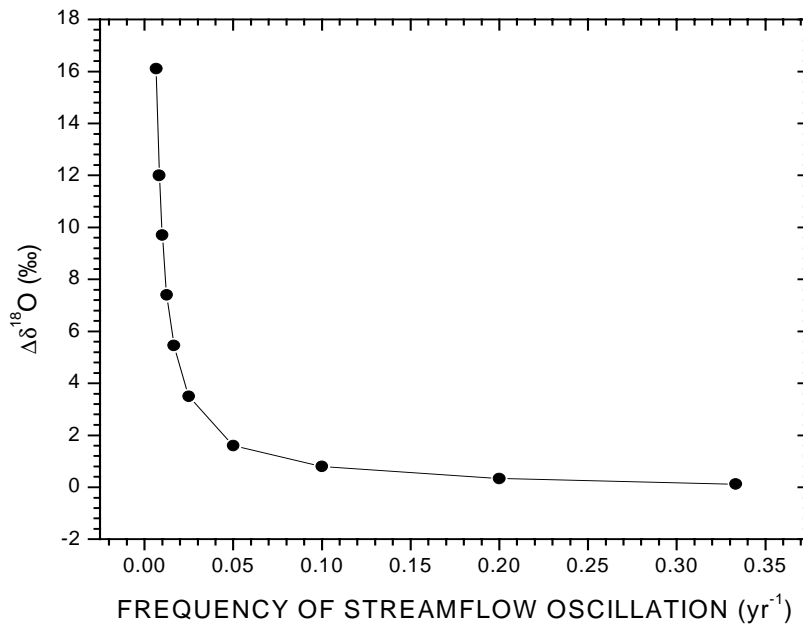


Figure 5-7. Relationship between the amplitude of oscillations in the $\delta^{18}\text{O}_L$ and the frequency component of oscillations in the Walker River discharge showing that the sensitivity of the $\delta^{18}\text{O}_L$ becomes exponentially large for lower frequency climatic forcing.

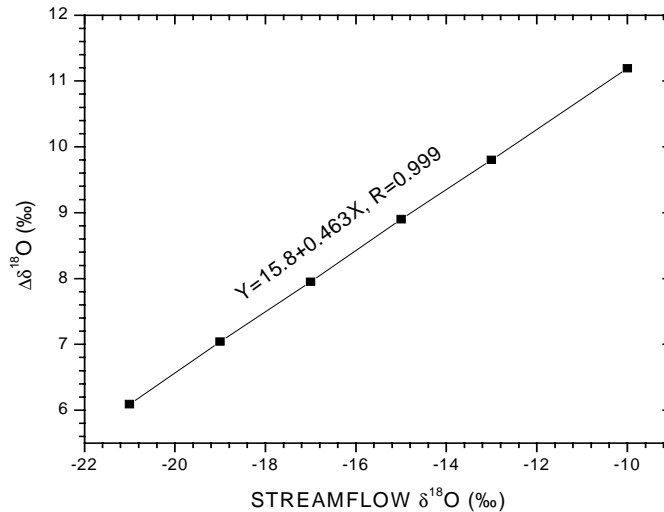


Figure 5-8. Relationship between the amplitude of oscillations in the $\delta^{18}\text{O}_L$ and the $\delta^{18}\text{O}_R$ value of the Walker River discharge showing that the sensitivity of the $\delta^{18}\text{O}_L$ is positively correlated with the value of $\delta^{18}\text{O}_R$.

In summary, changes in river discharge will lead to fluctuations in the $\delta^{18}\text{O}_L$ at different timescales, such as interannual, interdecadal, and centennial timescales. Most frequencies of variations in river discharge are reflected in the $\delta^{18}\text{O}_L$ and thereby $\delta^{18}\text{O}_C$ record and only slight changes are noticeable. The lower frequency component of the river flow signal tends to have higher spectral power in affecting the $\delta^{18}\text{O}_L$. This is consistent with observation from spectral analysis that lower frequency geophysical signal usually has larger spectral power.

5.4 Age model revision

The chronology of core WLC002 derived and presented in Chapter 4 is mainly based on nine AMS radiocarbon dates. Because of large uncertainty in conversion from radiocarbon dates to calendar ages (especially for those relatively young dates), here I use Table 1 and 2 in Stuiver et al. (1998) to reinterpret the radiocarbon dates and try to get their best probable calendar ages (Table 5-1). LH-2 in Figure 5-9 denotes the interval of interest from AD 800 to 1900, based on the age model presented in this figure. In chapter 4, it has been noted that the $\delta^{18}\text{O}$ record of Walker Lake has a great deal of similarity with the tree-ring-based Sacramento flow data over the last 1200 years. This similarity is not unexpected because both the Walker River and the Sacramento River receive water originating from the

snowmelt of the Sierra Nevada. In Appendix 2, I apply HIBAL (BENSON and PAILLET, 2002) on scaled Walker River flow data according to the Sacramento River flow records (MEKO et al., 2001) to simulate variations in the $\delta^{18}\text{O}_L$ of Walker Lake. Because the tree-ring-based Sacramento River flow record is believed to have superior advantage in age constraints, the simulated $\delta^{18}\text{O}_L$ record is therefore used as an extra age control to refine the $\delta^{18}\text{O}$ chronology of Walker Lake during the last 1200 years (Figure 5-10). Direct comparison of the simulated $\delta^{18}\text{O}_L$ and downcore $\delta^{18}\text{O}_C$ results from Walker Lake suggests that the base age (350 cm) of section LH-2 is close to AD 800 and validates the age constraints of the revised age model. The top age (40 cm) of section LH-2 is believed to be AD1900 according to the youngest radiocarbon date (CAMS 87139) and marked transition of $\delta^{18}\text{O}$ record, which was induced by a rapid lake level lowering beginning in ~1920s due to upstream impoundments and increasing water demands for irrigation. The new age model utilizes all AMS radiocarbon dates except the third and fifth points, where perturbations or turbidations might have occurred according the magnetic susceptibility and radiocarbon dates. In addition, this age model suggests that the topmost age of core WLC002 is close to AD 2000, the year when the core was extracted. This is consistent with the fact that the topmost sedimentary loss of the core is minor (ref. Figure 4-9).

Table 5-1 Revised calendar ages according to Table 1 and 2 in Stuiver et al. (1998)

CAMS Number	Section Number	Depth (cm)	^{14}C Age (yr BP)	Error (\pm yr)	Cal Year (AD/BC)	1- σ Error (yr)
87139	WLC002-5	40	35	35	1901	+5/-8
87140	WLC002-5	67	145	35	1807	+147/-135
87141	WLC002-4	84	335	35	1625	+14/-140
87142	WLC002-4	135	365	35	1495	+130/-40
87143	WLC002-3	196	695	35	1290	+90/-20
87144	WLC002-3	242	710	40	1285	+10/-20
87145	WLC002-3	267	740	45	1265	+20/-40
87146	WLC002-2	333	995	35	1025	+10/-10
87147	WLC002-1	452	2370	35	-406	+10/-10

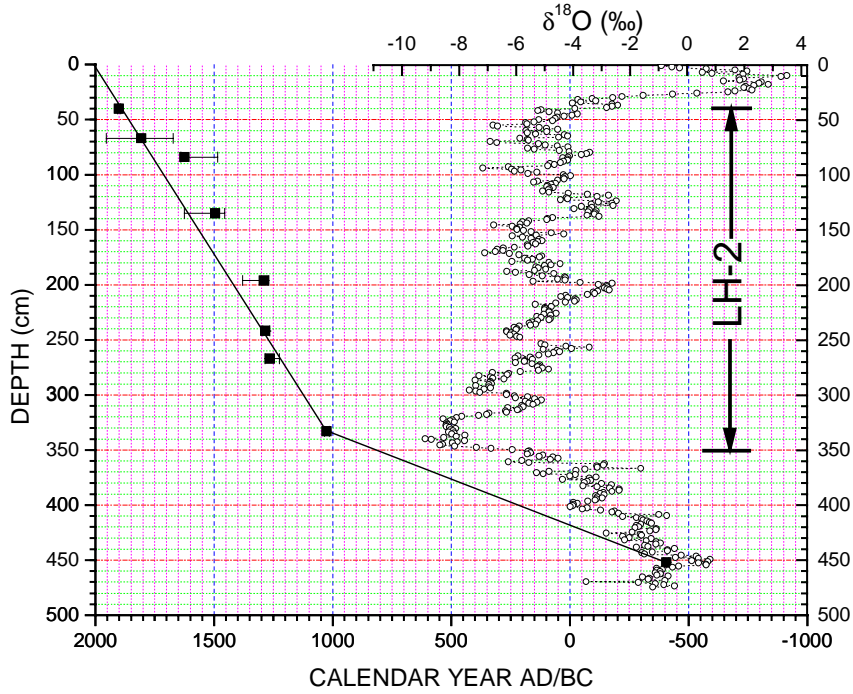


Figure 5-9 Plots of revised age model and original $\delta^{18}\text{O}$ results from Walker Lake. LH-2 denotes the interval of interest (AD 800 to 1900) according to this new age model.

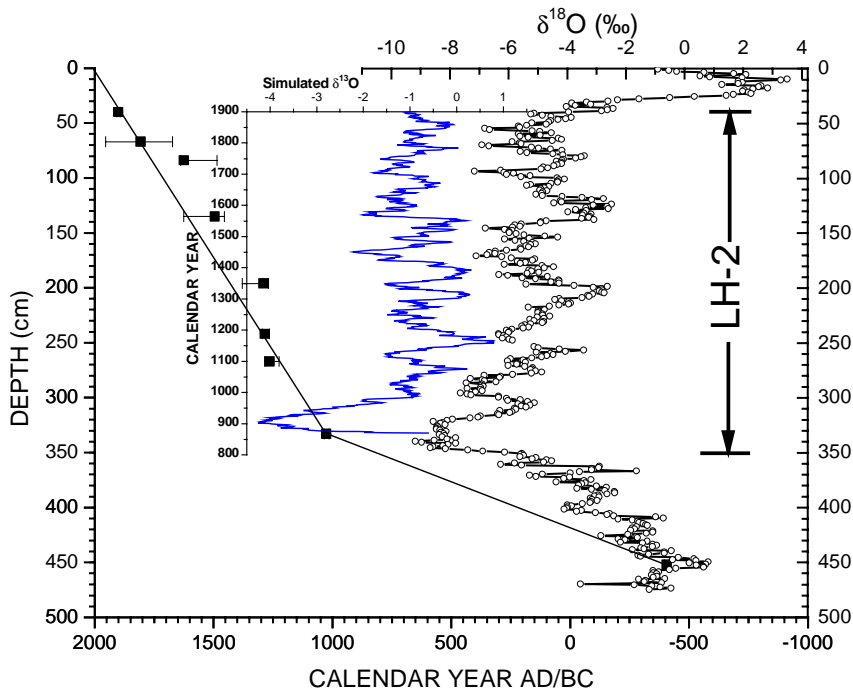


Figure 5-10 Plots of revised age model, original and simulated $\delta^{18}\text{O}$ results from Walker Lake. Embedded graph is a chronology of simulated $\delta^{18}\text{O}_L$ results of Walker Lake using the scaled Walker River flow data according to the tree-ring-based Sacramento River flow record (MEKO et al., 2001) and a hydrologic-isotopic model-HIBAL (BENSON and PAILLET, 2002).

5.5 Spectral analysis

The periodicities of a time series can be quantified through spectral analysis. The spectral analytical methods used here to identify and evaluate centennial to interdecadal variability in the Walker Lake proxy record include maximum entropy method (MEM) (BUTTKUS, 2000; HAYKIN, 1983), multitaper method (MTM) (PARK et al., 1987; PERCIVAL and WALDEN, 1993; THOMSON, 1982) and singular spectral analysis (SSA) (VAUTARD and GHIL, 1989; VAUTARD et al., 1992). MEM is based on approximating the time series by a linear autoregressive process (GHIL et al., 2002), which is very efficient at detecting frequency lines in stationary time series. However, the resolution and confidence of MEM results is dependent on the number of autoregressive (AR) terms, and for a high number of AR terms MEM often include spurious peaks. MTM reduces the variance of spectral estimates using a small set of data tapers or orthogonal window functions. The tapered time series are then Fourier transformed and a set of independent spectral estimates is computed (GHIL et al., 2002). MTM provides a corresponding statistical significance level for each independent spectral estimate, which is determined based on a red noise null hypothesis (MANN and LEES, 1996). SSA is a robust tool to decompose and reconstruct a climatic time series. The SSA technique is a variation of the classical empirical orthogonal function (EOF) analysis or principal component (PC) analysis applied to lag-correlation structures of time series. SSA decomposes time series into oscillatory patterns, trends, and noise. Spectral peaks are associated with oscillatory pairs of eigenvectors and the oscillatory components of a time series can be reconstructed using corresponding pairs of eigenvectors. The spectral analyses of MEM, MTM, and SSA used here were implemented using the SSA-MTM Toolkit (DETTINGER et al., 1995; GHIL et al., 2002).

5.6 Results and discussion

5.6.1 Interdecadal climatic oscillations

The $\delta^{18}\text{O}_\text{C}$ values of bulk inorganic carbonate sediments from Walker Lake range from -1.2 to -9.2 ‰ (PDB) during the period of 800 through 1900AD (Figure 5-9, A). The average resolution of the raw $\delta^{18}\text{O}_\text{C}$ record spanning 800 to 1900AD is 3.5 years per sample. A cubic spline is used to fit the raw

$\delta^{18}\text{O}_\text{C}$ record and the $\delta^{18}\text{O}_\text{C}$ record was extracted with a 3-year time step prior to spectral analysis. SSA is applied to decompose the $\delta^{18}\text{O}_\text{C}$ time series (Figure 5-11, B-D). The first four reconstructed components (RCs 1-4) account for 89% of the total variance. MTM spectra on RCs 1-4 indicate four dominant periodicities of 240, 90, 60, and 50 years at a confidence level of 99% (Figure 5-11, B). In addition, MTM spectral analyses on RCs 2-4 and RC 3 reveal that five cyclicities of 170, 140, 80, 60, and 50 years persist (Figure 5-11, C-D). In summary, the $\delta^{18}\text{O}_\text{C}$ record of Walker Lake spanning AD 800 to 1900 contains interdecadal fluctuations in hydrological balance that are centered around periods of roughly 90, 80, 60, and 50 years. It is noteworthy that two interdecadal periodicities that centered around 50 and 60 yr are present in all three reconstructions (RCs 1-4, RCs 2-4, and RC3).

Because there exists a great deal of similarity between the $\delta^{18}\text{O}_\text{C}$ record of Walker Lake and the tree-ring-based Sacramento River flow reconstructions (MEKO et al., 2001), spectral analysis on the tree-ring-based Sacramento River flow record has been performed to confirm or deny the interdecadal fluctuations in hydrologic balance. Unlike SSA on the $\delta^{18}\text{O}_\text{C}$ record of Walker Lake, the first eight reconstructed components (RCs 1-8) only account for 13.2 % of total variance. However, interdecadal (50-90 yr) oscillations are also present in the reconstructed Sacramento River flow record spanning AD 869 to 1900 (Figure 5-12).

Decadal to interdecadal modes of climatic variability are also detected in the carbonate record from Lake Turkana, Kenya during the last 4,000 years (HALFMAN et al., 1994), the $\delta^{13}\text{C}$ profile of *Globigerinoides ruber* from Gallipoli Terrace, Ionian sea over the last millennium (CINI CASTAGNOLI et al., 2002), and Nile River historical discharge record during AD 622-1470 (DE PUTTER et al., 1998). However, it is debatable whether decadal and interdecadal modes of climatic variability are induced by external forcing (solar radiative forcing) or internal forcing (ocean-atmospheric interactions). For example, the low-frequency interdecadal oscillations that are close to the 90-yr period are usually associated with the 88-yr Gleissberg cycle (EDDY, 1976) seen in sunspot and ^{14}C data (DAMON and SONETT, 1991). Global high-resolution paleoclimatic records reveal periodicities near 11, 18.6 and 22

yr that are in general attributed to an 11-yr sunspot, 18.6-yr lunar nodal, and 22-yr double sunspot cycles (CURRIE and FAIRBRIDGE, 1985; HALFMAN et al., 1994; MORNER and KARLEN, 1984). However, a coral-based SSTs record from the South Pacific (LINSLEY et al., 2000) suggested that some of the decadal oscillations observed in the Pacific Ocean might be ascribed to tropical forcing. Model experiments (LATIF and BARNETT, 1994) also suggested that about one-third of the low-frequency climate variability over the North Pacific and North America could be attributed to a cycle induced by ocean-atmospheric interactions. Minobe (1997) proposed that the interdecadal variability (50-70 yr) were likely to be an internal oscillation in the coupled atmosphere-ocean system.

More recently, Benson et al (2003b), based on Mono Lake $\delta^{18}\text{O}$ and its association with other PDO-related signals, suggested that the wetness of the Sierra Nevada was linked with the sign of PDO over the past three centuries. The Sacramento River discharge and the Walker Lake $\delta^{18}\text{O}$ records are compared with the Santa Barbara $\delta^{18}\text{O}$ record from *Neogloboquadrina dutertrei* (Figure 5-13). The Santa Barbara $\delta^{18}\text{O}$ signal was interpreted to reflect thermal fluctuations in the coastal California. The ^{18}O -enriched signatures of *N. dutertrei* usually indicate cold SSTs along the coastal California. Interestingly, most of cold SSTs events that occurred in the Santa Barbara Basin coincided with the Sierra droughts recorded in the Walker Lake $\delta^{18}\text{O}$ and tree-ring records (Figure 5-13). For example, the pervasive Sierra drought that occurred around AD 1100 (STINE, 1994) almost coincided with the cold SSTs in the Santa Barbara Basin. Conversely, the Sierra Nevada tended to receive more moisture during the periods with warm SSTs of the Santa Barbara Basin over the last millennium. Moreover, spectral analysis on the Santa Barbara $\delta^{18}\text{O}$ record suggested interdecadal thermal fluctuations (55, 70, and 90 yr) persisted in the interval spanning AD 1030 to 1905 (FIELD and BAUMGARTNER, 2000).

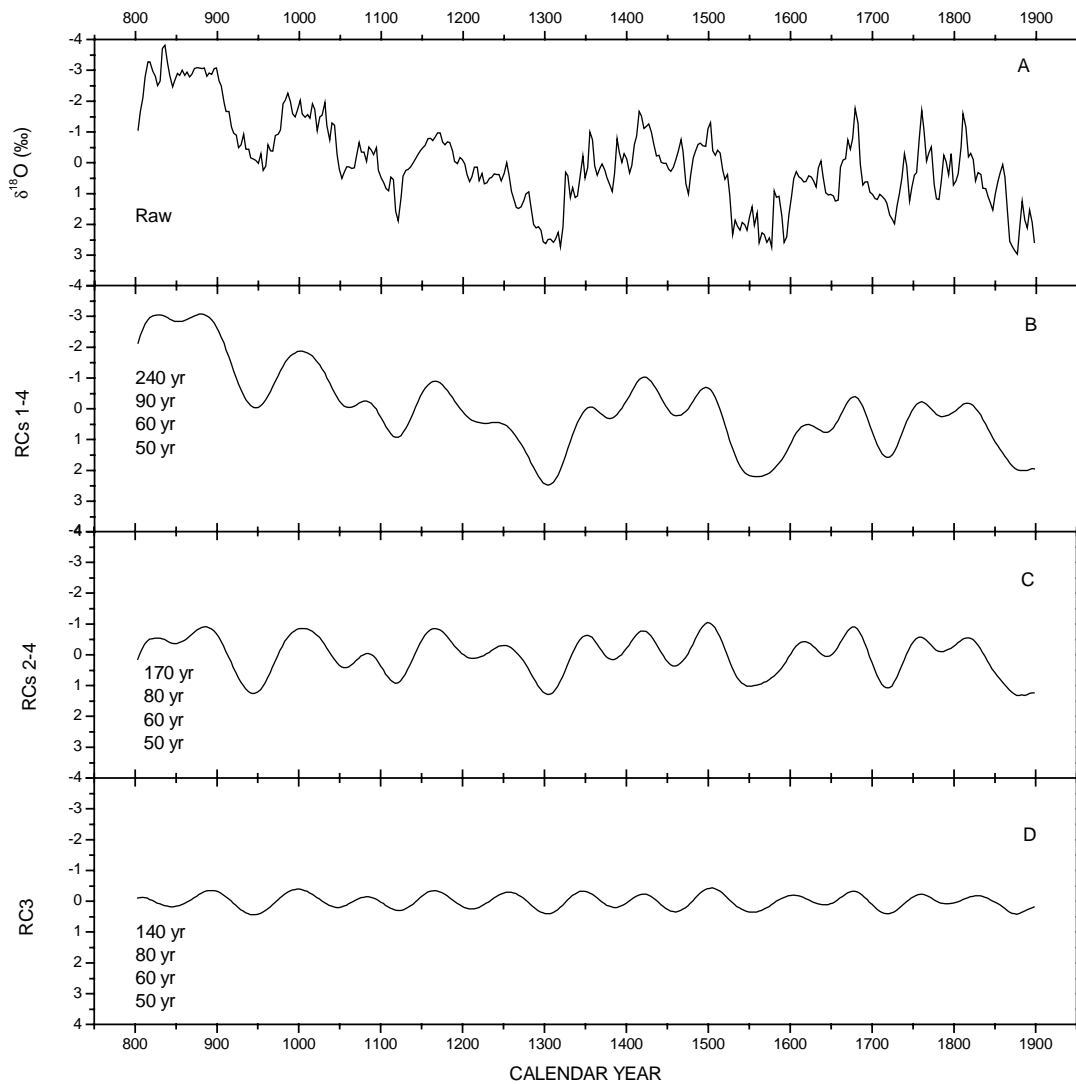


Figure 5-11. Singular spectrum analysis (SSA) (DETTINGER et al., 1995; VAUTARD and GHIL, 1989) on time series from Walker Lake for the intervals from 800 to 1900AD. A: Raw centered $\delta^{18}\text{O}_C$ record of bulk inorganic carbonate sediments. B: First four reconstructed components (RCs 1-4) derived from SSA. A cubic spline is used to extract the $\delta^{18}\text{O}_C$ data every 3-yr prior to SSA and SSA is implemented using the SSA-MTM Toolkit 4.1 (DETTINGER et al., 1995; GHIL et al., 2002). Window length N is 36. The first four RCs together account for 89% of total variance and have significant frequency lines of 240, 90, 60, and 50 yr. These frequency lines are detected using MultiTaper method (MTM) (PARK et al., 1987; PERCIVAL and WALDEN, 1993; THOMSON, 1982). C: The second to fourth reconstructed components (RCs 2-4) of SSA representing 27% of total variance and having dominant periodicities of 170, 80, 60, and 50 yr. D: The third reconstructed component (RC 3) accounting for 6.8 % of total variance and having dominant cyclicities of 140, 80, 60, and 50 yr.

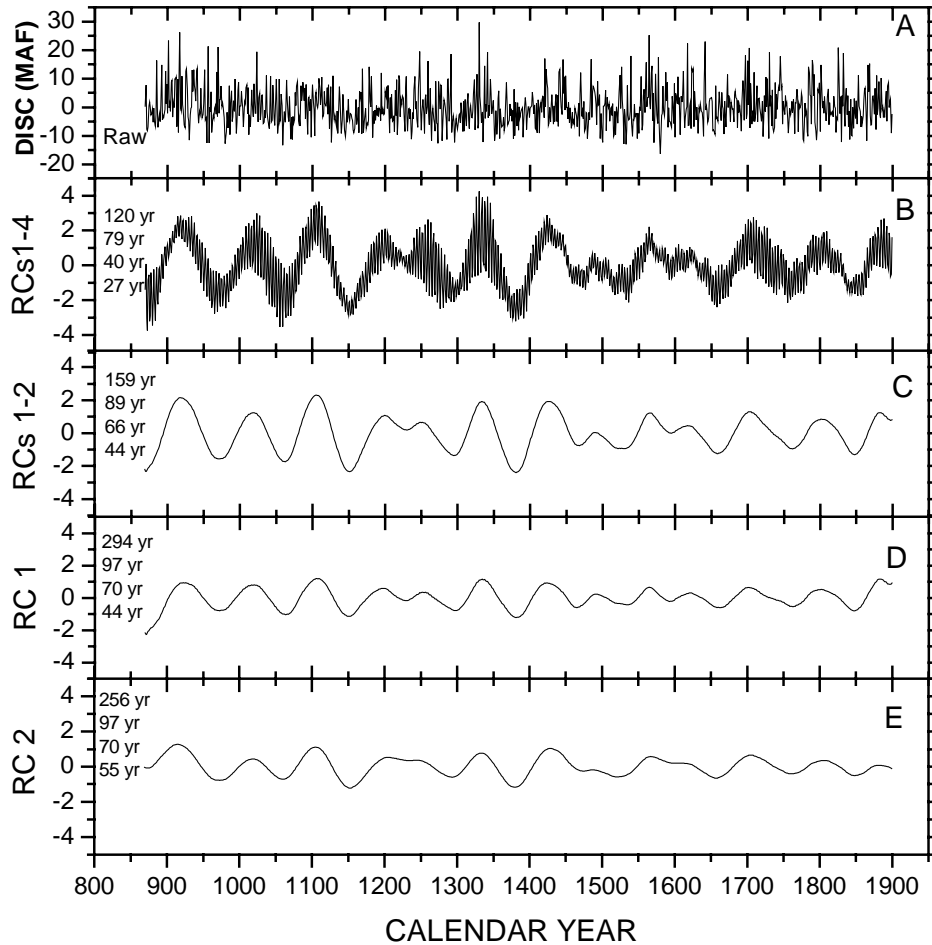


Figure 5-12. Singular spectrum analysis (SSA) (DETTINGER et al., 1995; VAUTARD and GHIL, 1989) on time series of the tree-ring based Sacramento River for the intervals from AD 869 to 1900. A: Centered river flow record (MEKO et al., 2001). MAF denotes million acre feet. B: First four reconstructed components (RCs 1-4) derived from SSA. SSA is implemented using the SSA-MTM Toolkit 4.1 (DETTINGER et al., 1995; GHIL et al., 2002). Window length N is 103. The first four RCs together account for 7.0 % of total variance and have significant frequency lines of 120, 79, 40, and 27 yr. These frequency lines are detected using MultiTaper method (MTM) (PARK et al., 1987; PERCIVAL and WALDEN, 1993; THOMSON, 1982). C: The first two reconstructed components (RCs 1-2) of SSA representing 3.6% of total variance and having dominant periodicities of 159, 89, 66, and 44 yr. D: The first reconstructed component (RC 1) accounting for 1.85 % of total variance and having dominant cyclicities of 294, 97, 70, and 44 yr. E: The second reconstructed component (RC 2) accounting for 1.77% of total variance and having dominant periodicities of 256, 97, 70, and 50 yr.

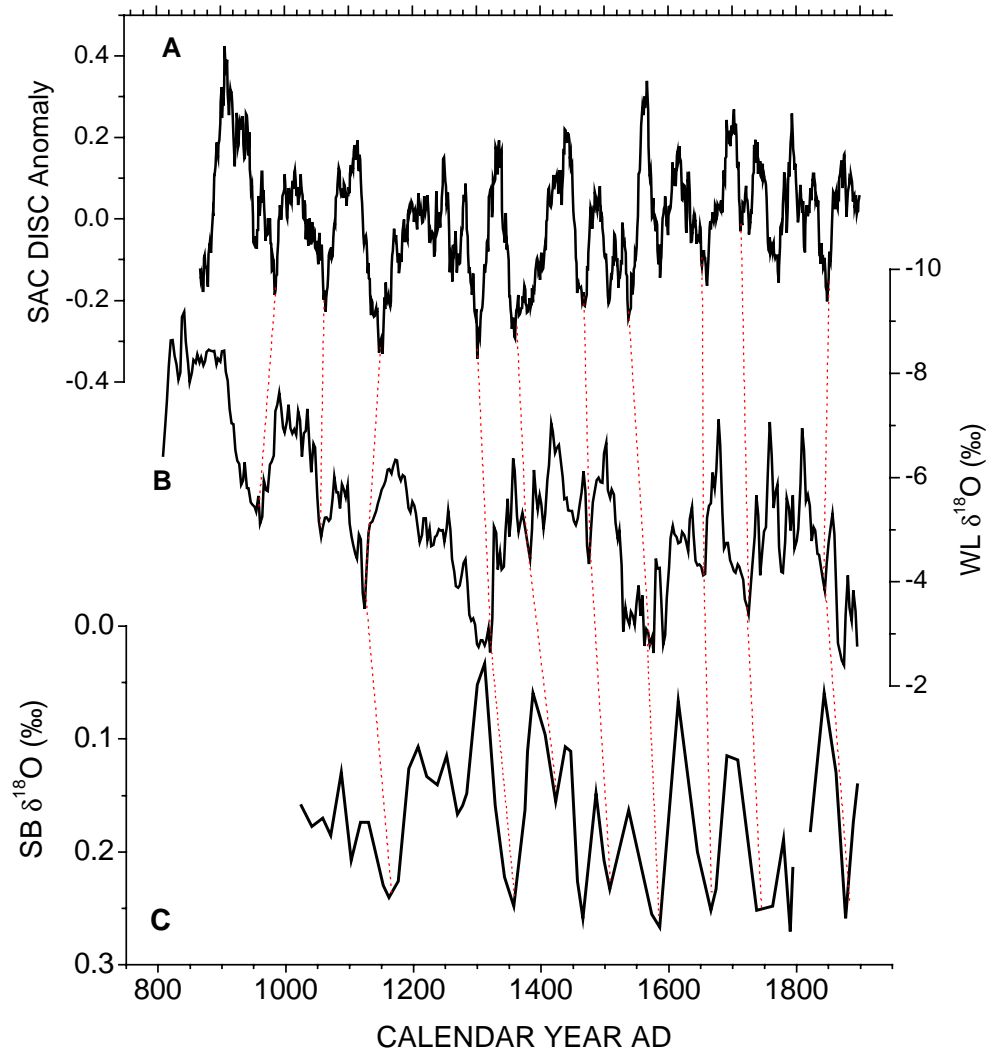


Figure 5-13 Comparison of the tree-ring reconstructed Sacramento River flow (MEKO et al., 2001), Walker Lake $\delta^{18}\text{O}$, and Santa Barbara $\delta^{18}\text{O}$ records (FIELD and BAUMGARTNER, 2000). The Sacramento discharge anomaly (upper panel: A) is calculated using the reconstructed river flow data and the Santa Barbara $\delta^{18}\text{O}$ record (lower panel C) is Lowess smoothing ($\ell=0.04$) of average *N. duterrei* $\delta^{18}\text{O}$ values (see Figure 7b in Field and Baumgartner, 2000).

Although the variance concentrations detected from the Walker Lake $\delta^{18}\text{O}$, the Sacramento River discharge, and the Santa Barbara $\delta^{18}\text{O}$ records are not exactly the same, most of them are within 50-70 yr, the most energetic periodicities of PDO-related climate variability (MINOBE, 1997). The fact that these two proxy records in the Sierra regions are almost in phase with fluctuations in the California Current suggests that the climate of the Sierra is linked the dynamics of the Pacific Ocean. During the

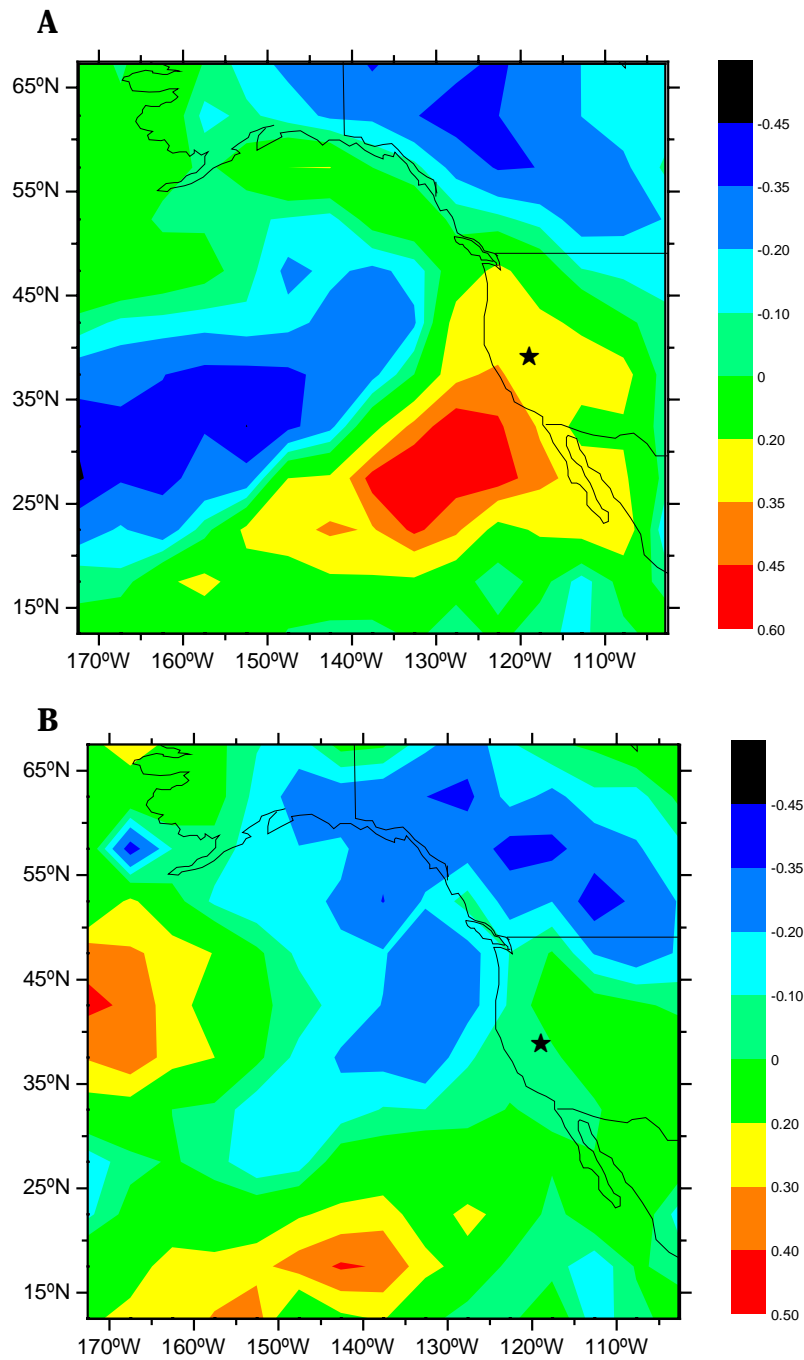


Figure 5-14 Regression analysis of the winter mean (January, February, and March) $5^{\circ} \times 5^{\circ}$ surface temperature (HadCRUTv dataset) against the West Walker River discharge during the positive PDO phase of 1978 to 2000 (A) and the negative PDO phase of 1948-1977 (B). Stars denote the geographical location of the Walker Lake Basin.

positive phase of PDO, wind stress field (WSF) appears to favor in delivering more moisture inland, weaken the California Current and coastal upwelling, and therefore create warm SSTs along coastal California. On the contrary, during the negative phase of PDO, WSF favors in strengthening the California Current and coastal upwelling, and leading cold SSTs along coastal California. As a result, WSF favorable in the Sierra moisture delivery is likely weakened and/or diverted.

As mentioned in Chapter 1, instrumental climatological data suggest that the wetness of the Sierra Nevada is linked with PDO on decadal time-scales even there is no robust correlation between the Sierra runoff and the PDO index on yearly base over the past 50-60 years. Detailed regression analyses of winter mean (January, February, March) surface temperature ($5^{\circ}\times 5^{\circ}$) against the West Walker River (WWR) flow reveal that the calendar-yearly WWR discharge was influenced by the SSTs of the North Pacific and surface air temperatures of Northwestern America (Figure 5-14). There were apparently three high correlation coefficient centers during the PDO positive phase, when the winter precipitation (snowfall) in the Sierra Nevada was positively correlated with the SSTs of the California Coast and negatively correlated with the SSTs of the central gyre. These correlations are statistically significant at the 95% confidence level. However, the mid-latitude storm track plays an important role in affecting on the winter precipitation in the Sierra Nevada either in the positive PDO phase or the negative PDO phase. This is related to the polarwards displacement of the mid-latitude storm track during the relatively warmer years and therefore less moisture reaching in the Sierra regions (STINE, 1994). Particularly, during the negative PDO phase, the surface air temperature of the Northwestern America became the primary factor in affecting on the snowfall of the Sierra Nevada.

5.6.2 Centennial timescale variability

Spectral analyses on the Walker Lake $\delta^{18}\text{O}$ and the reconstructed Sacramento River flow also revealed that centennial timescale climate and hydrologic oscillations that were centered around 120, 150, and 240 years persisted over the interval of AD 800 to 1900 (Figure 5-10 and 5-11). Century-scale modes of climatic variability have also been extracted in a variety of paleoclimatic records such as tree rings, ice

cores, marine and lacustrine sediments. For examples, the ^{14}C record from tree rings shows a pronounced 126-yr peak in the past 4000 years (STUIVER and BRAZIUNAS, 1993). A 2100-yr lake sediment-based salinity record from Rice Lake, a closed-basin lake in the northern Great Plains exhibits significant periodicities of 400, 200, 130 and 100 yr (YU and ITO, 1999).

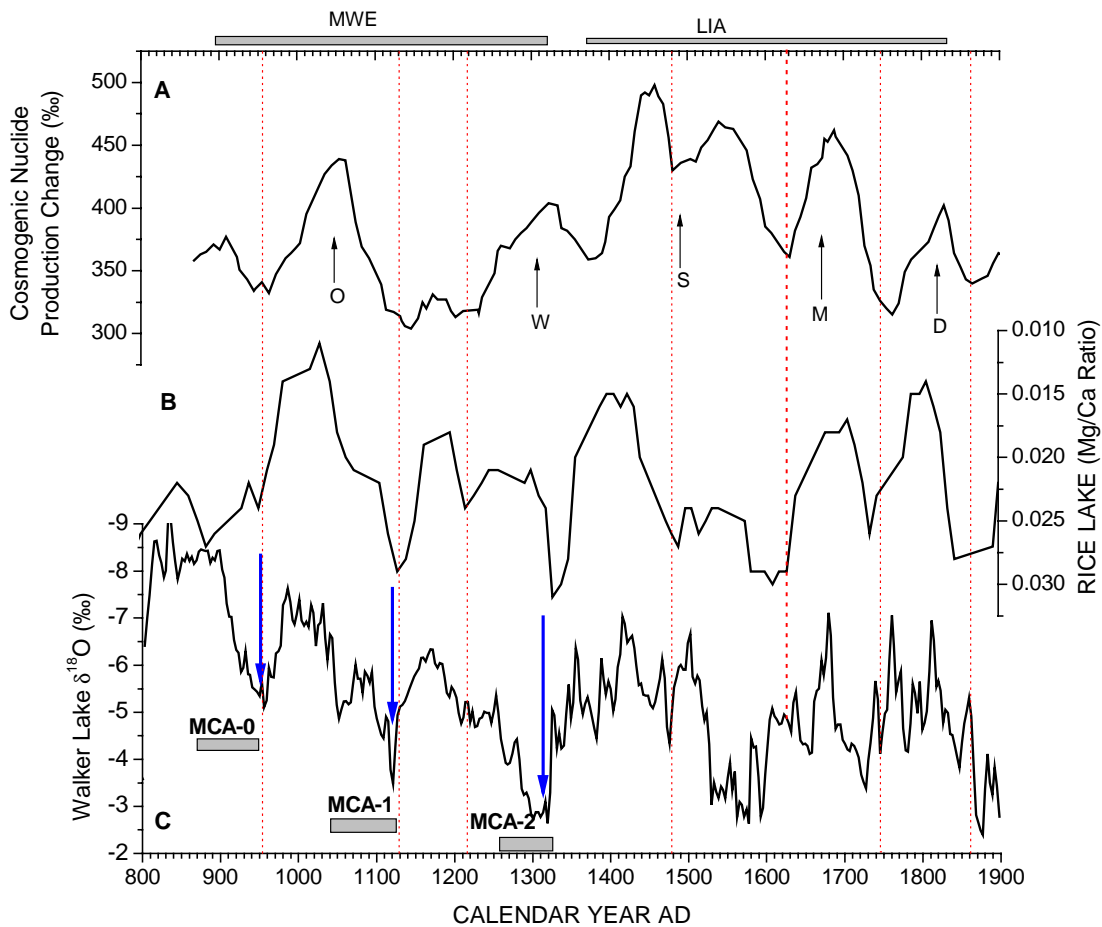


Figure 5-15. Correlation of paleoclimate and paleo-solar proxies. A) The record of the cosmogenic nuclide production changes (BARD et al., 2000; BARD et al., 2003). B) Mg/Ca molar ratio record from Rice Lake (YU and ITO, 1999). C) The $\delta^{18}\text{O}_\text{C}$ record of Walker Lake. Minima of solar activity: D-Dalton (1810 AD), M-Maunder (1645-1715), S-Spörer (1420-1530), W-Wolf (1280-1340), and O-Oort (1010-1050) (BARD et al., 2000; EDDY, 1976). MWE-Medieval Warm Epoch, LIA-Little Ice Age. Vertical dotted lines denote probable correlations among these records and three major arrows symbolize terminations of three major droughts that occurred during the MWE. MCA-Medieval Climate Anomaly. Note that MCA-1 (AD910-1110) and MCA-2 (AD 1210-1350) were previously proposed by Stine (1994).

It is recognized that the climate of the last millennium contained centennial to multicentennial variability that was characterized by the Medieval Warm Epoch (MWE) and the Little Ice Age (LIA) (LAMB, 1965). In the western United States, Stine (1994) described compelling evidence that two prolonged droughts persisted during the MWE. These two drought events are also recorded in the $\delta^{18}\text{O}$ record of Walker Lake (see Figure 5-15), and the timings of drought terminations are very close to those described by Stine (STINE, 1994). Moreover, these two pronounced droughts likely affected the Great Plains because the Mg/Ca molar ratio suggested low stands of Rice Lake, North Dakota during the MWE (FRITZ et al., 2000; YU et al., 2002). In addition, the $\delta^{18}\text{O}$ record of Walker Lake suggested that there were two short-life (60-80 yr) wet events during the first drought described by Stine (1994). This feature is also identifiable in the Mg/Ca ratio record of Rice Lake (see figure 5-15). The relatively wet events that occurred in the drought intervals of AD 910 to 1110 coincided with the sunspot minimum of Oort. The relatively good visual correlations among the ice-core based cosmogenic nuclide production, the Rice Lake Mg/Ca ratio, and the Walker Lake $\delta^{18}\text{O}$ records suggested that solar radiative activity played an important role in regulating lake levels on centennial timescales. The cosmogenic nuclide production is controlled by solar activity. When solar activity is high, the extended solar magnetic sweeps through interplanetary space and therefore more effectively shields the Earth from cosmic rays and reduces cosmogenic production (VAN GEEL et al., 1999). Low solar activity lets more cosmic rays enter the Earth's atmosphere and induces more cosmogenic production. The best-known low solar activity event is the Maunder Minimum (1645-1715) that coincided with the coldest times of the LIA (EDDY, 1976). The sun during the Maunder Minimum was 0.25% less bright than it was during the solar minimum of 1985-1986 (LEAN et al., 1992). Model experiment suggested that a lowering of 0.25% solar irradiance would lead to a global cooling of ~ 0.5 °C (RIND and OVERPECK, 1993). Changes in global temperature have an effect on the ocean-atmospheric circulations. Stine (1994) proposed that the mid-latitude storm track of the northern hemisphere likely remained to the north of California during the MWE, resulting in a less snowfall scenario in the Sierra Nevada. During the LIA,

because of an expansion of the circumpolar vortex, the mid-latitude storm track displaced southwards, leading to a more snowfall scenario in the Sierra Nevada. In addition, Lake Naivasha, an equatorial African lake, also recorded a drier climate than today during the MWE on the basis of a lithologic and diatom inferred salinity record (VERSCHUREN et al., 2000), indicating changes in solar irradiance played an important role in long-term moisture variability in this region.

In summary, the $\delta^{18}\text{O}$ record of Walker Lake documented centennial to interdecadal timescale variability over the interval of AD 800 to 1900. Oscillations in hydrologic balance of the lake basically reflect snowfall variability in the Sierra Nevada. At least, some century timescale oscillations may be attributed to changes in solar irradiance due to a great deal of similarity between ice-core-based cosmogenic production and the Walker Lake $\delta^{18}\text{O}$ records. Meanwhile, PDO-like interdecadal climate variability that centered on 60-80 yr persisted over the period of AD 800 to 1900. This PDO-like mode of climate variability was intimately linked with alterations in the California Current, indicating some of interdecadal oscillations were induced by ocean-atmosphere interactions.

APPENDIX 1 A WINDOWS PROGRAM FOR PALEOLAKE LEVEL RECONSTRUCTION FROM THE OXYGEN ISOTOPIC RECORD OF CLOSED- BASIN LAKE CARBONATES

A1.1 Abstract

A windows-based program has been developed to reconstruct past lake surface level changes from the oxygen isotopic composition ($\delta^{18}\text{O}$) record of carbonates in sediments from closed-basin lakes in arid-semiarid regions. The software program consists of three major integrated modules: a data acquisition and validation module, a model parameter settings module, and a modeling module. The modeling module includes three components: a hydrologic mass balance model, an isotopic mass balance model, and a paleolake level recovery model. These three modeling components work sequentially. The first two modeling components are designed to define modern hydrologic and isotopic systems in the study area by using historic daily stream gauge readings and modern observations of lake water $\delta^{18}\text{O}$ changes. The last modeling component is a tool to recover paleolake level changes based on the $\delta^{18}\text{O}$ record derived from the carbonate component of lake sediments. The software program provides a user-friendly visual interface that facilitates the input of modern hydrologic and isotopic data and the modeling of past lake surface level changes.

A1.2 Introduction

Closed-basin lakes have long been recognized as the potential informative source of terrestrial paleoclimate given their sensitivity to changes in hydrologic budget (METCALFE, 1997). The variability of closed-basin lake surface level changes in arid-semiarid regions is an effective climatic index in prehistoric times. Lake surface level changes are strongly connected with the lake water $\delta^{18}\text{O}$ (BENSON and PAILLET, 2002; HOSTETLER and BENSON, 1994) that is preserved in the carbonate fraction of closed-basin lake sediments (BENSON and PAILLET, 2002; LI and KU, 1997a; RICKETTS and

ANDERSON, 1998). In closed-basin systems most lake levels fluctuate on a seasonal to interannual timescale. Some lakes even have experienced large surface level drawdown over the past century (LI and KU, 1997a; RICKETTS and ANDERSON, 1998). In some cases, historic stream gauge readings and lake level changes have been documented back to the beginning of the last century. Coupled with modern stream and lake water $\delta^{18}\text{O}$ observations, this provides a unique opportunity to establish a linkage between lake surface level changes and lake water $\delta^{18}\text{O}$ variations. For those closed lakes whose hydrologic settings are relatively simple to define, this linkage can be used to reconstruct the past lake level changes by applying the $\delta^{18}\text{O}$ record of lake carbonate sediments.

One-dimension hydrologic mass balance models, either steady state or dynamic, have been well developed and successfully applied to lakes to define key components (typically evaporation) of hydrologic settings (MILNE, 1987). Also, several models based on isotopic mass balance have been proposed and applied in arid-semiarid closed-basin lakes (BENSON and PAILLET, 2002; HOSTETLER and BENSON, 1994; LI, 1995a; RICKETTS and ANDERSON, 1998). Current hydrologic and isotopic models can essentially be separated into homogeneous and heterogeneous models. In heterogeneous models (BENSON and PAILLET, 2002) the seasonal limnological stratification has been taken into account. Generally speaking, limnological stratification depends on lake physical settings, such as water depth, lake size, current vector, surface wind speed, thermal structure of water column, etc. Some of these physical properties are hard to constrain before the instrumental record. Since many medium to small-sized closed-basin lakes are relatively shallow and well mixed, especially in the winter season when the temperature gradient of water column is relatively small, lake water $\delta^{18}\text{O}$ is close to homogeneous. In comparison with open lake systems, however, most closed-basin lakes have much longer resident time accommodating water mixing. A homogeneous model is more effective in some closed-basin lakes where seasonal stratification is weak or absent. A few studies based on the homogeneous model have been reported (BENSON and PAILLET, 2002; LI, 1995a; RICKETTS and ANDERSON, 1998). This program adopts the homogeneous model.

However, most models developed to date have usually been designed for a specific lake. To attempt to broaden and facilitate the use of hydrologic and isotopic models, I have designed and implemented a windows-based program that is applicable to all closed-basin lakes where seasonal stratification is weak. The program provides a user-friendly visual interface in which the user defines two model parameters, an evaporation rate (E) and the fraction of advected air (f_{ad}). The model uses daily stream gauge readings as the primary input, and historic lake level and water $\delta^{18}\text{O}$ records as references for the hydrologic and isotopic mass balance modules. Since there are seven tables of program inputs and some of them can have a great number of records, such as daily stream gauge readings, the program adopts the Microsoft Access Database management strategy to handle the input data. The program offers its own data inputting, importing from an ASCII file, and editing interface. Also, it provides a module to export the modeling results to an ASCII file. This file can be easily loaded into Microsoft Excel or other professional plotting software for construction of different graph format.

A1.3 Program description

The application runs on modern IBM compatible PCs, with a single Pentium processor and a Windows 98, ME, 2000, NT, or XP operating system. The minimum system requirements are Pentium II 200 MHz processor, 32 MB RAM, and 20 MB of available disk space. These specifications may vary depending on the amount of input data and chosen model running step. The graphic user interface consists of three major components, data acquisition and validation, model parameter values and physical settings, and the modeling modules (fig. 1).

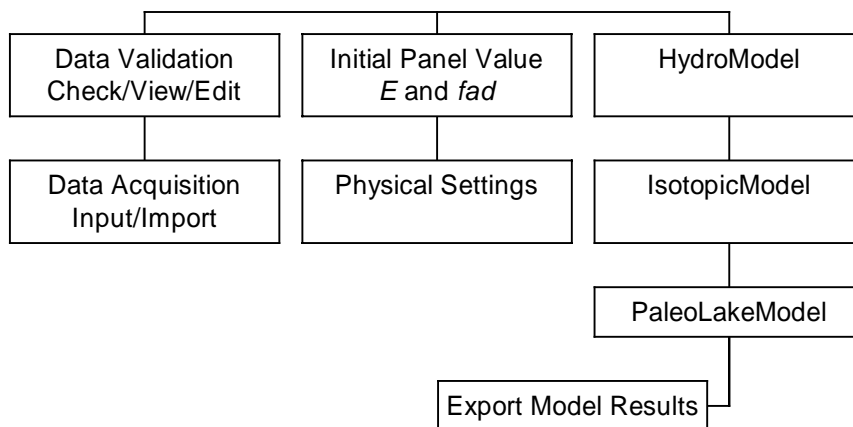


Fig. A1-1. A block diagram lists the major modules or components of the program. The left column functions as data acquisitions and validations. The middle column consists of two components; the physical settings (such as lake geometry) and tuning parameters (such as model parameters and model interval of interest). The right column includes three key modules plus a data export module.

A1.3.1 Data acquisition and validation

The model assumes that the following aspects of information are available; the lake geometry, the historic lake surface levels, daily stream gauge readings, the $\delta^{18}\text{O}$ of stream and lake water, the $\delta^{18}\text{O}$ record of lake carbonate sediments, and its corresponding age control. Usually, hydrologic models use polynomial equations to define the relationships between surface area, volume and lake water depth (BENSON and PAILLET, 2002). Instead, this program applies the spline interpolation technique to get the corresponding value. In the Data submenu, the program gives a graphic interface to compare the spline curve with that measured.

The record of historic stream gauge readings is the primary input variable for the hydrologic and isotopic mass balance modeling modules. This program uses the daily stream flow readings. The unit is in cubic feet per second (cfs). In the case of multiple stream inputs into the same lake, the sum of these stream gauge readings is applied.

The historic lake surface level (elevation) record is used as key references for hydrologic mass balance and paleolake level recovery modeling modules. In the hydrologic mass balance module the model uses this record as a baseline to determine the mean annual evaporation rate, while in the

paleolake level recovery module the model uses it as criteria to validate the model results. Lake surface level is input in meters above sea level. The $\delta^{18}\text{O}$ record of lake water is one of the most important parts of the input dataset and limits the applicability of this model to lakes where this data exist. The quality and length of the lake water $\delta^{18}\text{O}$ record directly affects the confidence interval of the model results. In the isotopic mass balance module the model uses this data as reference to define the fraction of advected air (f_{ad}). Its unit is in per mil (SMOW).

The carbonate $\delta^{18}\text{O}$ record is generally derived from the total inorganic carbon fraction (TIC) of sediments. Since most closed-basin lakes are saline, I recommend using deionized water to wash the sediments to remove salts, and then remove the organic matter by 2.5% HClO or 15% H₂O₂ before isotopic analysis (BENSON et al., 2002; LI et al., 2000). TIC $\delta^{18}\text{O}$ units are per mil (PDB).

Usually calibrated ²¹⁰Pb or ¹⁴C dates are used as age control. In the model, age unit is in years AD. The model automatically generates a time series of carbonate $\delta^{18}\text{O}$ record by using this age control and the raw carbonate $\delta^{18}\text{O}$ record. This time series serves as a basic input for the paleolake level recovery module.

The program gives an interface to display the input or imported data in graph or table format that facilitates the user to check, modify and validate the original dataset.

A1.3.2 Model parameters and physical settings

There are two model parameters (E and f_{ad}) that are defined by the model itself. The hydrologic and isotopic mass balance models determine E and f_{ad} , respectively. The program offers an interface to input physical settings (fig. 2). There are four types of information that need to be input; geometric, hydrologic, isotopic and dynamic parameters. For the hydrologic mass balance modeling, only geometric and hydrologic settings are needed. Obviously, the lake becomes dry when lake surface level reaches to the lake bottom elevation. On the other hand, the lake becomes an open lake system when its surface level exceeds the spill sill level. These two parameters are used as physical constraints to assure that the modeling processes are strictly under a closed-lake system. The fraction of stream water

(f) stands for the fraction of water that actually flows into the lake of interest since there maybe some water loss between the gauge station and the lake inlet. The isotopic and dynamic parameter settings are designed for the isotopic mass balance and paleolake level recovery models, which are not visible at the first stage of modeling, i.e. the HydroModel. The $\delta^{18}\text{O}$ of free air vapor, on-lake precipitation, and stream water need to be clear. For those lakes with multiple stream inlets, the stream $\delta^{18}\text{O}$ value should be the weighted average. α_{kin} is the kinetic fractionation factor, and the mean annual surface temperature, precipitation and relative humidity (RH) can be obtained from the local weather station. These values are stored in the same database file of the input dataset.

The screenshot shows a 'Settings...' dialog box with four sections:

- Geometric:**
 - Elevation of Lake Bottom m ASL: 1171.5
 - Spill Elevation m ASL: 1308.0
- Hydrologic:**
 - Fraction of Stream Water (f): 0.90
 - Precipitation (P) in cm: 12.7
 - Relative Humidity(%): 68
 - Evaporation (E) in cm: 140.0
- Isotopic:**
 - $\delta^{18}\text{O}$ of Stream Water (Ds): -13.6
 - $\delta^{18}\text{O}$ of Precipitation (Dp): -10.0
 - $\delta^{18}\text{O}$ of Free Air Vapor (Da): -21.0
- Dynamic:**
 - Temperature (T) in Degree C: 10.0
 - Kinetic Fractionation Factor (α_{kin}): 0.994

Buttons at the bottom: OK, Advance, Cancel.

Figure A1-2. A model parameter settings panel consists of four categories: geometric, hydrologic, isotopic, and dynamic settings.

A1.3.3 Modeling modules

This program integrates three modeling modules: hydrologic mass balance model (HydroModel), isotopic mass balance model (IsotopicModel), and paleolake level recovery model (PaleoLakeModel). The details of mathematical derivation are discussed in Appendix 2. These models work in a sequential fashion from the HydroModel to the IsotopicModel to the PaleoLakeModel. In the HydroModel, the program gives a graphic interface to define the key component of hydrologic setting, E . This is determined by fitting the lake surface level modeled with that observed. The model works in both directions, forward and backward. Once a good evaporation rate is selected, the modeled lake level curve usually fits the observed one well in both modes. If this is not the case, the hydrologic system of interest is not well defined. In other words, there may be other water sources or sinks in the system, such as groundwater discharge and recharge. This program does not take the groundwater input or output into account.

Provided that the hydrologic system appears to be adequately modeled, the IsotopicModel module is ready to define the isotopic behavior of the system. The $\delta^{18}\text{O}$ of lake water is affected by the $\delta^{18}\text{O}$ and fluxes of stream water, on-lake precipitation, and evaporation. The $\delta^{18}\text{O}$ of water vapor leaving lake surface is a function of the $\delta^{18}\text{O}$ of lake water, f_{ad} , relative humidity, and surface water temperature (BENSON and PAILLET, 2002; BENSON and WHITE, 1994). Most of them are measurable and kept constant in the model. f_{ad} is hard to measure and is defined through the IsotopicModel. The IsotopicModel uses the same technique as the HydroModel by fitting the predicted lake water $\delta^{18}\text{O}$ change curve with that observed. Also, it works in both directions to determine f_{ad} . The confidence or the quality of this determination depends on the length of the lake water $\delta^{18}\text{O}$ record.

Finally, using the $\delta^{18}\text{O}$ record of lake carbonates with the above parameters determined, the PaleoLakeModel can reproduce the lake level changes in the past. The historic lake level change record here is used as criteria to validate the model. Theoretically, it can only work backward as the lake level is unknown for the past. However, we can also assume the lake level in the past based on the predicted

curve produced by the backward method and run the model in forward mode again. Both methods should produce similar results of lake surface level changes in the past. Otherwise, there may be unknown perturbation, such as sediment bioturbation, lake sediment reworking, the accuracy of age controls, etc.

A1.4 Discussion

This software application was written specifically to facilitate data acquisition, model parameter settings, and hydrologic and isotopic modeling. The software program stores all data including model parameter settings in a Microsoft Access *.mdb file and uses the same jet database engine as Microsoft Access 2000. This enables the program to handle a large amount of input data and its data file format is completely compatible with Microsoft Access. In addition, the import module facilitates the input of lake system parameters and the export module enables the user to use additional plotting software to reproduce the graph of the model results.

Usually, most hydrologic models will accumulate the error when model goes away from the initial point. As this program adapts from two methods, forward and backward, this greatly reduces the accumulative error if the system is well defined. Successful application of this program relies on the quality of input dataset and the extent of knowledge of the system of interest.

All of the source codes are written in Visual Basic 6.0 and most of the program routines and modules are hardware-independent. A trial version of this software package is available online (<http://www.albany.edu/~fy7247>). The program runs in Windows 98/NT/ME/2000/XP operating system.

APPENDIX 2 RECONSTRUCTION OF LATE HOLOCENE EFFECTIVE MOISTURE AVAILABILITY IN THE WALKER LAKE BASIN

A2.1 Abstract

The oxygen isotopic signal ($\delta^{18}\text{O}$) preserved in down-core carbonate sediments has been analyzed in numerous studies to extract information on hydrologic and climatic conditions of the past. Since change in the $\delta^{18}\text{O}$ value of lake water ($\delta^{18}\text{O}_L$) in a closed-basin lake is not a simple function of the amount of change in lake level (or volume), the interpretation of the $\delta^{18}\text{O}$ preserved in down-core lacustrine proxy carbonates usually is not straightforward. Here I have developed a new approach to reconstructing variations in lake elevation using the down-core TIC $\delta^{18}\text{O}$ ($\delta^{18}\text{O}_C$) record. This new approach has been used in Walker Lake, and a high-resolution lake elevation record spanning the late Holocene has been produced. The reconstructed lake level record has been used to generate a modeled $\delta^{18}\text{O}$ ($\delta^{18}\text{O}_M$) record of carbonate precipitates with a hydrologic-isotopic balance model (HIBAL) (BENSON and PAILLET, 2002). The HIBAL-derived $\delta^{18}\text{O}_M$ results match well with the original $\delta^{18}\text{O}_C$ record. This demonstrated the ability of this approach to reconstructing past lake level changes using the $\delta^{18}\text{O}_C$ record extracted from down-core carbonate sediments. The reconstructed lake elevation record of Walker Lake is consistent in shape with Benson and Thompson's (1987) tufa elevation record of the lake except for the magnitude of lake level variations. The reconstructed results suggest that Walker Lake levels were probably very low during the interval from 800 to 900 AD, which is in agreement with Antevs (1952) calculations¹⁶. In addition, the reconstructed stream flow record of the Walker River indicates that the rapid refilling beginning in ~850AD was probably due to river

¹⁶ The small salt contents of Walker Lake suggest that it would accumulate in 1100 years.

diversions. This river flow record clearly indicates that the overall the climate of the Walker Lake basin during the Medieval Warm Epoch (MWE) was relatively wet relative to the Little Ice Age (LIA).

A2.2 Introduction

The lake level of a closed-basin lake is an effective indicator of hydrological conditions. Variations in the lake level of a closed-basin lake usually possess basin-wide signals of climatic and hydrologic variability. In the western Great Basin, many lakes (like Pyramid Lake, Walker Lake, Mono Lake, and Owens Lake) have headwaters originating from the Sierra Nevada snowpack. Variations in the lake level of these lakes have the potential to reflect changes in winter precipitation of the Sierra Nevada. A comparison of the reconstructed lake level records of some Great Basin lakes suggested that most of the lakes would experience approximately synchronous changes in their lake level (or size) since the mid-1800s if they were not anthropogenically perturbed (MILNE, 1987).

In the late Holocene, reconstruction of variations in lake level of the Great Basin lakes primarily relies on proxy data derived from shoreline, delta, and deepwater deposits of these lakes. In Walker Lake and Pyramid Lake, Benson and Thompson (1987) reconstructed the late Holocene elevation and chronology in both basins through dating shoreline tufa deposits. Their results suggested that both Pyramid Lake and Walker Lake fluctuated within a vertical range of ~23 and 30 m respectively, and experienced nearly synchronous variations in lake elevation during the late Holocene. In the Mono Lake basin, Stine (1990) suggested that Mono Lake fluctuated within a vertical range of 40 m in response to changes in effective inflow to the lake during the last 3,800 years. The reconstructed low lake stands of Walker Lake, Pyramid Lake, and Mono Lake during the interval between 2000 and 3000 years BP reflected a pervasive drier climate in this region (BRADBURY, 1987; BRADBURY et al., 1989).

Previous reconstructions of variations in lake level of Walker Lake, Pyramid Lake, and Mono Lake, however, have not yet yielded continuous high-resolution consistent records and have resulted in discrepant interpretations of regional climatic and hydrologic variability at some times during the late Holocene. This appears mostly due to the discontinuous nature of shoreline and/or shallow water

deposits studied. Recent studies of deepwater sediments in Pyramid Lake (BENSON et al., 2002) and Walker Lake (see chapters 1-4) have created nearly continuous high-resolution proxy records from both lakes. In particular, over the last 1200 years the $\delta^{18}\text{O}_C$ record from Walker Lake sediments shares many similarities with the Pyramid Lake record. Many wet-dry episodes recorded in the $\delta^{18}\text{O}_C$ record are also identifiable in a tree-ring based river flow record of the Sacramento River (MEKO et al., 2001). This implies that the Walker Lake $\delta^{18}\text{O}_C$ record probably possesses a high-resolution signal of regional climatic variability.

Since change in $\delta^{18}\text{O}_L$ in a closed-basin lake is not a simple linear function of change in lake level, the $\delta^{18}\text{O}_C$ record stored in down-core carbonate sediments usually requires a modeling approach to reconstruct variations in lake level. For example, Li (1995b) designed an isotopic modeling approach and applied it to Mono Lake to reconstruct a lake level curve in the historical interval, which is comparable with the actual lake level curve observed. In Lake Turkana, Kenya, Ricketts and Anderson (1998) applied a hydrologic and isotopic mass balance model on the $\delta^{18}\text{O}_C$ record to generate quantitative lake level variations in the historical intervals. Their results suggested that, in spite of using the $\delta^{18}\text{O}_C$ dataset with significant spatial variability, the $\delta^{18}\text{O}_C$ records could still be capable of reconstructing lake level change through model calculations.

In Pyramid Lake, detailed climatic and hydrologic data were obtained through direct observations and/or model simulations (HOSTETLER and BENSON, 1994). The model HIBAL was made to simulate variations in Pyramid Lake surface water $\delta^{18}\text{O}_L$ spanning 1985 to 1994 (BENSON and PAILLET, 2002). With this approach, both reconstruction and simulation are limited in the historical intervals, in which the climate and hydrological conditions are already known. This is because there are a number of parameters affecting the $\delta^{18}\text{O}_L$ value, such as the amount and $\delta^{18}\text{O}$ value of river water ($\delta^{18}\text{O}_R$), precipitation, and evaporation. These components are usually unknown or poorly constrained for the past prior to 1900AD. Besides, modeling simulations (BENSON and WHITE, 1994) indicated

that the $\delta^{18}\text{O}$ value of water vapor leaving off lake surface water is dependent on the $\delta^{18}\text{O}_L$ value and ambient climatic conditions (water temperature, relative humidity, wind speeds, etc).

In this part of this dissertation, a new approach to reconstructing variations in lake elevation in the past has been developed and used to produce a late Holocene lake level record of Walker Lake. Reconstruction results are validated using HIBAL and derived stream flow records to reproduce down-core $\delta^{18}\text{O}_C$ records.

A2.3 Reconstruction Model

The $\delta^{18}\text{O}_L$ value is thought to fluctuate with change in hydrological balance, and variations in $\delta^{18}\text{O}_L$ are assumed to be preserved in down-core carbonate sediments (BENSON and PAILLET, 2002; BENSON and WHITE, 1994). In fact, there is not a linear relationship between $\delta^{18}\text{O}_L$ and lake level (BENSON et al., 1991). In Walker Lake, lake level is a function of the amount of primary hydrologic components

(stream flow discharge (Q), on-lake precipitation (P), and evaporation (E)), $\frac{\partial V}{\partial t} = Q + P - E$, while

$\delta^{18}\text{O}_L$ (δ) is not only affected by these primary hydrologic components, but also the $\delta^{18}\text{O}$ values of

these hydrologic components, $\frac{\partial(V\delta)}{\partial t} = Q\delta_Q + P\delta_P - E\delta_E$. Moreover, the $\delta^{18}\text{O}$ value of water

vapor leaving the lake surface depends on $\delta^{18}\text{O}_L$ and ambient atmosphere conditions, such as lake surface temperature, relative humidity, and atmospheric stability (BENSON and WHITE, 1994),

$$\delta_E = \frac{\left[\frac{1 + \delta}{\alpha_{eq}} \right] - RHf_{ad}(1 + \delta_{ad})}{\left[\frac{1 - RH}{\alpha_{kin}} \right] + RH(1 - f_{ad})} - 1 \quad (\text{A2.0})$$

where RH is the relative humidity of the boundary layer over the lake surface, δ_{ad} is the $\delta^{18}\text{O}$ of advected water vapor, α_{eq} and α_{kin} are equilibrium and kinetic isotopic fractionation factors, and f_{ad} is the fraction of advected water vapor in the boundary layer over the lake surface.

The equation for δ_E above can be translated into a linear function, $\delta_E = a\delta + b$, where

$$a = \frac{\alpha_{kin}}{\alpha_{eq}(1 - RH + (1 - f_{ad})RH\alpha_{kin})} \text{ and}$$

$$b = \frac{\alpha_{kin} - (1 - RH)\alpha_{eq} - (1 - (1 - R_{ad})f_{ad})RH\alpha_{eq}\alpha_{kin}}{\alpha_{eq}(1 - RH + (1 - f_{ad})RH\alpha_{kin})} \times 10^3$$

The hydrologic and isotopic mass balance equations above can be transformed into the following step-functions,

$$V_2 - V_1 = (Q + P - E) \times (t_2 - t_1) \quad (\text{A2.1})$$

$$V_2\delta_1 + V_1\delta_2 - 2V_1\delta_1 = (Q\delta_Q + P\delta_P - E\delta_E) \times (t_2 - t_1) \quad (\text{A2.2})$$

Multiplying δ_Q on both sides of Equation A2.1 and then substituting $Q\delta_Q$ from Equation A2.1 into Equation A2.2, a step-function for V_2 is obtained as follows,

$$V_2 = \frac{V_1(2\delta_1 - \delta_2 - \delta_Q) - (P - E)\delta_Q(t_2 - t_1) + (P\delta_P - E\delta_E)(t_2 - t_1)}{\delta_1 - \delta_Q} \quad (\text{A2.3})$$

In a conventional hydrologic mass balance model, stream flow (Q) data usually needs to be known prior to modeling experiments while in this hydrologic and isotopic model, lake volume can be calculated using variations in $\delta^{18}\text{O}_L$ and other parameters, such as the $\delta^{18}\text{O}_L$ of stream flow, precipitation and evaporation including their $\delta^{18}\text{O}_L$ values.

A2.4 Model Data Acquisition

A2.4.1 Lake Water $\delta^{18}\text{O}_L$

The $\delta^{18}\text{O}_C$ record stored in down-core carbonate sediments from Walker Lake is the primary variable input available for reconstruction of lake level variations in the late Holocene. Modeling reconstruction needs data of variations in the $\delta^{18}\text{O}_L$ that is presumably in isotopic equilibrium with the $\delta^{18}\text{O}_C$ of inorganic carbonate precipitates.

Under conditions where there is slow inorganic carbonate precipitation, the oxygen isotopic fractionation between carbonates and host water is dependent on ambient water temperature (EPSTEIN et al., 1953; MCCREA, 1950), $t = 16.5 - 4.3(\Delta\delta) + 0.14(\Delta\delta)^2$, where t is water temperature in °C and $\Delta\delta$ is isotopic difference between inorganic carbonate precipitates (relative to PDB) and host water (relative to SMOW). Assuming that the host water temperature of Walker Lake is 22°C (BENSON et al., 1991), $\Delta\delta$ is 1.23 ‰. In fact, the isotopic fractionation is also related to carbonate phases. For calcite ($\Delta\delta = 3.95 - 0.232T$, Epstein et al. (1953) and O'Neil et al. (1969)) and aragonite ($\Delta\delta = 4.68 - 0.221T$, Grossman and Ku (1986)), their $\Delta\delta$ values are 1.15‰ and 0.182 ‰, respectively. The X-ray scan performed on core WLC84-8 (see Figure 11 in Benson et al.(1991)) indicated that monohydrocalcite is predominant throughout the upper 2-m section of the core and calcite is present in the lower part (2 to 12 m) of the core. A direct comparison of $\delta^{18}\text{O}_C$ and $\delta^{18}\text{O}_L$ indicates that the $\Delta\delta$ of the Walker Lake carbonate precipitates is relatively small (<1.0‰) in the interval of 1978 through 1990 and relatively large after 1990 (Figure A2-1). The large $\Delta\delta$ is likely to be induced by the uncertainties of ages. Also, more negative $\delta^{18}\text{O}$ of carbonates can be resulted from recrystallization of monohydrocalcite (JIMENEZ-LOPEZ et al., 2001). The original $\delta^{18}\text{O}_C$ record is smoothed via the three-point running average and then interpolated into an annual $\delta^{18}\text{O}_L$ dataset prior to the model reconstruction.

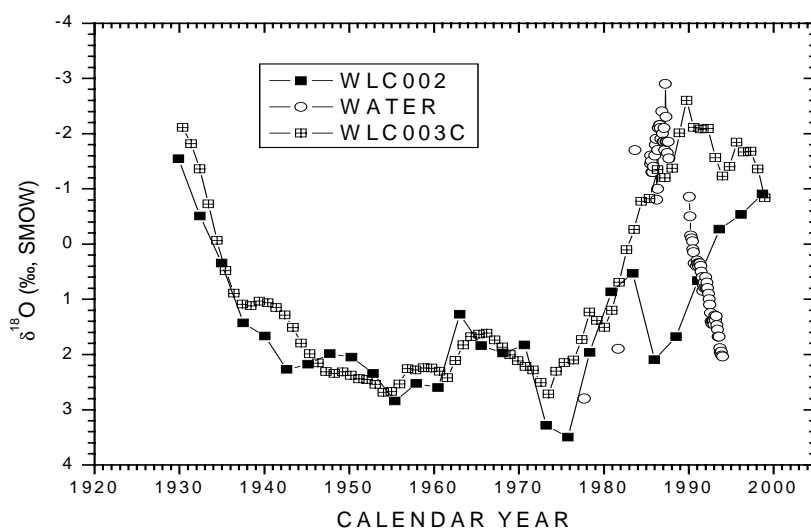


Figure A2-1. Comparison of measured and computed $\delta^{18}O_L$ records for Walker Lake. The measured $\delta^{18}O_L$ data were taken from Benson et al. (2002). Grossman and Ku's (1986) equation was used to compute corresponding $\delta^{18}O_L$ value for WLC002 and WLB-003C, assuming $T = 22^\circ C$. The computed $\delta^{18}O_L$ values were smoothed by the 6-point running average. Discrepancies among these records appear to be induced by the uncertainties of ages and possible minor loss at the top of WLC002.

A2.4.2 River Flow $\delta^{18}O_R$

The $\delta^{18}O_R$ value probably is the key to reconstruction of variations in lake level. Results of direct measurements for water samples collected at Wabuska gauging station indicate that the $\delta^{18}O_R$ varies from -14.85 to -12.25 (‰, SMOW) with an average of 13.6 ‰, SMOW (see Figure 2-10). The $\delta^{18}O_R$ value observed may not be representative of that in prehistoric times since agricultural irrigation has the potential to increase the $\delta^{18}O_R$ value of stream water. Besides, the Walker River is fed by headwaters originating from the Sierra Nevada snowpack. Variations in the $\delta^{18}O$ value of the Sierra Nevada snowpack during the past few thousand years remain unknown. However, the ice $\delta^{18}O$ record from Kilimanjaro in tropical Africa (THOMPSON et al., 2002) reveals that the ice $\delta^{18}O$ at this location fluctuated within -10 ± 2 (‰) over the last two thousand years. The modern (1991-1992) ice $\delta^{18}O$ record from Guliya, China (THOMPSON, 1996) also indicates large variations (-20 to -8 ‰) in ice isotopic composition.

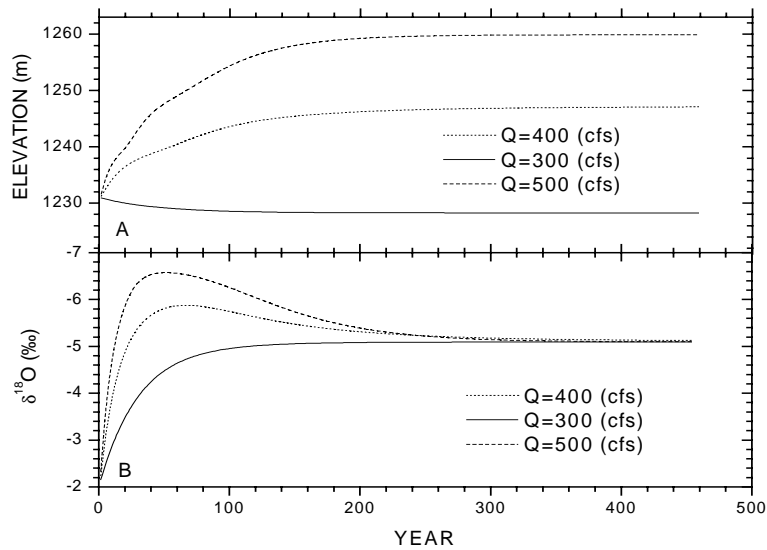


Figure A2-2. A) Response of lake level elevation to change in river discharge of the Walker River. B) Response of $\delta^{18}\text{O}_L$ to change in river discharge of the Walker River using a published hydrologic-isotopic model - HIBAL (BENSON and PAILLET, 2002). HIBAL simulations, using parameter values taken from the results of measurements in Pyramid Lake (BENSON et al., 2002), suggest that the steady-state $\delta^{18}\text{O}_L$ value is independent of the amount of river discharge of the Walker River.

To estimate the average $\delta^{18}\text{O}_R$ values of the past, the condition of steady-state is assumed. When stream discharge is held constant, a closed-basin lake level will ultimately reach a hydrologic steady state, a state without significant variations in lake level (Figure A2-2A). Moreover, when a lake maintains closed-basin conditions and stream flow is kept constant, it will achieve an isotopic steady state and its steady-state $\delta^{18}\text{O}_L$ value is independent of the amount of stream discharge (Figure A2-2B). In fact, the steady-state $\delta^{18}\text{O}_L$ value is positively correlated with the $\delta^{18}\text{O}_R$ value (Figure A2-3A) and negatively correlated with f_{ad} (Figure A2-3B). Further modeling experiments indicate that the steady-state $\delta^{18}\text{O}_L$ value is also independent of initial conditions (lake level and $\delta^{18}\text{O}_L$). However, the time to achieve a hydrologic-isotopic steady state is determined by the difference between initial and steady-state values of lake level and $\delta^{18}\text{O}_L$ as well as lake basin shape. Variations in both $\delta^{18}\text{O}_R$ and the amount of stream water affect the $\delta^{18}\text{O}_L$ value. Although detailed variations in $\delta^{18}\text{O}_R$ of the past remains largely

unknown, the $\delta^{18}\text{O}_\text{C}$ record preserved in down-core carbonate sediments may be used to determine a long-term average $\delta^{18}\text{O}_\text{R}$ value of the past.

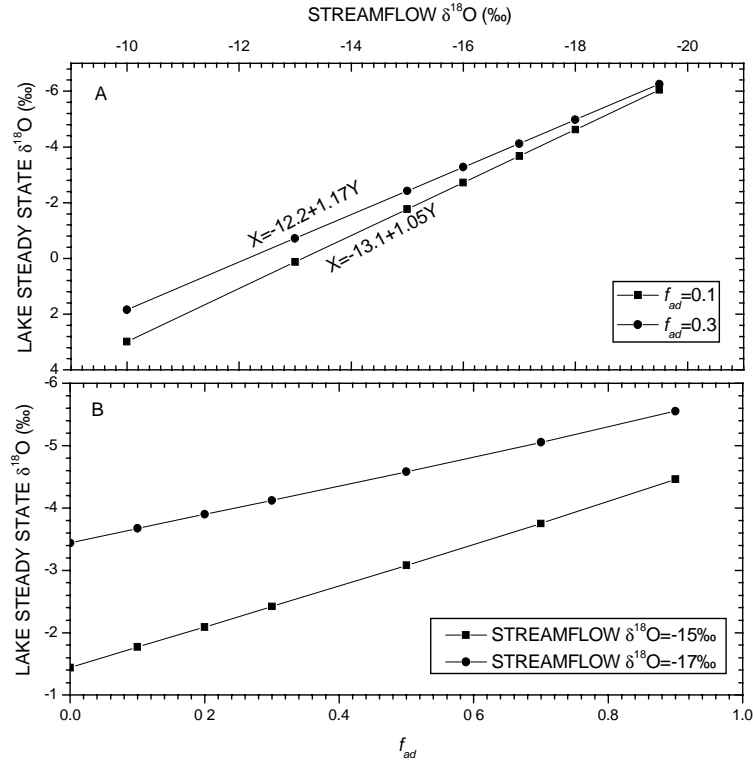


Figure A2-3. A) Linear correlation between steady-state $\delta^{18}\text{O}_\text{L}$ and $\delta^{18}\text{O}_\text{R}$. f_{ad} is the fraction of advected air in the thin boundary layer overlying the water surface of the lake. B) Correlation between steady-state $\delta^{18}\text{O}_\text{L}$ and f_{ad} based on HIBAL simulations.

A2.4.3 Model Parameters

A number of meteorological parameters (surface water temperature, on-lake precipitation, evaporation, relative humidity, f_{ad} , wind speed, etc) affect the oxygen and hydrogen isotopic distribution in an aquatic system. Most of these parameter values are taken from the measured data from Pyramid Lake obtained by Benson and Paillet (2002). The surface water temperature affects isotopic fractionation both between water vapor and surface water ($T=14.2^\circ\text{C}$) and between carbonate precipitates and host water ($T=22^\circ\text{C}$)¹⁷. Evaporation and on-lake precipitation rates are 135 and 12.5 cm yr⁻¹, respectively.

¹⁷ Carbonate precipitation usually occurs in late summer and early fall while water evaporation occurs perennially. Annual mean temperature value is taken from measured data from Pyramid Lake [Benson and Paillet, 2002].

Relative humidity and wind speed are 53% and 3.57 m s⁻¹, respectively. f_{ad} is the fraction of advected water vapor in the boundary layer overlying lake surface, ranging from 0.1 to 0.3.

A2.5 Model Results

The $\delta^{18}\text{O}_C$ record can be approximately divided into three intervals according to variations in the $\delta^{18}\text{O}_C$ value (see Figure A2-4). The average $\delta^{18}\text{O}_C$ values in the interval from 1000BC to 400AD, from 400AD to 1000AD, and from 800AD to 1900 AD are -1.22, -4.48, and -5.29 (‰, PDB). Assuming that steady-state $\delta^{18}\text{O}_L$ values in these three intervals are close to the average $\delta^{18}\text{O}_C$ values, the long-term average $\delta^{18}\text{O}_R$ value can be approximated with the linear function $\delta_R = -13.14 + 1.05\delta_L$ (for $f_{ad}=0.1$, see Figure A2-3A). For example, the average $\delta^{18}\text{O}_C$ value of the Walker Lake record (1990-2000AD)¹⁸ is -0.26 ‰, (PDB) and the calculated $\delta^{18}\text{O}_R$ value is -13.4 ‰ (SMOW), which is very close to the $\delta^{18}\text{O}_R$ value of -13.6 ‰, (SMOW) observed at the Wabuska during the period from 1985 to 1994. Noting that the calculated $\delta^{18}\text{O}_R$ values for stream water listed in Table A2-1 are long-term mean (LTM) values only for reconstruction purpose since the isotopic fractionation varies with a potential shift of down-core carbonate phase.

¹⁸ In comparison with the boxcore record WLB-003C in Figure 5-1, there is a 5-10 year loss of WLC-002 at the topmost section of the core.

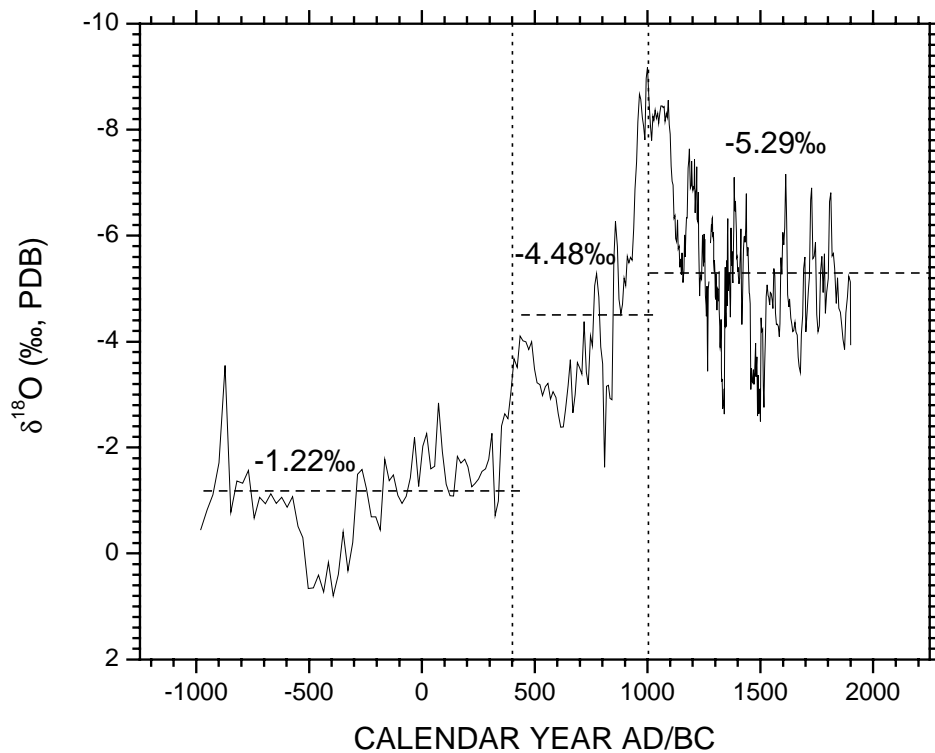


Figure A2-4. The TIC $\delta^{18}\text{O}_C$ record from Walker Lake divided into three stages with distinctive average $\delta^{18}\text{O}_C$ values. These isotopic values are used to infer $\delta^{18}\text{O}_R$ in corresponding stages.

Table A2-1 Input data and parameter values for reconstruction of the Walker Lake levels during the past 3,000 years

Input Data		Interval A (1000BC-400AD)	Interval B (400AD-1000AD)	Interval C (1000-1900AD)
$\delta^{18}\text{O}$	Carbonates ¹⁹ (‰, PDB)	-1.22	-4.48	-5.29
	Steam Water ²⁰ (‰, SMOW)	-14.4	-17.8	-18.7
Parameters	f_{ad}	0.1	0.1	0.1
	RH (%)	53	53	53
	T (°C)	14.2	14.2	14.2
	E (cm yr ⁻¹)	135	135	135
	P (cm yr ⁻¹)	12.5	12.5	12.5

¹⁹ Average $\delta^{18}\text{O}$ values indicated in Figure 5-4.

The reconstruction-modeling program was run separately in the three intervals. The smoothed (the 3-point running average) $\delta^{18}\text{O}_C$ record is the primary input variable for the reconstruction model. Reconstruction of lake level starts on the latest interval, Interval C (1000 AD-1900AD), as the Walker Lake level in ~1900 AD is known. The reconstruction model applies the parameter values listed in Table A2-1 and was run three times using a $\delta^{18}\text{O}_R$ value equal or close to the average $\delta^{18}\text{O}_R$ calculated (-18.7 ‰, SMOW). The model outputs three slightly different curves of lake elevation over the last 1,000 years (Figure A2-5A). All three curves match well with the historical (1900-2000AD) lake level record of Walker Lake. However, their initial lake elevations are a little different (1216 ± 8 m). The $\delta^{18}\text{O}_R$ value is sensitive to the reconstruction modeling. Here the midpoint elevation of 1216 m is picked for reconstruction of Interval B (400AD-1000AD). The model also was run three times and generated three reconstructed elevation curves of Walker Lake during 400-1000AD. The lake elevation in 400AD is reconstructed to be 1214 ± 8 m (Figure A2-5B). Since the lake level in 1000AD is reconstructed with ± 8 m uncertainty, the reconstructed lake level at 400AD has ± 16 m uncertainties. In the third interval the model was run three times and produced the lake level curves shown in Figure A2-5C. The lake elevation in 1000BC is reconstructed to be 1252 ± 14 m. As the lake level in 400AD has ± 16 m uncertainty, the maximum uncertainty of lake elevation in 1000BC is ± 30 m. Therefore, a continuous lake elevation record of the late Holocene Walker Lake is produced merging the reconstruction results presented in Figure A2-5A, A2-5B, and A2-5C.

²⁰ Calculated through equation: $\delta_{stream} = -13.14 + 1.05\delta_{lake}$ for $f_{ad}=0.1$.

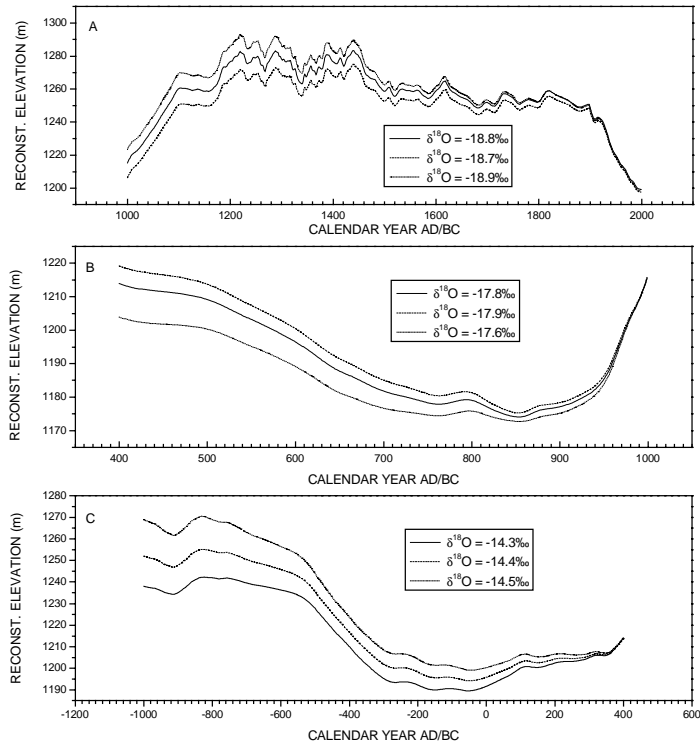


Figure A2-5. A) Reconstructed lake level elevation of Walker Lake for the period of 1000 to 2000AD using the reconstruction model and the inferred LTM value of $\delta^{18}\text{O}_R$. B) Reconstructed lake level elevation of Walker Lake for the period of 400 to 1000AD using the reconstruction model and the inferred LTM value of $\delta^{18}\text{O}_R$. C) Reconstructed lake level elevation of Walker Lake for the period of 1000BC to 400AD using the reconstruction model and the inferred LTM value of $\delta^{18}\text{O}_R$.

A2.6 Validation

A2.6.1 Walker River Discharge

Change in lake level of a closed-basin lake is a function of the amount of river discharge, evaporation, and on-lake precipitation. Change in lake level of Walker Lake can be simulated by assuming fixed mean annual values of evaporation (1.35 m) and on-lake precipitation (0.125 m). The Walker River discharge can also be estimated based on changes in lake elevation. On the basis of the reconstructed lake level record, continuous river discharge record for the Walker River is reconstructed (Figure A2-6A), assuming constant rates of on-lake precipitation and evaporation over the late Holocene. In Walker Lake, a continuous annual river flow record of the Walker River back to 1944 and a lake level record of Walker Lake back to 1861 have been documented (USGS). A 9-point-average historical river

flow²¹ of the Walker River is consistent in general with that calculated from the reconstructed lake elevation record (Figure A2-6B).

The tree-ring based river flow record of the Sacramento River is compared with the $\delta^{18}\text{O}_\text{C}$ -based river flow record of the Walker River (Figure A2-7). The intervals that show apparent correlation between these two reconstructed river flow records are not unexpected as historical stream flow records on both sides of the Sierra Nevada exhibit strong positive correlation (BENSON et al., 2002). However, the $\delta^{18}\text{O}_\text{C}$ -based river flow record of the Walker River clearly indicates that the climate in this region was relatively wet during the MWE relative to the LIA. This feature is opposite to the tree-ring based river flow record of the Sacramento River.

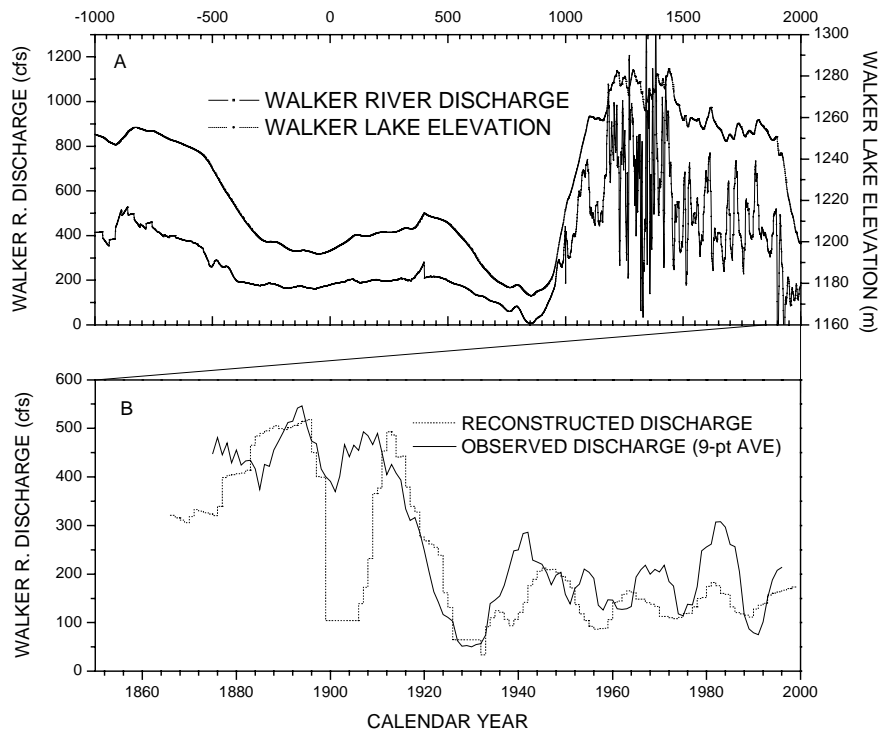


Figure A2-6. A) Reconstructed lake level elevation of Walker Lake and stream discharge of the Walker River during the late Holocene (3,000). B) Comparison of reconstructed and observed river discharge (USGS) records of the Walker River during the historic interval (1860-2000).

²¹ River flow record was taken from Milne's (1987) for the interval of 1871 through 1920 and from USGS statistic data for the interval of 1921 through 2000.

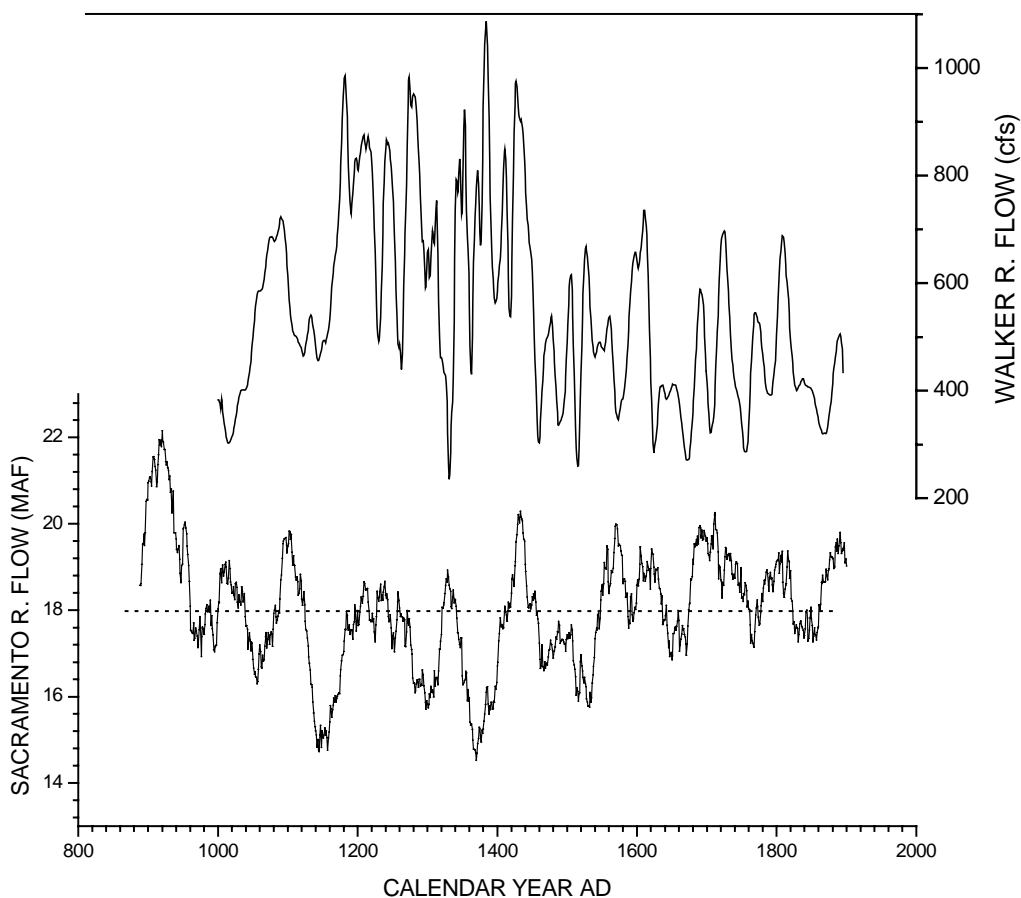


Figure A2-7. Comparing the reconstructed river flow record of the Walker River with the tree-ring based river flow record of the Sacramento River.

A2.6.2 Oxygen Isotopes

The reconstructed lake level record of Walker Lake is produced through the approach described in section A2.3, in which the model assumes that the lake is isotopically homogeneous. In fact, most closed-basin lakes, including Walker Lake, are limnologically stratified in summer and early fall and overturned in winter and early spring. However, isotopic modeling experiments indicate that the thermal-structure of the lake affects the $\delta^{18}\text{O}_L$ value only on yearly timescales (see Chapter 2). To validate the results produced by the reconstruction model, HIBAL is used to generate a $\delta^{18}\text{O}_M$ record of the lake carbonate using the reconstructed stream flow record of the Walker River.

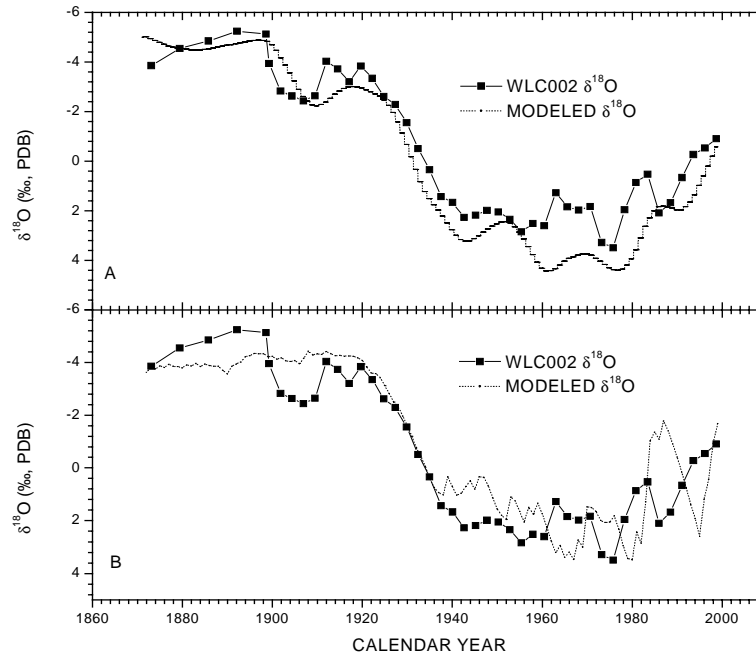


Figure A2-8. A) Comparing the HIBAL $\delta^{18}\text{O}_M$ record with the measured down-core TIC $\delta^{18}\text{O}_C$ record based on the reconstructed river flow of the Walker River. B) Comparing the HIBAL model-derived $\delta^{18}\text{O}$ record with the measured down-core TIC $\delta^{18}\text{O}_C$ record based on the measured river flow of the Walker River.

Because HIBAL requires lunar monthly meteorological and limnological parameter data, the results of measurements of these parameters from Pyramid Lake listed in Table 2-1 were used. The $\delta^{18}\text{O}_M$ record is generated separately due to substantial variations in LTM $\delta^{18}\text{O}_R$ values of the Walker River water, using fixed mean annual values of evaporation (1.35 m), on-lake precipitation (0.125 m), and f_{ad} (0.1). In the historical (1870-2000) interval, the Walker River probably experienced large changes in the $\delta^{18}\text{O}_R$ value. The mean value of $\delta^{18}\text{O}_R$ measured in a period of 1985 through 1994 is -13.6 ‰ (SMOW) and may be not representative of the historical $\delta^{18}\text{O}_R$ values of the Walker River since the results from running HIBAL suggest that the $\delta^{18}\text{O}_M$ values of the historical interval would reach ~ 10 ‰, (PDB) if a -13.6 (‰) value of $\delta^{18}\text{O}_R$ was assigned. Using the same $\delta^{18}\text{O}_R$ value (-18.7 ‰) of river flow that is assigned for lake level reconstruction for the last 1000 years, two $\delta^{18}\text{O}$ curves were generated using the reconstructed and actual river flow records (Figure A2-8A and Figure A2-8B). Both

$\delta^{18}\text{O}_M$ curves are in good agreement with the $\delta^{18}\text{O}_C$ record extracted from down-core (WLC-002) carbonate sediments. In addition, the HIBAL $\delta^{18}\text{O}_M$ results derived from the actual river flow data (USGS) captures two negative $\delta^{18}\text{O}$ excursions that occurred in the El Niño wet years of 1982/83 and 1997/98.

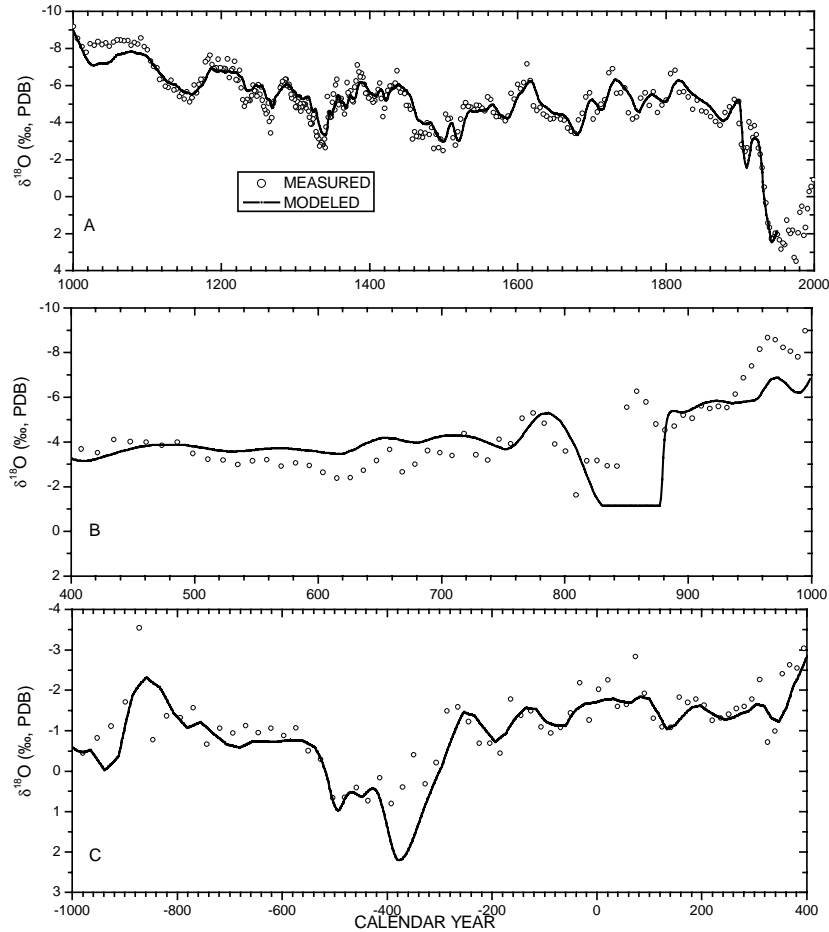


Figure A2-9. A) Comparing the HIBAL $\delta^{18}\text{O}_M$ record with the measured down-core TIC $\delta^{18}\text{O}_C$ record based on the reconstructed river flow of the Walker River spanning 1000 to 1900 AD. B) Comparing the HIBAL $\delta^{18}\text{O}_M$ record with the measured down-core TIC $\delta^{18}\text{O}_C$ record based on the reconstructed river flow of the Walker River spanning 400 to 1000 AD. C) Comparing the HIBAL $\delta^{18}\text{O}_M$ record with the measured down-core TIC $\delta^{18}\text{O}_C$ record based on the reconstructed river flow of the Walker River spanning 1000BC to 400 AD.

For the intervals from 1000 to 1900AD, from 400 to 1000AD, and from 1000BC to 400AD, the LTM $\delta^{18}\text{O}_R$ values of the Walker River are the same as those that are assigned for lake level reconstruction (-18.7, -17.8, and -14.4, respectively). HIBAL runs separately in these intervals, using the reconstructed river discharge data. The HIBAL $\delta^{18}\text{O}_M$ records are compared with the original $\delta^{18}\text{O}_C$ record (see Figure A2-9A, Figure A2-9B, and Figure A2-9C). The HIBAL $\delta^{18}\text{O}_C$ record closely matches the late Holocene $\delta^{18}\text{O}_C$ record of Walker Lake (Figure A2-10A). This demonstrates that fluctuations in the river flow record of the Walker River are the primary contributor to the variations in the $\delta^{18}\text{O}_C$ signal preserved in down-core carbonate sediments.

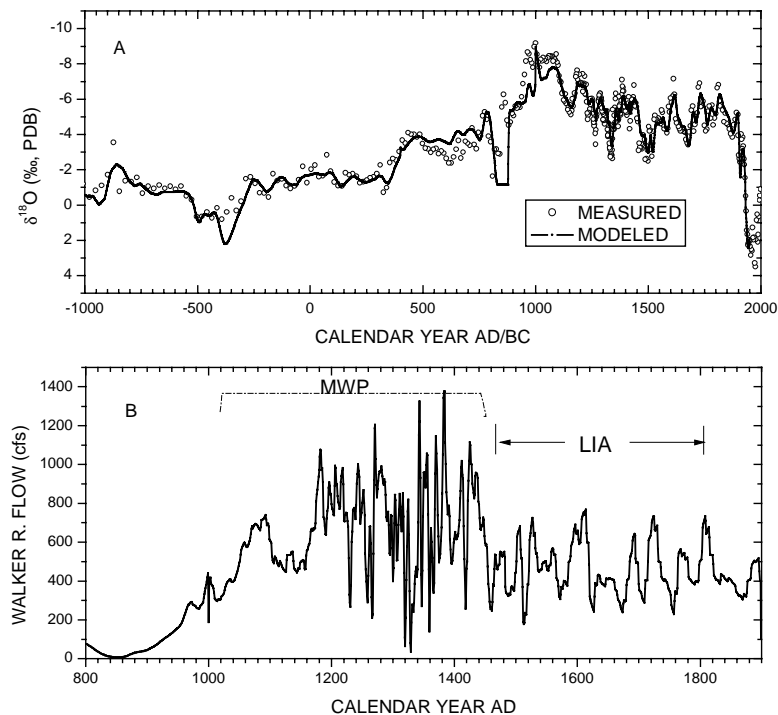


Figure A2-10. A) Comparing the HIBAL $\delta^{18}\text{O}_C$ record with the measured down-core TIC $\delta^{18}\text{O}_C$ record based on the reconstructed river flow of the Walker River spanning 1000BC to 2000 AD. B) Reconstructed Walker River discharge record spanning 800 to 1900.

A2.7 Discussion

I have presented an isotopic modeling approach to reconstruction of lake levels of Walker Lake and demonstrated the ability of the model to recover the history of lake level changes both in the historical

interval and in the late Holocene. The reconstructed hydrological conditions have been used to simulate variations in the $\delta^{18}\text{O}$ of down-core carbonate sediments through the model HIBAL. Results indicate that most variations in $\delta^{18}\text{O}_C$ extracted from down-core carbonate sediments can be ascribed to fluctuations in stream discharge. In addition, the $\delta^{18}\text{O}_R$ value is also an important factor that affects the $\delta^{18}\text{O}_L$ value. The LTM $\delta^{18}\text{O}_R$ value can be inferred from the $\delta^{18}\text{O}_C$ record of Walker Lake. Since the mineralogical phase of carbonate precipitates may vary from the early stage (1000BC-400AD) to the late one (400-2000AD) and the isotopic fractionation is related to carbonate phases, the average $\delta^{18}\text{O}_C$ value of bulk carbonate sediments is a composite result of $\delta^{18}\text{O}_R$, hydrological conditions, and isotopic fractionations. Therefore, the calculated LTM $\delta^{18}\text{O}_R$ value (-14.4 ‰) in the interval of 1000BC-400AD does not necessarily represent the actual $\delta^{18}\text{O}_R$ value of the Walker River. However, this LTM $\delta^{18}\text{O}_R$ value proves to be useful in $\delta^{18}\text{O}_C$ -based lake level reconstruction.

The reconstructed lake level record is consistent in shape with the tufa chronology (BENSON and THOMPSON, 1987) in which Walker Lake was in a relatively high stand 3000 years ago, in a relatively low stand between 2000-1000 years ago, and desiccated²² at ~850 AD, and then refilled and reached the highest lake stands during the late Holocene. This $\delta^{18}\text{O}_C$ -inferred desiccation of Walker Lake in ~850 is remarkably in agreement with the results from salt accumulation calculations (ANTEVS, 1952). However, this rapid refilling beginning in ~900AD signaled a wet climate during the MWE in the Walker Lake Basin (Figure A2-10B). This finding is opposite to tree stump data (STINE, 1994) and the tree-ring based river flow record of the Sacramento River (MEKO et al., 2001). In fact, if the hydrologic variations in the tree-ring-based data of the Sacramento River are applied or scaled into the Walker River, the HIBAL model results suggest that the magnitudes of fluctuations in lake level and $\delta^{18}\text{O}_L$ are within 10 meters and 2 ‰, respectively (Figure A2-11). This is apparently not the case for Walker Lake over the last ~1000 years because variations in $\delta^{18}\text{O}_C$ are larger than 2 ‰.

²² It simply denotes the water depth of Walker Lake was less than 5 m then.

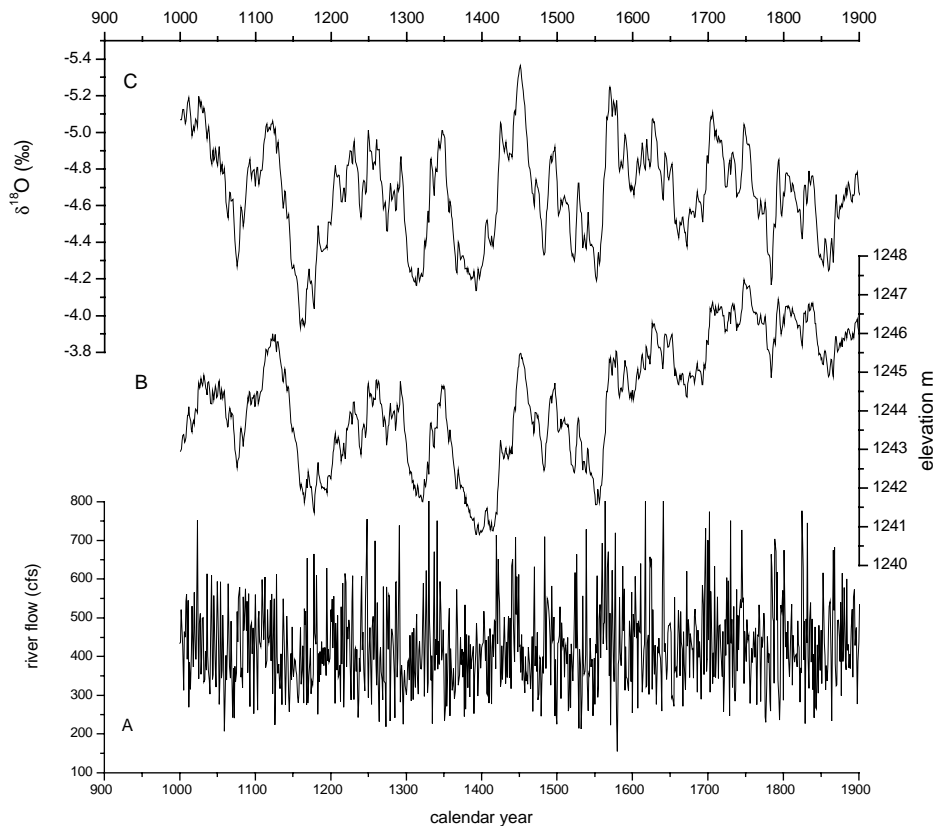


Figure A2-11. Modeled fluctuations in the Walker River discharge (panel A), Walker Lake level (panel B), and lake water $\delta^{18}\text{O}_L$ (panel C). Scaled annual Walker River discharge data (panel A) is based on the tree-ring-based Sacramento River flow (MEKO et al., 2001) and correlation of historic streamflow records (BENSON et al., 2002). Modeled Walker Lake elevations are inferred through a simple mass balance model (MILNE, 1987), assuming fixed rates of evaporation (135 cm per year) and on-lake precipitation (12.5 cm per year). The $\delta^{18}\text{O}_L$ data are modeled through HIBAL. Note that the magnitude of variations in $\delta^{18}\text{O}_L$ is within 2 ‰, which is far less than that of actual variations recorded and extracted.

Certainly, the isotopic reconstruction model is based on the assumption that the extracted downcore $\delta^{18}\text{O}_C$ signatures are representative to the $\delta^{18}\text{O}_L$ of host water when carbonates formed. Previous studies (SPENCER, 1977) suggested that monohydrocalcite is the dominant phase of carbonate precipitates today and subject to recrystallization (BENSON et al., 1991). More recent studies (JIMENEZ-LOPEZ et al., 2001) suggested that recrystallization of monhydrocalcite would create anomalously low $\delta^{18}\text{O}_L$ signatures on carbonates that have not had the opportunity for further exchange with the surrounding medium. The pseudo-isotopic signatures may be preserved or entirely erased depending on

post-depositional processes and ambient media conditions (JIMENEZ-LOPEZ et al., 2001). Thus, question about whether the large variability of downcore $\delta^{18}\text{O}$ in Walker Lake was induced by the climate or geochemical processes or simply a combination of the two remains.

If the $\delta^{18}\text{O}_C$ is representative to the $\delta^{18}\text{O}_L$ of host water when carbonates formed, then the reconstructed results are valid. Under this circumstances, the Walker Lake climate over the last millennium is characterized by wet MWE) and dry LIA. A climate regime shift probably occurred in ~1440 AD. Recent observations indicate that the Walker Lake Basin received abnormal moisture during the recent two major El Niño events that occurred in the 1982/83 and 1997/98. In spite of the fact that the Walker Lake Basin sits at a hinge point with respect to the effects of the El Niño Southern Oscillation (ENSO), the inferred wet MWE climate of the Walker Lake Basin pinpoints strong ENSO-like activity during the MWE in this region and highlights possible changes in the linkage between the low-frequency ENSO behavior and the Walker Lake Basin precipitation. In the following chapter, I will discuss the primary climatic frequency found from the $\delta^{18}\text{O}$ record preserved in down-core carbonate sediments, and climatic and hydrologic variability in this region over the past millennium.

Lastly, the reconstructed results presented here are subject to modify or correct due to the complications of post-depositional geochemical processes and ambient conditions. Examination of downcore carbonate crystals is a useful excise, but it will not help much in interpretation of the isotopic results extracted. One possible solution is to examine the δD and $\delta^{18}\text{O}$ of downcore organic matter like lipid.

**APPENDIX 3 RESULTS OF MEASUREMENTS OF TOTAL INORGANIC
CARBON, TOTAL CARBON, OXYGEN AND CARBON ISOTOPIC
COMPOSITIONS**

A3.1 Box-core WLB-003C

Table A3-1 Geochemical and isotopic results of bulk sediments from box core WLB-003C

Number	Depth (mm)	Age (Cal Yr)	TOC (wt %C)	TIC (wt %C)	$\delta^{13}\text{C}$ (‰)	$\delta^{18}\text{O}$ (‰)
3C0-5	2.5	2000.6	5.15	2.69	3.813	0.292
3C5-10	7.5	1999.8	3.12	2.48	3.508	0.496
3C10-15	12.5	1999.0	3.46	1.80	3.029	-1.183
3C15-20	17.5	1998.1	2.94	1.67	3.273	-0.603
3C20-25	22.5	1997.3	4.03	1.09	1.873	-3.194
3C25-30	27.5	1996.5	4.46	1.12	2.381	-2.310
3C30-35	32.5	1995.6	5.06	1.48	3.112	-1.108
3C35-40	37.5	1994.8	5.01	1.50	3.210	-1.127
3C40-45	42.5	1994.0	5.20	1.37	2.758	-1.481
3C45-50	47.5	1993.1	5.25	1.63	3.032	-0.984
3C50-55	52.5	1992.3	5.04	1.62	2.942	-1.440
3C55-60	57.5	1991.5	4.75	1.38	2.532	-2.785
3C60-65	62.5	1990.6	4.27	1.05	1.335	-3.765
3C65-70	67.5	1989.8	3.11	1.95	3.093	-1.442
3C70-75	72.5	1988.9	3.25	1.98	3.670	-1.122
3C75-80	77.5	1988.1	3.45	0.97	1.619	-3.885
3C80-85	82.5	1987.2	2.08	2.43	3.609	0.153
3C85-90	87.5	1986.3	2.45	2.01	3.406	-0.569
3C90-96	93.0	1985.4	2.91	1.80	3.427	-0.569
3C96-101	98.5	1984.4	3.58	1.19	2.057	-1.860
3C101-106	103.5	1983.6	4.50	1.11	2.071	-1.261
3C106-111	108.5	1982.7	4.24	1.69	3.168	0.386
3C111-116	113.5	1981.8	4.37	2.10	3.835	1.983
3C116-121	118.5	1980.9	4.03	2.36	3.726	1.274
3C121-126	123.5	1980.1	3.93	1.81	2.929	1.074
3C126-131	128.5	1979.2	3.38	2.06	3.333	1.294
3C131-136	133.5	1978.3	2.91	2.70	3.775	1.913
3C136-141	138.5	1977.4	3.05	1.91	2.972	1.375
3C141-147	144.0	1976.4	2.83	1.58	2.804	0.516
3C147-153	150.0	1975.4	2.38	3.15	3.985	3.564

Number	Depth (mm)	Age (Cal Yr)	TOC (wt %C)	TIC (wt %C)	$\delta^{13}\text{C}$ (‰)	$\delta^{18}\text{O}$ (‰)
3C153-158	155.5	1974.4	3.12	3.12	3.909	3.137
3C158-163	160.5	1973.5	3.51	2.17	3.408	2.149
3C163-168	165.5	1972.6	-2.55	2.55	3.659	2.161
3C168-173	170.5	1971.7	3.76	2.66	3.797	2.586
3C173-178	175.5	1970.8	4.29	2.63	3.687	2.510
3C178-183	180.5	1969.9	4.04	2.61	3.571	2.019
3C183-188	185.5	1969.0	4.35	2.67	3.687	1.812
3C188-193	190.5	1968.0	4.21	2.79	3.594	1.657
3C193-198	195.5	1967.1	3.92	3.11	3.801	2.028
3C198-203	200.5	1966.2	4.47	2.74	3.727	1.821
3C203-208	205.5	1965.3	4.61	2.30	3.535	1.375
3C208-213	210.5	1964.4	5.06	1.96	2.993	1.195
3C213-218	215.5	1963.4	4.73	2.15	3.112	1.744
3C218-223	220.5	1962.5	3.89	3.00	3.533	2.249
3C223-228	225.5	1961.6	3.82	3.13	3.590	2.568
3C228-233	230.5	1960.6	4.24	3.12	3.652	2.806
3C233-238	235.5	1959.7	3.98	3.18	3.634	2.746
3C238-243	240.5	1958.8	4.57	2.03	3.038	1.158
3C243-248	245.5	1957.8	4.19	2.34	3.271	1.958
3C248-253	250.5	1956.9	3.30	3.03	3.398	2.550
3C253-258	255.5	1955.9	3.25	3.38	3.605	2.988
3C258-263	260.5	1955.0	3.26	2.99	3.268	2.634
3C263-268	265.5	1954.0	3.15	2.89	3.072	2.546
3C268-273	270.5	1953.1	3.01	3.24	3.415	2.639
3C273-278	275.5	1952.1	3.07	3.46	3.456	2.626
3C278-283	280.5	1951.2	3.25	3.18	3.304	2.267
3C283-288	285.5	1950.2	2.88	3.43	3.390	2.194
3C288-293	290.5	1949.2	2.64	3.89	3.481	2.485
3C293-298	295.5	1948.3	2.64	3.40	3.364	2.320
3C298-303	300.5	1947.3	2.22	3.85	3.415	2.317
3C303-308	305.5	1946.3	2.12	4.26	3.440	2.404
3C308-313	310.5	1945.3	2.36	3.59	3.361	2.037
3C313-318	315.5	1944.4	2.38	3.55	3.278	1.695
3C318-323	320.5	1943.4	2.43	3.42	3.169	1.492
3C323-328	325.5	1942.4	2.39	3.51	3.224	1.362
3C328-333	330.5	1941.4	2.50	3.46	3.041	0.983
3C333-338	335.5	1940.4	2.55	3.58	3.157	0.907
3C338-343	340.5	1939.4	2.43	3.74	3.224	1.012
3C343-348	345.5	1938.4	2.42	3.84	3.256	1.058
3C348-353	350.5	1937.4	2.36	4.07	3.234	1.218
3C353-358	355.5	1936.4	2.35	4.09	3.249	1.402
3C358-363	360.5	1935.4	2.20	4.01	3.224	0.765
3C363-368	365.5	1934.4	2.32	3.67	3.132	0.020

Number	Depth (mm)	Age (Cal Yr)	TOC (wt %C)	TIC (wt %C)	$\delta^{13}\text{C}$ (‰)	$\delta^{18}\text{O}$ (‰)
3C368-373	370.5	1933.4	2.13	3.64	3.004	-0.988
3C373-378	375.5	1932.4	1.95	3.61	2.870	-1.518
3C378-383	380.5	1931.4	1.98	2.93	2.720	-1.901
3C383-388	385.5	1930.4	1.86	2.91	2.642	-2.412
3C388-393	390.5	1929.4	1.79	2.73	2.706	-2.260
3C393-396	394.5	1928.5	2.03	2.67	2.391	-2.452

Table A4-2 Stable isotopic results of ostracode shells (*L. ceriotuberosa*) from box core WLB-003C

Number	Depth (mm)	Age (Cal. Yr)	$\delta^{13}\text{C}$ (‰)	$\delta^{18}\text{O}$ (‰)
1	10	1999.4	1.036	1.091
2	25	1996.9	-0.359	3.529
3	35	1995.2	-0.368	4.706
4	45	1993.6	-0.031	4.915
5	55	1991.9	0.440	5.804
6	65	1990.2	-0.100	3.936
7	75	1988.5	0.490	5.370
8	85	1986.8	-0.305	0.783
9	96	1984.9	-0.320	2.631
10	106	1983.1	0.366	-0.493
11	116	1981.4	0.057	7.259
12	126	1979.6	0.169	5.679
13	136	1977.9	-0.735	3.350
14	147	1975.9	-0.308	6.028
15	158	1973.9	-0.125	6.273
16	168	1972.1	-0.010	9.433
17	178	1970.3	0.016	8.100
18	188	1968.5	0.126	6.842
19	198	1966.7	0.120	6.356
20	208	1964.8	-0.358	8.411
21	218	1963.0	0.454	8.580
22	228	1961.1	-0.442	5.448
23	238	1959.2	-0.371	5.543
24	248	1957.4	-0.457	6.101
25	258	1955.5	-0.472	6.420
26	268	1953.6	-0.917	7.244
27	278	1951.6	-0.843	7.642
28	288	1949.7	-1.051	9.046
29	298	1947.8	-0.569	10.552

Number	Depth (mm)	Age (Cal. Yr)	$\delta^{13}\text{C}$ (‰)	$\delta^{18}\text{O}$ (‰)
30	308	1945.8	-0.705	3.425
31	318	1943.9	-1.032	3.401
32	328	1941.9	-0.663	3.455
33	338	1939.9	-0.558	1.527
34	348	1937.9	-0.829	2.843
35	358	1935.9	-0.987	2.157
36	368	1933.9	-1.407	1.508
37	378	1931.9	-1.785	0.331
38	388	1929.9	-1.855	0.453
39	395	1928.4	-1.822	1.016

A3.2 Piston Core WLC002

Table A3-3 Geochemical and isotopic results of bulk sediments from piston core WLC002

Number	Depth (cm)	TIC (wt % C)	CaCO ₃ (%)	$\delta^{13}\text{C}$ (‰)	$\delta^{18}\text{O}$ (‰)
2-5-0-1	0.5	2.12	17.67	3.619	-0.904
2-5-1-2	1.5	1.84	15.33	3.533	-0.534
2-5-2-3	2.5	2.04	17.00	3.621	-0.268
2-5-3-4	3.5	2.12	17.67	3.917	0.665
2-5-4-5	4.5	2.20	18.33	3.991	1.680
2-5-5-6	5.5	2.42	20.17	3.855	2.097
2-5-6-7	6.5	1.60	13.33	3.153	0.530
2-5-7-8	7.5	1.69	14.08	3.225	0.866
2-5-8-9	8.5	2.43	20.25	3.691	1.962
2-5-9-10	9.5	2.82	23.50	4.008	3.497
2-5-10-11	10.5	2.94	24.50	3.895	3.286
2-5-11-12	11.5	1.95	16.25	3.376	1.831
2-5-12-13	12.5	2.40	20.00	3.516	1.978
2-5-13-14	13.5	2.32	19.33	3.466	1.842
2-5-14-15	14.5	2.25	18.75	3.397	1.274
2-5-15-16	15.5	2.99	24.92	3.609	2.603
2-5-16-17	16.5	2.78	23.17	3.459	2.523
2-5-17-18	17.5	3.04	25.33	3.426	2.844
2-5-18-19	18.5	2.78	23.17	3.234	2.344
2-5-19-20	19.5	2.88	24.00	3.271	2.049
2-5-20-21	20.5	2.90	24.17	3.206	1.988
2-5-21-22	21.5	3.56	29.67	3.241	2.180
2-5-22-23	22.5	3.83	31.92	3.350	2.272
2-5-23-24	23.5	3.57	29.75	3.269	1.671
2-5-24-25	24.5	3.63	30.25	3.362	1.429
Number	Depth	TIC	CaCO₃	$\delta^{13}\text{C}$	$\delta^{18}\text{O}$

	(cm)	(wt % C)	(%)	(‰)	(‰)
2-5-25-26	25.5	3.46	28.83	3.132	0.346
2-5-26-27	26.5	3.68	30.67	3.058	-0.507
2-5-27-28	27.5	3.53	29.42	2.896	-1.542
2-5-28-29	28.5	2.74	22.83	2.760	-2.284
2-5-29-30	29.5	2.21	18.42	2.738	-2.611
2-5-30-31	30.5	2.01	16.75	2.412	-3.337
2-5-31-32	31.5	1.65	13.75	1.653	-3.835
2-5-32-33	32.5	2.07	17.25	2.223	-3.199
2-5-33-34	33.5	1.78	14.83	1.584	-3.724
2-5-34-35	34.5	1.30	10.83	1.222	-4.026
2-5-35-36	35.5	2.13	17.75	2.670	-2.636
2-5-36-37	36.5	2.75	22.92	2.678	-2.431
2-5-37-38	37.5	1.93	16.08	2.783	-2.626
2-5-38-39	38.5	2.51	20.92	2.667	-2.822
2-5-39-40	39.5	1.82	15.17	1.850	-3.942
2-5-40-41	40.5	1.21	10.08	1.517	-5.124
2-5-41-42	41.5	1.32	11.00	1.375	-5.235
2-5-42-43	42.5	1.42	11.83	1.789	-4.844
2-5-43-44	43.5	1.56	13.00	1.925	-4.542
2-5-44-45	44.5	2.54	21.17	2.587	-3.853
2-5-45-46	45.5	2.63	21.92	2.484	-4.042
2-5-46-47	46.5	2.26	18.83	2.324	-4.310
2-5-47-48	47.5	2.36	19.67	2.459	-4.552
2-5-48-49	48.5	2.03	16.92	2.385	-4.630
2-5-49-50	49.5	1.66	13.83	2.201	-5.207
2-5-50-51	50.5	2.03	16.92	2.282	-4.718
2-5-51-52	51.5	0.93	7.75	1.942	-5.378
2-5-52-53	52.5	0.77	6.42	1.926	-5.664
2-5-53-54	53.5	0.88	7.33	1.649	-5.615
2-5-54-55	54.5	0.28	2.33	-2.263	-6.810
2-5-55-56	55.5	0.51	4.25	-1.530	-6.642
2-5-56-57	56.5	1.51	12.58	1.671	-5.195
2-5-57-58	57.5	1.38	11.50	1.758	-4.927
2-5-58-59	58.5	1.88	15.67	2.462	-4.533
2-5-59-60	59.5	1.53	12.75	1.465	-5.657
2-5-60-61	60.5	1.74	14.50	2.562	-4.923
2-5-61-62	61.5	1.03	8.58	1.186	-5.609
2-5-62-63	62.5	1.37	11.42	1.713	-5.319
2-5-63-64	63.5	2.34	19.50	2.589	-4.299
2-5-64-65	64.5	2.36	19.67	2.592	-4.188
2-5-65-66	65.5	1.89	15.75	2.512	-4.510
2-5-66-67	66.5	1.04	8.67	0.688	-5.873
2-5-67-68	67.5	1.12	9.33	1.258	-5.608

Number	Depth (cm)	TIC (wt % C)	CaCO ₃ (%)	δ ¹³ C (‰)	δ ¹⁸ O (‰)
2-5-68-69	68.5	1.45	12.08	1.903	-5.568
2-5-69-70	69.5	0.27	2.25	-3.903	-6.905
2-5-70-71	70.5	0.30	2.50	-2.684	-6.676
Gap					
2-4-0-1	79.5	2.63	21.92	3.428	-3.418
2-4-1-2	80.5	2.23	18.58	3.363	-3.524
2-4-2-3	81.5	2.42	20.17	3.432	-3.707
2-4-3-4	82.5	2.47	20.58	3.424	-4.125
2-4-4-5	83.5	3.06	25.50	3.790	-4.183
2-4-5-6	84.5	2.58	21.50	3.317	-4.364
2-4-6-7	85.5	2.22	18.50	3.037	-4.206
2-4-7-8	86.5	2.92	24.33	3.561	-4.190
2-4-8-9	87.5	2.53	21.08	3.107	-4.335
2-4-9-10	88.5	2.23	18.58	3.361	-4.447
2-4-10-11	89.5	2.37	19.75	3.134	-4.808
2-4-11-12	90.5	3.42	28.50	3.163	-4.658
2-4-12-13	91.5	2.86	23.83	2.788	-4.886
2-4-13-14	92.5	0.13	1.08	-2.754	-6.269
2-4-14-15	93.5	0.17	1.42	-4.155	-7.162
2-4-15-16	94.5	0.50	4.17	0.205	-6.155
2-4-16-17	95.5	0.87	7.25	1.814	-5.825
2-4-17-18	96.5	1.01	8.42	1.186	-6.059
2-4-18-19	97.5	1.38	11.50	2.920	-5.269
2-4-19-20	98.5	0.66	5.50	0.780	-5.582
2-4-20-21	99.5	1.28	10.67	2.603	-4.341
2-4-21-22	100.5	2.07	17.25	3.317	-4.094
2-4-22-23	101.5	1.81	15.08	2.875	-4.287
2-4-23-24	102.5	2.02	16.83	3.424	-4.330
2-4-24-25	103.5	2.37	19.75	3.572	-4.319
2-4-25-26	104.5	2.07	17.25	3.190	-4.546
2-4-26-27	105.5	1.26	10.50	2.692	-5.248
2-4-27-28	106.5	1.36	11.33	2.168	-5.381
2-4-28-29	107.5	2.18	18.17	3.168	-4.622
2-4-29-30	108.5	2.38	19.83	3.697	-4.778
2-4-30-31	109.5	2.08	17.33	3.342	-4.904
2-4-31-32	110.5	2.05	17.08	3.589	-4.925
2-4-32-33	111.5	2.58	21.50	3.476	-4.693
2-4-33-34	112.5	2.30	19.17	3.486	-4.834
2-4-34-35	113.5	2.23	18.58	3.421	-4.872
2-4-35-36	114.5	1.80	15.00	3.024	-5.072
2-4-36-37	115.5	1.96	16.33	3.435	-4.846
2-4-37-38	116.5	1.93	16.08	3.587	-4.177
2-4-38-39	117.5	1.61	13.42	2.943	-3.493

Number	Depth (cm)	TIC (wt % C)	CaCO ₃ (%)	δ ¹³ C (‰)	δ ¹⁸ O (‰)
2-4-39-40	118.5	2.75	22.92	3.842	-2.760
2-4-40-41	119.5	1.88	15.67	2.895	-3.162
2-4-41-42	120.5	1.10	9.17	2.032	-4.236
2-4-42-43	121.5	1.34	11.17	3.073	-4.193
2-4-43-44	122.5	0.70	5.83	1.472	-4.448
2-4-44-45	123.5	1.81	15.08	2.928	-2.490
2-4-45-46	124.5	1.56	13.00	3.455	-3.109
2-4-46-47	125.5	2.24	18.67	3.836	-2.637
2-4-47-48	126.5	2.64	22.00	3.417	-3.366
2-4-48-49	127.5	2.67	22.25	3.818	-2.595
2-4-49-50	128.5	1.96	16.33	3.355	-3.710
2-4-50-51	129.5	2.14	17.83	3.207	-3.341
2-4-51-52	130.5	1.30	10.83	2.802	-3.975
2-4-52-53	131.5	1.76	14.67	3.395	-3.421
2-4-53-54	132.5	1.96	16.33	3.710	-3.193
2-4-54-55	133.5	1.79	14.92	3.227	-3.474
2-4-55-56	134.5	2.34	19.50	3.305	-3.228
2-4-56-57	135.5	2.28	19.00	3.202	-3.256
2-4-57-58	136.5	2.12	17.67	3.135	-3.503
2-4-58-59	137.5	2.79	23.25	3.334	-3.093
2-4-59-60	138.5	2.09	17.42	2.279	-4.717
2-4-60-61	139.5	2.32	19.33	2.823	-4.904
2-4-61-62	140.5	3.31	27.58	2.945	-4.915
2-4-62-63	141.5	1.78	14.83	2.555	-5.561
2-4-63-64	142.5	1.91	15.92	2.519	-5.781
2-4-64-65	143.5	1.76	14.67	2.525	-5.612
2-4-65-66	144.5	1.26	10.50	2.377	-5.855
2-4-66-67	145.5	0.94	7.83	1.745	-6.792
2-4-67-68	146.5	1.17	9.75	2.134	-6.129
2-4-68-69	147.5	1.80	15.00	2.598	-5.877
2-4-69-70	148.5	1.61	13.42	2.372	-5.983
2-4-70-71	149.5	1.70	14.17	2.567	-5.975
2-4-71-72	150.5	1.56	13.00	2.411	-5.737
2-4-72-73	151.5	1.04	8.67	1.308	-5.474
2-4-73-74	152.5	1.33	11.08	2.750	-4.764
2-4-74-75	153.5	2.48	20.67	3.201	-4.320
2-4-75-76	154.5	1.31	10.92	1.593	-5.295
2-4-76-77	155.5	0.84	7.00	0.339	-6.130
2-4-77-78	156.5	1.04	8.67	1.598	-5.775
2-4-78-79	157.5	1.54	12.83	1.375	-5.477
2-4-79-80	158.5	1.68	14.00	2.826	-5.189
2-4-80-81	159.5	1.99	16.58	2.795	-5.091
2-4-81-82	160.5	2.01	16.75	2.624	-5.243

Number	Depth (cm)	TIC (wt % C)	CaCO ₃ (%)	δ ¹³ C (‰)	δ ¹⁸ O (‰)
2-4-82-83	161.5	2.03	16.92	2.657	-5.400
2-4-83-84	162.5	2.13	17.75	2.738	-5.317
2-4-84-85	163.5	2.12	17.67	2.800	-5.603
2-4-85-86	164.5	2.56	21.33	2.821	-5.583
2-4-86-87	165.5	1.64	13.67	2.519	-6.065
2-4-87-88	166.5	1.46	12.17	2.624	-6.449
2-4-88-89	167.5	1.40	11.67	2.520	-6.656
2-4-89-90	168.5	2.04	17.00	2.696	-6.459
2-4-90-91	169.5	1.13	9.42	1.445	-6.731
2-4-91-92	170.5	0.77	6.42	0.567	-7.100
2-4-92-93	171.5	1.01	8.42	2.222	-6.232
2-4-93-94	172.5	1.23	10.25	2.348	-5.902
2-4-94-95	173.5	1.79	14.92	3.597	-5.105
2-4-95-96	174.5	2.10	17.50	3.787	-5.181
2-4-96-97	175.5	1.47	12.25	2.379	-5.699
2-4-97-98	176.5	1.59	13.25	2.783	-5.426
2-4-98-99	177.5	1.31	10.92	2.995	-5.598
2-3-0-1	178.5	0.21	1.75	1.052	-6.144
2-3-1-2	179.5	1.14	9.50	3.416	-4.847
2-3-2-3	180.5	2.11	17.58	4.078	-4.458
2-3-3-4	181.5	1.30	10.83	3.033	-4.778
2-3-4-5	182.5	1.19	9.92	3.591	-4.999
2-3-5-6	183.5	1.20	10.00	3.594	-5.299
2-3-6-7	184.5	1.56	13.00	3.552	-5.218
2-3-7-8	185.5	1.86	15.50	3.742	-4.960
2-3-8-9	186.5	0.83	6.92	1.911	-5.359
2-3-9-10	187.5	0.77	6.42	1.486	-6.322
2-3-10-11	188.5	0.89	7.42	1.906	-6.024
2-3-11-12	189.5	1.57	13.08	3.349	-4.675
2-3-12-13	190.5	0.99	8.25	1.537	-5.532
2-3-13-14	191.5	1.02	8.50	2.331	-5.082
2-3-14-15	192.5	1.48	12.33	3.329	-4.292
2-3-15-16	193.5	1.72	14.33	3.449	-4.278
2-3-16-17	194.5	0.97	8.08	2.819	-4.545
2-3-17-18	195.5	1.05	8.75	3.054	-4.280
2-3-18-19	196.5	0.54	4.50	0.310	-5.403
2-3-19-20	197.5	0.67	5.58	2.533	-3.760
2-3-20-21	198.5	1.30	10.83	3.025	-2.631
2-3-21-22	199.5	1.15	9.58	2.545	-3.108
2-3-22-23	200.5	1.31	10.92	3.375	-2.822
2-3-23-24	201.5	1.52	12.67	3.569	-2.811
2-3-24-25	202.5	1.66	13.83	3.548	-2.899
2-3-25-26	203.5	1.88	15.67	3.570	-2.813

Number	Depth (cm)	TIC (wt % C)	CaCO ₃ (%)	δ ¹³ C (‰)	δ ¹⁸ O (‰)
2-3-26-27	204.5	2.01	16.75	3.579	-2.733
2-3-27-28	205.5	1.65	13.75	3.458	-3.132
2-3-28-29	206.5	1.65	13.75	3.459	-3.294
2-3-29-30	207.5	1.44	12.00	3.342	-3.246
2-3-30-31	208.5	1.29	10.75	3.392	-3.496
2-3-31-32	209.5	0.80	6.67	2.875	-4.261
2-3-32-33	210.5	0.69	5.75	2.902	-4.421
2-3-33-34	211.5	0.78	6.50	2.879	-4.194
2-3-34-35	212.5	1.13	9.42	3.411	-3.943
2-3-35-36	213.5	1.33	11.08	3.303	-3.889
2-3-36-37	214.5	1.42	11.83	3.241	-3.946
2-3-37-38	215.5	1.15	9.58	3.125	-4.277
2-3-38-39	216.5	0.87	7.25	2.869	-4.605
2-3-39-40	217.5	0.33	2.75	2.346	-5.320
2-3-40-41	218.5	0.08	0.67	-9999	-9999
2-3-41-42	219.5	0.90	7.50	3.218	-4.771
2-3-42-43	220.5	1.41	11.75	3.068	-4.988
2-3-43-44	221.5	1.03	8.58	2.814	-4.983
2-3-44-45	222.5	0.85	7.08	2.758	-4.999
2-3-45-46	223.5	1.30	10.83	2.872	-4.841
2-3-46-47	224.5	1.21	10.08	2.807	-4.835
2-3-47-48	225.5	1.21	10.08	2.910	-4.594
2-3-48-49	226.5	1.44	12.00	2.761	-5.023
2-3-49-50	227.5	1.59	13.25	3.030	-4.793
2-3-50-51	228.5	0.96	8.00	2.602	-5.274
2-3-51-52	229.5	1.65	13.75	2.913	-5.127
2-3-52-53	230.5	2.19	18.25	3.081	-4.798
2-3-53-54	231.5	1.77	14.75	2.888	-4.841
2-3-54-55	232.5	1.39	11.58	2.736	-5.245
2-3-55-56	233.5	1.34	11.17	2.750	-5.445
2-3-56-57	234.5	1.46	12.17	2.811	-5.537
2-3-57-58	235.5	1.69	14.08	2.951	-5.315
2-3-58-59	236.5	1.42	11.83	2.741	-5.500
2-3-59-60	237.5	1.18	9.83	2.573	-5.886
2-3-60-61	238.5	0.94	7.83	2.493	-6.071
2-3-61-62	239.5	0.61	5.08	2.471	-5.969
2-3-62-63	240.5	1.04	8.67	2.684	-6.004
2-3-63-64	241.5	0.26	2.17	2.399	-6.336
2-3-64-65	242.5	0.32	2.67	2.442	-6.324
2-3-65-66	243.5	1.34	11.17	2.509	-6.171
2-3-66-67	244.5	0.92	7.67	2.500	-6.082
2-3-67-68	245.5	0.71	5.92	2.264	-6.213
2-3-68-69	246.5	0.67	5.58	2.539	-5.981

Number	Depth (cm)	TIC (wt % C)	CaCO ₃ (%)	δ ¹³ C (‰)	δ ¹⁸ O (‰)
2-3-69-70	247.5	0.32	2.67	2.455	-5.866
2-3-70-71	248.5	0.00	0.00	-9999	-9999
2-3-71-72	249.5	0.00	0.00	-9999	-9999
2-3-72-73	250.5	0.00	0.00	-9999	-9999
2-3-73-74	251.5	0.00	0.00	-9999	-9999
2-3-74-75	252.5	0.00	0.00	-9999	-9999
2-3-75-76	253.5	0.40	3.33	2.588	-5.125
2-3-76-77	254.5	1.80	15.00	2.777	-4.993
2-3-77-78	255.5	2.51	20.92	2.970	-4.256
2-3-78-79	256.5	3.63	30.25	3.139	-3.439
2-3-79-80	257.5	2.10	17.50	2.910	-4.057
2-3-80-81	258.5	1.87	15.58	2.734	-5.048
2-3-81-82	259.5	2.37	19.75	2.850	-4.567
2-3-82-83	260.5	2.88	24.00	2.793	-4.478
2-3-83-84	261.5	2.08	17.33	2.624	-4.689
2-3-84-85	262.5	1.64	13.67	2.610	-4.870
2-3-85-86	263.5	2.09	17.42	2.538	-5.207
2-3-86-87	264.5	1.54	12.83	2.487	-5.935
2-3-87-88	265.5	1.49	12.42	2.579	-5.501
2-3-88-89	266.5	1.35	11.25	2.457	-6.032
2-3-89-90	267.5	1.39	11.58	2.748	-5.420
2-3-90-91	268.5	0.58	4.83	2.600	-5.695
2-3-91-92	269.5	0.99	8.25	2.628	-5.712
2-3-92-93	270.5	2.01	16.75	2.749	-6.016
2-3-93-94	271.5	1.59	13.25	2.850	-5.438
2-3-94-95	272.5	2.26	18.83	2.730	-5.172
2-3-95-96	273.5	2.40	20.00	2.964	-5.204
2-3-96-97	274.5	2.57	21.42	2.928	-5.248
2-3-97-98	275.5	2.92	24.33	3.024	-5.082
2-3-98-99	276.5	3.22	26.83	2.953	-4.859
2-2-0-1	277.5	2.63	21.92	2.690	-5.213
2-2-1-2	278.5	1.62	13.50	2.312	-5.854
2-2-2-3	279.5	1.76	14.67	2.215	-6.824
2-2-3-4	280.5	2.26	18.83	2.402	-6.265
2-2-4-5	281.5	2.10	17.50	2.432	-6.311
2-2-5-6	282.5	1.27	10.58	2.152	-7.299
2-2-6-7	283.5	1.65	13.75	2.400	-6.898
2-2-7-8	284.5	1.91	15.92	2.350	-6.819
2-2-8-9	285.5	1.87	15.58	2.186	-6.428
2-2-9-10	286.5	0.57	4.75	1.422	-7.439
2-2-10-11	287.5	2.01	16.75	2.191	-6.899
2-2-11-12	288.5	1.68	14.00	2.023	-6.916
2-2-12-13	289.5	1.96	16.33	2.219	-6.856

Number	Depth (cm)	TIC (wt % C)	CaCO ₃ (%)	δ ¹³ C (‰)	δ ¹⁸ O (‰)
2-2-13-14	290.5	1.48	12.33	2.248	-6.948
2-2-14-15	291.5	1.37	11.42	1.959	-7.410
2-2-15-16	292.5	1.38	11.50	2.147	-6.950
2-2-16-17	293.5	2.06	17.17	2.166	-6.898
2-2-17-18	294.5	2.12	17.67	2.171	-7.119
2-2-18-19	295.5	0.86	7.17	1.243	-7.639
2-2-19-20	296.5	1.17	9.75	2.007	-7.412
2-2-20-21	297.5	0.88	7.33	1.951	-7.277
2-2-21-22	298.5	1.52	12.67	2.308	-6.333
2-2-22-23	299.5	1.66	13.83	2.337	-6.339
2-2-23-24	300.5	1.54	12.83	2.151	-6.066
2-2-24-25	301.5	1.63	13.58	2.221	-5.600
2-2-25-26	302.5	1.59	13.25	2.100	-6.018
2-2-26-27	303.5	1.45	12.08	2.107	-5.342
2-2-27-28	304.5	2.76	23.00	2.612	-5.112
2-2-28-29	305.5	1.75	14.58	1.987	-5.674
2-2-29-30	306.5	2.39	19.92	2.644	-5.264
2-2-30-31	307.5	1.98	16.50	2.309	-5.557
2-2-31-32	308.5	1.96	16.33	2.426	-5.405
2-2-32-33	309.5	1.83	15.25	2.336	-5.795
2-2-33-34	310.5	1.76	14.67	2.318	-5.751
2-2-34-35	311.5	1.82	15.17	2.234	-6.295
2-2-35-36	312.5	1.72	14.33	2.531	-5.887
2-2-36-37	313.5	2.78	23.17	2.693	-5.949
2-2-37-38	314.5	2.58	21.50	2.263	-6.374
2-2-38-39	315.5	2.41	20.08	2.207	-6.329
2-2-39-40	316.5	1.96	16.33	1.837	-6.954
2-2-40-41	317.5	2.03	16.92	1.513	-7.031
2-2-41-42	318.5	1.63	13.58	1.375	-7.315
2-2-42-43	319.5	1.48	12.33	1.176	-7.913
2-2-43-44	320.5	1.36	11.33	1.232	-8.095
2-2-44-45	321.5	1.42	11.83	1.030	-8.556
2-2-45-46	322.5	1.14	9.50	1.088	-8.231
2-2-46-47	323.5	0.72	6.00	0.782	-8.311
2-2-47-48	324.5	0.82	6.83	0.486	-8.157
2-2-48-49	325.5	0.76	6.33	0.496	-8.434
2-2-49-50	326.5	0.66	5.50	0.408	-8.417
2-2-50-51	327.5	0.79	6.58	0.272	-8.450
2-2-51-52	328.5	0.70	5.83	0.450	-8.448
2-2-52-53	329.5	0.78	6.50	0.616	-8.334
2-2-53-54	330.5	0.44	3.67	0.162	-8.123
2-2-54-55	331.5	0.46	3.83	0.226	-8.306
2-2-55-56	332.5	0.57	4.75	0.474	-8.212

Number	Depth (cm)	TIC (wt % C)	CaCO ₃ (%)	δ ¹³ C (‰)	δ ¹⁸ O (‰)
2-2-56-57	333.5	0.45	3.75	-0.041	-8.367
2-2-57-58	334.5	0.29	2.42	-0.331	-8.173
2-2-58-59	335.5	1.15	9.58	0.424	-8.256
2-2-59-60	336.5	0.82	6.83	0.266	-7.799
2-2-60-61	337.5	0.80	6.67	0.112	-8.101
2-2-61-62	338.5	1.56	13.00	0.360	-8.532
2-2-62-63	339.5	1.79	14.92	0.293	-9.180
2-2-63-64	340.5	0.56	4.67	-0.346	-8.967
2-2-64-65	341.5	0.75	6.25	0.348	-7.806
2-2-65-66	342.5	1.64	13.67	0.749	-8.060
2-2-66-67	343.5	1.56	13.00	0.649	-8.232
2-2-67-68	344.5	1.40	11.67	0.675	-8.572
2-2-68-69	345.5	1.88	15.67	0.797	-8.668
2-2-69-70	346.5	1.88	15.67	0.920	-8.149
2-2-70-71	347.5	1.72	14.33	0.921	-7.393
2-2-71-72	348.5	2.29	19.08	0.850	-6.876
2-2-72-73	349.5	1.77	14.75	0.560	-6.133
2-2-73-74	350.5	1.74	14.50	0.322	-5.538
2-2-74-75	351.5	1.75	14.58	-0.090	-5.588
2-2-75-76	352.5	1.93	16.08	-0.412	-5.491
2-2-76-77	353.5	2.03	16.92	-0.810	-5.608
2-2-77-78	354.5	2.01	16.75	-0.530	-5.060
2-2-78-79	355.5	1.63	13.58	-0.110	-5.195
2-2-79-80	356.5	1.66	13.83	0.461	-4.703
2-2-80-81	357.5	1.61	13.42	-0.097	-4.527
2-2-81-82	358.5	1.98	16.50	-0.651	-4.800
2-2-82-83	359.5	2.08	17.33	-0.862	-5.795
2-2-83-84	360.5	2.00	16.67	-0.276	-6.270
2-2-84-85	361.5	2.40	20.00	0.625	-5.549
2-2-85-86	362.5	1.81	15.08	0.638	-2.901
2-2-86-87	363.5	1.86	15.50	0.791	-2.927
2-2-87-88	364.5	1.81	15.08	0.590	-3.173
2-2-88-89	365.5	1.79	14.92	0.545	-3.155
2-2-89-90	366.5	1.92	16.00	1.260	-1.631
2-2-90-91	367.5	1.93	16.08	0.397	-3.583
2-2-91-92	368.5	2.02	16.83	0.288	-3.900
2-2-92-93	369.5	2.06	17.17	-0.074	-4.842
2-2-93-94	370.5	2.11	17.58	-0.069	-5.283
2-2-94-95	371.5	2.20	18.33	0.418	-5.053
2-2-95-96	372.5	2.17	18.08	0.913	-3.919
2-2-96-97	373.5	2.22	18.50	1.101	-4.110
2-2-97-98	374.5	2.28	19.00	1.563	-3.188
2-2-98-99	375.5	2.20	18.33	1.090	-3.423

Number	Depth (cm)	TIC (wt % C)	CaCO ₃ (%)	δ ¹³ C (‰)	δ ¹⁸ O (‰)
2-2-99-100	376.5	2.30	19.17	0.920	-4.376
2-1-0-1	377.5	2.31	19.25	1.455	-3.386
2-1-1-2	378.5	2.11	17.58	1.619	-3.507
2-1-2-3	379.5	2.26	18.83	1.468	-3.607
2-1-3-4	380.5	2.20	18.33	1.648	-3.000
2-1-4-5	381.5	2.46	20.50	1.833	-2.658
2-1-5-6	382.5	2.14	17.83	1.614	-3.657
2-1-6-7	383.5	2.43	20.25	1.717	-3.166
2-1-7-8	384.5	2.24	18.67	1.720	-2.720
2-1-8-9	385.5	2.24	18.67	1.724	-2.388
2-1-9-10	386.5	2.36	19.67	1.712	-2.380
2-1-10-11	387.5	2.20	18.33	1.599	-2.642
2-1-11-12	388.5	2.11	17.58	1.411	-2.945
2-1-12-13	389.5	2.12	17.67	1.350	-3.056
2-1-13-14	390.5	2.03	16.92	1.335	-2.912
2-1-14-15	391.5	2.06	17.17	1.035	-3.208
2-1-15-16	392.5	2.06	17.17	1.108	-3.151
2-1-16-17	393.5	2.16	18.00	1.188	-2.980
2-1-17-18	394.5	2.04	17.00	1.126	-3.185
2-1-18-19	395.5	2.06	17.17	1.048	-3.221
2-1-19-20	396.5	2.05	17.08	0.795	-3.484
2-1-20-21	397.5	2.05	17.08	0.381	-3.995
2-1-21-22	398.5	1.98	16.50	0.597	-3.847
2-1-22-23	399.5	1.90	15.83	0.588	-3.995
2-1-23-24	400.5	1.90	15.83	0.560	-4.016
2-1-24-25	401.5	1.81	15.08	0.841	-4.103
2-1-25-26	402.5	2.10	17.50	1.265	-3.510
2-1-26-27	403.5	1.82	15.17	1.447	-3.676
2-1-27-28	404.5	1.81	15.08	2.036	-3.033
2-1-28-29	405.5	1.81	15.08	2.226	-2.547
2-1-29-30	406.5	1.90	15.83	2.287	-2.637
2-1-30-31	407.5	1.99	16.58	2.344	-2.409
2-1-31-32	408.5	1.96	16.33	2.421	-0.987
2-1-32-33	409.5	1.58	13.17	1.907	-0.716
2-1-33-34	410.5	1.88	15.67	1.912	-2.266
2-1-34-35	411.5	1.87	15.58	2.298	-1.778
2-1-35-36	412.5	1.80	15.00	2.165	-1.598
2-1-36-37	413.5	1.72	14.33	1.821	-1.548
2-1-37-38	414.5	1.68	14.00	1.779	-1.406
2-1-38-39	415.5	1.37	11.42	1.868	-1.318
2-1-39-40	416.5	1.53	12.75	1.920	-1.257
2-1-40-41	417.5	1.68	14.00	2.220	-1.631
2-1-41-42	418.5	1.84	15.33	2.007	-1.778

Number	Depth (cm)	TIC (wt % C)	CaCO ₃ (%)	δ ¹³ C (‰)	δ ¹⁸ O (‰)
2-1-42-43	419.5	1.59	13.25	2.155	-1.703
2-1-43-44	420.5	1.51	12.58	2.449	-1.829
2-1-44-45	421.5	1.71	14.25	2.689	-1.084
2-1-45-46	422.5	1.65	13.75	2.233	-1.088
2-1-46-47	423.5	1.50	12.50	1.665	-1.303
2-1-47-48	424.5	1.37	11.42	1.520	-1.926
2-1-48-49	425.5	1.56	13.00	0.932	-2.840
2-1-49-50	426.5	1.49	12.42	1.773	-1.647
2-1-50-51	427.5	1.69	14.08	1.791	-1.600
2-1-51-52	428.5	1.72	14.33	1.685	-2.260
2-1-52-53	429.5	1.54	12.83	2.107	-2.028
2-1-53-54	430.5	2.32	19.33	3.062	-1.266
2-1-54-55	431.5	1.78	14.83	3.120	-2.189
2-1-55-56	432.5	1.92	16.00	3.190	-1.432
2-1-56-57	433.5	2.07	17.25	2.860	-1.080
2-1-57-58	434.5	1.97	16.42	2.546	-0.943
2-1-58-59	435.5	1.83	15.25	2.579	-1.097
2-1-59-60	436.5	1.59	13.25	2.597	-1.484
2-1-60-61	437.5	1.50	12.50	2.619	-1.376
2-1-61-62	438.5	1.41	11.75	2.254	-1.778
2-1-62-63	439.5	2.59	21.58	1.979	-0.446
2-1-63-64	440.5	2.17	18.08	2.520	-0.689
2-1-64-65	441.5	2.29	19.08	1.805	-0.691
2-1-65-66	442.5	2.48	20.67	2.564	-1.220
2-1-66-67	443.5	2.02	16.83	2.651	-1.587
2-1-67-68	444.5	2.01	16.75	2.730	-1.492
2-1-68-69	445.5	2.21	18.42	2.694	-0.208
2-1-69-70	446.5	2.09	17.42	2.431	0.319
2-1-70-71	447.5	1.82	15.17	2.177	-0.408
2-1-71-72	448.5	1.79	14.92	1.682	0.396
2-1-72-73	449.5	3.15	26.25	1.306	0.802
2-1-73-74	450.5	2.60	21.67	1.094	0.163
2-1-74-75	451.5	2.62	21.83	1.279	0.729
2-1-75-76	452.5	2.38	19.83	1.072	0.405
2-1-76-77	453.5	3.34	27.83	1.266	0.653
2-1-77-78	454.5	2.56	21.33	0.954	0.663
2-1-78-79	455.5	1.84	15.33	0.719	-0.297
2-1-79-80	456.5	2.38	19.83	0.744	-0.510
2-1-80-81	457.5	2.39	19.92	1.218	-1.069
2-1-81-82	458.5	1.85	15.42	1.400	-0.875
2-1-82-83	459.5	3.12	26.00	1.536	-1.063
2-1-83-84	460.5	1.38	11.50	1.365	-0.947
2-1-84-85	461.5	2.40	20.00	1.498	-1.123

Number	Depth (cm)	TIC (wt % C)	CaCO ₃ (%)	δ ¹³ C (‰)	δ ¹⁸ O (‰)
2-1-85-86	462.5	3.69	30.75	1.508	-0.940
2-1-86-87	463.5	2.71	22.58	1.389	-1.063
2-1-87-88	464.5	2.89	24.08	1.273	-0.670
2-1-88-89	465.5	1.76	14.67	1.173	-1.567
2-1-89-90	466.5	2.98	24.83	1.349	-1.329
2-1-90-91	467.5	2.91	24.25	1.415	-1.369
2-1-91-92	468.5	3.43	28.58	1.342	-0.775
2-1-92-93	469.5	0.28	2.33	0.157	-3.547
2-1-93-94	470.5	0.83	6.92	0.836	-1.713
2-1-94-95	471.5	1.37	11.42	0.975	-1.108
2-1-95-96	472.5	1.41	11.75	1.198	-0.823
2-1-96-97	473.5	2.00	16.67	1.558	-0.449
2-1-97-98	474.5	1.07	8.92	1.699	-1.200

A3.3 Piston Core WLC-001

Table A3-4 Geochemical and isotopic results of bulk sediments from piston core WLC001

Section	Depth (cm)	δ ¹³ C (‰)	δ ¹⁸ O (‰)	Section	Depth (cm)	δ ¹³ C (‰)	δ ¹⁸ O (‰)
1-6	35.5	2.503	-4.457	1-6	60.5	3.321	-4.484
1-6	36.5	2.369	-4.894	1-5	61.5	3.578	-4.147
1-6	37.5	2.256	-5.117	1-5	62.5	3.564	-3.687
1-6	38.5	2.051	-5.432	1-5	63.5	3.530	-3.955
1-6	39.5	1.798	-6.196	1-5	64.5	3.679	-4.078
1-6	40.5	1.865	-6.171	1-5	65.5	3.680	-4.210
1-6	41.5	0.929	-6.630	1-5	66.5	3.724	-4.322
1-6	42.5	-0.489	-7.473	1-5	67.5	3.350	-4.254
1-6	43.5	1.576	-6.348	1-5	68.5	3.006	-4.606
1-6	44.5	1.828	-5.648	1-5	69.5	3.078	-4.985
1-6	45.5	2.344	-5.188	1-5	70.5	3.244	-4.768
1-6	46.5	2.422	-5.034	1-5	71.5	2.742	-5.292
1-6	47.5	2.086	-4.683	1-5	72.5	3.053	-5.030
1-6	48.5	2.804	-4.018	1-5	73.5	-6.176	-9.596
1-6	49.5	2.476	-4.614	1-5	74.5	3.026	-3.945
1-6	50.5	2.159	-5.627	1-5	75.5	2.893	-4.693
1-6	51.5	1.116	-5.964	1-5	76.5	3.260	-4.767
1-6	52.5	-4.493	-7.481	1-5	77.5	3.490	-4.599
1-6	53.5	-1.287	-7.117	1-5	78.5	3.504	-4.727
1-6	54.5	2.075	-5.217	1-5	79.5	3.709	-4.762
1-6	55.5	2.113	-4.979	1-5	80.5	3.463	-5.056
1-6	56.5	3.033	-4.561	1-5	81.5	3.447	-4.852
1-6	57.5	3.198	-4.183	1-5	82.5	3.582	-4.802
1-6	58.5	0.681	-5.599	1-5	83.5	3.936	-4.100
1-6	59.5	1.111	-5.369	1-5	84.5	3.868	-3.797

Note: Missing values are represented by -9999.

REFERENCE

- Anderson R. Y. (1992) Long-term changes in the frequency of occurrence of El Niño events. In *El Niño: Historical and Paleoclimatic Aspects of the Southern Oscillation* (ed. V. Markgraf), pp. 193-200. Cambridge University Press.
- Antevs. (1952) Cenozoic climates of the Great Basin. *Geologisch Rundschau* **40**, 94-108.
- Bard E., Raisbeck G., Yiou F., and Jouzel J. (2000) Solar irradiance during the last 1200 years based on cosmogenic nuclides. *Tellus, Series B: Chemical and Physical Meteorology* **52**(3), 985-992.
- Bard E., Raisbeck G., Yiou F., and Jouzel J. (2003) Reconstructed Solar Irradiance Data, IGBP PAGES/World Data Center for Paleoclimatology, Data Contribution Series #2003-006. NOAA/NGDC Paleoclimatology Program, Boulder CO, USA.
- Barnett T. P., Hasselmann K., and Chelliah M. (1999) Detection and attribution of recent climate change: a status report. *Bulletin of the American Meteorological Society* **80**(12), 2631-59.
- Benedict C. R. (1978) The fractionation of stable carbon isotopes in photosynthesis. *What's New Plant Physiol.* **9**, 13-16.
- Benson L., Liddicoat J., Smoot J., Sarna-Wojcicki A., Negrini R., and Lund S. (2003a) Age of the Mono Lake excursion and associated tephra. *Quaternary Science Reviews* **22**(2-4), 135-140.
- Benson L., Linsley B., Smoot J., Mensing S., Lund S., Stine S., and Sarna-Wojcicki A. (2003b) Influence of the Pacific decadal oscillation on the climate of the Sierra Nevada, California and Nevada. *Quaternary Research* **59**(2), 151-159.
- Benson L., Lund S., Paillet F., Smoot J., Kester C., Mensing S., Meko D., Lindström S., Kashgarian M., and Rye R. (2002) Holocene multidecadal and multicentennial droughts affecting Northern California and Nevada. *Quaternary Science Reviews* **21**(4-6), 659-682.
- Benson L., Mensing S., Burdett J., Lund S., and Kashgarian M. (1997) Nearly synchronous climate change in the Northern Hemisphere during the last glacial termination. *Nature* **388**(6639), 263-265.
- Benson L. and Paillet F. (2002) HIBAL: A hydrologic-isotopic-balance model for application to paleolake systems. *Quaternary Science Reviews* **21**(12-13), 1521-1539.
- Benson L., White L. D., and Rye R. (1996) Carbonate deposition, Pyramid Lake Subbasin, Nevada: 4. Comparison of the stable isotope values of carbonate deposits (tufas) and the Lahontan lake-level record. *Palaeogeography, Palaeoclimatology, Palaeoecology* **122**(1-4), 45-76.
- Benson L. V. (1994) Stable isotopes of oxygen and hydrogen in the Truckee River-Pyramid Lake surface-water column. 1. Data analysis and extraction of paleoclimatic information. *Limnology and oceanography* **39**(2), 344-355.
- Benson L. V. (1999) Records of millennial-scale climate change from the Great Basin of the Western United States. In *Mechanisms of Global Climate Change at Millennial Time Scales*, Vol. 112 (ed. L. D. Keigwin), pp. 203-225. American Geophysical Union.
- Benson L. V., Currey D. R., Dorn R. I., Lajoie K. R., Oviatt C. G., Robinson S. W., Smith G. I., and Stine S. (1990) Chronology of expansion and contraction of four Great Basin lake systems during the past 35 000 years. *Palaeogeography, Palaeoclimatology, Palaeoecology* **78**(3-4), 241-286.

- Benson L. V. and Leach D. L. (1979) Uranium transport in the Walker River Basin, California and Nevada. *Journal of Geochemical Exploration* **11**(3), 227-248.
- Benson L. V., Meyers P. A., and Spencer R. J. (1991) Change in the size of Walker Lake during the past 5000 years. *Palaeogeography, Palaeoclimatology, Palaeoecology* **81**(3-4), 189-214.
- Benson L. V. and Spencer R. J. (1983) A hydrological reconnaissance study of the Walker River Basin, California and Nevada. *U.S. Geological Survey Open-File Report 83-740*, 53.
- Benson L. V. and Thompson R. S. (1987) Lake-level variation in the Lahontan basin for the past 50 000 years. *Quaternary Research* **28**(1), 69-85.
- Benson L. V. and White J. W. C. (1994) Stable isotopes of oxygen and hydrogen in the Truckee River-Pyramid Lake surface-water system. 3. Source of water vapor overlying Pyramid Lake. *Limnology & Oceanography* **39**(8), 1945-1958.
- Beutel M. W., Horne A. J., Roth J. C., and Barratt N. J. (2001) Limnological effects of anthropogenic desiccation of a large, saline lake, Walker Lake, Nevada. *Hydrobiologia* **466**, 91-105.
- Biondi F., Lange C. B., Hughes M. K., and Berger W. H. (1997) Inter-decadal signals during the last millennium (AD 1117-1992) in the varve record of Santa Barbara Basin, California. *Geophysical Research Letters* **24**(2), 193-196.
- Bradbury J. P. (1987) Late Holocene diatom paleolimnology of Walker Lake, Nevada. *Arch. Hydrobiol./ Suppl.* **79**(1), 1-27.
- Bradbury J. P., Forester R. M., and Thompson R. S. (1989) Late Quaternary paleolimnology of Walker Lake, Nevada. *Journal of Paleolimnology* **1**(4), 249-267.
- Bradley R. S. (2000) Climate paradigms for the last millennium. *A Joint Newsletter of the Past Global Changes Project (PAGES) and the Climate Variability and Predictability Project (CLIVAR)* **8**(1), 2-3.
- Bradley R. S. and Jones P. D. (1993) "Little Ice Age" summer temperature variations: their nature and relevance to recent global warming trends. *Holocene* **3**(4), 367-376.
- Buttkus B. (2000) *Spectral analysis and filter theory in applied geophysics*. Springer-Verlag.
- Calder J. A. and Parker P. L. (1973) Geochemical implications of induced changes in ¹³C fractionation by blue algae. *Geochim. Cosmochim. Acta* **37**, 133-140.
- Campbell I. D., Campbell C., Apps M. J., Rutter N. W., and Bush A. B. G. (1998) Later Holocene ~1500 yr climatic periodicities and their implications. *Geology* **26**(5), 471-473.
- Chivas A. R., De Deckker P., and Shelly J. M. G. (1985) Strontium content of ostracods indicates lacustrine palaeosalinity. *Nature* **316**(6025), 251-253.
- Chu G., Gu Z., Wang W., Liu T., Liu J., Sun Q., and Lu H. (2002) The 'Mediaeval Warm Period' drought recorded in Lake Huguangyan, tropical South China. *Holocene* **12**(5), 511-516.
- Cini Castagnoli G., Bonino G., and Taricco C. (2002) Long term solar-terrestrial records from sediments: Carbon isotopes in planktonic foraminifera during the last millennium. *Advances in Space Research* **29**(10), 1537-1549.
- Cioccale M. A. (1999) Climatic fluctuations in the central region of Argentina in the last 1000 years. *Quaternary International* **62**, 35-47.
- Clarke F. W. (1924) *The data of geochemistry*.
- Cole J. E., Overpeck J. T., and Cook E. R. (2002) Multiyear La Niña events and persistent drought in the contiguous United States. *Geophys. Res. Lett.* **29**(13), 25-1.
- Cook E. R., Meko D. M., Stahle D. W., and Cleaveland M. K. (1999) Drought reconstructions for the continental United States. *Journal of Climate* **12**(4), 1145-1163.

- Cook E. R., Palmer J. G., and D'Arrigo R. D. (2002) Evidence for a 'Medieval Warm Period' in a 1,100 year tree-ring reconstruction of past austral summer temperatures in New Zealand. *Geophysical Research Letters* **29**(14), 12-1 - 12-4.
- Cooper J. J. and Koch D. L. (1984) Limnology of a desertic terminal lake, Walker Lake, Nevada, USA. *Hydrobiologia* **118**, 275-292.
- Covich A. and Stuiver M. (1974) Changes in oxygen 18 as a measure of long-term fluctuations in tropical lake levels and molluscan populations. *Limnol. Oceanogr.* **19**, 682-691.
- Craig H. (1953) The geochemistry of the stable carbon isotopes. *Geochim. Cosmochim. Acta* **37**, 53-92.
- Crowley T. J. and Lowery T. A. (2000) How warm was the Medieval Warm Period? *Ambio* **29**(1), 51-54.
- Currie R. G. and Fairbridge R. W. (1985) Periodic 18.6-year and cyclic 11-year induced drought and flood in northeastern China and some global implications. *Quaternary Science Reviews* **4**(2), 109-134.
- Curtis J. H., Hodell D. A., and Brenner M. (1996) Climate variability on the Yucatan Peninsula (Mexico) during the past 3500 years, and implications for Maya cultural evolution. *Quaternary Research* **46**(1), 37-47.
- Damon P. E. and Sonett C. P. (1991) Solar and terrestrial components of the atmospheric 14C variation spectrum. In *The Sun in time* (ed. C. P. Sonett), pp. 360-388. University of Arizona Press.
- D'Arrigo R., Villalba R., and Wiles G. (2001) Tree-ring estimates of Pacific decadal climate variability. *Climate Dynamics* **18**(3-4), 219-224.
- Davis J. O. (1982) Bits and pieces: The last 35,000 years in the Lahotan area. In *Man and Environment in the Great Basin* (ed. J. F. O'Connell), pp. 53-75. Soc. Amer. Archaeol.
- De Putter T., Loutre M. F., and Wansard G. (1998) Decadal periodicities of Nile River historical discharge (A.D. 622-1470) and climatic implications. *Geophysical Research Letters* **25**(16), 3193-3196.
- Dean W. (2002) A 1500-year record of climatic and environmental change in Elk Lake, Clearwater County, Minnesota II: Geochemistry, mineralogy, and stable isotopes. *Journal of Paleolimnology* **27**(3), 301-319.
- deMenocal P. B. (2001) Cultural responses to climate change during the late holocene. *Science* **292**(5517), 667-673.
- Dettinger M. D., Ghil M., Strong C. M., Weibel W., and Yiou P. (1995) Software expedites singular-spectrum analysis of noisy time series. *EOS, Trans, American Geophysical Union*, v. **76**(2), 12,14,21.
- Deuser W. G., Degens E. T., and Guillard R. R. L. (1968) Carbon isotope relationships between plankton and seawater. *Geochim. Cosmochim. Acta* **32**, 657-660.
- Dunbar R. B., Wellington G. M., Colgan M. W., and Glynn P. W. (1994) Eastern Pacific sea surface temperature since 1600 A.D.: the $\delta^{18}\text{O}$ record of climate variability in Galapagos corals. *Paleoceanography* **9**(2), 291-315.
- Eddy J. A. (1976) The Maunder minimum. *Science* **192**, 1189-1202.
- Encyclopedia. (1999) Encarta Encyclopedia 99 Program Manager. Encarta, Microsoft Cooperation, Redmond, WA, USA, 1999.
- Epstein S., Buchsbaum R., Lowenstam H. A., and Urey H. C. (1953) Revised carbonate-water isotopic temperature scale. *Geochim. Cosmochim. Acta* **4**, 213-224.

- Esper J., Cook E. R., and Schweingruber F. H. (2002) Low-frequency signals in long tree-ring chronologies for reconstructing past temperature variability. *Science* **295**(5563), 2250-2253.
- Field D. B. and Baumgartner T. R. (2000) A 900 year stable isotope record of interdecadal and centennial change from the California current. *Paleoceanography* **15**(6), 695-708.
- Fritz S. C., Engstrom D. R., Ito E., Yu Z., and Laird K. R. (2000) Hydrologic variation in the northern Great Plains during the last two millennia. *Quaternary Research* **53**(2), 175-184.
- Ghil M., Allen M. R., Dettinger M. D., Ide K., Kondrashov D., Mann M. E., Robertson A. W., Saunders A., Tian Y., Varadi F., and Yiou P. (2002) Advanced spectral methods for climatic time series. *Rev. Geophys.* **40**(1), 3:1-42.
- Ghil M. and Vautard R. (1991) Interdecadal oscillations and the warming trend in global temperature time series. *Nature* **350**(6316), 324-327.
- Glantz M. H. (1996) *Currents of Changes: El Niño's Impact on Climate and Society*. Cambridge University Press.
- Gonfiantini R. (1965) Environmental effects in the evaporation of salt water. *Atti Società Toscana National Science Pisa* **72**, 5-22.
- Gonfiantini R. (1986) Environmental isotopes in lake studies. In *Handbook of Environmental Isotope Geochemistry* (ed. J. C. Fontes), pp. 113-168. Elsevier.
- Gong D. Y., Wang S. W., and Zhu J. H. (2000) Surplus summer rainfall along the middle to lower reaches of Changjiang River in the 1990s. *Acta Geographica Sinica* **55**(5), 567-575.
- Graham N. E. (1994) Decadal-scale climate variability in the tropical and North Pacific during the 1970s and 1980s: observations and model results. *Climate Dynamics* **10**(3), 135-162.
- Graumlich L. J. (1993) A 1000-year record of temperature and precipitation in the Sierra Nevada. *Quaternary Research* **39**(2), 249-255.
- Grayson D. K. (1993) *The desert's past : a natural prehistory of the Great Basin*. Smithsonian Institution Press.
- Grissino-Mayer H. D. (1996) A 2129-year reconstruction of precipitation for northwestern New Mexico, USA. In *Tree Rings, Environment, and Humanity; Radiocarbon* (ed. J. S. Dean, D. M. Meko, and T. W. Swetnam), pp. 191-204.
- Grossman E. L. and Ku T. L. (1986) Oxygen and carbon isotope fractionation in biogenic aragonite: temperature effects. *Chemical Geology (Isotope Geoscience Section)* **59**(1), 59-74.
- Grove J. M. (1988) *The Little Ice Age*. Methuen.
- Halfman J. D., Johnson T. C., and Finney B. P. (1994) New AMS dates, stratigraphic correlations and decadal climatic cycles for the past 4 ka at Lake Turkana, Kenya. *Palaeogeography, Palaeoclimatology, Palaeoecology* **111**(1-2), 83-98.
- Halley E. (1715) On the cause of the saltiness of the ocean, and the several lakes that emit no rivers. *Philosophical Transactions of the Royal Society of London* **6**, 169.
- Haykin S. (1983) *Nonlinear methods of spectral analysis*. Springer-Verlag.
- Hendy E. J., Lough J. M., Isdale P. J., Gagan M. K., Alibert C. A., and McCulloch M. T. (2002) Abrupt decrease in tropical pacific sea surface salinity at end of little ice age. *Science* **295**(5559), 1511-1514.
- Herczeg A. L. and Fairbanks R. G. (1987) Anomalous carbon isotope fractionation between atmospheric CO₂ and dissolved inorganic carbon induced by intense photosynthesis. *Geochimica et Cosmochimica Acta* **51**(4), 895-899.
- Hodell D. A., Brenner M., Curtis J. H., and Guilderson T. (2001) Solar forcing of drought frequency in the Maya lowlands. *Science* **292**(5520), 1367-1370.

- Hodell D. A., Curtis J. H., and Brenner M. (1995) Possible role of climate in the collapse of Classic Maya civilization. *Nature* **375**(6530), 391-394.
- Hoffmann G., Jouzel J., and Johnsen S. (2001) Deuterium excess record from central Greenland over the last millenium: Hints of a North Atlantic signal during the Little Ice Age. *Journal of Geophysical Research D: Atmospheres* **106**(13), 14265-14274.
- Holmes J. A. (1996) Trace-element and stable-isotope geochemistry of non-marine ostracod shells in Quaternary palaeoenvironmental reconstruction. *Journal of Paleolimnology* **15**(3), 223-235.
- Hostetler S. W. and Benson L. V. (1994) Stable isotopes of oxygen and hydrogen in the Truckee River-Pyramid Lake surface-water system. 2. A predictive model of $\delta^{18}\text{O}$ and ^2H in Pyramid Lake. *Limnology and oceanography* **39**(2), 356-364.
- Houghton J. G. (1969) *Characteristics of rainfall in the Great Basin*. Ph.D dissertation, University of Oregon.
- Hughes M. K. and Diaz H. F. (1994) Was there a " Medieval Warm Period" and if so, where and when? *Climatic Change* **26**, 109-142.
- Hughes M. K. and Funkhouser G. (1996) Extremes of moisture availability reconstructed from tree rings for recent millennia in the Great Basin of Western North America. In *Varved sediment records of recent seasonal-millennial environmental variability*, Vol. 141 (ed. J. Jouzel), pp. 99-107. Springer-Verlag.
- Hughes M. K. and Graumlich L. J. (1996) Multimillennial dendroclimatic studies from the western United States. In *Climatic Variations and Forcing Mechanisms of the Last 2000 Years*, Vol. 141 (ed. J. Jouzel), pp. 109-124. Springer-Verlag.
- Hutchinson G. E. (1937) A contribution to the limnology of arid regions. *Connecticut Academy of Arts and Sciences Transactions* **33**, 47-132.
- Jimenez-Lopez C., Caballero E., Huertas F. J., and Romanek C. S. (2001) Chemical, mineralogical and isotope behavior, and phase transformation during the precipitation of calcium carbonate minerals from intermediate ionic solution at 25°C. *Geochimica et Cosmochimica Acta* **65**(19), 3219-3231.
- Jones P. D., Osborn T. J., and Briffa K. R. (2001) The evolution of climate over the last millennium. *Science* **292**(5517), 662-667.
- Jones P. D., Wigley T. M. L., and Wright P. B. (1986) Global temperature variations between 1861 and 1984. *Nature* **322**, 430-4.
- Keigwin L. D. (1996) The Little Ice Age and Medieval Warm Period in the Sargasso Sea. *Science* **274**(5292), 1504-1508.
- Kempe S. and Kazmierczak J. (1990) Calcium carbonate supersaturation and the formation of in situ calcified stromatolites. In *Facets of Modern Biogeochemistry* (ed. A. Spitzzy), pp. 255-278. Springer-Verlag.
- Knutson T. R., Manabe S., and Daifang G. (1997) Simulated ENSO in a global coupled ocean-atmosphere model: multidecadal amplitude modulation and CO₂ sensitivity. *Journal of Climate* **10**(1), 138-161.
- Koch D. L., Cooper J. J., Lider E. L., Jacobson R. L., and Spencer R. J. (1979) *Investigations of Walker Lake, Nevada: dynamic ecological relationships*. University of Nevada.
- Laird K. R., Fritz S. C., and Cumming B. F. (1998) A diatom-based reconstruction of drought intensity, duration, and frequency from Moon Lake, North Dakota: A sub-decadal record of the last 2300 years. *Journal of Paleolimnology* **19**(2), 161-179.

- Laird K. R., Fritz S. C., Maasch K. A., and Cumming B. F. (1996) Greater drought intensity and frequency before AD 1200 in the northern Great Plains, USA. *Nature* **384**(6609), 552-554.
- Lamb H. H. (1965) The early Medieval warm epoch and its sequel. *Palaeogeography, Palaeoclimatology, Palaeoecology* **1**, 13-37.
- Lamb H. H. (1995) *Climate, history and the modern world*. Routledge.
- Latif M. and Barnett T. P. (1994) Causes of decadal climate variability over the North Pacific and North America. *Science* **266**(5185), 634-637.
- Lean J., Skumanich A., and White O. (1992) Estimating the Sun's radiative output during the Maunder Minimum. *Geophysical Research Letters* **19**(15), 1591-1594.
- Levy D. B., Erickson T. A., Moore J. C., Schramke J. A., and Esposito K. J. (1999) The shallow ground water chemistry of arsenic, fluorine, and major elements: Eastern Owens Lake, California. *Applied Geochemistry* **14**(1), 53-65.
- Li H. C. (1995) Isotope geochemistry of Mono Basin, California: Applications to paleoclimate and paleohydrology. PhD dissertation, University of Southern California.
- Li H. C. and Ku T. L. (1997a) $\delta^{13}\text{C}$ - $\delta^{18}\text{O}$ covariance as a paleohydrological indicator for closed-basin lakes. *Palaeogeography, Palaeoclimatology, Palaeoecology* **133**(1-2), 69-80.
- Li H.-C. and Ku T.-L. (1997b) Decadal hydroclimatic variability in the western coastal United States: Temporal and spatial variations in precipitation, streamflow and lake level. *Proceedings of 13th Annual Pacific Climate (PACCLIM) Workshop, April 15-18, 1996. Interagency Ecological Program, Technical Report 53*, 79-91.
- Li H. C., Stott L. D., Bischoff J. L., Ku T. L., and Lund S. P. (2000) Climate variability in East-Central California during the past 1000 years reflected by high-resolution geochemical and isotopic records from Owens Lake sediments. *Quaternary Research* **54**(2), 189-197.
- Linsley B. K., Wellington G. M., and Schrag D. P. (2000) Decadal sea surface temperature variability in the subtropical south pacific from 1726 to 1997 A.D. *Science* **290**(5494), 1145-1148.
- Mann M. E., Bradley R. S., and Hughes M. K. (2000) Long-term variability in the El Niño/Southern Oscillation and associated teleconnections. In *El Niño and the southern oscillation : multiscale variability and global and regional impacts* (ed. V. Markgraff), pp. 496. Cambridge University Press.
- Mann M. E. and Lees J. M. (1996) Robust estimation of background noise and signal detection in climatic time series. *Climatic Change* **33**(3), 409-445.
- Mantua N. J., Francis R. C., Hare S. R., Zhang Y., and Wallace J. M. (1997) A Pacific interdecadal climate oscillation with impacts on salmon production. *Bulletin - American Meteorological Society* **78**(6), 1069-1079.
- McCrea J. M. (1950) On the isotopic chemistry of carbonates and a paleotemperature scale. *J. Chem. Phys.* **18**, 849-857.
- McKenzie J. A. (1985) Carbon isotopes and productivity in the lacustrine and marine environment. In *Chemical processes in lakes* (ed. W. Stumm), pp. 99-118. Wiley.
- McKenzie J. A. and Eberli G. P. (1987) Indications for abrupt Holocene climatic change: late Holocene oxygen isotope stratigraphy of the Great Salt Lake, Utah. In *Abrupt climatic change. Proc. 1985* (ed. W. H. Berger), pp. 127-136. Reidel.
- McKenzie J. A. and Hollander D. J. (1993) Oxygen-isotope record in recent carbonate sediments from Lake Greifen, Switzerland (1750-1986): Application of continental isotopic indicator for evaluation of change in climate and atmospheric circulation

- patterns. In *Climate change in continental isotopic records*, Vol. Geophysical monograph 78 (ed. P. K. Swart), pp. 101-111. American Geophysical Union.
- Meko D. M., Therrell M. D., Baisan C. H., and Hughes M. K. (2001) Sacramento river flow reconstructed to A.D. 869 from tree rings. *Journal of the American Water Resources Association* **37**(4), 1029-1038.
- Merlivat L. and Jouzel J. (1979) Global climatic interpretation of the deuterium-oxygen 16 relationship for precipitation. *Journal of Geophysical Research* **84**(C8), 5029-5033.
- Metcalfe S. E. (1997) Palaeolimnological records of climate change in Mexico -- frustrating past, promising future? *Quaternary International* **43-44**, 111-116.
- Meyers P. A. (1990) Impacts of Late Quaternary fluctuations in water level on the accumulation of sedimentary organic matter in Walker Lake, Nevada. *Palaeogeography, Palaeoclimatology, Palaeoecology* **78**(3-4), 229-240.
- Milne W. (1987) *A comparison of reconstructed lake-level records since the mid-1800s of some Great Basin lakes*. Thesis, Colorado School of Mine.
- Milne W. and Benson L. V. (1987) A comparison of reconstructed lake-level records since the mid-1800's of some Great Basin lakes. *American Geophysical Union, 1987 fall meeting* **68**(44), 1274.
- Minobe S. (1997) A 50-70 year climatic oscillation over the North Pacific and North America. *Geophysical Research Letters* **24**(6), 683-686.
- Mook W. G., Bommerson J. C., and Staverman W. H. (1974) Carbon isotope fractionation between dissolved bicarbonate and gaseous carbon dioxide. *Earth Planet. Sci. Lett.* **22**, 169-176.
- Morner N. A. and Karlen W. (1984) Climatic changes on a yearly to millennial basis. Geological, historical and instrumental records. Proceedings of the 2nd Nordic symposium, Stockholm, May 16-20 1983. In *Climatic changes on a yearly to millennial basis*, pp. 667. Reidel.
- Mosley-Thompson E., Thompson L. G., Grootes P. M., and Gundestrup N. (1990) Little Ice Age (neoglacial) paleoenvironmental conditions at Siple Station, Antarctica. *Annals of Glaciology* **14**, 199-204.
- Muñoz A., Ojeda J., and Sánchez-Valverde B. (2002) Sunspot-like and ENSO/NAO-like periodicities in lacustrine laminated sediments of the Pliocene Villarroya Basin (La Rioja, Spain). *Journal of Paleolimnology* **27**(4), 453-463.
- NDEP. (2003) State of Nevada Surface Water Monitoring Network: Walker River Basin (<http://ndep.nv.gov/bwqp/WalkerMap.html>). Nevada Division of Environmental Protection, Carson City, Nevada.
- Newton M. S. and Grossman E. L. (1988) Late Quaternary chronology of tufa deposits, Walker Lake, Nevada. *Journal of Geology* **96**(4), 417-433.
- NRC. (1998) *Decade-to-century-scale climate variability and change : a science strategy*. National Academy Press.
- O'Neil J. R., Clayton R. N., and Mayeda T. K. (1969) Oxygen isotopic fractionation in divalent metal carbonates. *J. Chem. Phys.* **51**, 5547-5558.
- Park J., Lindberg C. R., and Vernon F. L. I. (1987) Multitaper spectral analysis of high-frequency seismograms. *J. Geophys. Res.* **92**, 12675-12684.
- Peng T. H. and Broecker W. (1980) Gas exchange rates for three closed-basin lakes. *Limnol. Oceanogr.* **25**(5), 789-796.
- Percival D. B. and Walden A. T. (1993) *Spectral Analysis for Physical Applications*. Cambridge University Press.

- Pfister C., Luterbacher J., Schwarz-Zanetti G., and Wegmann M. (1998) Winter air temperature variations in western Europe during the Early and High Middle Ages (AD 750-1300). *Holocene* **8**(5), 535-552.
- Quay P. D., Emerson S. R., Quay B. M., and Devol A. H. (1986) The carbon cycle for Lake Washington - a stable isotope study. *Limnology & Oceanography* **31**(3), 596-611.
- Quinn T. M., Crowley T. J., Taylor F. W., Kim S. J., and Stossel A. (1996) New stable isotope results from a 173-year coral from Espiritu Santo, Vanuatu. *Geophysical Research Letters* **23**(23), 3413-3416.
- Redmond K. T. and Koch R. W. (1991) Surface climate and streamflow variability in the western United States and their relationship to large-scale circulation indices. *Water Resources Research* **27**(9), 2381-2399.
- Ricketts R. D. and Anderson R. F. (1998) A direct comparison between the historical record of lake level and the $\delta^{18}\text{O}$ signal in carbonate sediments from Lake Turkana, Kenya. *Limnology and Oceanography* **43**(5), 811-822.
- Riebsame W. E., Changnon S. A., and Karl T. R. (1991) *Drought and natural resources management in the United States: impacts and implications of the 1987-89 drought*. Westview Press.
- Rind D. and Overpeck J. (1993) Hypothesized causes of decade-to-century-scale climate variability: climate model results. *Quaternary Science Reviews* **12**(6), 357-374.
- Rittenour T. M., Brigham-Grette J., and Mann M. E. (2000) El Nino-like climate teleconnections in New England during the late Pleistocene. *Science* **288**(5468), 1039-1042.
- Rodbell D. T., Enfield D. B., Newman J. H., Seltzer G. O., Anderson D. M., and Abbott M. B. (1999) An 15,000-year record of El Nino-driven alluviation in Southwestern Ecuador. *Science* **283**(5401), 516-520.
- Rush F. E. (1970) Hydrologic regime of Walker Lake, Mineral County, Nevada. *U.S. Geol. Surv. Hydrol. Atlas HA415*.
- Russell I. C. (1885) Geological history of Lake Lahontan, a Quaternary lake of northwestern Nevada. *U.S. Geol. Surv. Monogr.* **11**, 288.
- Scuderi L. A. (1993) A 2000-yr tree ring record of annual temperatures in the Sierra Nevada Mountains. *Science* **259**(5100), 1433-1436.
- Smith A. J., Engstrom D. R., Panek V. A., Donovan J. J., and Ito E. (2002) Climate-driven hydrologic transients in lake sediment records: Multiproxy record of mid-Holocene drought. *Quaternary Science Reviews* **21**(4-6), 625-646.
- Smith B. N. and Epstein S. (1971) Two categories of $^{13}\text{C}/^{12}\text{C}$ ratios for high plants. *Plant Physiol.* **47**, 380-384.
- Smith C. (2002) Native Peoples of North America: Agricultural Societies in Pre-European Times Southwestern U.S. and Northwestern Mexico (<http://www.cabrillo.cc.ca.us/~crsmith/southwest.html>). Cabrillo College, Aptos, CA.
- Smith G. H. (1998) The History of the Comstock Lode. *Nevada Bureau of Mines and Geology*, 328.
- Spencer R. J. (1977) *Silicate and carbonate sediment-water relations in Walker Lake, Nevada*. Thesis, University of Nevada.
- Spero H. J., Bijma J., Lea D. W., and Bernis B. E. (1997) Effect of seawater carbonate concentration on foraminiferal carbon and oxygen isotopes. *Nature* **390**(6659), 497-500.
- Stahle D. W., Gay D. A., Cleaveland M. K., Blanton D. B., and Therrell M. D. (1998) The Lost Colony and Jamestown droughts. *Science* **280**(5363), 564-567.

- Stine S. (1990) Late Holocene fluctuations of Mono Lake, eastern California. *Palaeogeography, Palaeoclimatology, Palaeoecology* **78**(3-4), 333-381.
- Stine S. (1994) Extreme and persistent drought in California and Patagonia during mediaeval time. *Nature* **369**(6481), 546-549.
- Stuiver M. (1970) Oxygen and carbon isotope ratios of fresh water carbonates as climatic indicators. *J. Geophys. Res.* **75**, 5247-5257.
- Stuiver M. and Braziunas T. F. (1993) Sun, ocean, climate and atmospheric $^{14}\text{CO}_2$: an evaluation of causal and spectral relationships. *Holocene* **3**(4), 289-305.
- Stuiver M. and Reimer P. J. (1993) Extended ^{14}C data base and revised CALIB 3.0 ^{14}C age calibration program. *Radiocarbon* **35**(1), 215-230.
- Stuiver M., Reimer P. J., and Braziunas T. F. (1998) High-precision radiocarbon age calibration for terrestrial and marine samples. *Radiocarbon* **40**(3), 1127-1151.
- Talbot M. R. and Kelts K. (1990) Paleolimnological signatures from carbon and oxygen isotopic ratios in carbonates from organic carbon-rich lacustrine sediments. In *Lacustrine basin exploration - case studies and modern analogs* (ed. B. J. Katz), pp. 99-112. AAPG Memoir 50.
- Talbot M. R. A. (1990) A review of the palaeohydrological interpretation of carbon and oxygen isotopic ratios in primary lacustrine carbonates. *Chemical geology* **80**(4), 261-280.
- Tenzer G. E., Meyers P. A., and Knoop P. (1997) Sources and distribution of organic and carbonate carbon in surface sediments of Pyramid Lake, Nevada. *Journal of Sedimentary Research A: Sedimentary Petrology and Processes* **67**(5), 884-890.
- Thomas J. M. (1995) Water budget and salinity of Walker Lake, western Nevada. In *U.S. Geological Survey Fact Sheet FS-115-95*, pp. 4.
- Thompson L. G. (1996) Climatic changes for the last 2000 years from ice-core evidence in tropical ice cores. In *Climatic Variations and Forcing Mechanisms*, Vol. I41 (ed. J. Jouzel), pp. 281-295. Springer-Verlag.
- Thompson L. G., Mosley-Thompson E., Dansgaard W., and Grootes P. M. (1986) The Little Ice Age as recorded in the stratigraphy of the tropical Quelccaya Ice Cap. *Science* **234**(4774), 361-364.
- Thompson L. G., Mosley-Thompson E., Davis M. E., Henderson K. A., Brecher H. H., Zagorodnov V. S., Mashiotto T. A., Lin P.-N., Mikhailenko V. N., Hardy D. R., and Beer J. (2002) Kilimanjaro Ice Core Records: Evidence of Holocene Climate Change in Tropical Africa. *Science* **298**(5593), 589-593.
- Thomson D. J. (1982) Spectrum estimation and harmonic analysis. *Proc. IEEE* **70**, 1055-1096.
- Trenberth K. E. and Hurrell J. W. (1994) Decadal atmosphere-ocean variations in the Pacific. *Climate Dynamics* **9**(6), 303-319.
- Urban F. E., Cole J. E., and Overpeck J. T. (2000) Influence of mean climate change on climate variability from a 155-year tropical Pacific coral record. *Nature* **407**(6807), 989-993.
- Van Geel B., Van der Plicht J., Dergachev V. A., Meijer H. A. J., Raspopov O. M., and Renssen H. (1999) The role of solar forcing upon climate change. *Quaternary Science Reviews* **18**(3), 331-338.
- Vautard R. and Ghil M. (1989) Singular spectrum analysis in nonlinear dynamics, with applications to paleoclimatic time series. *Physica D* **35**, 395-424.
- Vautard R., Yiou P., and Ghil M. (1992) Singular-spectrum analysis: A toolkit for short, noisy chaotic signals. *Physica D Nonlinear phenomena*. **58**(1-4), 95.

- Verschuren D., Laird K. R., and Cumming B. F. (2000) Rainfall and drought in equatorial east Africa during the past 1,100 years. *Nature* **403**(6768), 410-414.
- Von Grafenstein U., Trimborn P., Alefs J., Erlenkeuser H., and Muller J. (1996) A 200 year mid-European air temperature record preserved in lake sediments: an extension of the $\delta^{18}\text{O}_p$ -air temperature relation into the past. *Geochimica et Cosmochimica Acta* **60**(21), 4025-4036.
- Woodhouse C. A. and Overpeck J. T. (1998) 2000 years of drought variability in the central United States. *Bulletin of the American Meteorological Society* **79**(12), 2693-2714.
- Xia J., Engstrom D. R., and Ito E. (1997a) Geochemistry of ostracode calcite: part 2. The effects of water chemistry and seasonal temperature variation on *Candona rawsoni*. *Geochimica et Cosmochimica Acta* **61**(2), 383-391.
- Xia J., Ito E., and Engstrom D. R. (1997b) Geochemistry of ostracode calcite: part 1. An experimental determination of oxygen isotope fractionation. *Geochimica et Cosmochimica Acta* **61**(2), 377-382.
- Yu Z. and Eicher U. (1998) Abrupt climate oscillations during the last deglaciation in central North America. *Science* **282**(5397), 2235-2238.
- Yu Z. and Ito E. (1999) Possible solar forcing of century-scale drought frequency in the northern Great Plains. *Geology* **27**(3), 263-266.
- Yu Z., Ito E., Engstrom D. R., and Fritz S. C. (2002) A 2100-year trace-element and stable-isotope record at decadal resolution from Rice Lake in the Northern Great Plains, USA. *Holocene* **12**(5), 605-617.
- Zhang Y., Wallace J. M., and Battisti D. S. (1997) ENSO-like Interdecadal Variability: 1900-93. *Journal of Climate* **10**(5), 1004-1020.
- Zheng Y. F. (1999) Oxygen isotope fractionation in carbonate and sulfate minerals. *Geochemical Journal* **33**(2), 109-126.
- Zhou G.-T. and Zheng Y.-F. (2003) An experimental study of oxygen isotope fractionation between inorganically precipitated aragonite and water at low temperatures. *Geochimica et Cosmochimica Acta* **67**(3), 387-399.

VITA

Name: Fasong Yuan

Major: Earth Sciences

Specialty: Environmental Geochemistry and Paleoclimatology

Biographical Sketch:

Born in Hangzhou, Zhejiang Province, People's Republic of China in 1963. Attended Zhejiang University and received B.S. in Earth Sciences (1986) and M.S. in Environmental Chemistry (1989). Served as Environmental Specialist for the city of Hangzhou with the Department of Municipal Services from 1989 to 1998. Doctoral work began in 1998 at the University at Albany, State University of New York.

Other Professional Experience:

Graduate Teaching Assistant: University at Albany (1998-2002)

Graduate Research Assistant: SUNY Research Foundation (1999 and 2001)

Graduate Award: SUNY Benevolent Award (2003)

Permanent Address: 36A, Nandu Garden, Hangzhou, PR China 310012

E-Mail: fy7247@yahoo.com